Nonstationary Stochastic Dynamics of Neuronal Membranes

Marco Paulo Ferreira Brigham

▶ To cite this version:

HAL Id: tel-01186526
https://theses.hal.science/tel-01186526

Submitted on 25 Aug 2015

Nonstationary Stochastic Dynamics
of Neuronal Membranes

Dynamique Stochastique Non-Stationnaire
de la Membrane Neuronale

Marco Paulo Ferreira Brigham

Thèse de Doctorat en Neurosciences Computationnelles

Université Pierre et Marie Curie (UPMC)
École Doctorale Cerveau, Cognition, Comportement

Soutenue le 27 Avril 2015, avec le Jury composé de:

Arvind Kumar	Rapporteur
Ruben Moreno-Bote	Rapporteur
Bruno Delord	Président du Jury
Michèle Thieullen	Examinateur
Alain Destexhe	Directeur de Thèse

Laboratory of Computational Neuroscience
Unité de Neurosciences, Information et Complexité (UNIC, UPR-3293),
Centre National de la Recherche Scientifique (CNRS), Gif-sur-Yvette, France

To my dear grandmother Maria Isabel for the gift of curiosity,

and to my dear friend Ian Gilbert for being proud to where it lead.

Summary

Neurons are complex cells that require contributions from many fields of scientific expertise in order to advance our knowledge of their function and inner workings. Neuroscientists often simplify the description of these cells into a small set of quantities such as the time-evolving voltage in the cell body and level of neuronal discharge. However minimalistic, such description enables to capture important aspects that are relevant for information exchange between neurons and their dynamical characteristics. Membrane potential dynamics and neuronal discharge (or spikes) are causally related since spikes from connected neurons drive the evolution of membrane potential that leads to the firing of the neuron. The membrane potential encodes information on the state of the neuron but also on the activity level of afferent neuronal populations. Computational models of neuronal activity for neurons and populations of neurons are often based on this causal relationship. Improving our knowledge of the dynamical properties of membrane potential evolution may lead to more accurate models of neural activity and potentially contribute to our understanding of neuronal dynamics and information exchange between neurons. Such is the main objective and motivation of this work.

The characterization of membrane potential fluctuations is the principal subject of this thesis with focus on neuron models with passive membrane, i.e. without spiking mechanism. An important aspect is the "noisy" evolution of membrane potential due to irregular inputs received from numerous other neurons in the network. The key question is therefore expressed in probabilistic terms: *For given statistics of presynaptic spikes, what are the statistics of membrane potential fluctuations?* One popular approach is to model membrane potential fluctuations as noise with suitable characteristics, or at a lower level, to do so with synaptic input. This approach is very effective and is supported by a large body of analytical results that contributes to its overall tractability. However, it will no longer account for spike timing information that may be relevant for the particular neuronal system and function under investigation.

The main contribution from this thesis is a modeling framework that explicitly takes into account the effects of individual presynaptic spikes in the evolution of membrane potential. Applied to simple but popular neuronal models often used in computational studies, this framework yields exact results for the statistical description of membrane potential fluctuations under highly variable synaptic input rate that is thought to reflect behaving conditions. These results may benefit computational models of neuronal activity with improved statistical accuracy. Statistical inference models of biological and dynamical characterization of neurons and connected populations may also benefit from more precise data generation models. These exact descriptions contribute to future work establishing biological and dynamical conditions under which more tractable noise models are sufficient to fully capture neuronal dynamics.

Résumé

Les neurones sont des cellules complexes qui font appel à l'expertise de plusieurs domaines scientifiques pour faire évoluer notre connaissance sur leurs fonctions et mécanismes internes. Malgré cette complexité, la description des neurones peut se réduire à un nombre limité de quantités telles que l'évolution temporelle du voltage à l'intérieur du corps cellulaire et la fréquence de décharge neuronale. Une telle description réussit à capturer des aspects clés de l'échange d'information entre les neurones et de leur évolution dynamique. Le potentiel de membrane et la fréquence de décharge ont un lien de causalité car les potentiels d'action des neurones en amont régissent l'évolution du potentiel de membrane, qui à son tour mène à la décharge neuronale. Le potentiel de membrane encode de l'information sur l'état du neurone mais aussi sur le niveau d'activité des populations afférentes. Les modèles computationnels d'activité neuronale pour des neurones individuels ainsi que leurs populations, sont souvent basés sur cette relation causale. L'avancement de la connaissance des propriétés dynamiques du potentiel de membrane pourrait aboutir à des modèles d'activité neuronale plus précis et contribuer ainsi à notre compréhension sur la dynamique neuronale et d'échange d'information entre neurones. Ceci constitue l'objectif principal et la motivation de ce travail.

La caractérisation des fluctuations du potentiel de membrane est donc le sujet principal de cette thèse et elle s'applique aux modèles de neurones à membrane passive, sans mécanisme de décharge neuronale. L'évolution bruitée du potentiel de membrane est un aspect très important, conséquence des entrées synaptiques irrégulières reçues de nombreux neurones appartenant aux populations afférentes. La question clé s'exprime en termes probabilistes: *Etant donné les statistiques des entrées présynaptiques, quelles sont les statistiques des fluctuations du potentiel de membrane ?* Une approche fréquemment utilisée est celle de modéliser directement les fluctuations du potentiel de membrane avec un processus aléatoire de bruit ou alors de le faire au niveau des entrées synaptiques. Cette approche est très efficace et soutenue par un corps important de résultats analytiques, ce qui contribue à la facilité de leur traitement. Cependant, l'information des temps de décharge neuronale est perdue, alors que celle-ci pourrait se révéler importante pour la compréhension du système et des fonctions neuronales en question.

La contribution principale de cette thèse est de dériver un formalisme analytique qui tient compte explicitement des effets des temps de décharge neuronaux. Ce formalisme a été appliqué à des modèles neuronaux simples, souvent utilisés dans des études computationnelles, sous des entrées synaptiques à taux variable. Nous avons obtenu des résultats analytiques exacts, ainsi que des approximations très efficaces pour ce type de système non stationnaire. Ces résultats pourraient contribuer aux modèles computationnels d'activité neuronale. Les modèles d'inférence statistique pour la caractérisation des neurones en termes biologiques et dynamiques pourraient en bénéficier aussi, permettant l'éventuel développement de modèles statistiques sous-jacents plus précis. Ces résultats analytiques pourront donc contribuer à établir les conditions biologiques et dynamiques sous lesquelles des modèles de bruit de plus simple traitement seraient suffisants pour capturer la dynamique neuronale.

Acknowledgments

I wish to thank my thesis supervisor Alain Destexhe for the opportunity to undertake this PhD and freedom to develop what became its main line of research. His patience and support helped me through the most challenging periods with drive and motivation to cover always a little bit more of ground. I wish to thank Yves Frégnac for his steady support and academic advice, and Kirsty Grant for her guidance on how to successfully steer PhD studies. I also thank Frédéric Chavane and Arvind Kumar for hosting my FACETS-ITN internships and for many refreshing and stimulating discussions.

My scientific development was guided by numerous exchanges with Claude Bedard who kindly directed me to relevant techniques from physics and mathematics. I wish to thank Michelle Rudolph for the precious feedback on the first article, Jan Antolik for heated and interesting discussions on modeling strategies, Mathieu Galtier for his advice on scientific writing, Bartosz Telenczuk, Yann Zerlaut, Lyle Muller and Sarah Goethals for many interesting exchanges on stochastic modeling. I am grateful to the members of UNIC for welcoming me to their ranks and enriching me with stimulating scientific discussions, with special thanks to administrative and I.T. staff for taking excellent care of paperwork and computing needs. I thank my fellow FACETS-ITN students for their friendship and exchanges during the workshops across Europe.

I am indebted to Suresh Nampuri for his help in revising of the first article and troubleshooter of last resort when math would just not add up. My deep gratitude also goes to Ana Paixão for her unrelenting support during this period and for helping revise word by word many of the texts comprising this thesis. Both are true masters of many trades but most particularly, masters of time. I thank Paul Bressloff for the colorful advice on non-Markovian process that changed the course of my PhD.

This work would not have been possible without the unwavering support of my family and close friends throughout the years. I specially thank Mauro and Eduardo Brigham, Gisela Costa, Solaiman Amensour, my parents and grandparents for their presence and support.

I am very thankful for the financial and institutional support given by FACETS-ITN, the Human Brain Project and the European Institute of Theoretical Neuroscience (EITN).

Finally, I would like to thank the members of the jury for kindly reviewing this thesis.

Contents

Part I

Introduction

Chapter 1

General Introduction

This chapter provides a general introduction to the subject and motivation of this thesis, and relevant research context. This is complementary to the various introductions from subsequent chapters.

1.1 Synopsis

The dynamical evolution of neurons is often described in terms of membrane potential fluctuations and neuronal discharge. Such characterization is a vast simplification of the inner workings of this complex cell. Nevertheless, it seems to capture important processes that are relevant for information exchange between neurons. Membrane potential fluctuations are variations in the voltage difference between inside and outside of the cell, and are due to neuronal discharge, or spikes, from other neurons in the network. Outgoing spikes occur under particular conditions of membrane potential evolution that are often modeled by the crossing of a voltage threshold. Spikes have a major role in the exchange of information between neurons whereas membrane potential fluctuations are an important characterization of their dynamical states. The level of activity of afferent neural networks is inherently sampled by the neuron and this information is encoded in membrane potential fluctuations. Computational models of neuronal activity, at the level of neurons and populations of neurons, account for this causal relationship between presynaptic activity, membrane potential fluctuations and neuronal discharge. Improving our knowledge of the dynamical properties of membrane potential fluctuations may lead to more accurate models of neural activity and potentially contribute to our understanding of neuronal dynamics and information exchange between neurons. Such is the main objective and motivation of this work.

The characterization of membrane potential fluctuations is the subject of this thesis and the focus is on neuron models with passive membrane, i.e. without spiking mechanism. The *membrane equation* describes how electrical currents generated from incoming spikes are translated into membrane potential evolution. The membrane equation is often formulated in deterministic terms such that a particular time course of input current results in the same trace of membrane potential. This reflects the experimental fact that subjecting a biological neuron to the same sequence of presynaptic spikes results in very similar membrane potential evolution. However, the timing of incoming spikes and synapses that receive them are considered random from the perspective of the neuron. This results in complex membrane potential evolution that is due to the contribution of numerous irregular, or "noisy", synaptic inputs received from other neurons in the network. Such complex dynamics are best described in probabilistic terms notwithstanding the deterministic response to synaptic input, since deterministic functions of random quantities are in general random quantities as well. The key question of this study is therefore expressed in probabilistic terms: *For given statistics of presynaptic spikes, what are the*

statistics of membrane potential fluctuations?

Computational models of neuronal activity often start with the specification of the membrane equation and noise model for synaptic input. Membrane equation models vary in complexity to reflect the desired level of biological detail. Current and conductance synapses are two important categories of the synapse model and specify how synaptic input translates to membrane potential fluctuations. Current synapses lead to unbounded variation of membrane potential whereas conductance synapses drive the evolution between minimum and maximum values. Conductance-based models have higher biological accuracy and current-based models lead to simpler and often more tractable analytical descriptions. The later may also yield good approximations to membrane dynamics under certain synaptic input regimes.

Several strategies have been applied to model the stochastic nature of membrane potential fluctuations. The membrane potential can be directly modeled as a noise process that reflects basic statistical properties of membrane fluctuations, typically their mean and variance. Another possibility is to model the synaptic input as a noise process with appropriate statistical properties. Noise processes that are typically used in both cases are supported by a large body of analytical results that contributes to their tractability. Among these are white noise, Gaussian noise, Wiener process, Ornstein-Uhlenbeck process, etc. Modeling membrane potential or synaptic input with these noise processes will no longer account for spike timing information since the objective is to capture the statistical effects of synaptic input rather than spike times themselves. This is a trade-off in accuracy versus tractability, which is made under the assumption that the statistical properties of these noise processes provides the most relevant contribution to membrane potential dynamics. Depending on the particular neuronal system and neuronal function under investigation, this hypothesis has been shown to be very effective and in some cases quite sufficient. Under some other conditions however, these approaches are not entirely successful since higher order statistics of synaptic input may play an important role in membrane potential dynamics.

The proposed approach is to explicitly consider the effect of individual presynaptic spikes in the evolution of membrane potential. This should provide access to exact statistics of membrane potential fluctuations by integration of cause and effect mechanisms. This is the case for the simple but popular class of neuronal models adopted in this study that is often used in computational studies. These exact results apply to current and conductance synapse models under highly variable synaptic input regimes that are thought to reflect behaving conditions. This improvement in statistical accuracy opens the way to refine existing models of *transfer function* that links membrane potential evolution to neuronal discharge. This transfer function is a core element of computational models of neuronal activity since it compresses internal dynamics of neurons into an input to output firing relationship. Statistical inference models of biological and dynamical characterization of neurons and their afferent neural networks also benefit from these results since data generation models can be made more precise. These exact descriptions may enable to develop new approximations and estimate the accuracy of existing ones. They contribute to future work regarding biological and dynamical conditions under which higher order statistics are essential to fully capture neuronal dynamics. This would contribute to establish the validity domain of more tractable noise models.

Further details on the modeling assumptions and possible applications of this work are presented next.

1.2 Framework Description

The main features and assumptions of the neuron model and key principles leading to the analytical results developed in this thesis are presented here.

The neuron model is a point neuron without spatial extent that is characterized by a single time-evolving value of membrane potential. As illustrated in Fig. 1.1, there is some simplification when going from biological neuron, to morphological model and finally to point neuron. The underlying assumption is that the membrane equation will account for the most important biological processes that are relevant to the particular research question. The focus is on the biological properties related to synapse type (current or conductance), the characteristics of synaptic input (noise model) and the statistical properties of nonstationary membrane dynamics. This leads to a passive and linear neuronal membrane without spiking mechanism that is represented schematically in Fig. 1.1 by a point neuron with input edges only.
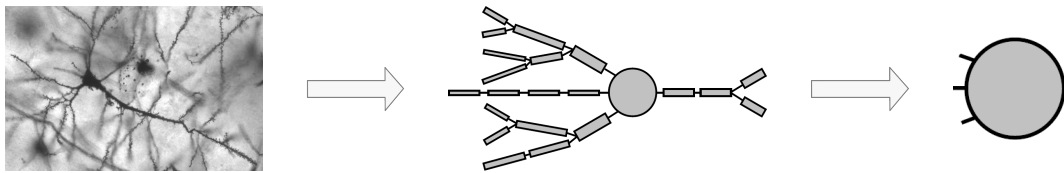

Figure 1.1 – *Two common levels of simplification when modeling biological neurons (left). Some models take into consideration the spatial extent of the neuron by characterizing membrane potential values at different physical locations (middle). The adopted neuron model is a point neuron without spatial extent that is described by a single time-evolving value of membrane potential (right).*

The two final assumptions regard the statistics of presynaptic spikes and how synaptic input is generated from them. Presynaptic spikes are assumed to be generated by *Poisson point processes* (PPP) with intensity that can vary in time and synaptic input is shot noise generated from these spikes. The shot noise assumption is motivated by experimental studies showing that presynaptic spikes elicit stereotypical responses under low activity regimes [Hodgkin et al., 1952, Hodgkin and Huxley, 1952, Fatt and Katz, 1952, Curtis and Eccles, 1960]. This neglects changes in synaptic response due to synaptic saturation and short term plasticity that are certainly relevant in many synaptic input regimes of interest. Neglecting them however, provides a reasonable first approximation. The Poisson assumption may not always hold, even for cells undergoing spontaneous activity in the absence of external experimental stimuli [Rodieck et al., 1962]. However, this hypothesis has significant tractability advantages and is often adopted in computational studies. As shown in the article of Chapter 5 on synaptic correlations, PPP can be used to build more complex synaptic input models. The relevant background information and techniques are developed in Chapter 2.

The scheme in Fig. 1.2 illustrates these elements and assumptions: (1) Presynaptic spike times are generated by a PPP (2) to produce synaptic input in the form of shot noise (3) that drives membrane potential evolution.
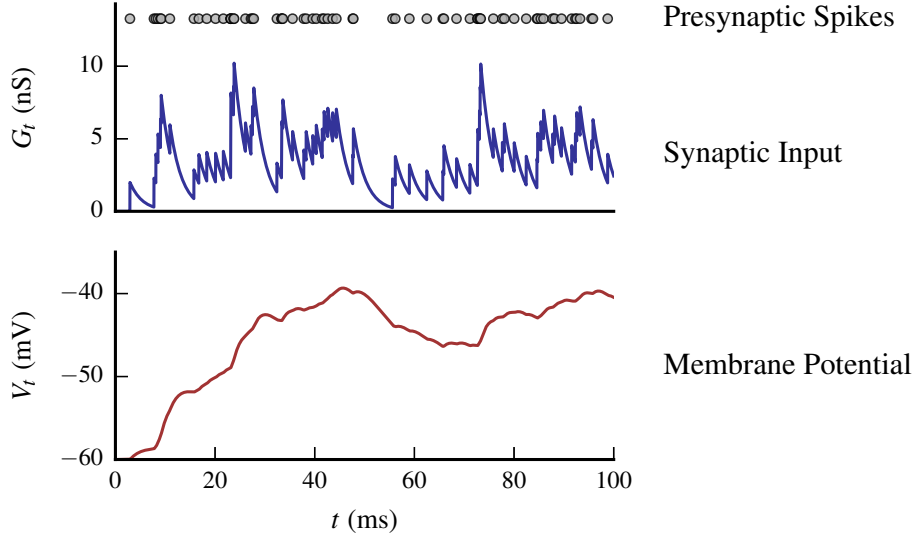
Figure 1.2 – *General scheme of the model: Presynaptic spikes produce synaptic input (top) that drives membrane potential fluctuations (bottom). Spike arrival times are generated by a Poisson point process with intensity that can vary in time. The synaptic input is shot noise generated by superposition of individual responses to presynaptic spikes.*

As can be appreciated from this figure, the neuron model is a deterministic system with random inputs, since synaptic drive and membrane potential fluctuations are deterministic functions of random spike arrival times.

The quantities of interest are the value of membrane potential at different times, noted $V_t \equiv V(t)$ for the value at time t and $V_1, \ldots, V_K$ for the values of V_t at times $t_1 \geq t_2 \geq \ldots t_K$. The statistical properties of V_t characterize aspects such as mean value of membrane potential $\langle V_t \rangle$, variance $\left\langle (V_t - \langle V_t \rangle)^2 \right\rangle \equiv \langle\langle V_t^2 \rangle\rangle$ and probability density $p(V_t = v_t)$. The probabilistic nature of membrane potential is encoded in $p(v_t)$. For example, the mean value of membrane potential $\langle V_t \rangle$ is obtained from $p(v_t)$ as follows:

$$\langle V_t \rangle = \int v_t \, p(v_t) \, dv_t$$

where the integral runs over all possible values of V_t.

The approach proposed in this thesis is to model membrane potential fluctuations as a transformation of presynaptic spikes generated by PPP. The first step is to determine the effect of an arbitrary set of presynaptic spikes on membrane potential evolution. This defines the PPP transformation for the neuronal membrane model of interest. In the second step, the statistics of the PPP transformation are derived under the PPP. This requires access to the density of presynaptic spike times $\xi \equiv \{x_1, x_2, \ldots x_n\}$, represented informally as $p(\xi)$, and to the solution of the membrane equation $V(t, \xi)$ for arbitrary sets of presynaptic spike times ξ. This is illustrated in Fig. 1.3 where the effect of individual presynaptic spikes can be appreciated in the membrane potential trace.
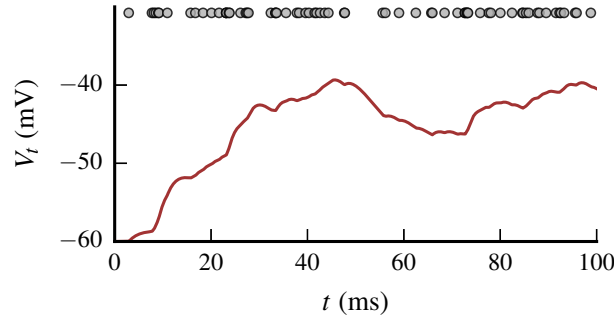
Figure 1.3 – *Modeling the transformation of presynaptic spike to membrane potential fluctuations. Each presynaptic spike contributes to the evolution of membrane potential V_t.*

The key steps in deriving exact membrane potential statistics for a particular neural membrane model are the following:

1. Determine the solution of the membrane equation $V(t, \xi)$ for arbitrary sets of presynaptic spike times ξ generated by PPP

2. The transformation $V(t, \xi)$ is analyzed and decomposed into one or several generic PPP transformations

3. The statistics of V_t are accessible for those cases where the underlying PPP transformations are exactly or approximately tractable

This approach enables to obtain the statistical properties of V_t from the solution of the membrane equation $V(t, \xi)$ and the density of presynaptic arrival times $p(\xi)$. Returning to the previous example of evaluating $\langle V_t \rangle$, this is equivalent to the following operation:

$$\langle V_t \rangle = \int v_t \, p(v_t) \, dv_t = \int V(t, \xi) \, p(\xi) \, d\xi$$

1.3 Applications

These analytical results may find applications in the context of statistical analysis of experimental data and certain aspects of computational neuroscience models.

Intracellular recordings provide direct access to statistical properties of membrane potential fluctuations. The recordings at the soma reflect important biological characteristics of the neuron, such as the number of excitatory and inhibitory synapses $N_{\{e,i\}}$, the synaptic time constant $\tau_{\{e,i\}}$ and synaptic strength $h_{\{e,i\}}$ of synaptic input. The dynamical state of afferent populations is likewise reflected in the statistics of fluctuations. This is illustrated in Fig. 1.4 where a schematic intracellular recording is made at the soma of a neuron.
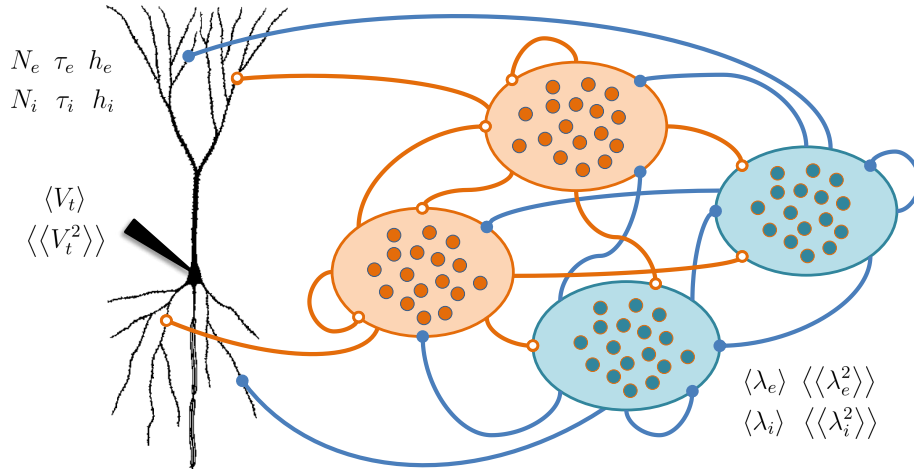
Figure 1.4 – *Membrane potential fluctuations carry information of the biological properties of the neuron and the activity of afferent neural networks. The black arrow represents an intracellular electrode recording the membrane potential V_t from which the mean $\langle V_t \rangle$ and variance $\langle\langle V_t^2 \rangle\rangle$ can be calculated. The activity of afferent neural networks is often characterized in terms of the mean $\langle \lambda_{e,i} \rangle$ and variance $\langle\langle \lambda_{e,i}^2 \rangle\rangle$ of neuronal discharge. Important biological properties include the number of excitatory and inhibitory synapses $N_{e,i}$, the synaptic time constant $\tau_{e,i}$ and synaptic strength $h_{e,i}$.*

The raw data from intracellular recording is often processed to extract its statistical characteristics. This provides a compact representation of the data that in order to yield insight into biological properties and afferent population dynamics requires the interpretation of a statistical inference model. The typical scheme is illustrated in Fig. 1.5 and involves two levels of modeling: how the data was generated (statistical model) and how to estimate the parameters from the data (statistical inference model).
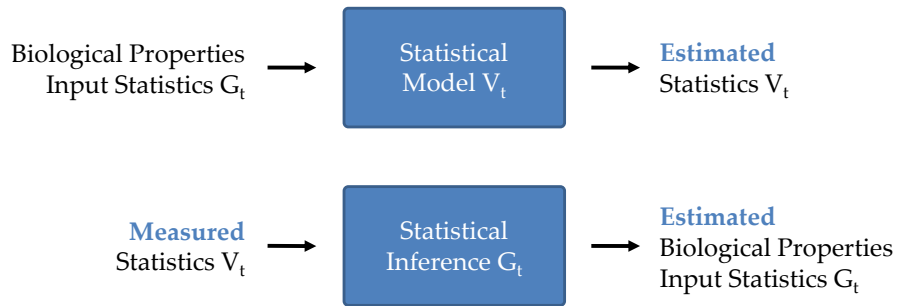
Figure 1.5 – *Common scheme for inference of biological and dynamical properties of neurons from experimental measurements of membrane potential.*

A statistical model of V_t has a set of parameters corresponding to biological and synaptic input characteristics that when specified result in the prediction of V_t statistics. This is the level of statistical modeling developed in this thesis. A statistical inference model corresponds to the inverse problem under the assumption that membrane potential dynamics are well represented by the statistical model, and the observed traces of V_t are realizations generated under particular sets of parameters. The statistical inference step evaluates the likelihood of particular parameters sets given the observed data. An example is provided by the *VmD* method [Rudolph et al., 2005, 2007] that estimates mean and variance of excitatory and inhibitory synaptic in-

put from recordings of membrane potential at different levels of injected current. This class of statistical inference models relate the statistics of V_t measurements to biological properties and synaptic input characteristics and the results developed in this thesis may provide basis for improvement. Firstly, their exact nature provides more accurate statistical models of V_t for non-stationary synaptic input. Secondly, analytical access to higher order statistics of V_t may enable to extract additional information from raw data. Thirdly, statistical inference models critically depend on the ability to assign probabilities to measured data for given parameters. An important result from this work are the accurate approximations for the nonstationary probability distribution of V_t.

Another important aspect is the contribution of high order statistics in the description of membrane potential dynamics. Synaptic input and membrane potential fluctuations are often modeled by more tractable noise processes with appropriate statistical properties [Tuckwell, 1988a, Burkitt, 2006a,b, Gerstner et al., 2014]. The spike timing information is no longer present in such descriptions since the objective is to capture basic statistical properties of synaptic input, such as mean and variance. This is illustrated in Fig. 1.6 where synaptic input generated from shot noise and Ornstein-Uhlenbeck (OU) processes with equal mean and variance are shown for a simple membrane model with single conductance synapse type (excitatory). The OU process does not represent individual postsynaptic responses to spike arrivals, and may display negative conductance that is without biophysical meaning. In terms of higher order statistics, the OU process has cumulants of order higher than two equal to zero, whereas shot noise has non-zero cumulants of all orders. As shown in this figure, these differences affect the standard deviation of V_t, in addition to its higher order statistics (not shown but similar to Fig. 1.9). The central moments expansion (CME), that is also developed in this work, can be used to show that the mean of V_t is mostly affected by the mean and variance of input conductance, whereas its standard deviation has important contributions from third and fourth order cumulants. In particular, the third order cumulant of input conductance contributes to decrease the standard deviation of V_t seen in this figure.
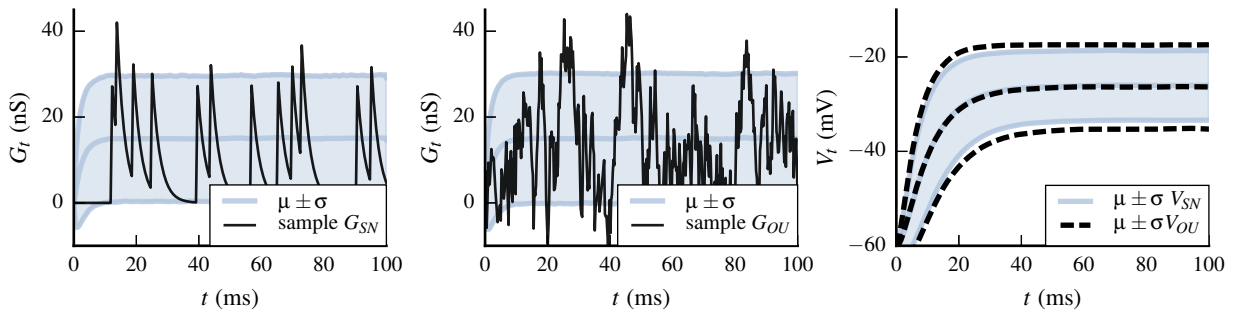
Figure 1.6 – *Simple membrane model with a single conductance synapse type (excitatory). Comparison of synaptic input generated from shot noise process G_{SN} (left), Ornstein-Uhlenbeck process G_{OU} (center) and corresponding mean and standard deviation of V_t (right). The synaptic input has the same mean and standard deviation but differs in higher order statistics. The synaptic input realizations are not visually similar and the membrane potential generated from G_{SN} has lower standard deviation.*

The OU process and similar noise models are successful in other synaptic input regimes, such as the diffusion limit where fluctuations of the input are small when compared to the mean. This is illustrated in Fig. 1.7 where realizations of synaptic input from both processes are very similar and result in equally similar mean and standard deviation of V_t. The contribution of higher order statistics of shot noise to the standard deviation of V_t is quite small in this regime.
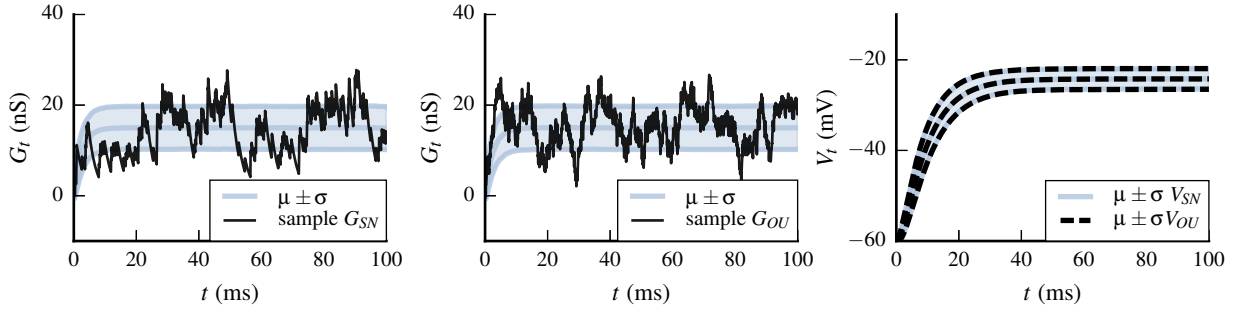
Figure 1.7 – *Same comparison as Fig. 1.6 but in the diffusion limit regime where fluctuations of the input are small when compared to the mean. The realizations of synaptic input are visually very similar and result in equally similar mean and standard deviation of V_t.*

The effects of high order statistics are also present in more complex membrane models, such as the example shown below with two conductance synapse types (excitatory and inhibitory) and nonstationary rates. The mean and variance of V_t and synaptic input are shown in Fig. 1.8. The excitatory input $G_e(t)$ of the neuron is stationary with constant mean and standard deviation (in gray). The inhibitory input $G_i(t)$ is highly variable as can be seen by time-varying mean and standard deviation. These nonstationary statistics reflect alternating periods of spiking activity that results in time-varying evolution of membrane potential statistics. This can be appreciated by the evolution of mean and standard deviation in the lower plot. Two time points t_a and t_b are marked in the abscissa of the lower plot and correspond to local minimum and maximum in the mean of V_t.
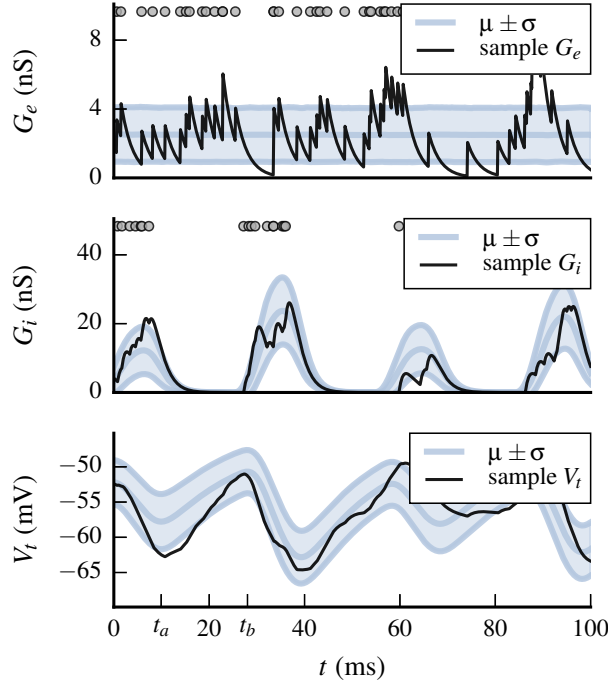
Figure 1.8 – *Neuron model with excitatory and inhibitory conductance synapses under nonstationary inhibitory input. Excitatory conductances G_e (top) and inhibitory conductances G_i (middle) drive the membrane potential evolution V_t (bottom). Single realizations of G_e, G_i and V_t are shown in black, mean and standard deviation ($\mu \pm \sigma$) are shown in gray.*

In order to illustrate the importance of higher order statistics, consider the values of V_t at times

t_a and t_b. The distribution of membrane potential at those times can be estimated from the histograms in Fig. 1.9. The histograms display the relative count of values that fall into a discrete number of bins covering the range of observed values. Near t_a, the local minimum, the distribution of membrane potential $p(V_t)$ is not well captured by a gaussian density as shown in the left plot of Fig. 1.9, whereas at time t_b, the local maximum, the gaussian fit is much improved. In the right plot of this figure, higher order statistics (third and fourth order) are used to approximate the distribution of V_t with more accurate results. Statistical models of membrane potential fluctuations with second order statistics would not be able to fully capture the dynamics of this particular example.
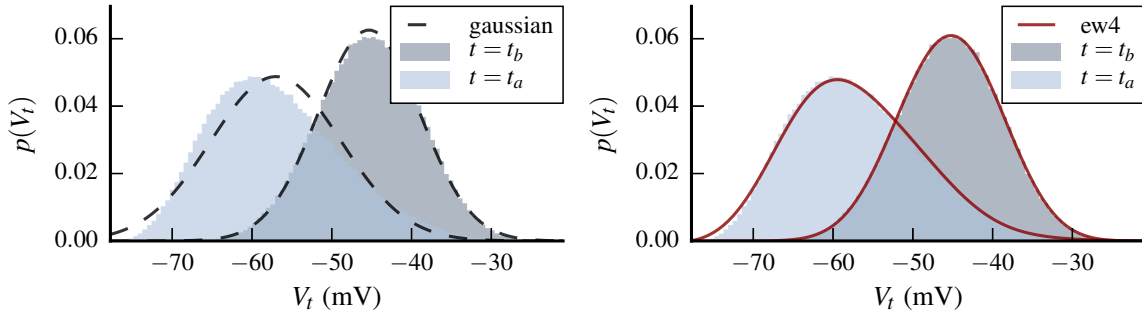
Figure 1.9 – *Histograms of membrane potential distribution $p(V_t)$ measured at two different times t_a and t_b corresponding to local minimum and local maximum, respectively. Gaussian approximation (left, black dash) is calculated from empirical mean and variance and manages to capture well the distribution at time t_b, but is less successful at time t_a. An approximation based on higher order statistics (fourth order) is able to better capture the time evolution of $p(V_t)$.*
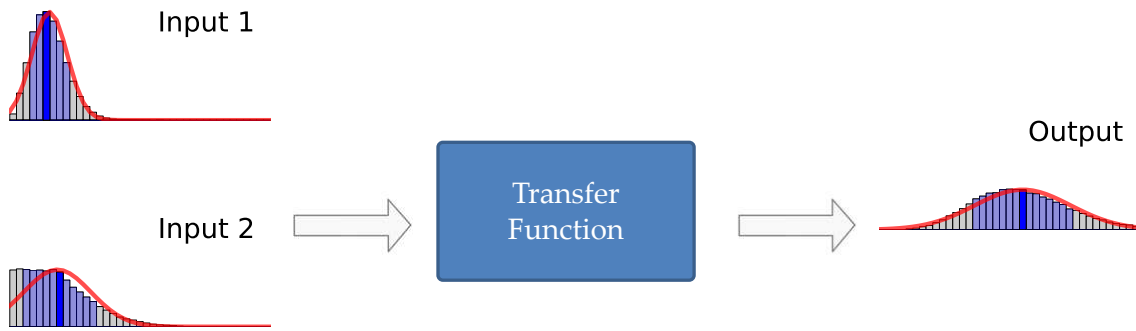
Figure 1.10 – *Overview scheme of transfer function: statistics of presynaptic activity are the input and an estimation of neuronal discharge under those input conditions is the output.*

Membrane potential statistics are important in the development of the *transfer function* for computational models of neural activity. This function encodes the relationship between neuronal discharge rate of the neuron at time t' and the presynaptic input rate at an earlier time $t \leq t'$. This is illustrated in Fig. 1.10 where histograms of presynaptic activity and neuronal discharge are represented for the same neuron over many realizations. The transfer function for a given neuron model is typically derived as follows: (1) the statistical relationship between synaptic input and V_t is first derived and (2) the probability of neuronal discharge for a given level of V_t is evaluated. A high degree of information compression is captured by the transfer function: encoding and encapsulating all aspects regarding biological properties and membrane dynamics that matter in regards to spiking activity. The first step may benefit from the exact statistics

for synaptic input with nonstationary rate that are derived in this work. The second step often involves evaluating the membrane potential distribution $p(V_t)$ and as illustrated in Fig. 1.9, may be improved from the inclusion of higher order statistics. The transfer function can be cast as a *first passage problem* [Amit and Brunel, 1997, Brunel, 2000] that is related to the *density of crossings* [Rice, 1944, Badel, 2011]. The later requires statistical description of both membrane potential level and its rate of change, which are readily accessible for conductance synapses in the present formalism.

1.4   State of the Art and Main Contributions

The theoretical basis from this work can be found in two important developments: the basic membrane model for the *integrate-and-fire neuron* introduced by Lapicque [Lapicque, 1907, Abbott, 1999] and the discovery and modeling of shot noise by Campbell and Schottky [Campbell, 1909, Schottky, 1918].

Lapique's membrane model describes deterministic current input and was later extended to include stochastic currents, conductances and other biophysical aspects [Stein, 1965, Verveen and DeFelice, 1974]. Further developments include non-linear membrane potential dynamics, synaptic plasticity and adaptation but are not addressed here [Tuckwell, 1988b,a, Dayan and Abbott, 2001, Gerstner et al., 2014].

Shot noise processes are simple yet powerful models of stochastic input that correspond to the superposition of impulse responses arriving at random times according to a Poisson law. The early works of Campbell and Schottky described current fluctuations in vacuum tubes but many applications were later found in biology [Stevens, 1972, Siebenga et al., 1973], acoustics [Kuno and Ikegaya, 1973], optics [Rousseau, 1971, Picinbono et al., 1970], wireless communications [Venkataraman et al., 2006] and many other fields [Snyder and Miller, 1991, Parzen, 1999]. Whereas Campbell derived the expressions for the stationary mean and variance of shot noise, in-depth analysis of their probabilistic structure was performed by S.O. Rice (in addition to many important properties of Gaussian processes) [Rice, 1944, 1945]. A modern review of more recent developments are presented in Refs. [Rice, 1977, Snyder and Miller, 1991, Parzen, 1999]. Shot noise has a simple mathematical form but can display nonstationary and non-Markovian characteristics: a time-varying rate of random arrival times yields nonstationary shot noise, and the process is in general non-Markovian for a single state variable [Masoliver, 1987, Lund et al., 1999], with a notable exception being the exponential kernel. The shot noise assumption is motivated by experimental studies showing that presynaptic spikes elicit stereotypical responses under low activity regimes [Hodgkin et al., 1952, Hodgkin and Huxley, 1952, Fatt and Katz, 1952, Curtis and Eccles, 1960]. This neglects changes in synaptic response due to synaptic saturation and short term plasticity that are certainly relevant but provides a reasonable first approximation.

Poisson point processes are a natural model of random input arrival times that are distributed according to a Poisson law that may vary in time. Application-oriented treatments of PPP theory and PPP transformations can be found in Refs. [Moller and Waagepetersen, 2003, Streit, 2010]. Shot noise is an example of *Filtered Poisson Process* [Snyder and Miller, 1991, Parzen, 1999] that is generated by linear transformations of PPP. The Poisson assumption may not hold in all cases [Rodieck et al., 1962] but is very tractable and popular in computational studies.

Membrane potential fluctuations are often studied as the starting point of neuronal population activity models (but see Refs. [Stein, 1967, Bevan et al., 1979, Verveen and DeFelice, 1974]) where in general conductance-based shot noise input is analyzed with constant rate and par-

ticular shot noise kernels (for example, exponential kernel [Richardson and Gerstner, 2005, Rudolph and Destexhe, 2005] and alpha kernel [Kuhn et al., 2004]). The exact solution for conductance shot noise has been first obtained by Wolff and Lindner for exponential kernel with constant rate [Wolff and Lindner, 2008, 2010]. Other studies have analyzed the case of nonstationary shot noise input for exponential kernel conductance and arbitrary kernel for currents [Cai et al., 2006, Amemori and Ishii, 2001, Burkitt, 2006b].

The main contributions of this thesis are the derivation of exact membrane potential statistics in the general case of nonstationary shot noise with arbitrary kernel and their approximate formulation in terms of the central moments expansion (CME). These results were applied to several questions in computational neuroscience: the statistics of neuron models with multiple independent synapse types, the statistical effects of afferent network inhomogeneities per synapse type, the population-level statistics for inhomogeneities in neuronal input characteristics, the effects of correlations between synapse types, including strictly causal correlations and an estimate of timescale for membrane potential memory effects.

1.5   Thesis Outline

The developments of this thesis are presented in two parts: *Analytical Tools* and *Research Articles*.

In the first part, the analytical tools and techniques leading to the derivation of exact membrane potential statistics are presented in Chapter 2. This chapter is more technical in content and presentation and contains several results not included in the presented research articles but may be useful for future work. The basic properties of PPP and their transformations are presented in Sec. 2.1. The membrane equation is analyzed in terms of those transformations and their exact statistics are derived under the PPP. The general solution is presented in Sec. 2.2 and is applied to models of current and conductance synapses and a more general model with both synapse types. The asymptotic and stationary limits of the model are analyzed in Sec. 2.3 and the popular model of random Dirac Delta sums is analyzed under PPP transformations in Sec. 2.4. A more general type of PPP is presented in Sec. 2.5 and CME is introduced in Sec. 2.6. Several results and derivations are included in the Appendix A.

In the second part, the research articles developed in this thesis are presented together with a compact introduction to each article. The article *Nonstationary filtered shot noise processes and applications to neuronal membranes* is presented in Chapter 3 and analyzes the simple case of a single conductance synapse. The effects of variation in synaptic properties are investigated in Chapter 4 with the article *The impact of synaptic conductance inhomogeneities on membrane potential statistics*. The effects of causal correlations in membrane potential statistics is explored in Chapter 5 with the article *How causal correlations between synaptic inputs affect membrane potential fluctuations*. The memory effects of membrane potential are analyzed and estimated in Chapter 6 in the article *Estimating stochastic process memory in neuronal membranes*.

A general discussion of this work and future research directions are presented in Chapter 7.

Chapter 2

Analytical Tools

The key concepts and techniques that underlie the analytical results developed in this thesis are presented here. These techniques are used to derive the statistical properties of membrane potential fluctuations from the statistics of synaptic input, and are developed in the formalism of Poisson point process (PPP) transformations that is briefly reviewed in Sec. 2.1. This presentation is slower-paced and more general than in the research articles included in Chapters 3 to 6. The exact statistics for passive membrane equations with current and conductance synapses under nonstationary shot noise input are derived in Sec. 2.2. Their asymptotic and stationary limits are investigated in Sec. 2.3. The popular synaptic input model of Dirac delta functions is analyzed under this formalism in Sec. 2.4. A more general type of PPP is presented in Sec. 2.5 and the central moments expansion (CME) is introduced in Sec. 2.6. Several results and derivations are included in the Appendix A.

2.1 Poisson Point Processes

The evolution of membrane potential for a passive neuronal membrane model can be expressed as a transformation of presynaptic spike times. Since the statistics of spike times are assumed to follow a Poisson law, the formalism of PPP provides a natural model for investigating these transformations. Basic definitions and statistical properties of stochastic processes constructed from transformations of PPP are first reviewed in Secs. 2.1.1 and 2.1.2. The membrane equations for current and conductance synapses are first-order linear ordinary differential equations (ODEs) that when receiving shot noise input correspond to particular PPP transformations as shown in Sec. 2.1.3. Their statistical properties are investigated in Sec. 2.1.4.

2.1.1 Poisson Point Processes in the Real Line

Poisson point processes model the distribution of points in arbitrary dimensions. The coordinates of stars in a small section of the sky or the location of trees in a forest provide examples in two or three spatial dimensions. In one dimension they can provide a model for the generation of presynaptic spike times.

A PPP $\Xi\left(\mathcal{S}, \lambda\right)$ that generates points or event times in an interval $\mathcal{S} \subseteq \mathbb{R}$ of the real line is characterized by a non-negative *rate function* $\lambda(x) \geq 0$ such that the quantity $m(\mathcal{S}) \equiv \int_{\mathcal{S}} \lambda(x)\, dx$ is finite for any bounded interval $\mathcal{S}$. A PPP is said to be homogeneous if the rate function $\lambda(t) = \lambda$ is constant and inhomogeneous otherwise.

A realization of the PPP is a set $\xi \equiv \{n \geq 0, \{x_1, \ldots, x_n\} \in \mathcal{S}\}$ that specifies the number of points n and their locations $\{x_1, \ldots, x_n\} \in \mathcal{S}$. These points are associated with presynaptic

spike times of synaptic input. In order to simplify notations n is made implicit and ξ represents the event times in order to write more compact expressions such as $\sum_{x_j \in \xi} g(t, x_j)$.

A realization ξ is obtained through a two-step sampling procedure: an integer $n \geq 0$ is drawn from a Poisson distribution with mean $m(\mathcal{S})$; and for $n > 0$, each x_j is independent and identically distributed (i.i.d.) with probability density $p(x_j) = \lambda(x_j)/m(\mathcal{S})$. The condition of finite $m(\mathcal{S})$ over bounded $\mathcal{S}$ ensures a finite number of event times for realizations ξ over bounded $\mathcal{S}$. A well-known and simple implementation of this procedure is included in the Appendix A.1. Examples of PPP realizations for both homogeneous and inhomogeneous PPP are shown in Fig. 2.1.
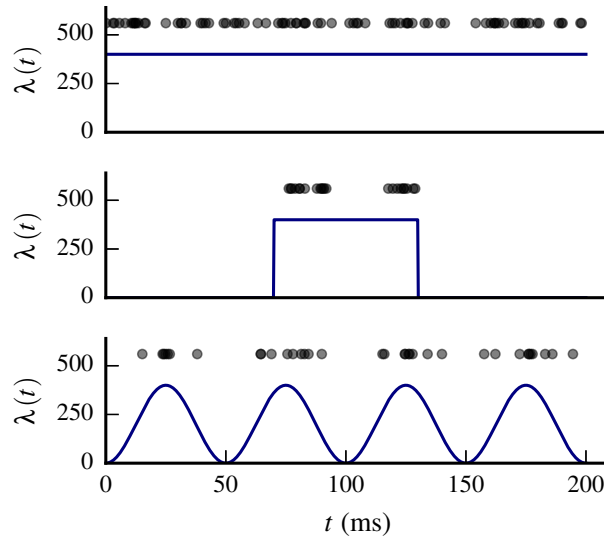
Figure 2.1 – *Examples of rate function $\lambda(t)$ for homogeneous PPP (top) and inhomogeneous PPP (middle and bottom). The event times $x_j \in \xi$ of realization ξ are represented by gray dots above the rate function.*

The statistics of event arrivals and the estimation of rate function from a set of realizations ξ have important applications in the analysis of spiking data, for example. Here the main focus is on statistical properties of PPP transformations that are presented next.

2.1.2 PPP Transformations

Let $F(t, \xi)$ be a transformation of Ξ that evaluates to a real number for any realization ξ and real parameter $t \in \mathcal{S}$. The transformation $F(t, \xi)$ is assumed to be invariant under permutation of $x_j \in \xi$ when written as a regular function $F(t, x_1, \ldots, x_n)$ such that $F(t, x_1, \ldots, x_n) = F(t, \{x_1, \ldots, x_n\})$. The expectation of $F(t, \xi)$ under Ξ is evaluated according to the two-step sampling procedure described earlier.

$$
\begin{aligned}
\langle F(t, \xi) \rangle &= \int F(t, \xi) \, p(\xi) \, d\xi \\
&= \sum_{n=0}^{+\infty} p(n) \int_{\mathcal{S}} \cdots \int_{\mathcal{S}} F(t, x_1, \ldots, x_n) \, p(x_1, \ldots, x_n | n) \, dx_1 \ldots dx_n \\
&= \sum_{n=0}^{+\infty} p(n) \int_{\mathcal{S}} \cdots \int_{\mathcal{S}} F(t, x_1, \ldots, x_n) \prod_{j=1}^{n} p(x_j) \, dx_j
\end{aligned}
$$

with,

$$p(n) = e^{-m(\mathcal{S})} \frac{(m(\mathcal{S}))^n}{n!} \qquad\qquad p(x_j) = \frac{\lambda(x_j)}{m(\mathcal{S})}$$

This results in the ensemble average over the number of events n and their arrival times $\{x_1, \ldots, x_n\}$:

$$\langle F(t,\xi) \rangle = \sum_{n=0}^{\infty} \frac{1}{n!} e^{-m(\mathcal{S})} \int_{\mathcal{S}} \cdots \int_{\mathcal{S}} F(t, x_1, \ldots, x_n) \prod_{j=1}^{n} \lambda(x_j)\, dx_j \qquad (2.1)$$

where the expectation $\langle F(t,\xi) \rangle$ only exists if right side exists as well.

The quantities evaluated by Eq. (2.1) are ensemble averages that correspond to repetition of transformation $\langle F(t,\xi) \rangle$ over a large number of realizations ξ and averaging over the same value of parameter t. This is illustrated in Fig. 2.2 where realizations from a particular transformation $F(t,\xi)$ are shown and the value of $\langle F(t,\xi) \rangle$ is evaluated over a range of 100 ms. The transformation $F(t,\xi)$ may be a continuous function of parameter t even though ξ is a discrete set of points.
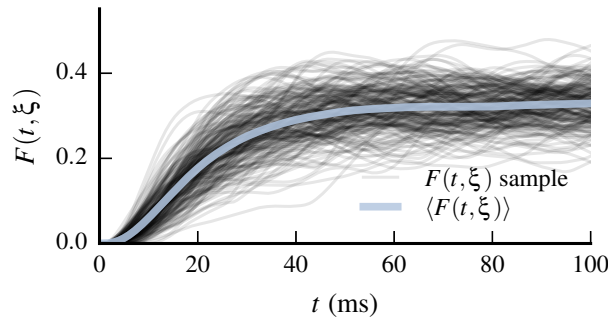
Figure 2.2 – *Example of a PPP transformation $F(t,\xi)$ that is a continuous function of parameter t. One hundred realizations of $F(t,\xi)$ are superposed and the value of the mean $\langle F(t,\xi) \rangle$ is evaluated from 0 to 100 ms.*

The key observation is that a single realization ξ fully determines the transformation $F(t,\xi)$. The expectation of $F(t,\xi)$ under Ξ therefore yields the statistics of the *slave stochastic process* $F_t \equiv F(t,\xi)$. Higher order moments or cumulants of F_t are obtained by forming the relevant products of $F(t,\xi)$ before taking the expectation. For example, the variance $\langle\langle F_t^2 \rangle\rangle$ is obtained by evaluating the expectations $\langle F(t,\xi)^2 \rangle$-$\langle F(t,\xi) \rangle^2$. The same follows for higher order statistics involving the values $F_1, \ldots, F_K$ at times $t_1 \geq t_2 \geq \ldots t_K$, where we write $\langle F_1 \cdots F_K \rangle$ for joint moments and $\langle\langle F_1 \cdots F_K \rangle\rangle$ for joint cumulants. For example, the moment $\langle F_1 F_2^2 \rangle$ is evaluated with the expectation $\langle F(t_1,\xi)\, F(t_2,\xi)^2 \rangle$. An example of PPP transformation is shown in Fig. 2.3 where the entire time course of F_t is determined by ξ.
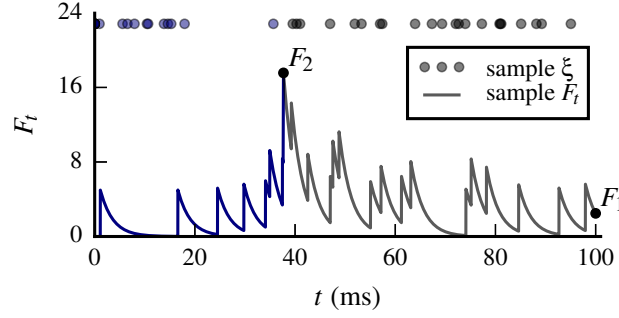
Figure 2.3 – *Shot noise is an example of PPP transformation. The realization ξ fully determines the slave stochastic process $F_t \equiv F(t, \xi)$. Shot noise is a causal transformation where the value of $F(t_2, \xi) \equiv F_2$ is determined by event arrivals $x_j \in \xi$ up to t_2 (in blue) and is not affected by events later than t_2 (in gray). The gray dots represent the location of input arrival times $x_j \in \xi$.*

Modeling the time evolution of systems with PPP transformations requires the notion of causality. We therefore focus on transformations that are causal in the parameter t, such that arrivals $x_j \in \xi$ later than t cannot affect the value of $F(t, \xi)$. A shot noise process is an example of causal transformation since it generates a superposition of unitary impulse responses that only affect the process at times later than the response arrival times.

$$F(t, \xi) = \sum_{x_j \in \xi} g(t - x_j)\, H(t - x_j) = \sum_{x_j \in \xi} g(t, x_j) \tag{2.2}$$

where ξ is the set of shot noise arrival times, $g(t - x_j)\, H(t - x_j)$ is the impulse response function at time t for arrival time $x_j \in \xi$ and $H(u)$ is the Heaviside function. The function $g(t - x_j)$ is also known as *shot noise kernel*.

A realization of shot noise is shown in Fig. 2.3 and illustrates the characteristic superposition of unitary impulse responses. The shot response function or shot noise kernel $g(u)$ is assumed to decay sufficiently fast for all joint cumulants to exist. Some popular choices of shot noise kernels [Gilbert and Pollak, 1960, Verveen and DeFelice, 1974] are illustrated in Fig. 2.4.
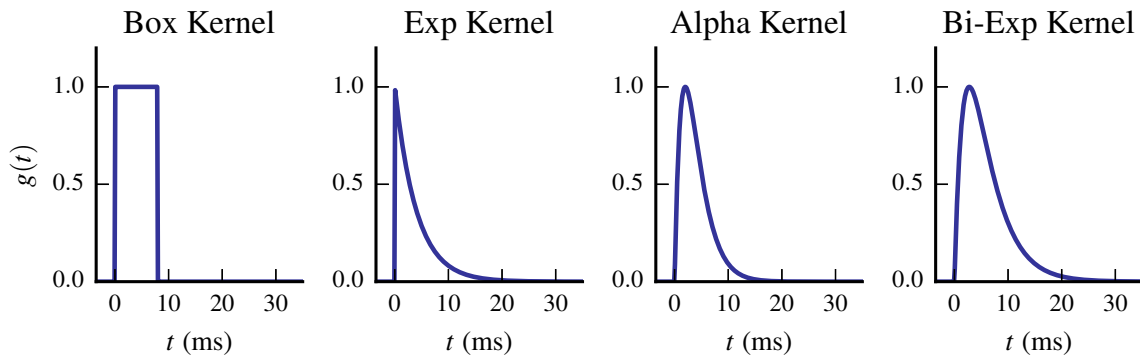
Figure 2.4 – *Popular shot noise kernels $g(u)$ in the literature: box, exponential, alpha, and bi-exponential.*

The analytical expressions for the shot noise kernels from Fig. 2.4 are presented below. Their scaling is such as to yield the same stationary mean $\langle F_t \rangle$. In the Appendix A.7 are presented expressions for stationary and nonstationary statistics up to second order cumulants under constant rate. The nonstationary versions include the transient effects in the build-up to the

stationary regime.

$$g(t,x)_{\text{box}} = h\, H(\tau_s - (t-x))\, H(t-x)$$

$$g(t,x)_{\text{exp}} = h\, e^{-\frac{t-x}{\tau_s}}\, H(t-x)$$

$$g(t,x)_{\text{alpha}} = h\, \frac{t-x}{\tau_s}\, e^{-\frac{t-x}{\tau_s}}\, H(t-x)$$

$$g(t,x)_{\text{bi-exp}} = h\, \frac{\tau_s}{\tau_s - \tau_r} \left(e^{-\frac{t-x}{\tau_s}} - e^{-\frac{t-x}{\tau_r}} \right) H(t-x)$$

2.1.3 Membrane Equation as PPP transformation

The membrane equation is formulated as a linear first-order ODE. The membrane equation for current synapses of a single synapse type is given by:

$$\tau_m \frac{d}{dt} V(t) = E_l - V(t) + R_m\, I(t) \tag{2.3}$$

where τ_m is the membrane time constant, E_l is the resting potential, R_m is the membrane resistance. The membrane potential $V(t)$ is a filtered version of synaptic input $I(t)$ since the ODE changes the spectral characteristics of $I(t)$. It is an additive noise process since noise in the input is added to $V(t)$.

The membrane equation for conductance synapses of a single synapse type are given by:

$$\tau_m \frac{d}{dt} V(t) = E_l - V(t) + (E_e - V(t)) \frac{1}{g_l} G(t) \tag{2.4}$$

where E_e is the excitatory reversal potential and g_l is the leak conductance. This is a multiplicative noise process since noise in the input multiplies or modulates $V(t)$.

The membrane equation for both types of synapse are particular cases of the general form of linear first-order ODE shown below with its solution:

$$\tau \frac{d}{dt} Y(t) = -Q(t)\, Y(t) + J(t) \tag{2.5}$$

$$Y(t) = \frac{1}{\tau} \int J(z)\, e^{-\frac{1}{\tau} \int_z^t Q(u)\, du}\, dz \tag{2.6}$$

where τ is a time constant and $Q(t)$ and $J(t)$ are the inputs to the system.

The filtering of shot noise input by Eq. (2.5) corresponds to four scenarios depending on whether the inputs are shot noise or deterministic functions:

1. $J(t,\xi)$ is shot noise and $Q(t)$ is a function of time

2. $Q(t,\xi)$ is shot noise and $J(t)$ is a function of time

3. Both inputs are the same shot noise process ($J(t,\xi) = Q(t,\xi)$)

4. $J(t,\xi_1)$ and $Q(t,\xi_2)$ are shot noise from realizations of independent PPP Ξ_1 and Ξ_2

The first case generates filtered process with additive noise and results in integrated *random sums*:

$$Y(t,\xi) = \frac{1}{\tau} \int \sum_{x_i \in \xi} j(z, x_i)\, e^{-\frac{1}{\tau} \int_z^t Q(u)\, du}\, dz$$

where $j(t, x)$ is the shot noise kernel of $J(t, \xi)$.

The second case generates filtered process with multiplicative noise and results in integrated *random products*:

$$Y(t, \xi) = \frac{1}{\tau} \int J(z) \prod_{x_j \in \xi} e^{-\frac{1}{\tau} \int_z^t g(u, x_j) du} \, dz$$

where $g(t, x)$ is the shot noise kernel of $Q(t, \xi)$.

The third case results in integrated *generalized random sums*:

$$Y(t, \xi) = \frac{1}{\tau} \int \sum_{x_i \in \xi} g(z, x_i) \prod_{x_j \in \xi} e^{-\frac{1}{\tau} \int_z^t g(u, x_j) du} \, dz$$

The fourth case is a combination of the first two since the expectation Eq. (2.1) can be evaluated independently for each PPP.

A small remark regarding the naming of PPP transformations. The term random sums is borrowed from R. Streit [Streit, 2010] and by analogy random products and generalized random sums is adopted for the other two cases. There doesn't seem to be much convergence in the literature regarding the naming of these PPP transformations.

2.1.4 Statistics of PPP transformations

In this section we review the basic statistics of random products, random sums, generalized random sums and the integral transform.

Random products are introduced first since they are necessary to obtain the characteristic function of random sums. Random products are factorizations of the form $F(t, \xi) = \prod_{x_j \in \xi} f(t, x_j)$ and their mean and joint moments are evaluated as follows:

$$\langle F_t \rangle = \sum_{n=0}^{\infty} \frac{1}{n!} e^{-m(\mathcal{S})} \left(\int_{\mathcal{S}} f(t, x) \, \lambda(x) \, dx \right)^n = \exp \left(\int_{\mathcal{S}} (f(t, x) - 1) \, \lambda(x) \, dx \right)$$

$$\langle F_1 \ldots F_K \rangle = \left\langle \prod_{x_j \in \xi} \prod_{k=1}^{K} f(t_k, x_j) \right\rangle = \exp \left(\int_{\mathcal{S}} (f(t_1, x) \cdots f(t_K, x) - 1) \, \lambda(x) \, dx \right) \quad (2.7)$$

Random sums are factorisations of the form $F(t, \xi) = \sum_{x_j \in \xi} f(t, x_j)$. The shot noise process G_t from Eq. (2.2) is a causal random sum with $f(t, x_j) = g(t - x_j) H(t - x_j)$. As in the previous case, their statistical properties can be obtained explicitly from the expectation Eq. (2.1). However, the *characteristic function* $\phi(s_1, \ldots, s_K)$ of random sums has an analytical form that leads to simpler derivation of relevant statistical properties.

$$\phi(s_1, \ldots, s_K) \equiv \left\langle e^{is_1 F_1 + \cdots + is_K F_K} \right\rangle = \left\langle \prod_{k=1}^{K} e^{is_k \sum_{x_j \in \xi} f(t_k, x_j)} \right\rangle = \left\langle \prod_{x_j \in \xi} \prod_{k=1}^{K} e^{is_k f(t_k, x_j)} \right\rangle$$

The expectation of the random product on the right side can be evaluated by Eq. (2.7) and yields the general form of the *Campbell Theorem* [Campbell, 1909]:

$$\phi(s_1, \ldots, s_K) = \exp \left(\int_{\mathcal{S}} \left(e^{\sum_{k=1}^{K} is_k f(t_k, x)} - 1 \right) \lambda(x) \, dx \right) \quad (2.8)$$

The probability density function (pdf) of random sums have known analytical forms for a small number of shot noise kernels, among which the exponential kernel [Gilbert and Pollak, 1960]. The joint pdf, moments and cumulants of random sums are directly obtained from the characteristic function, as follows:

$$p(F_1, \ldots, F_K) = \frac{1}{(2\pi)^K} \int_{\mathbb{R}} \cdots \int_{\mathbb{R}} e^{\sum_{k=1}^{K} -is_k F_k} \phi(s_1, \ldots, s_K) \, ds_1 \ldots ds_K \tag{2.9}$$

$$\langle F_1 \cdots F_K \rangle = \left(\frac{1}{i} \frac{d}{ds_1} \right) \cdots \left(\frac{1}{i} \frac{d}{ds_K} \right) \phi(s_1, \ldots, s_K) \Big|_{s_1 = \cdots = s_K = 0} \tag{2.10}$$

$$\langle\langle F_1 \cdots F_K \rangle\rangle = \left(\frac{1}{i} \frac{d}{ds_1} \right) \cdots \left(\frac{1}{i} \frac{d}{ds_K} \right) \ln \phi(s_1, \ldots, s_K) \Big|_{s_1 = \cdots = s_K = 0} \tag{2.11}$$

In particular, the mean and joint cumulants of random sums have the following well-known expressions:

$$\langle F_t \rangle = \int_{\mathcal{S}} f(t, x) \, \lambda(x) \, dx \tag{2.12}$$

$$\langle\langle F_1 \ldots F_K \rangle\rangle = \int_{\mathcal{S}} f(t_1, x) \cdots f(t_K, x) \, \lambda(x) \, dx \tag{2.13}$$

The expectation of more general forms of random sums are given by the *Slivnyak-Mecke Theorem* [Slivnyak, 1962, Mecke, 1967]:

$$\left\langle \sum_{x_j \in \xi} f\left(t, x_j, \xi_{\backslash x_j}\right) \right\rangle = \int_{\mathcal{S}} \langle f(t, x, \xi) \rangle \, \lambda(x) \, dx \tag{2.14}$$

where $\xi_{\backslash x_j}$ is the set of events ξ except element x_j. In particular, the expectation of random sum of products that is relevant for conductance synapses is given by:

$$\left\langle \sum_{x_j \in \xi} f(t, x_j) \prod_{x_k \in \xi} g(t, x_k) \right\rangle = \langle g(t, \xi) \rangle \int_{\mathcal{S}} f(t, x) \, g(t, x) \, \lambda(x) \, dx$$

The third and last PPP transformation is the integral transform. The properties of causal PPP transformations under the integral sign are now investigated. Following [Rice, 1945] and integral transform of $F(t, \xi)$ in the interval $\mathcal{U} \subseteq \mathbb{R}$ and in regards to a bounded function $w(u, \mathcal{U})$ can be defined as follows:

$$SF(\mathcal{U}, \xi) = \int_{\mathcal{U}} F(u, \xi) \, w(u, \mathcal{U}) \, du$$

The mean and joint moments of the integral transform are calculated by interchanging the infinite sum and integrals of the expectation Eq. (2.1) with the integral of the transform. Assuming this leads to well defined quantities,

$$\langle SF \rangle = \left\langle \int_{\mathcal{U}} F(u, \xi) \, w(u, \mathcal{U}) \, du \right\rangle = \int_{\mathcal{U}} \langle F(u, \xi) \rangle \, w(u, \mathcal{U}) \, du \tag{2.15}$$

In the remainder of this document we'll assume that the integral of the transform can be interchanged with the integrals and infinite sum of the expectation. Under such conditions, the autocovariance yields:

$$\langle SF_1\,SF_2 \rangle = \left\langle \int_{\mathcal{U}_1} F(u_1,\xi)\,w\,(u_1,\mathcal{U}_1)\,du_1 \int_{\mathcal{U}_1} F(u_2,\xi)\,w\,(u_2,\mathcal{U}_2)\,du_2 \right\rangle$$

$$= \int_{\mathcal{U}_1}\int_{\mathcal{U}_2} \langle F(u_1,\xi)\,F(u_2,\xi) \rangle\,w\,(u_1,\mathcal{U}_1)\,w\,(u_2,\mathcal{U}_2)\,du_1\,du_2$$

Which generalizes for joint moments of any order:

$$\langle SF_1 \cdots SF_K \rangle = \left\langle \prod_{k=1}^{K} \int_{\mathcal{U}_k} F(u_k,\xi)\,w\,(u_k,\mathcal{U}_k)\,du_k \right\rangle$$

$$= \int_{\mathcal{U}_1} \cdots \int_{\mathcal{U}_K} \langle F(u_1,\xi) \cdots F(u_K,\xi) \rangle \prod_{k=1}^{K} w\,(u_k,\mathcal{U}_k)\,du_k$$

Since joint cumulants are expressed as partitions of joint moments, the following equality also holds:

$$\langle\langle SF_1 \cdots SF_K \rangle\rangle = \int_{\mathcal{U}_1} \cdots \int_{\mathcal{U}_K} \langle\langle F(u_1,\xi) \cdots F(u_K,\xi) \rangle\rangle \prod_{k=1}^{K} w\,(u_k,\mathcal{U}_k)\,du_k \tag{2.16}$$

As shown in the Appendix A.3, this equality also holds for the more general case of N independent PPP.

2.2 General Solution

The general form of the solution can be evaluated using the statistics of the relevant PPP transformations under the integral sign. The mean and high order cumulants of the filtered process Y_t are obtained by forming the relevant products of $Y(t,\xi)$ and evaluating the expectation Eq. (2.1). We consider the case where both $Q(t,\xi)$ and $J(t,\xi)$ are shot noise generated from the same PPP, and assume without loss of generality the initial value $Y(t_0) = 0$ for $t \leq t_0$ and $\mathcal{U}_i =]t_0, t_i]$. The solution of the system for and arbitrary realization is given by:

$$Y(t,\xi) = \frac{1}{\tau} \int_{\mathcal{U}} J(z,\xi)\,e^{-\frac{1}{\tau}\int_z^t Q(u,\xi)\,du} dz$$

Applying Eqs. (2.15) and (2.16) yields:

$$\langle Y_t \rangle = \frac{1}{\tau} \int_{\mathcal{U}} \left\langle J(z,\xi)\,e^{-\frac{1}{\tau}\int_z^t Q(u,\xi)\,du} \right\rangle dz \tag{2.17}$$

$$\langle\langle Y_1 \cdots Y_K \rangle\rangle = \frac{1}{\tau^K} \int_{\mathcal{U}_1} \cdots \int_{\mathcal{U}_K} \left\langle\left\langle \prod_{k=1}^{K} J(z_k,\xi)\,e^{-\frac{1}{\tau}\int_{z_k}^{t_k} Q(u,\xi)\,du} \right\rangle\right\rangle dz_1 \ldots dz_K \tag{2.18}$$

The cases where only one of the inputs depends on ξ (i.e. $R(t,\xi)$ and $Q(t)$ and $R(t)$ and $Q(t,\xi)$)

are evaluated by taking the expectation on the stochastic term and using the properties of random sums and random products, respectively.

The case where $Q(t, \xi_1)$ and $R(t, \xi_2)$ are shot noise generated from independent PPP Ξ_1 and Ξ_2 are evaluated under multivariate PPP $\boldsymbol{\Xi}$ with 2 independent components. The expectation under this PPP with N independent components is detailed in Appendix A.3. For the mean and autocovariance,

$$\langle Y_t \rangle = \frac{1}{\tau} \int\limits_{\mathcal{U}} \langle R(z, \xi_1) \rangle \left\langle e^{-\frac{1}{\tau} \int_z^t Q(u, \xi_2)\, du} \right\rangle dz$$

$$\langle\langle Y_1\, Y_2 \rangle\rangle = \frac{1}{\tau^2} \int\limits_{\mathcal{U}_1} \int\limits_{\mathcal{U}_2} \left\langle \left\langle R(z_1, \xi_1)\, e^{-\frac{1}{\tau} \int_{z_1}^{t_1} Q(u_1, \xi_2) du_1}\, R(z_2, \xi_1)\, e^{-\frac{1}{\tau} \int_{z_2}^{t_2} Q(u_2, \xi_2) du_2} \right\rangle \right\rangle dz_1\, dz_2$$

with,

$$\left\langle \left\langle R(z_1, \xi_1)\, e^{-\frac{1}{\tau} \int_{z_1}^{t_1} Q(u_1, \xi_2) du_1}\, R(z_2, \xi_1)\, e^{-\frac{1}{\tau} \int_{z_2}^{t_2} Q(u_2, \xi_2) du_2} \right\rangle \right\rangle$$

$$= \langle R(z_1, \xi_1)\, R(z_2, \xi_1) \rangle \left\langle e^{-\frac{1}{\tau} \int_{z_1}^{t_1} Q(u_1, \xi_2) du_1 - \frac{1}{\tau} \int_{z_2}^{t_2} Q(u_2, \xi_2) du_2} \right\rangle$$

$$- \langle R(z_1, \xi_1) \rangle \langle R(z_2, \xi_1) \rangle \left\langle e^{-\frac{1}{\tau} \int_{z_1}^{t_1} Q(u_1, \xi_2) du_1} \right\rangle \left\langle e^{-\frac{1}{\tau} \int_{z_2}^{t_2} Q(u_2, \xi_2) du_2} \right\rangle$$

2.2.1 Additive Noise

The well-known case of filtering with additive noise is revisited and applies to membrane models with current synapses. We start with the general form given by Eq. (2.5) and assume $Q(t)$ is a deterministic function and $J(t) = J(t, \xi)$ is shot noise:

$$\tau \frac{d}{dt} Y(t) = -Q(t)\, Y(t) + J(t, \xi) \qquad\qquad J(t, \xi) = \sum_{x_j \in \xi} r(t, x_j)$$

The solution Eq. (2.6) is expressed by an integrated random sum:

$$Y(t, \xi) = \frac{1}{\tau} \int\limits_{\mathcal{U}} J(z, \xi)\, e^{-\frac{1}{\tau} \int_z^t Q(u)\, du}\, dz = \sum_{t_i \in \xi} \frac{1}{\tau} \int\limits_{\mathcal{U}} j(z, t_i)\, e^{-\frac{1}{\tau} \int_z^t Q(u)\, du}\, dz$$

$$\equiv \sum_{x_i \in \xi} y(t, t_i)$$

The cumulants of this filtered process are obtained by evaluating the expectation for terms containing $J(z, \xi)$ with the cumulants of random sums Eqs. (2.13) and (2.13), yielding:

$$\langle Y_t \rangle = \frac{1}{\tau} \int\limits_{\mathcal{U}} \int\limits_{\mathcal{S}} j(z, x)\, e^{-\frac{1}{\tau} \int_z^t Q(u)\, du}\, \lambda(x)\, dx\, dz$$

$$\langle\langle Y_1 \cdots Y_K \rangle\rangle = \frac{1}{\tau^K} \int\limits_{\mathcal{U}_1} \cdots \int\limits_{\mathcal{U}_K} \int\limits_{\mathcal{S}} \prod_{k=1}^{K} j(z_k, x)\, e^{-\frac{1}{\tau} \int_{z_k}^{t_k} Q(u)\, du}\, \lambda(x)\, dx\, dz_1 \cdots dz_K$$

The probability density of Y_t can be evaluated with the characteristic function $\phi(s)$ of random sums by inverse Fourier transform (Eq. (2.9)), yielding:

$$p(Y_t = z) = \frac{1}{2\pi} \int\limits_{\mathbb{R}} \exp\left(-isz + \int\limits_{\mathcal{S}} \left(e^{isy(t, x)} - 1 \right) \lambda(x)\, dx \right) ds \tag{2.19}$$
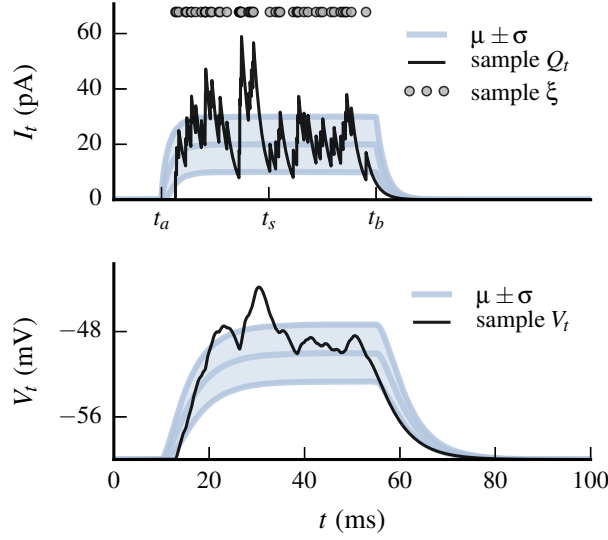
Figure 2.5 – *Single realization and basic statistics of membrane model with single current-based synapse type (excitatory). (Top) Random input arrival times $x_j \in \xi$ generate nonstationary shot noise current $I_t \equiv Q(t, \xi)$. (Bottom) Nonstationary membrane potential response $V_t \equiv V(t, \xi)$ driven by the shot noise input. The input arrival times are distributed with a variable Poisson rate $\lambda(t)$ that restricts the arrivals to occur between t_a and t_b. A single realization of random arrival times ξ is represented by gray dots (top), realizations of I_t and V_t are shown in black. The mean and standard deviation ($\mu \pm \sigma$) of both processes are shown in gray and are clearly nonstationary.*

The membrane equation for current-based synapses (Eq. (2.3)) can be recovered by the following transformation of variables:

$$V(t) = Y(t) + E_L \qquad\qquad Q(t) = 1 \qquad\qquad J(t, \xi) = R\, I(t, \xi)$$

In order to illustrate the exact nature of these results with nonstationary input dynamics, we introduce the protocol from the article in Chapter 3 where the synaptic input is restricted to occur between t_a and $t_b \geq t_a$ with a constant Poisson rate λ. This corresponds to the rate function $\lambda(t)$ from the middle plot in Figure 2.1. Single realizations of shot noise input I_t and the membrane potential time course V_t are shown in Fig. 2.5. The mean and standard deviation ($\mu \pm \sigma$) of both processes are clearly nonstationary since they vary in time. A comparison between numerical simulations and analytical predictions for this model show excellent agreement, as illustrated in Fig. 2.6 for the mean, standard deviation and autocorrelation. The autocorrelation at times t_1 and t_2 of process F_t is given by $\rho(F_1 F_2) = \langle\langle F_1 F_2 \rangle\rangle / (\sigma(F_1)\, \sigma(F_2))$ where $\langle\langle F_1 F_2 \rangle\rangle$ is the autocovariance at times t_1 and t_2 and $\sigma(F_t)$ is the standard deviation at time t. A comparison between the empirical distribution and analytical prediction of Eq. (2.19) is shown in Fig. 2.7.

The numerical simulations were generated with exponential kernel $g(t-x)_{exp} = h \exp\left(-(t-x)/\tau_s\right)$ for excitatory current. The rate function is represented in the middle plot of Fig. 2.1 with rate $\lambda = 1000$ Hz when the PPP is active. Other parameters are $\tau_m = 0.02$ s, $E_l = -0.06$ V, $R = 100\text{E}6$ Ω, $h = 10\text{E-}12$ A, and $\tau_s = 0.002$ s.

This model can be easily extended to N synapse types by considering the multivariate form Ξ of the PPP with N independent components. For clarity we now write $Q(t) = 1$.

$$\tau \frac{d}{dt} Y(t) = -Y(t) + J(t, \boldsymbol{\xi}) \qquad\qquad J(t, \boldsymbol{\xi}) = \sum_{n=1}^{N} \sum_{x_j \in \xi_n} r_n(t, x_j)$$
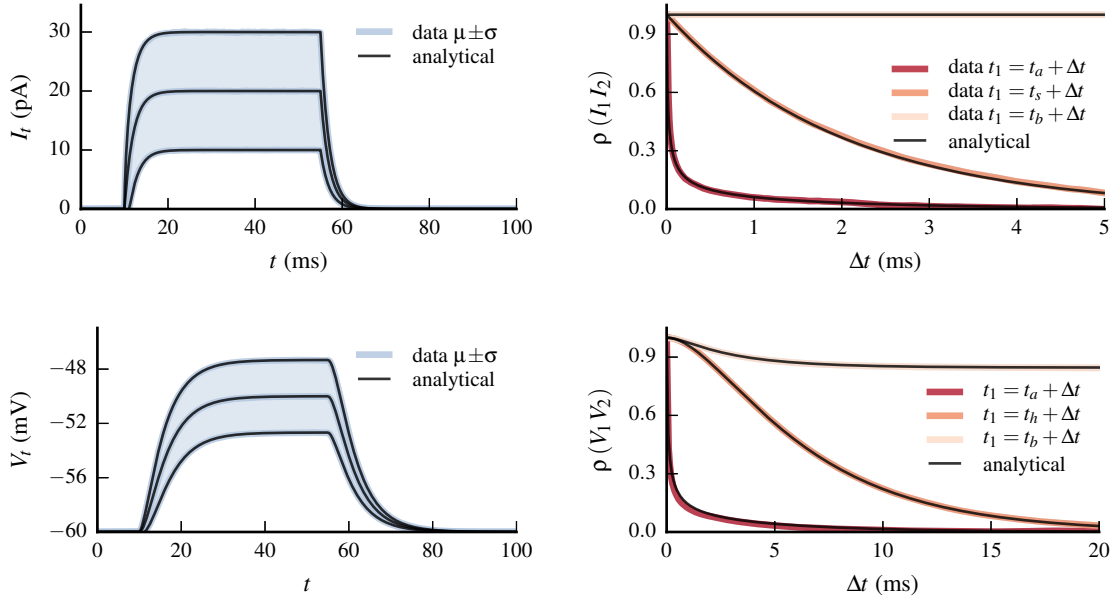
Figure 2.6 – *Comparison with numerical simulations for nonstationary mean and standard deviation (left) and the autocorrelation of the shot noise process I_t and membrane potential V_t. There is excellent agreement between the simulations (gray and colored lines) and the analytic predictions (black lines) with the respective lines overlapping. The autocorrelation ρ is evaluated at t_a, t_s, and t_b corresponding respectively to the onset of PPP activity, quasi-stationary I_t, and extinction of PPP activity.*

The solution Eq. (2.6) is expressed as a sum over each independent shot noise process:

$$Y(t, \boldsymbol{\xi}) = \frac{1}{\tau} \int_{\mathcal{U}} e^{-\frac{t-z}{\tau}} \sum_{n=1}^{N} J_n(z, \xi_n) \, dz$$

The cumulants of this filtered process have the same form as those of the previous case with the expectations evaluated under the multivariate PPP Ξ.

$$\langle Y_t \rangle = \frac{1}{\tau} \int_{\mathcal{U}} e^{-\frac{t-z}{\tau}} \sum_{n=1}^{N} \langle J_n(z) \rangle \, dz \tag{2.20}$$

$$\langle\langle Y_1 \cdots Y_K \rangle\rangle = \frac{1}{\tau^K} \int_{\mathcal{U}_1} \cdots \int_{\mathcal{U}_K} \sum_{n_1=1}^{N} \cdots \sum_{n_K=1}^{N} \left\langle \left\langle \prod_{k=1}^{K} J_{n_k}(z_k) \, e^{-\frac{t_k - z_k}{\tau}} \right\rangle \right\rangle dz_1 \cdots dz_K \tag{2.21}$$

The linearity of the expectation and properties of cumulants yield the solution:

$$\langle Y_t \rangle = \frac{1}{\tau} \int_{\mathcal{U}} e^{-\frac{t-z}{\tau}} \sum_{n=1}^{N} \int_{\mathcal{S}} j_n(z, x) \, \lambda_n(x) \, dx \, dz$$

$$\langle\langle Y_1 \cdots Y_K \rangle\rangle = \frac{1}{\tau^K} \int_{\mathcal{U}_1} \cdots \int_{\mathcal{U}_K} \sum_{n=1}^{N} \int_{\mathcal{S}} \prod_{k=1}^{K} j_n(z_k, x) \, e^{-\frac{t_k - z_k}{\tau}} \, \lambda_n(x) \, dx \, dz_1 \cdots dz_K$$
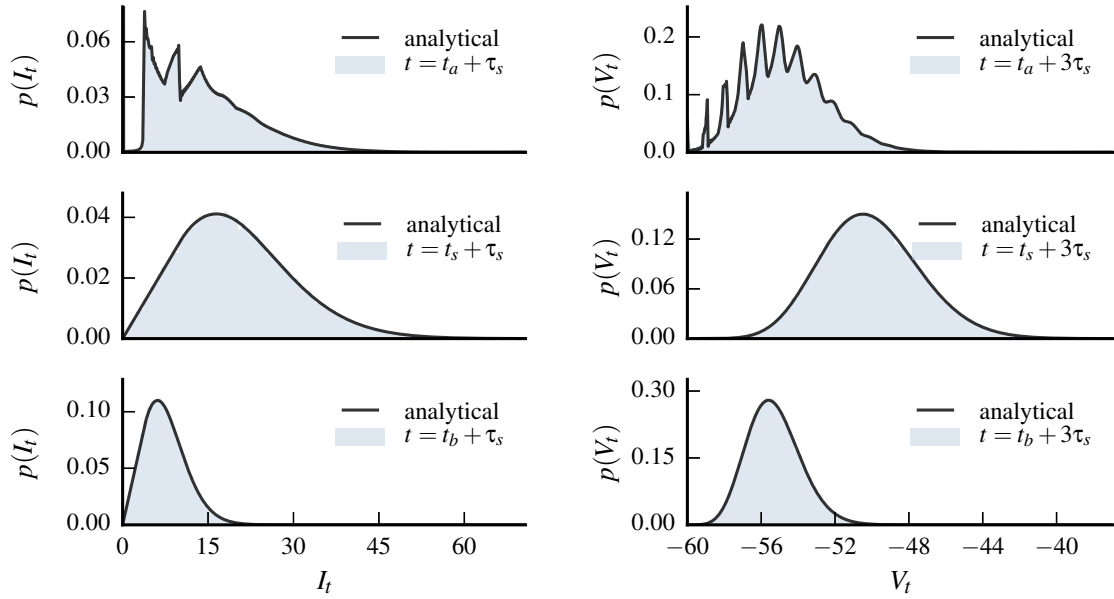
Figure 2.7 – *Comparison with numerical simulations for nonstationary probability density function of synaptic current $p(I_t)$ (left) and membrane potential $p(V_t)$ (right). Data histograms of empirical distributions from simulations (gray) are compared with analytic predictions (black lines) at times t_a, t_s, and t_b.*

2.2.2 Multiplicative Noise

The case of multiplicative noise corresponds to conductance synapses and is developed in the articles of Chapters 3 and 4. In particular, the case of a single synapse type can be expressed as a pure multiplicative noise process as shown in the article of Chapter 3. This leads to shorter expressions by avoiding the usage of Slivnyak-Mecke Theorem. The solution for the case of two independent shot noise inputs and a time dependent current is briefly derived here and the complete derivation for the case $J(t) = 0$ is provided in Appendix A.4. Comparisons with numerical simulations are shown in the relevant articles.

Starting with the general form given by Eq. (2.5) and assuming $J(t)$ is a deterministic function and $Q(t, \xi_1)$ and $Q(t, \xi_2)$ are independent shot noise inputs:

$$\tau \frac{d}{dt} Y(t) = (w_1 - Y(t)) Q_1(t, \xi_1) + (w_1 - Y(t)) Q_1(t, \xi_2) + J(t) \tag{2.22}$$

$$Q_n(t, \xi_n) = \sum_{x_j \in \xi_n} g_n(t, x_j) \quad \text{with } n \in \{1, 2\} \tag{2.23}$$

The solution Eq. (2.6) is expressed as a generalized random sum. Writing $Q_0(u, \boldsymbol{\xi}) = 1 + Q(t, \xi_1) + Q(t, \xi_2)$,

$$Y(t, \xi) = \frac{1}{\tau} \int_{\mathcal{U}} (w_1 Q_1(t, \xi_1) + Q_2(t, \xi_2) + J(z)) \, e^{-\frac{1}{\tau} \int_z^t Q_0(u, \boldsymbol{\xi}) \, du} \, dz$$

$$= \frac{1}{\tau} \int_{\mathcal{U}} \left(\sum_{n=1}^{2} w_n \sum_{x_j \in \xi_n} g_n(t, x_j) + J(z) \right) e^{-\frac{t-z}{\tau}} \prod_{m=1}^{2} e^{-\frac{1}{\tau} \int_z^t g_m(u, \xi_m) \, du} \, dz$$

The cumulants of this filtered process are obtained by evaluating the expectation for terms containing $Q_n(t, \xi_n)$ with the cumulants of random sums Eqs. (2.13) and (2.13), yielding:

$$\langle Y_t \rangle = \frac{1}{\tau} \int_{\mathcal{U}} \left\langle \left(\sum_{n=1}^{2} w_n Q_n(z, \xi_n) + J(z) \right) e^{-\frac{1}{\tau} \int_z^t Q_0(u, \boldsymbol{\xi}) \, du} \right\rangle dz$$

$$\langle\langle Y_1 \cdots Y_K \rangle\rangle = \frac{1}{\tau^K} \int_{\mathcal{U}_1} \cdots \int_{\mathcal{U}_K} \left\langle \left\langle \prod_{k=1}^{K} \left(\sum_{n=1}^{2} w_n Q_n(z_k, \xi_n) + J(z_k) \right) e^{-\frac{1}{\tau} \int_{z_k}^{t_k} Q_0(u, \boldsymbol{\xi}) \, du_k} \right\rangle \right\rangle dz_1 \ldots dz_K$$

The key expectations are given by:

$$\left\langle Q_n(z, \xi_n) e^{-\frac{1}{\tau} \int_z^t Q_0(u, \boldsymbol{\xi}) \, du} \right\rangle = \left\langle e^{-\frac{1}{\tau} \int_z^t Q_0(u, \boldsymbol{\xi}) \, du} \right\rangle \int_{-\infty}^{z} g_n(z, x) e^{-\frac{1}{\tau} \int_z^t g_n(u, x) du} \lambda_n(x) \, dx$$

$$\left\langle \prod_{k=1}^{K} e^{-\frac{1}{\tau} \int_{z_k}^{t_k} Q_n(u) \, du} \right\rangle = \exp\left(\int_{\mathcal{S}} \left(\prod_{k=1}^{K} e^{-\frac{1}{\tau} \int_{z_k}^{t_k} g_n(u, x) du} - 1 \right) \lambda_n(x) \, dx \right)$$

The cumulants of V_t are recovered with the following transformation:

$$\langle V_t \rangle = (E_e - E_i) \langle Y_t \rangle + E_l \qquad\qquad \langle\langle V_1 \cdots V_K \rangle\rangle = (E_e - E_i)^K \langle\langle Y_1 \cdots Y_K \rangle\rangle$$

with,

$$Q_n(t, \xi_n) = \frac{1}{g_l} G_n(t, \xi_n) \qquad J(t) = RI(t) \qquad w_n = \frac{E_n - E_l}{E_e - E_i}$$

2.2.3 General Case

The general case considered here has three independent shot noise inputs and a periodic reversal potential $U(t)$. Two shot noise processes generate input current and a third shot noise process generates input conductance. The input currents model additive noise to simulate measurement error, are generated with high frequency rate and have opposite signs. The PPP Ξ_1, Ξ_2 modeling current input have constant rate η and generate zero mean current $J(t, \xi_1, \xi_2) = J_1(t, \xi_1) + J_2(t, \xi_2)$. The third PPP Ξ_3 modeling input conductance has the rate function $\lambda(t) = \lambda H(t - t_a) H(t_b - t)$ illustrated in the middle plot of Fig. 2.1.

$$\tau \frac{d}{dt} Y(t) = -Y(t) + (U(t) - Y(t)) Q(t) + J(t) \tag{2.24}$$

with,

$$J_1(t, \xi_1) = \sum_{x_i \in \xi_1} f(t - x_i) H(t - x_i) \qquad\qquad U(t) = 1 - U_0 \sin(2\pi\omega t)$$

$$J_2(t, \xi_2) = \sum_{x_k \in \xi_2} f(t - x_k) H(t - x_k) \qquad\qquad Q(t, \xi_3) = \sum_{x_j \in \xi_3} g(t - x_j) H(t - x_j)$$

The mean and autocovariance are given below and the derivation is provided in Appendix A.5.

$$\langle Y_t \rangle = \frac{1}{\tau} \int_{\mathcal{U}} \left(1 - U_0 \sin(2\pi\omega z)\right) e^{-\frac{t-z}{\tau}} \left\langle Q(z,\xi_3) e^{-\frac{1}{\tau} \int_z^t Q(u,\xi_3) du} \right\rangle dz$$

$$\langle\langle Y_1 Y_2 \rangle\rangle = \frac{1}{\tau^2} \int_{\mathcal{U}_1} \int_{\mathcal{U}_2} \left(1 - U_0 \sin(2\pi\omega z_1)\right) \left(1 - U_0 \sin(2\pi\omega z_2)\right)$$

$$\left\langle\left\langle Q(z_1,\xi_3)\, Q(z_2,\xi_3)\, e^{-\frac{1}{\tau}\int_{z_1}^{t_1} Q(u,\xi_3)\,du - \frac{1}{\tau}\int_{z_2}^{t_2} Q(v,\xi_3)\,dv} \right\rangle\right\rangle dz_1\, dz_2$$

$$+ \frac{2}{\tau^2} \int_{\mathcal{U}_1} \int_{\mathcal{U}_2} \langle\langle J(x_1,\xi_1,\xi_2)\, J(x_2,\xi_1,\xi_2) \rangle\rangle \left\langle\left\langle e^{-\frac{1}{\tau}\int_{x_1}^{t_1} Q(u,\xi_3)\,du - \frac{1}{\tau}\int_{x_2}^{t_2} Q(v,\xi_3)\,dv} \right\rangle\right\rangle dx_1\, dx_2$$

Comparison with numerical simulations are shown in Fig. 2.8 and display excellent agreement with the analytical predictions.
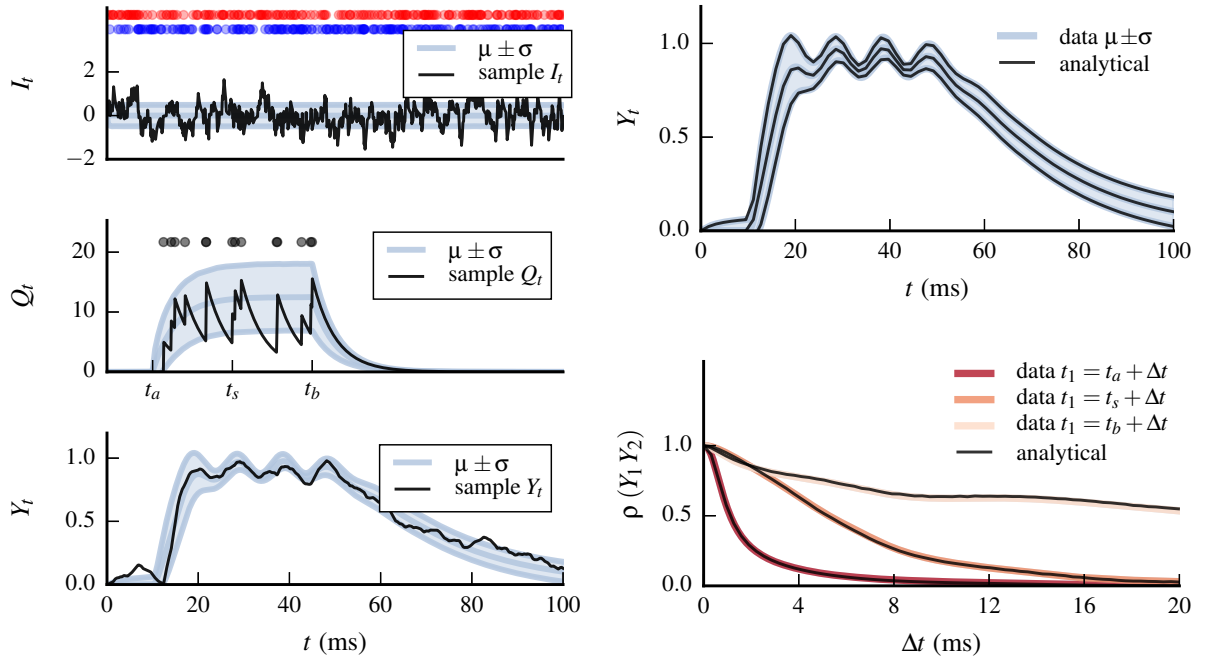
Figure 2.8 – *Filtering of three independent shot noise processes. A zero mean current I_t is generated by two shot noise processes with constant rate (left top). A multiplicative noise Q_t is generated by the third process and is only active between t_a and $t_b \geq t_a$ (left middle). The filtered process Y_t has a time-varying reversal potential (left bottom). Single realizations of J_t, Q_t and Y_t are shown in black, mean and standard deviation ($\mu \pm \sigma$) is shown in gray. Comparison between simulations (gray) and analytic prediction (black) for the mean and standard deviation ($\mu \pm \sigma$) of system response Y_t (right top). Comparison between simulations (colors) and analytic prediction (black) for the autocorrelation ρ of system response Y_t at times $t_b \geq t_s \geq t_a$ (right bottom).*

The cumulants of V_t are recovered with the following transformation:

$$\langle V_t \rangle = (E_e - E_L)\, \langle Y_t \rangle + E_L \qquad\qquad \langle\langle V_1 \cdots V_K \rangle\rangle = (E_e - E_L)^K \langle\langle Y_1 \cdots Y_K \rangle\rangle$$

with

$$J(t,\xi_1,\xi_2) = R\, I_1(t,\xi_1) + R\, I_2(t,\xi_2) \quad Q(t,\xi_3) = \frac{1}{g_l}\, G(t,\xi_3) \quad E(t) = U(t)\,(E_e - E_l) + E_l$$

The numerical simulations were generated with exponential kernel for current and conductance inputs. The current inputs have constant rate of 2000 Hz, and the conductance rate function is represented in the middle plot of Fig. 2.1 with rate $\lambda = 500$ Hz when the PPP is active. Other parameters are $\tau = 0.02$ s, $h = 0.5\text{E-}12$ A and $\tau_s = 0.0005$ s for current inputs and $h = 5\text{E-}9$ S and $\tau_s = 0.005$ s for conductance input.

2.3 Asymptotic and Stationary Limits

The statistical properties of long running shot noise process Q_t and system response Y_t are analyzed in this section. A shot noise process generated from an homogeneous PPP will reach a stationary regime after an initial transient period, assuming the appropriate convergence properties of the shot noise kernel to ensure the finiteness of cumulants (Eq. (2.13)). This may no longer be the case under inhomogeneous PPP. However, an asymptotic limit may exist for certain periodic rate functions such as the example from Fig. 2.9.

The stationary or asymptotic limits of shot noise process Q_t are obtained by setting the origin of event arrivals T_0 at infinity ($T_0 \to -\infty$). The stationary and asymptotic limits of system response Y_t are obtained by setting the start of input integration t_0 in the same limit ($t_0 = T_0$, $T_0 \to -\infty$). The filtering of Q_t may eventually be decoupled from the starting time of event arrivals, as shown in the lower plots of the same Figure. Finally, the limit where Y_t is driven by stationary or asymptotic Q_t and the initial Q_t transients are neglected, is obtained by setting $T_0 \to -\infty$ and keeping t_0 finite.
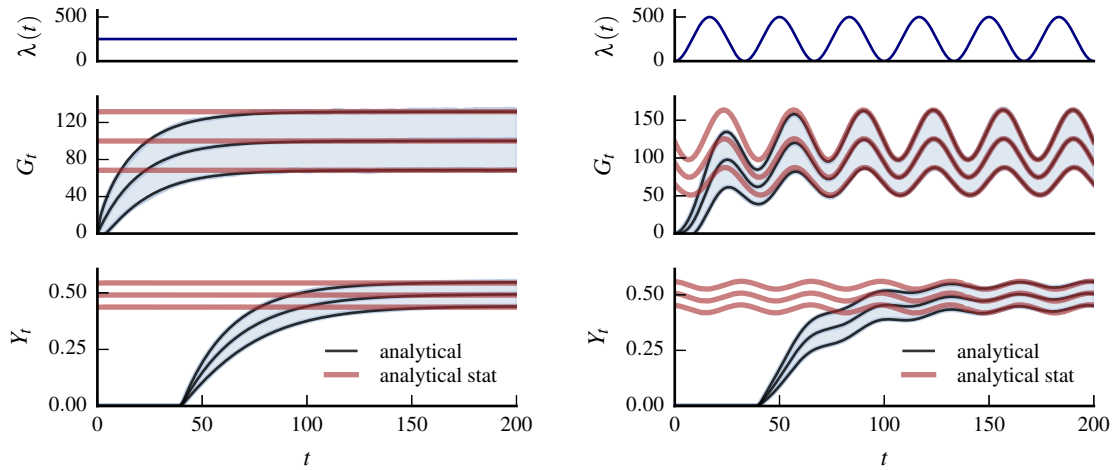
Figure 2.9 – *(Left) Transformations of homogeneous PPP may have have stationary limits (red). (Right) Inhomogeneous PPP may display an asymptotic limit that is nonstationary (red). The stationary and asymptotic limits are obtained by setting the origin of event arrivals T_0 at infinity ($T_0 \to -\infty$).*

For example, the stationary or asymptotic limits of $\langle Q_t \rangle$ and $\langle Y_t \rangle$ illustrated in Fig. 2.9, are

given by:

$$\langle Q_t \rangle = \lim_{T_0 \to -\infty} \int_{T_0}^{t} g(t-x)\,\lambda(x)\,dx$$

$$\langle Y_t \rangle = \lim_{T_0 \to -\infty} 1 - \frac{1}{\tau} \int_{t_0}^{t} \exp\left(-\frac{t-z}{\tau} + \int_{T_0}^{t} \left(e^{-\frac{1}{\tau}\int_z^t g(u-x)\,H(u-x)\,du} - 1\right)\lambda(x)\,dx\right)dz \quad \text{with } t_0 = T_0$$

2.4   Random Dirac Delta Sums

Synaptic input under certain parameter regimes is well modeled by sums of Dirac delta functions that result in a jump of the filtered process $Y(t)$ for each presynaptic spike. In this section we apply the formalism of PPP transformation by replacing the shot noise kernel $g(t - x_i)$ with a Dirac delta function $h\,\tau_s\,\delta(u - x)$. This corresponds to the limit of sharply peaked shot noise and has been very successfully used in previous studies [Burkitt, 2001, Richardson, 2004].

The random product expectation Eq. (2.7) for random Dirac delta sums is given by:

$$\left\langle e^{-\frac{1}{\tau}\int_z^t Q(u,\xi)\,du} \right\rangle = \exp\left(\int_{\mathcal{S}} \left(e^{-\frac{h\tau_s}{\tau}(H(t-x)-H(z-x))} - 1\right)\lambda(x)\,dx\right)$$

$$\left\langle e^{-\frac{1}{\tau}\int_{z_1}^{t_1} Q(u,\xi)\,du - \frac{1}{\tau}\int_{z_2}^{t_2} Q(u,\xi)\,du} \right\rangle = \exp\left(\int_{\mathcal{S}} \left(e^{-\frac{h\tau_s}{\tau}(H(t_1-x)-H(z_1-x))-\frac{h\tau_s}{\tau}(H(t_2-x)-H(z_2-x))} - 1\right)\lambda(x)\,dx\right)$$

These expressions can be written in a more compact form in terms of the integrated rate function by reordering the integration limits of the expectation: $\{z_1, t_1, z_2, t_2\} \to \{x_1, x_2, x_3, x_4\}$ with $x_1 \geq x_2 \geq x_3 \geq x_4$. Writing $\gamma_k = \left(1 - e^{-\frac{kh\tau_s}{\tau}}\right)$ and assuming $t_1 \geq t_2$,

$$\left\langle e^{-\frac{1}{\tau}\int_z^t Q(u,\xi)\,du} \right\rangle = e^{-\gamma_1(m(t)-m(z))}$$

$$\left\langle e^{-\frac{1}{\tau}\int_{z_1}^{t_1} Q(u,\xi)\,du - \frac{1}{\tau}\int_{z_2}^{t_2} Q(u,\xi)\,du} \right\rangle = \begin{cases} e^{-\gamma_1(m(z_1)-m(z_2)+m(t_1)-m(t_2))-\gamma_2(m(t_2)-m(z_1))} & \text{for } t_2 \geq z_1 \\ e^{-\gamma_1(m(t_1)-m(z_1)+m(t_2)-m(z_2))} & \text{otherwise} \end{cases}$$

The cumulants for the filtered process with a single synapse type and nonstationary input are derived in Appendix A.6. A comparison between predictions and numerical simulations is shown in Fig. 2.10 for decreasing ratios of shot noise kernel time constant τ_s and relaxation time τ of Y_t.
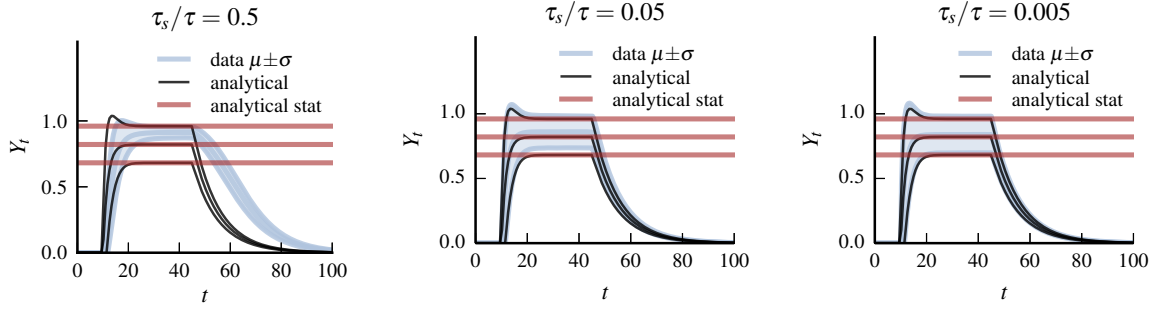
Figure 2.10 – *Replacing the shot noise kernel with a Dirac delta yields the limit of sharply peaked shot noise filtering. In each plot from left to right, the shot noise kernel time constant τ_s is successively divided by a factor of 10 while keeping the same value for the system response time constant τ. The scale variable h is successively increased by the same amount in order to ensure the same stationary mean shot noise input. Comparison between simulations (gray) and analytic prediction with random Dirac delta sums (black) for the mean and standard deviation ($\mu \pm \sigma$) of system response Y_t. The stationary limit has very simple analytic forms and is shown in red.*

The stationary limit yields very compact expressions:

$$\langle Y_t \rangle_{\text{stat}} = \frac{\lambda \tau\, \gamma_1}{1 + \lambda \tau\, \gamma_1} \qquad\qquad \langle\langle Y_1\, Y_2 \rangle\rangle_{\text{stat}} = \frac{\tau \lambda\,(2\gamma_1 - \gamma_2)}{(1 + \tau\lambda\gamma_1)^2 (2 + \tau\lambda\gamma_2)}\, e^{-(1+\lambda\gamma_1)\frac{t_1-t_2}{\tau}}$$

As expected, the stationary limit is only a good approximation whenever the typical rate of change of $\lambda(t)$ is small compared to the relaxation time τ of Y_t. The autocovariance of the system response Y_t is greatly reduced in the limit of sharply peaked shot noise filtering. This is illustrated in Fig. 2.11 by comparing the line $t_b + \Delta t$ between left and right plots.
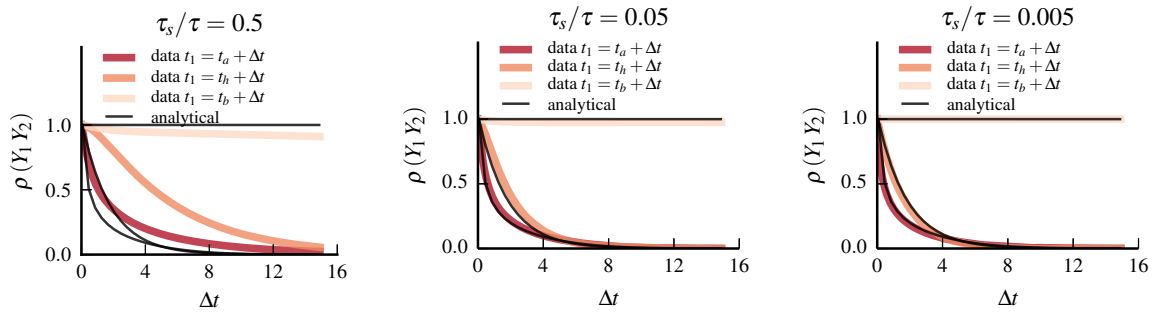
Figure 2.11 – *Comparison between simulations (colors) and analytic prediction with random Dirac delta sums (black) for the autocorrelation ρ of system response Y_t at the same evaluation points as in Figure 2.10.*

Please note that Dirac delta sums are not random sums since they dot not share the same characteristic function given by Eq. (2.8) that requires the impulse response function to be an actual function rather than a distribution [Streit, 2010].

2.5 Compound PPP Transformations

Shot noise processes are particular types of random sums and belongs to a larger family of stochastic processes called *Filtered Poisson Process* [Snyder and Miller, 1991, Parzen, 1999, Streit, 2010] that is characterized by linear transformations of PPP. This family includes transformations of *Compound PPP* where marks $\boldsymbol{\theta}_j$ are generated independently from the points x_j. This

enables to extend the synaptic input model to include variations in shot noise kernel shape, scale, etc. This leads to the following generalization of shot noise:

$$F(t, \xi^{\boldsymbol{\theta}}) = \sum_{x_j \in \xi^{\boldsymbol{\theta}}} f(t, x_j, \boldsymbol{\theta}_j)\, H(t - x_j) \tag{2.25}$$

where $\xi^{\boldsymbol{\theta}} = \{(x_1, \boldsymbol{\theta}_1), \ldots, (x_n, \boldsymbol{\theta}_n)\}$ is a realization of the compound PPP with mark $\boldsymbol{\theta}_j$ associated with point x_j. The marks are used to model the biological parameters $\boldsymbol{\theta} = \{\theta_1, \ldots, \theta_l\}$ of the shot noise kernel. For example, the exponential and alpha kernels have two biological parameters $\boldsymbol{\theta} = \{h, \tau_s\}$ to characterize synaptic strength and synaptic time constant of impulse responses.

The independence of the marks in regards to the points greatly simplifies the analysis of these PPP transformations. The expectation of $F(t, \xi)$ under the compound process Ξ given by:

$$\left\langle F(t, \xi^{\boldsymbol{\theta}}) \right\rangle = \sum_{n=0}^{\infty} \frac{1}{n!}\, e^{-m(\mathcal{S})} \int_{\mathcal{S}} \cdots \int_{\mathcal{S}} \int_{\Theta} \cdots \int_{\Theta} F\left(t, (x_1, \boldsymbol{\theta}_1), \ldots, (x_n, \boldsymbol{\theta}_n)\right) \prod_{j=1}^{n} p(\boldsymbol{\theta}_j)\, d\boldsymbol{\theta}_j\, \lambda(x_j)\, dx_j \tag{2.26}$$

where integrals over the density $p(\boldsymbol{\theta})$ are replaced by the respective sums for parameters with discrete values.

Variations in postsynaptic responses are expected to occur due to biological differences in synapses and their impact in membrane potential statistics is explored in the article presented in Chapter 4. Synaptic inhomogeneities are modeled by introducing individual synapses with specific biological parameters for each type. Each synapse is driven by an independent shot noise processes with rate adjusted to yield the desired cumulative rate. The limit of large number of synapses is modeled by generalized shot noise processes of the form Eq. (2.25), one for each synapse type. This limit is approached quite rapidly, as discussed in the article and illustrated in Fig. 2.12 for synaptic time constant inhomogeneities $\tau_s \sim p(\tau_s)$. In the left plot of this figure, presynaptic spikes from five synapses are color-coded to reflect the synapse of origin. The synaptic responses are added to form the total synaptic output of the synapse type. The right plot shows a realization of the limiting case. Even for a small number of synapses it may be difficult to distinguish between the cases individually and a small difference is shown in the variance.
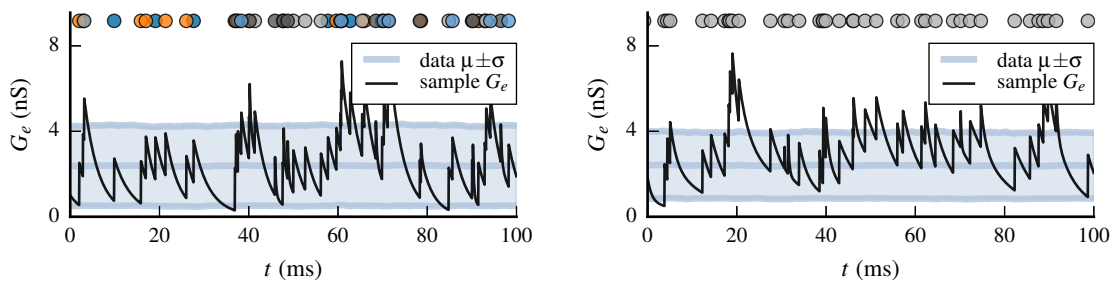
Figure 2.12 – *Example of synaptic input generated with synaptic time constant inhomogeneities $\tau_s \sim p(\tau_s)$. Small number of synapses ($N_e = 5$) with individual τ_s belonging to the same synapse type (left) and the limit of very large number of synapses where postsynaptic responses are generated with different τ_s for each spike arrival (right). The presynaptic spikes are color-coded to represent the synapse of origin (left). This figure shows the limit case already yields quite good approximations even for a small number of synapses, depending on particular synaptic time constant distributions $p(\tau_s)$ and simulation parameters.*

The Slivnyak-Mecke theorem is still valid for transformations of compound PPP since the probabilistic structure of the PPP is not changed. This enables to reuse the previous results under compound PPP as shown in the article from Chapter 4.

2.6 Central Moments Expansion

The central moments expansion (CME) enables to evaluate the contribution of shot noise cumulants to the statistics of the membrane equation with conductance synapses. This corresponds to the *Delta Method* [Cramér, 1946, Oehlert, 1992] for approximating expectations of random variable transformations. For the case of single conductance synapse type presented in the article of Chapter 3, the mean of the filtered process is given by:

$$\langle Y_t \rangle = 1 - \frac{1}{\tau} \int_{\mathcal{U}} e^{-\frac{t-z}{\tau}} \left\langle e^{-\frac{1}{\tau} \int_z^t Q(u) du} \right\rangle dz \tag{2.27}$$

The purpose of the CME is to approximate the expectation inside the integral. This is done by Taylor expansion of the integrated shot noise and only keeping the first and second order terms. The mean integrated shot noise is first factored from the expectation in order to yield a series in central moments of integrated shot noise.

$$\left\langle e^{-\frac{1}{\tau} \int_z^t Q(u) \, du} \right\rangle = e^{-\frac{1}{\tau} \int_z^t \langle Q(u) \rangle du} \left\langle e^{-\frac{1}{\tau} \int_z^t (Q(u) - \langle Q(u) \rangle) \, du} \right\rangle$$

$$\simeq e^{-\frac{1}{\tau} \int_z^t \langle Q(u) \rangle du} \left(1 + \frac{1}{2} \left\langle \left(-\frac{1}{\tau} \int_z^t (Q(u) - \langle Q(u) \rangle) \, du \right)^2 \right\rangle \right)$$

$$= e^{-\frac{1}{\tau} \int_z^t \langle Q(u) \rangle du} \left(1 + \frac{1}{2\tau^2} \int_z^t \int_z^t \langle \langle Q(u_1) \, Q(u_2) \rangle \rangle \, du_1 \, du_2 \right)$$

Inserting into the integral of Eq. (2.27) yields the CME approximation of the mean of the filtered process.

$$\langle Y_t \rangle_2 = \langle Y_t \rangle_0 - \frac{1}{\tau} \int_{\mathcal{U}} e^{-\frac{t-z}{\tau}} \frac{1}{2\tau^2} \int_z^t \int_z^t \langle \langle Q(u_1) \, Q(u_2) \rangle \rangle \, du_1 \, du_2 \, dz \tag{2.28}$$

with,

$$\langle Y_t \rangle_0 = 1 - \frac{1}{\tau} \int_{\mathcal{U}} e^{-\frac{t-z}{\tau}} e^{-\frac{1}{\tau} \int_z^t \langle Q(u) \rangle du} \, dz$$

The term $\langle Y_t \rangle_0$ is the deterministic solution for mean shot noise input $\langle Q(u) \rangle$, i.e. without shot noise fluctuations. The deterministic solution overestimates the mean of the filtered process, which can be verified by applying Jensen's inequality [Jensen, 1906] to the exponential function and concluding that $\langle \exp(X) \rangle \geq \exp(\langle X \rangle)$. Applying this inequality to the mean of the filtered process, yields:

$$\langle Y_t \rangle = 1 - \frac{1}{\tau} \int_{\mathcal{U}} e^{-\frac{t-z}{\tau}} \left\langle e^{-\frac{1}{\tau} \int_z^t Q(u) du} \right\rangle dz \leq 1 - \frac{1}{\tau} \int_{\mathcal{U}} e^{-\frac{t-z}{\tau}} e^{\langle -\frac{1}{\tau} \int_z^t Q(u) du \rangle} \, dz = \langle Y_t \rangle_0$$

The positive quantity $\Delta Y_t \equiv \langle Y_t \rangle_0 - \langle Y_t \rangle$ determines the correction due to stochastic input. The

CME for the mean (Eq. (2.28)) indicates that shot noise autocovariance is directly proportional to the amplitude of ΔY_t. This relationship can be illustrated by transformations of shot noise parameters that leave the mean unchanged. For example, by inversely varying rate and size parameter h. The mean of shot noise is linearly proportional to rate $\lambda(t)$ and h, whereas autocovariance scales linearly with rate but quadratically with h (even in nonstationary case, see Eqs. 2.12 and 2.13). Dividing the rate by $\alpha > 0$ and multiplying h by the same factor keeps the mean constant but increases the autocovariance by a factor of α, i.e. the scaling transformation $(\lambda(t), h) \mapsto (\lambda(t)/\alpha, h\,\alpha)$ yields $\langle\langle Q_1 Q_2\rangle\rangle \mapsto \alpha\,\langle\langle Q_1 Q_2\rangle\rangle$. This can be verified by applying the Campbell theorem (Eqs. 2.12 and 2.13) to the scaling transformation:

$$\langle\langle Q_t \rangle\rangle \mapsto \alpha\,h \int_{\mathcal{S}} f(t,x)\,\frac{\lambda(x)}{\alpha}\,dx = h \int_{\mathcal{S}} f(t,x)\,\lambda(x)\,dx = \langle\langle Q_t \rangle\rangle$$

$$\langle\langle Q_1 Q_2 \rangle\rangle \mapsto (\alpha\,h)^2 \int_{\mathcal{S}} f(t_1,x)\,f(t_2,x)\,\frac{\lambda(x)}{\alpha}\,dx = \alpha\,\langle\langle Q_1 Q_2 \rangle\rangle$$

This is illustrated in Fig. 2.13 where the scaling transformation $(\lambda(t), h) \mapsto (\lambda(t)/\alpha, h\,\alpha)$ is applied to different values of α.
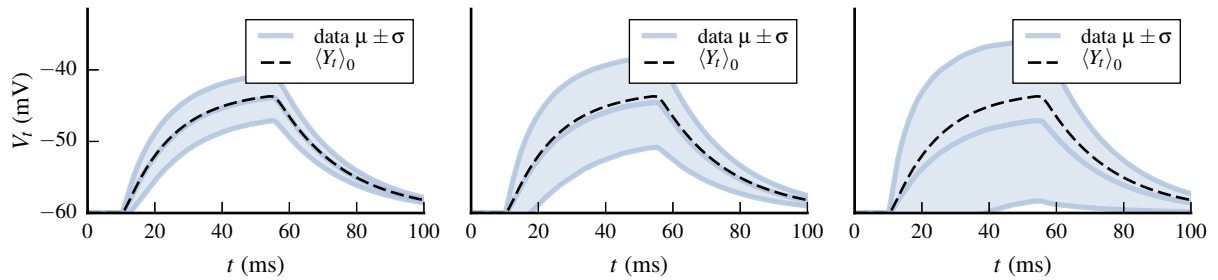

Figure 2.13 – *Analyzing the scaling of system parameters using the central moments expansion (CME). Scaling transformation $(\lambda(t), h) \mapsto (\lambda(t)/\alpha, h\,\alpha)$ with $\alpha = 1$ (left), $\alpha = 4$ (middle) and $\alpha = 16$ (right). The deterministic solution $\langle Y_t \rangle_0$ with mean shot noise input (black dash) is always greater than the mean of the filtered process $\langle Y_t \rangle_t$ due to the convexity of exponential function (Jensen's inequality). The difference between them $\Delta Y_t \equiv \langle Y_t \rangle_0 - \langle Y_t \rangle$ is the correction due to stochastic input. The CME for $\langle Y_t \rangle_t$ indicates that ΔY_t increases by reducing the rate of shot noise rate while increasing the mean in order to maintain constant mean of shot noise.*

The Fig. 2.13 also shows the variance of the filtered process increasing with α. This is expected since the scaling transformation increases the variance and this generally leads to increased variance of the filtered process (certainly in the stationary case). However, the variance increase seen in this figure could be mainly due to the autocovariance of shot noise or one of its higher order cumulants. In order to investigate the dominant contribution, the CME can be developed for the autocovariance of the filtered process. The first order CME for this cumulant is obtained by keeping terms up to second order in shot noise:

$$\langle\langle Y_1 Y_2 \rangle\rangle_1 = \frac{1}{\tau^4} \int_{\mathcal{U}_1} \int_{\mathcal{U}_2} e^{-\frac{1}{\tau}\int_{z_1}^{t_1}(1+\langle Q(u)\rangle)du - \frac{1}{\tau}\int_{z_2}^{t_2}(1+\langle Q(v)\rangle)dv} \int_{z_1}^{t_1} \int_{z_2}^{t_2} \langle\langle Q(u_1)\,Q(u_2)\rangle\rangle\,du_1\,du_2\,dz_1\,dz_2$$

$$(2.29)$$

The second order CME involves up to fourth order cumulants of integrated shot noise and is provided in Chapter 3. Additional work is required to establish the convergence properties of

the CME. Numerical simulations in the parameter regime of neuronal membranes show excellent results for the mean, and often very good results for the first order of autocovariance. The second order of the autocovariance appears to have the same order of accuracy as the mean, which is consistent with being second order in the delta method. For example, keeping third and fourth orders in the Taylor expansion for the mean either does not provide significant improvements or results in worse approximations. In the later case, in order to improve on the second order for the mean, many more terms are often required since the argument of the exponential grows large very fast (in this parameter regime).

The stationary limit of the filtered process yields the statistics under shot noise input with constant rate after dissipation of initial transients. The cumulants for this regime can be obtained by placing the onset of input arrival times at $-\infty$ and replacing the mean and second order cumulants of shot noise in Eqs (2.28) and (2.29) with their stationary limits. After integration by parts,

$$\langle Y_t \rangle_0 = \frac{\langle Q \rangle}{1 + \langle Q \rangle} \tag{2.30}$$

$$\langle Y_t \rangle_2 = \langle Y_t \rangle_0 - \frac{\langle\langle Q^2 \rangle\rangle}{(1 + \langle Q \rangle)^2} \frac{1}{\tau} \int\limits_{-\infty}^{t} e^{-\frac{t-z}{\tau}(1+\langle Q \rangle)} \, r \, (t - z) \, dz \tag{2.31}$$

$$\langle\langle Y_1 \, Y_2 \rangle\rangle_1 = \frac{\langle\langle Q^2 \rangle\rangle}{(1 + \langle Q \rangle)^2} \frac{1}{\tau^2} \int\limits_{-\infty}^{t_1} \int\limits_{-\infty}^{t_2} e^{-\frac{t_1 - z_1 + t_2 - z_2}{\tau}(1+\langle Q \rangle)} \, r \, (|z_1 - z_2|) \, dz_1 \, dz_2 \tag{2.32}$$

where $\langle Q \rangle$, $\langle\langle Q^2 \rangle\rangle$ and $\langle\langle Q_1 \, Q_2 \rangle\rangle = \langle\langle Q^2 \rangle\rangle \, r \, (|t_1 - t_2|)$ are respectively the mean, variance and autocovariance of stationary shot noise.

These expressions consistent with previous analytical estimates for the mean and standard deviation derived with alternative approaches: Fokker-Planck methods for exponential kernel shot noise Richardson and Gerstner [2005], Rudolph and Destexhe [2005] and shot noise approach for alpha kernel Kuhn et al. [2004]. The extension to the autocovariance of exponential and alpha kernels is provided in the article of Chapter 3.

The case of N independent shot noise inputs requires some changes in the expansion technique. The deterministic solution $\langle Y_t \rangle_0$ in this case is given by:

$$\langle Y_t \rangle_0 = \frac{1}{\tau} \int\limits_{-\infty}^{t} e^{-\frac{1}{\tau} \int_z^t \langle Q_0(u) \rangle du} \sum_{n=1}^{N} w_n \, \langle Q_n(z) \rangle \, dz \tag{2.33}$$

Directly expanding the exponential of integrated shot noise would result in mixed products of moments and central moments:

$$\left\langle Q(z)_n \, e^{-\frac{1}{\tau} \int_z^t Q_n(u) \, du} \right\rangle$$

$$= e^{-\frac{1}{\tau} \int_z^t \langle Q_n(u) \rangle du} \left(\langle Q_n(z) \rangle + \sum_{m=1}^{+\infty} \frac{1}{m!} \left\langle Q_n(z) \left(-\frac{1}{\tau} \int\limits_z^t (Q_n(u) - \langle Q_n(u) \rangle) \, du \right)^m \right\rangle \right)$$

An expansion purely in terms of central moments can be obtained after some preparatory work

that is detailed in the article of Chapter 4. The basic idea is to transform the mean of shot noise into a central moment prior to the Taylor expansion and only keeping terms up to the second order of every component.

$$\left\langle Q_n(z) \, e^{-\frac{1}{\tau}\int_z^t Q_n(u)du} \right\rangle$$
$$= e^{-\frac{1}{\tau}\int_z^t \langle Q_n(u)\rangle du} \left(\left\langle (Q_n(z) - \langle Q_n(z)\rangle) \, e^{-\frac{1}{\tau}\int_z^t (Q_n(u)-\langle Q_n(u)\rangle)du} \right\rangle + \langle Q_n(z)\rangle \left\langle e^{-\frac{1}{\tau}\int_z^t (Q_n(v)-\langle Q_n(v)\rangle)dv} \right\rangle \right)$$

This for the mean of the filtered process with N independent shot noise inputs:

$$\langle Y_t\rangle_2 = \langle Y_t\rangle_0 + \frac{1}{\tau} \int_{-\infty}^t e^{-\frac{1}{\tau}\int_z^t \langle Q_0(u)\rangle du}$$
$$\sum_{n=1}^N \left(-\frac{1}{\tau} \int_z^t w_n \, \langle\langle Q_n(z) \, Q_n(u)\rangle\rangle \, du \right.$$
$$\left. + w_n \, \langle Q_n(z)\rangle \, \frac{1}{2\tau^2} \int_z^t \int_z^t \sum_{m=1}^N \langle\langle Q_m(u_1) \, Q_m(u_2)\rangle\rangle \, du_1 \, du_2 \right) dz$$

$$(2.34)$$

Extending to joint moments is performed in similar manner and yields for the first order of autocovariance:

$$\langle\langle Y_1 \, Y_2\rangle\rangle_1 = \frac{1}{\tau^2} \int_{-\infty}^{t_1} \int_{-\infty}^{t_2} e^{-\frac{1}{\tau}\int_{z_1}^{t_1} \langle Q_0(u_1)\rangle du_1 - \frac{1}{\tau}\int_{z_2}^{t_2} \langle Q_0(u_2)\rangle du_2}$$
$$\sum_{n=1}^N \left(w_n^2 \, \langle\langle Q_n(z_1) \, Q_n(z_2)\rangle\rangle \right.$$
$$+ \sum_{m=1}^N \sum_{m'=1}^N w_n \, w_m \, \langle Q_n(z_1)\rangle \, \langle Q_m(z_2)\rangle \, \frac{1}{\tau^2} \int_{z_1}^{t_1} \int_{z_2}^{t_2} \langle\langle Q_{m'}(u_1) \, Q_{m'}(u_2)\rangle\rangle \, du_1 \, du_2$$
$$- \sum_{l=1}^N w_n \, w_l \left(\langle Q_n(z_1)\rangle \, \frac{1}{\tau} \int_{z_1}^{t_1} \langle\langle Q_l(u_1) \, Q_l(z_2)\rangle\rangle \, du_1 \right.$$
$$\left. \left. + \langle Q_n(z_2)\rangle \, \frac{1}{\tau} \int_{z_2}^{t_2} \langle\langle Q_l(u_2) \, Q_l(z_1)\rangle\rangle \, du_2 \right) \right) dz_1 \, dz_2$$

$$(2.35)$$

The structure of the CME for N independent shot noise inputs confirms the important role of the autocovariance for the mean and autocovariance of the filtered process. The simple scaling transformations performed earlier are very informative of the statistical properties of the filtered process. A more robust analysis may require the second order of the autocovariance, depending on the convergence properties for the relevant parameter regime.

Proceeding as previously yields the stationary limits.

$$\langle Y_t\rangle_0 = \frac{1}{\langle Q_0\rangle} \sum_{n=1}^N w_n \, \langle Q_n\rangle \tag{2.36}$$

$$\langle Y_t \rangle_2 = \langle Y_t \rangle_0 - \sum_{n=1}^{N} \frac{1}{\langle Q_0 \rangle} \left(w_n - \langle Y_t \rangle_0 \right) \langle\langle Q_n^2 \rangle\rangle \frac{1}{\tau} \int_{-\infty}^{t} e^{-\frac{t-z}{\tau}\langle Q_0 \rangle} r_n(t-z) \, dz \qquad (2.37)$$

$$\langle\langle Y_1 Y_2 \rangle\rangle_1 = \sum_{n=1}^{N} \left(w_n - \langle Y_t \rangle_0 \right)^2 \langle\langle Q_n^2 \rangle\rangle \frac{1}{\tau^2} \int_{-\infty}^{t_1} \int_{-\infty}^{t_2} e^{-\frac{t_1 - z_1 + t_2 - z_2}{\tau}\langle Q_0 \rangle} r_n(|z_1 - z_2|) \, dz_1 \, dz_2$$

$$(2.38)$$

where $\langle Q_n \rangle$, $\langle\langle Q_n^2 \rangle\rangle$ and $\langle\langle Q_n(t_1) Q_n(t_2) \rangle\rangle = \langle\langle Q_n^2 \rangle\rangle r(|t_1 - t_2|)$ are respectively the mean, variance and autocovariance of stationary shot noise conductance $Q_n(t)$.

The stationary limit of CME for the variance of V_t is obtained by setting y setting $t_1 = t_2 = t$ in Eq. (2.38). This can be used to analyze the impact of shot noise rate changes in the variance of V_t. Changing the rate of shot noise conductance will change its variance by the same factor since the autocovariance of shot noise is linearly proportional to rate $\lambda(t)$ (see Eq. (2.12)). In consequence, varying the stationary rate of a single conductance input will vary the variance of V_t according to Eq. (2.38). Several experimental studies have measured decrease of V_t variance on stimulus onset that is accompanied by an increase of mean V_t [Churchland et al., 2010]. Such reduction of variance can be caused by a decrease of synaptic input rate. The observed simultaneous increase of mean V_t would imply a reduction in inhibitory input rate, as illustrated in Fig. 2.13.
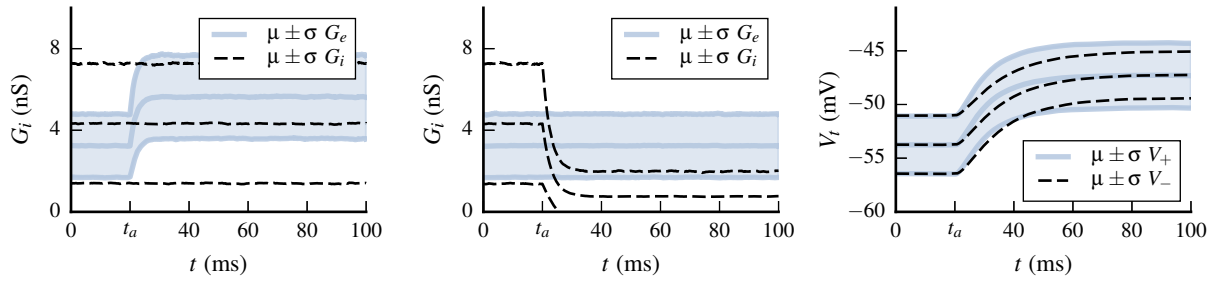
Figure 2.14 – *The mean V_t can be increased by raising the rate of excitatory conductance (left) or by decreasing the rate of inhibitory conductance (middle). These scenarios lead to opposite changes of V_t variance (conductance rate increase/decrease corresponds to V_+ and V_-, respectively) (right). The simultaneous increase V_t mean and decrease of V_t variance that is consistent with several experimental studies may occur by decrease of inhibitory conductance rate.*

Appendix A

A.1 Sampling Procedure

Sampling inhomogeneous PPPs in more than one dimension requires some care (see [Streit, 2010]), and may be performed with an acceptance-rejection procedure. This method can also be used in one dimension (see [Brette, 2009] for more general cases). An alternative and well-known procedure was adopted in this work, but can only be applied for PPPs in one dimension.

1. Evaluate the cumulative distribution of $p(x)$ in the interval $\mathcal{S} = [0, T]$ given by $\Phi(t) = m(t)/m(T)$

2. There is a one-to-one correspondence between $\Phi(t)$ and t since $\Phi(t)$ is a strictly increasing function of t

3. Draw the number of points n from Poisson distribution with rate $m(T)$

4. Sample N points $\{y_1, \ldots, y_N\}$ uniformly between 0 and 1, which is the range of $\Phi(t)$ since $\Phi(0) = m(0)/m(T) = 0$ and $\Phi(T) = m(T)/m(T) = 1$

5. The realization $\xi = \{x_1, \ldots, x_N\}$ is obtained by $\Phi^{-1}(y_n) = x_n$

A.2 Numerical Integration of Membrane Equation

The numerical integration schemes used in the simulations are described here. These schemes assume constant input between integration time steps, which results in sampling the input with time step Δt.

Current Synapses

Consider the membrane equation for N synapse types, given by:

$$\tau_m \frac{d}{dt} V(t) = E_l - V(t) + \sum_{n=1}^{N} R_m I_n(t)$$

where τ_m is the membrane time constant, E_l is the leak potential, R_m is the membrane resistance and $I_n(t)$ is the shot noise current for synapse type n.

The solution $V(t + \Delta t)$ at time $t + \Delta t$ for an initial value $V(t)$ at time t is given by:

$$V(t + \Delta t) = V(t) e^{-\frac{\Delta t}{\tau_m}} + \sum_{n=1}^{N} \frac{1}{\tau_m} \int_{t}^{t+\Delta t} \left(E_l + \sum_{n=1}^{N} R_m I_n(z) \right) e^{-\frac{t + \Delta t - z}{\tau_m}} \, dz$$

Using the fact that input is constant between integration steps yields the solution:

$$V(t + \Delta t) = V(t)\, e^{-\frac{\Delta t}{\tau_m}} + \left(E_l + \sum_{n=1}^{N} R_m\, I_n(t) \right)\left(1 - e^{-\frac{\Delta t}{\tau_m}} \right)$$

Conductance Synapses

The numerical integration of current synapses follows the same scheme. The membrane equation for N synapse types, given by:

$$\tau_m \frac{d}{dt} V(t) = E_l - V(t) + \sum_{n=1}^{N} (E_n - V(t))\, \frac{1}{g_l}\, G_n(t)$$

where τ_m is the membrane time constant, E_l is the leak potential, g_l is the leak conductance, E_n is the synaptic reversal potential for synapse type n, $G_n(t)$ is the shot noise conductance for synapse type n.

The solution $V(t + \Delta t)$ at time $t + \Delta t$ for an initial value $V(t)$ at time t is given by:

$$V(t + \Delta t) = V(t)\, e^{-\frac{1}{\tau_m g_l} \int_t^{t+\Delta t} G_0(u)\, du} + \sum_{n=1}^{N} \frac{1}{\tau_m} \int_t^{t+\Delta t} \left(E_l + \sum_{n=1}^{N} E_n \frac{1}{g_l} G_n(z) \right) e^{-\frac{1}{\tau_m g_l} \int_z^{t+\Delta t} G_0(u)\, du}\, dz$$

where $\frac{1}{g_l} G_0(t) = 1 + \sum_{n=1}^{N} \frac{1}{g_l} G_n(t)$.

Using the fact that input is constant between integration steps yields the solution:

$$V(t + \Delta t) = V(t)\, e^{-\frac{\Delta t}{\tau_m g_l} G_0(t)} + \frac{g_l}{G_0(t)} \left(E_l + \sum_{n=1}^{N} E_n \frac{1}{g_l} G_n(t) \right)\left(1 - e^{-\frac{\Delta t}{\tau_m g_l} G_0(t)} \right)$$

A.3 Cumulants of Integral PPP Transformations

Joint cumulants are expressed in terms of products of moments according to the following combinatorial expression:

$$\langle\langle X_1 \ldots X_K \rangle\rangle = \sum_{\pi} (|\pi| - 1)! (-1)^{|\pi|-1} \prod_{B \in \pi} \left\langle \prod_{i \in B} X_i \right\rangle$$

where π runs through the list of all partitions of $\{1, \ldots, K\}$, B runs through the list of all blocks of the partition π, and $|\pi|$ is the number of parts in the partition.

Assuming the infinite sum and integrals the expectation commutes with the integrals of $SI(\mathcal{U}_K, \xi)$

for $1 \leq k \leq K$,

$$
\begin{aligned}
\langle\langle SF_1 \cdots SF_K \rangle\rangle &= \sum_\pi (|\pi| - 1)!(-1)^{|\pi|-1} \prod_{B\in\pi} \left\langle \prod_{i\in B} SF(\mathcal{U}_i, \xi) \right\rangle \\
&= \sum_\pi (|\pi| - 1)!(-1)^{|\pi|-1} \prod_{B\in\pi} \left\langle \prod_{i\in B} \int_{\mathcal{U}_i} F(u_i, \xi)\, h(u_i, \mathcal{U}_i)\, du_i \right\rangle \\
&= \int_{\mathcal{U}_1} \cdots \int_{\mathcal{U}_K} \sum_\pi (|\pi| - 1)!(-1)^{|\pi|-1} \prod_{B\in\pi} \left\langle \prod_{i\in B} F(u_i, \xi) \right\rangle \prod_{k=1}^K h(u_k, \mathcal{U}_K)\, du_k \\
&= \int_{\mathcal{U}_1} \cdots \int_{\mathcal{U}_K} \langle\langle F(u_1, \xi) \cdots F(u_K, \xi) \rangle\rangle \prod_{k=1}^K h(u_k, \mathcal{U}_K)\, du_k
\end{aligned}
$$

This property can be extended to multivariate PPP with N independent components $\Xi_1(\mathcal{S}, \lambda_1)$ to $\Xi_N(\mathcal{S}, \lambda_N)$ with realizations $\boldsymbol{\xi} \equiv \{\xi_1, \ldots, \xi_N\}$ [Cox and Isham, 1980]. The cumulants of the transformation $F(t, \boldsymbol{\xi})$ are obtained under the expectation:

$$
\begin{aligned}
\langle F(t, \boldsymbol{\xi}) \rangle_{\boldsymbol{\Xi}} = \sum_{n_1=0}^\infty \cdots \sum_{n_N=0}^\infty \frac{1}{n_1!}\, e^{-m_1(\mathcal{S})} \cdots \frac{1}{n_N!}\, e^{-m_N(\mathcal{S})} \\
\int_{\mathcal{S}_1} \cdots \int_{\mathcal{S}} \cdots \int_{\mathcal{S}} \cdots \int_{\mathcal{S}} F\left(t, x_1^1, \ldots, x_{n_1}^1, \ldots, x_1^N, \ldots, x_{n_N}^N\right) \prod_{n=1}^N \prod_{j_n=1}^{n_N} \lambda_l(x_{j_n}^n)\, dx_{j_n}^n
\end{aligned}
$$

where x_k^n is the time of the k-th event from realization ξ_n.

The extension for transformations of independent PPP assumes that the product of infinite sums and integrals of the multivariate expectation commutes with the integrals of $SI(\mathcal{U}_K, \xi)$ for $1 \leq k \leq K$,

$$
\begin{aligned}
\langle\langle SF_1 \cdots SF_K \rangle\rangle_{\boldsymbol{\Xi}} &= \int_{\mathcal{U}_1} \cdots \int_{\mathcal{U}_K} \sum_\pi (|\pi| - 1)!(-1)^{|\pi|-1} \prod_{B\in\pi} \left\langle \prod_{i\in B} F(u_i, \boldsymbol{\xi}) \right\rangle_{\boldsymbol{\Xi}} \prod_{k=1}^K h(u_k, \mathcal{U}_K)\, du_k \\
&= \int_{\mathcal{U}_1} \cdots \int_{\mathcal{U}_K} \langle\langle F(u_1, \boldsymbol{\xi}) \cdots F(u_K, \boldsymbol{\xi}) \rangle\rangle_{\boldsymbol{\Xi}} \prod_{k=1}^K h(u_k, \mathcal{U}_K)\, du_k
\end{aligned}
$$

A.4   Two Independent Conductance Inputs

The derivation of exact cumulants for the membrane equation with conductance synapses is presented here. Consider the following ODE with two independent shot noise inputs:

$$
\tau \frac{d}{dt} Y(t) = -Y(t)\left(1 + Q_E(t) + Q_I(t)\right) + w_E\, Q_E(t) + w_I\, Q_I(t)
$$

$$
Q_E(t) = \sum_{x_i \in \xi_E} g(t - x_i)\, H(t - x_i) \qquad\qquad w_E = \frac{E_E - E_L}{E_E - E_I}
$$

$$
Q_I(t) = \sum_{x_i \in \xi_I} g(t - x_i)\, H(t - x_i) \qquad\qquad w_I = \frac{E_I - E_L}{E_E - E_I}
$$

The solution is given by:

$$Y(t, \xi_E, \xi_I) = Y(t_0) \, e^{-\frac{1}{\tau} \int_{t_0}^{t} (1 + Q_E(u) + Q_I(u)) du} + \frac{1}{\tau} \int_{t_0}^{t} (w_E \, Q_E(z) + w_I \, Q_I(z)) \, e^{-\frac{1}{\tau} \int_{z}^{t} (1 + Q_E(u) + Q_I(u)) \, du} \, dz$$

Setting $Y(t_0) = 0$ and $t_0 \to -\infty$,

$$Y(t, \xi_E, \xi_I) = \frac{1}{\tau} \int_{-\infty}^{t} (w_E \, Q_E(z) + w_I \, Q_I(z)) \, e^{-\frac{1}{\tau} \int_{z}^{t} (1 + Q_E(u) + Q_I(u)) \, du} \, dz$$

For 2nd order moments:

$$Y(t_1, \xi_E, \xi_I) \, Y(t_2, \xi_E, \xi_I) = \frac{1}{\tau^2} \int_{-\infty}^{t_1} \int_{-\infty}^{t_2} (w_E \, Q_E(z_1) + w_I \, Q_I(z_1)) \, (w_E \, Q_E(z_2) + w_I \, Q_I(z_2))$$

$$e^{-\frac{1}{\tau} \int_{z}^{t} (1 + Q_E(u_1) + Q_I(u_1)) du_1 - \frac{1}{\tau} \int_{z}^{t} (1 + Q_E(u_2) + Q_I(u_2)) du_2} \, dz_1 \, dz_2$$

In terms of cumulants:

$$\langle Y_t \rangle = \frac{1}{\tau} \int_{-\infty}^{t} e^{-\frac{t-z}{\tau}} \left\langle (w_E \, Q_E(z) + w_I \, Q_I(z)) \, e^{-\frac{1}{\tau} \int_{z}^{t} (Q_E(u) + Q_I(u)) \, du} \right\rangle dz$$

$$= \frac{1}{\tau} \int_{-\infty}^{t} e^{-\frac{t-z}{\tau}} \left(w_E \left\langle Q_E(z) \, e^{-\frac{1}{\tau} \int_{z}^{t} Q_E(u) \, du} \right\rangle \left\langle e^{-\frac{1}{\tau} \int_{z}^{t} Q_I(v) \, dv} \right\rangle \right.$$

$$\left. + w_I \left\langle Q_I(z) \, e^{-\frac{1}{\tau} \int_{z}^{t} Q_I(u) \, du} \right\rangle \left\langle e^{-\frac{1}{\tau} \int_{z}^{t} Q_E(v) \, dv} \right\rangle \right) dz$$

$$= \frac{1}{\tau} \int_{-\infty}^{t} e^{-\frac{t-z}{\tau}} \left\langle e^{-\frac{1}{\tau} \int_{z}^{t} Q_E(u) \, du} \right\rangle \left\langle e^{-\frac{1}{\tau} \int_{z}^{t} Q_I(v) \, dv} \right\rangle$$

$$\left(w_E \int_{-\infty}^{z} g_E(z - x) \, e^{-\frac{1}{\tau} \int_{z}^{t} g_E(u - x) \, du} \, \lambda_E(x) \, dx + w_I \int_{-\infty}^{z} g_I(z - y) \, e^{-\frac{1}{\tau} \int_{z}^{t} g_I(u_2 - x) du_2} \, \lambda_I(y) \, dy \right) dz$$

For the autocovariance,

$$\langle\langle Y_1 \, Y_2\rangle\rangle = \frac{1}{\tau^2} \int\limits_{-\infty}^{t_1} \int\limits_{-\infty}^{t_2} e^{-\frac{t_1-z_1+t_2-z_2}{\tau}} \left\langle\left\langle (w_E \, Q_E(z_1) + w_I \, Q_I(z_1)) \, (w_E \, Q_E(z_2) + w_I \, Q_I(z_2)) \right.\right.$$

$$\left.\left. e^{-\frac{1}{\tau}\int_{z_1}^{t_1}(Q_E(u_1)+Q_I(u_1))du_1 - \frac{1}{\tau}\int_{z_2}^{t_2}(Q_E(u_2)+Q_I(u_2))du_2}\right\rangle\right\rangle dz_1 \, dz_2$$

$$= \frac{1}{\tau^2} \int\limits_{-\infty}^{t_1} \int\limits_{-\infty}^{t_2} e^{-\frac{t_1-z_1+t_2-z_2}{\tau}}$$

$$\left(w_E^2 \left\langle\left\langle Q_E(z_1) \, e^{-\frac{1}{\tau}\int_{z_1}^{t_1}(Q_E(u_1)+Q_I(u_1)) \, du_1} \, Q_E(z_2) \, e^{-\frac{1}{\tau}\int_{z_2}^{t_2}(Q_E(u_2)+Q_I(u_2))du_2}\right\rangle\right\rangle \right.$$

$$+ w_I^2 \left\langle\left\langle Q_I(z_1) \, e^{-\frac{1}{\tau}\int_{z_1}^{t_1}(Q_E(u_1)+Q_I(u_1))du_1} \, Q_I(z_2) \, e^{-\frac{1}{\tau}\int_{z_2}^{t_2}(Q_E(u_2)+Q_I(u_2))du_2}\right\rangle\right\rangle$$

$$+ w_E \, w_I \left\langle\left\langle Q_E(z_1) \, e^{-\frac{1}{\tau}\int_{z_1}^{t_1}(Q_E(u_1)+Q_I(u_1))du_1} \, Q_I(z_2) \, e^{-\frac{1}{\tau}\int_{z_2}^{t_2}(Q_E(u_2)+Q_I(u_2))du_2}\right\rangle\right\rangle$$

$$\left. + w_E \, w_I \left\langle\left\langle Q_I(z_1) \, e^{-\frac{1}{\tau}\int_{z_1}^{t_1}(Q_E(u_1)+Q_I(u_1))du_1} \, Q_E(z_2) \, e^{-\frac{1}{\tau}\int_{z_2}^{t_2}(Q_E(u_2)+Q_I(u_2))du_2}\right\rangle\right\rangle \right) dz_1 \, dz_2$$

where,

$$\left\langle Q_S(z_1) \, Q_S(z_2) \, e^{-\frac{1}{\tau}\int_{z_1}^{t_1}(Q_E(u)+Q_I(u)) \, du - \frac{1}{\tau}\int_{z_2}^{t_2}(Q_E(v)+Q_I(v)) \, dv}\right\rangle$$

$$= \left\langle Q_S(z_1) \, Q_S(z_2) \, e^{-\frac{1}{\tau}\int_{z_1}^{t_1} Q_E(u_1)du_1 - \frac{1}{\tau}\int_{z_2}^{t_2} Q_E(u_2)du_2}\right\rangle \left\langle e^{-\frac{1}{\tau}\int_{z_1}^{t_1} Q_I(u_1)du_1 - \frac{1}{\tau}\int_{z_2}^{t_2} Q_I(v)dv}\right\rangle$$

$$= \left\langle e^{-\frac{1}{\tau}\int_{z_1}^{t_1} Q_E(u) \, du - \frac{1}{\tau}\int_{z_2}^{t_2} Q_E(u_2) \, du_2}\right\rangle \left\langle e^{-\frac{1}{\tau}\int_{z_1}^{t_1} Q_I(u) \, du - \frac{1}{\tau}\int_{z_2}^{t_2} Q_I(u_2) \, du_2}\right\rangle$$

$$\left(\int\limits_{-\infty}^{\min(t_1,t_2)} g_S(z_1-x) \, g_S(z_2-x) \, e^{-\frac{1}{\tau}\int_{z_1}^{t_1} g_S(u_1-x)du_1 - \frac{1}{\tau}\int_{z_2}^{t_2} g_S(u_2-x)du_2} \lambda_S(x) \, dx \right.$$

$$+ \int\limits_{-\infty}^{t_1} g_S(z_1-x) \, e^{-\frac{1}{\tau}\int_{z_1}^{t_1} g_S(u_1-x)du_1 - \frac{1}{\tau}\int_{z_2}^{t_2} g_S(u_2-x)du_2} \lambda_S(x) \, dx$$

$$\left. \int\limits_{-\infty}^{t_2} g_S(z_2-y) \, e^{-\frac{1}{\tau}\int_{z_1}^{t_1} g_S(u_1-y)du_1 - \frac{1}{\tau}\int_{z_2}^{t_2} g_S(u_2-y) \, du_2} \lambda_S(y) \, dy \right)$$

and,

$$\left\langle Q_E(z_1) \, Q_I(z_2) \, e^{-\frac{1}{\tau}\int_{z_1}^{t_1}(Q_E(u_1)+Q_I(u_1))du_1 - \frac{1}{\tau}\int_{z_2}^{t_2}(Q_E(u_2)+Q_I(u_2))du_2}\right\rangle$$

$$= \left\langle Q_E(z_1) \, e^{-\frac{1}{\tau}\int_{z_1}^{t_1} Q_E(u_1)du_1 - \frac{1}{\tau}\int_{z_2}^{t_2} Q_E(u_2)du_2}\right\rangle \left\langle Q_I(z_2) \, e^{-\frac{1}{\tau}\int_{z_1}^{t_1} Q_I(u_1)du_1 - \frac{1}{\tau}\int_{z_2}^{t_2} Q_I(u_2)du_2}\right\rangle$$

$$= \left\langle e^{-\frac{1}{\tau}\int_{z_1}^{t_1} Q_E(u_1)du_1 - \frac{1}{\tau}\int_{z_2}^{t_2} Q_E(u_2)du_2}\right\rangle \left\langle e^{-\frac{1}{\tau}\int_{z_1}^{t_1} Q_I(u_1)du_1 - \frac{1}{\tau}\int_{z_2}^{t_2} Q_I(u_2)du_2}\right\rangle$$

$$\int\limits_{-\infty}^{t_1} g_E(z_1-x) \, e^{-\frac{1}{\tau}\int_{z_1}^{t_1} g_E(u_1-x)du_1 - \frac{1}{\tau}\int_{z_2}^{t_2} g_E(u_2-x)du_2} \lambda_E(x) \, dx$$

$$\int\limits_{-\infty}^{t_2} g_I(z_2-y) \, e^{-\frac{1}{\tau}\int_{z_1}^{t_1} g_I(u_1-y)du_1 - \frac{1}{\tau}\int_{z_2}^{t_2} g_I(u_2-y) \, du_2} \lambda_I(y) \, dy$$

Yielding:

$$\langle Y_1 \, Y_2 \rangle = \frac{1}{\tau^2} \int\limits_{-\infty}^{t_1} \int\limits_{-\infty}^{t_2} e^{-\frac{t_1 - z_1 + t_2 - z_2}{\tau}} \left\langle e^{-\frac{1}{\tau} \int_{z_1}^{t_1} Q_E(u_1) du_1 - \frac{1}{\tau} \int_{z_2}^{t_2} Q_E(u_2) \, du_2} \right\rangle \left\langle e^{-\frac{1}{\tau} \int_{z_1}^{t_1} Q_I(u_1) du_1 - \frac{1}{\tau} \int_{z_2}^{t_2} Q_I(u_2) \, du_2} \right\rangle$$

$$\left(w_E^2 \int\limits_{-\infty}^{\min(t_1, t_2)} g_E(z_1 - x) \, g_E(z_2 - x) \, e^{-\frac{1}{\tau} \int_{z_1}^{t_1} g_E(u_1 - x) du_1 - \frac{1}{\tau} \int_{z_2}^{t_2} g_E(u_2 - x) du_2} \lambda_E(x) \, dx \right.$$

$$+ w_I^2 \int\limits_{-\infty}^{\min(t_1, t_2)} g_I(z_1 - y) \, g_I(z_2 - y) \, e^{-\frac{1}{\tau} \int_{z_1}^{t_1} g_I(u_1 - y) du_1 - \frac{1}{\tau} \int_{z_2}^{t_2} g_I(u_2 - y) \, du_2} \lambda_I(y) \, dy$$

$$+ \left(w_E \int\limits_{-\infty}^{t_1} g_E(z_1 - x) \, e^{-\frac{1}{\tau} \int_{z_1}^{t_1} g_E(u_1 - x) du_1 - \frac{1}{\tau} \int_{z_2}^{t_2} g_E(u_2 - x) du_2} \lambda_E(x) \, dx \right.$$

$$\left. + w_I \int\limits_{-\infty}^{t_1} g_I(z_1 - x) \, e^{-\frac{1}{\tau} \int_{z_1}^{t_1} g_E(u_1 - x) du_1 - \frac{1}{\tau} \int_{z_2}^{t_2} g_E(u_2 - x) du_2} \lambda_I(x) \, dx \right)$$

$$\left(w_E \int\limits_{-\infty}^{t_2} g_I(z_2 - x) \, e^{-\frac{1}{\tau} \int_{z_1}^{t_1} g_I(u_1 - x) du_1 - \frac{1}{\tau} \int_{z_2}^{t_2} g_I(u_2 - x) du_2} \lambda_E(x) \, dx \right.$$

$$\left. \left. + w_I \int\limits_{-\infty}^{t_2} g_I(z_2 - x) \, e^{-\frac{1}{\tau} \int_{z_1}^{t_1} g_I(u_1 - x) du_1 - \frac{1}{\tau} \int_{z_2}^{t_2} g_I(u_2 - x) du_2} \lambda_I(x) \, dx \right) \right)$$

A.5 General Case

In this appendix the expectations for general case of linear first-order ODE filtering with shot noise input $R(t, \xi) = \sum_{x_j \in \xi} f(t - x_j) \, H(t - x_j)$ and $Q(t, \xi) = \sum_{x_k \in \xi} g(t - x_k) \, H(t - x_k)$ are derived. Applying the Slivnyak's theorem to the generalized random sums,

$$\langle Y_t \rangle = \int\limits_{\mathcal{U}} \left\langle e^{-\frac{1}{\tau} \int_z^t Q(u, \xi) \, du} \right\rangle \int\limits_{\mathcal{S}} f(z, x) \, e^{-\frac{1}{\tau} \int_z^t g(u, x) \, du} \lambda(x) \, dx \, dz$$

$$\langle Y_1 \, Y_2 \rangle = \int\limits_{\mathcal{U}} \int\limits_{\mathcal{U}} \left\langle e^{-\frac{1}{\tau} \int_{z_1}^{t_1} Q(u, \xi) \, du - \int_{z_2}^{t_2} Q(v, \xi) \, dv} \right\rangle$$

$$\left(\int\limits_{\mathcal{S}} f(z_1, x) \, f(z_2, x) \, e^{-\frac{1}{\tau} \int_{z_1}^{t_1} g(u, x) \, du - \frac{1}{\tau} \int_{z_2}^{t_2} g(v, x) \, dv} \lambda(x) \, dx \right.$$

$$+ \int\limits_{\mathcal{S}} f(z_1, x) \, e^{-\frac{1}{\tau} \int_{z_1}^{t_1} g(u, y) \, du - \frac{1}{\tau} \int_{z_2}^{t_2} g(v, y) \, dv} \lambda(y) \, dy$$

$$\left. \int\limits_{\mathcal{S}} f(z_2, w) \, e^{-\frac{1}{\tau} \int_{z_1}^{t_1} g(u, w) \, du - \frac{1}{\tau} \int_{z_2}^{t_2} g(v, w) \, dv} \lambda(w) \, dw \right) dz_1 \, dz_2$$

For the example with three independent PPP Ξ_1, Ξ_2 and Ξ_3:

$$\langle Y_t \rangle = \frac{1}{\tau} \int_{\mathcal{U}} \left\langle \left((1 - E_0 \sin(2\pi\omega z)) Q(z,\xi_3) + I_1(z,\xi_1) - I_2(z,\xi_3) \right) e^{-\frac{1}{\tau} \int_z^t (1+Q(u,\xi_3))du} \right\rangle dz$$

$$= \frac{1}{\tau} \int_{\mathcal{U}} (1 - E_0 \sin(2\pi\omega z)) e^{-\frac{t-z}{\tau}} \left\langle Q(z,\xi_3) e^{-\frac{1}{\tau} \int_z^t Q(u,\xi_3)du} \right\rangle dz$$

The autocovariance is given by:

$$\langle\langle Y_1 Y_2 \rangle\rangle = \frac{1}{\tau^2} \int_{\mathcal{U}} \int_{\mathcal{U}} \left\langle \left\langle \left((1 - E_0 \sin(2\pi\omega z_1)) Q(z_1,\xi_3) + I_1(z_1,\xi_1) - I_2(z_1,\xi_2) \right) e^{-\frac{1}{\tau} \int_{z_1}^{t_1} (1+Q(u,\xi_3))du} \right. \right.$$

$$\left. \left. \left((1 - E_0 \sin(2\pi\omega z_2)) Q(z_2,\xi_3) + I_1(z_2,\xi_1) - I_2(z_2,\xi_2) \right) e^{-\frac{1}{\tau} \int_{z_2}^{t_2} (1+Q(v,\xi_3))dv} \right\rangle \right\rangle dz_1\, dz_2$$

$$= \frac{1}{\tau^2} \int_{\mathcal{U}} \int_{\mathcal{U}} (1 - E_0 \sin(2\pi\omega z_1)) (1 - E_0 \sin(2\pi\omega z_2))$$

$$\left\langle \left\langle Q(z_1,\xi_3)\, Q(z_2,\xi_3)\, e^{-\frac{1}{\tau} \int_{z_1}^{t_1} Q(u,\xi_3)\,du - \frac{1}{\tau} \int_{z_2}^{t_2} Q(v,\xi_3)\,dv} \right\rangle \right\rangle dz_1\, dz_2$$

$$+ \frac{1}{\tau^2} \int_{\mathcal{U}} \int_{\mathcal{U}} \langle\langle (I_1(x_1,\xi_1) - I_2(x_1,\xi_2)) (I_1(x_2,\xi_1) - I_2(x_2,\xi_2)) \rangle\rangle \left\langle e^{-\frac{1}{\tau} \int_{x_1}^{t_1} Q(u,\xi_3)\,du - \frac{1}{\tau} \int_{x_2}^{t_2} Q(v,\xi_3)\,dv} \right\rangle dx_1\, dx_2$$

where $\langle I_1(t) \rangle = \langle I_2(t) \rangle$ leads once more to important simplifications. In the last integral for example,

$$\langle\langle (I_1(x_1,\xi_1) - I_2(x_1,\xi_2)) (I_1(x_2,\xi_1) - I_2(x_2,\xi_2)) \rangle\rangle$$
$$= \langle (I_1(x_1,\xi_1) - I_2(x_1,\xi_2)) (I_1(x_2,\xi_1) - I_2(x_2,\xi_2)) \rangle - \langle I_1(x_1,\xi_1) - I_2(x_1,\xi_2) \rangle \langle I_1(x_2,\xi_1) - I_2(x_2,\xi_2) \rangle$$
$$= \langle\langle I_1(x_1,\xi_1)\, I_1(x_2,\xi_1) \rangle\rangle + \langle\langle I_2(x_1,\xi_2)\, I_2(x_2,\xi_2) \rangle\rangle$$

A.6 Random Dirac Delta Sums

Consider synaptic input in the form of random Dirac delta sums $Q(t) = \sum_{t_k \in \xi} h\tau_s\, \delta(t - t_k)$. Writing $\gamma_k = \left(1 - e^{-\frac{kh\tau_s}{\tau}} \right)$,

$$\left\langle e^{-\frac{1}{\tau} \int_z^t Q(u,\xi)\,du} \right\rangle = \exp\left(\int_{\mathcal{S}} \left(e^{-\frac{h\tau_s}{\tau} \int_z^t \delta(u-x)\,du} - 1 \right) \lambda(x)\, dx \right)$$

$$= \exp\left(\int_{\mathcal{S}} \left(e^{-\frac{h\tau_s}{\tau} (H(t-x) - H(z-x))} - 1 \right) \lambda(x)\, dx \right) = \exp\left(\left(e^{-\frac{h\tau_s}{\tau}} - 1 \right) \int_z^t \lambda(x)\, dx \right)$$

$$= \exp\left(-\gamma_1 (m(t) - m(z)) \right)$$

$$\left\langle e^{-\frac{1}{\tau} \int_{z_1}^{t_1} Q(u,\xi)\,du - \frac{1}{\tau} \int_{z_2}^{t_2} Q(u,\xi)\,du} \right\rangle = \exp\left(\int_{\mathcal{S}} \left(e^{-\frac{h\tau_s}{\tau} (H(t_1-x) - H(z_1-x)) - \frac{h\tau_s}{\tau} (H(t_2-x) - H(z_2-x))} - 1 \right) \lambda(x)\, dx \right)$$

Reordering the limits of the shot noise integrals $\{z_1, t_1, z_2, t_2\} \to \{x_1, x_2, x_3, x_4\}$ with $x_1 \geq x_2 \geq$

$x_3 \geq x_4$ enables the following compact notation:

$$\left\langle e^{-\frac{1}{\tau} \int_{z_1}^{t_1} Q(u,\xi)\,du - \frac{1}{\tau} \int_{z_2}^{t_2} Q(u,\xi)\,du} \right\rangle$$

$$= \exp\Bigg(- \gamma_1(m(x_3) - m(x_4) + m(x_1) - m(x_2))$$

$$- \gamma_2(m(x_2) - m(x_3))\left(H(t_2 - z_1)\,H(t_1 - t_2) + H(t_1 - z_2)\,H(t_2 - t_1)\right)\Bigg)$$

$$= \begin{cases} e^{-\gamma_1(m(z_1) - m(z_2) + m(t_1) - m(t_2)) - \gamma_2(m(t_2) - m(z_1))} & \text{for } t_2 \geq z_1 \\ e^{-\gamma_1(m(t_1) - m(z_1) + m(t_2) - m(z_2))} & \text{otherwise} \end{cases}$$

The solution of the filtered process has the following form with $\mathcal{U}_i = [t_0, t_i[$,

$$Y(t) = 1 - e^{-\frac{t-t_0}{\tau} - \sum_{t_j \in \xi} \frac{h\tau_s}{\tau} \int_{t_0}^{t} \delta(u - t_j)\,du} - \frac{1}{\tau}\int_{\mathcal{U}} e^{-\frac{t-z}{\tau} - \sum_{t_j \in \xi} \frac{h\tau_s}{\tau} \int_{z}^{t} \delta(u - t_j)\,du}\,dz$$

The mean of the filtered process is given by:

$$\langle Y_t \rangle = 1 - e^{-\frac{t-t_0}{\tau}}\left\langle e^{-\sum_{t_j \in \xi} \frac{h\tau_s}{\tau} \int_{t_0}^{t} \delta(u - t_j)\,du} \right\rangle - \frac{1}{\tau}\int_{\mathcal{U}} e^{-\frac{t-z}{\tau}}\left\langle e^{-\sum_{t_j \in \xi} \frac{h\tau_s}{\tau} \int_{z}^{t} \delta(u - t_j)\,du} \right\rangle dz$$

$$= 1 - e^{-\frac{1}{\tau}(t - t_0 + \tau\gamma_1 m(t))} - \frac{1}{\tau}\int_{\mathcal{U}} e^{-\frac{1}{\tau}(t - z + \tau\gamma_1(m(t) - m(z)))}\,dz$$

In the case of constant input rate $\lambda(t) = \lambda$,

$$\frac{1}{\tau}\int_{t_0}^{t} e^{-(1+\lambda\tau\gamma_1)\frac{t-z}{\tau}}\,dz = \frac{1}{1 + \lambda\tau\gamma_1}\left(1 - e^{-(1+\lambda\tau\gamma_1)\frac{t-t_0}{\tau}}\right)$$

$$\langle Y_t \rangle = 1 - e^{-(1+\lambda\tau\gamma_1)\frac{t-t_0}{\tau}} - \frac{1}{1 + \lambda\tau\gamma_1}\left(1 - e^{-(1+\lambda\tau\gamma_1)\frac{t-t_0}{\tau}}\right) = \frac{\lambda\tau\gamma_1}{1 + \lambda\tau\gamma_1}\left(1 - e^{-(1+\lambda\tau\gamma_1)\frac{t-t_0}{\tau}}\right)$$

The stationary limit this yields the following compact result:

$$\langle Y_t \rangle_{\text{stat}} = \frac{\lambda\tau\gamma_1}{1 + \lambda\tau\gamma_1}$$

The autocovariance of the filtered process is given by:

$$\langle\langle Y_1 Y_2 \rangle\rangle = \left\langle\left\langle e^{-\frac{1}{\tau}\int_{t_0}^{t_1}(1+Q(u,\xi))du - \frac{1}{\tau}\int_{t_0}^{t_2}(1+Q(v,\xi))dv} \right\rangle\right\rangle$$

$$+ \frac{1}{\tau}\int_{\mathcal{U}_1}\left\langle\left\langle e^{-\frac{1}{\tau}\int_{z_1}^{t_1}(1+Q(u,\xi))du - \frac{1}{\tau}\int_{t_0}^{t_2}(1+Q(v,\xi))dv} \right\rangle\right\rangle dz_1$$

$$+ \frac{1}{\tau}\int_{\mathcal{U}_2}\left\langle\left\langle e^{-\frac{1}{\tau}\int_{t_0}^{t_1}(1+Q(u,\xi))du - \frac{1}{\tau}\int_{z_2}^{t_2}(1+Q(v,\xi))dv} \right\rangle\right\rangle dz_2$$

$$+ \frac{1}{\tau^2}\int_{\mathcal{U}_1}\int_{\mathcal{U}_2}\left\langle\left\langle e^{-\frac{1}{\tau}\int_{z_1}^{t_1}(1+Q(u,\xi))du - \frac{1}{\tau}\int_{z_2}^{t_2}(1+Q(v,\xi))dv} \right\rangle\right\rangle dz_1\,dz_2$$

The last term can be split in two integrals in order to use the compact formulation of the auto-covariance.

$$\frac{1}{\tau^2} \int_{t_0}^{t_1} \int_{t_0}^{t_2} \left\langle \left\langle e^{-\frac{1}{\tau}\int_{z_1}^{t_1}(1+Q(u,\xi))du - \frac{1}{\tau}\int_{z_2}^{t_2}(1+Q(v,\xi))dv} \right\rangle \right\rangle dz_1\, dz_2$$

$$= \frac{2}{\tau^2} \int_{t_0}^{t_2} \int_{t_0}^{z1} \left\langle \left\langle e^{-\frac{1}{\tau}\int_{z_1}^{t_1}(1+Q(u,\xi))du - \frac{1}{\tau}\int_{z_2}^{t_2}(1+Q(v,\xi))dv} \right\rangle \right\rangle dz_1\, dz_2$$

$$+ \frac{1}{\tau^2} \int_{t_2}^{t_1} \int_{t_0}^{t_2} \left\langle \left\langle e^{-\frac{1}{\tau}\int_{z_1}^{t_1}(1+Q(u,\xi))du - \frac{1}{\tau}\int_{z_2}^{t_2}(1+Q(v,\xi))dv} \right\rangle \right\rangle dz_1\, dz_2$$

$$= \frac{2}{\tau^2} \int_{t_0}^{t_2} \int_{t_0}^{z1} e^{-\frac{1}{\tau}(t_1-z_1+t_2-z_2+\tau\gamma_1(m(z_1)-m(z_2)+m(t_1)-m(t_2))+\gamma_2(m(t_2)-m(z_1)))} dz_1\, dz_2$$

$$+ \frac{1}{\tau^2} \int_{t_2}^{t_1} \int_{t_0}^{t_2} e^{-\frac{1}{\tau}(t_1-z_1+t_2-z_2+\tau\gamma_1(m(t_1)-m(z_1)+m(t_2)-m(z_2)))} dz_1\, dz_2$$

In the case of constant input rate $\lambda(t) = \lambda$,

$$\frac{1}{\tau^2} \int_{t_0}^{t_1} \int_{t_0}^{t_2} \left\langle \left\langle e^{-\frac{1}{\tau}\int_{z_1}^{t_1}(1+Q(u,\xi))du - \frac{1}{\tau}\int_{z_2}^{t_2}(1+Q(v,\xi))dv} \right\rangle \right\rangle dz_2\, dz_1$$

$$= \frac{2}{\tau^2} \int_{t_0}^{t_2} e^{-\frac{1}{\tau}(t_1-z_1+\tau\lambda\gamma_1(t_1-t_2)+\tau\lambda\gamma_2(t_2-z_1))} \int_{t_0}^{z_1} e^{-\frac{1}{\tau}(t_2-z_2+\tau\lambda\gamma_1(z_1-z_2))} dz_2\, dz_1$$

$$+ \frac{1}{\tau^2} \int_{t_2}^{t_1} e^{-\frac{1}{\tau}(t_1-z_1+\tau\lambda\gamma_1(t_1-z_1))} \int_{t_0}^{t_2} e^{-\frac{1}{\tau}(t_2-z_2+\tau\lambda\gamma_1(t_2-z_2))} dz_2\, dz_1$$

$$- \frac{1}{\tau^2} \int_{t_0}^{t_1} e^{-\frac{1}{\tau}(t_1-z_1+\tau\lambda\gamma_1(t_1-z_1))} dz_1 \int_{t_0}^{t_2} e^{-\frac{1}{\tau}(t_2-z_2+\tau\lambda\gamma_1(t_2-z_2))} dz_2$$

$$= \frac{2\, e^{-(1+\tau\lambda\gamma_1)\frac{t_1-t_2}{\tau}}}{\tau(1+\tau\lambda\gamma_1)} \int_{t_0}^{t_2} e^{-(2+\tau\lambda\gamma_2)\frac{t_2-z_1}{\tau}} \left(1 - e^{-(1+\tau\lambda\gamma_1)\frac{z_1-t_0}{\tau}}\right) dz_1$$

$$- \frac{1}{\tau^2} \int_{t_0}^{t_2} e^{-(1+\tau\lambda\gamma_1)\frac{t_1-z_1}{\tau}} dz_1 \int_{t_0}^{t_2} e^{-(1+\tau\lambda\gamma_1)\frac{t_2-z_2}{\tau}} dz_2$$

$$= \frac{2\, e^{-(1+\tau\lambda\gamma_1)\frac{t_1-t_2}{\tau}}}{1+\tau\lambda\gamma_1} \left(\frac{1}{2+\tau\lambda\gamma_2} \left(1 - e^{-(2+\tau\lambda\gamma_2)\frac{t_2-t_0}{\tau}}\right) \right.$$

$$\left. - \frac{1}{1-\tau\lambda\gamma_1+\tau\lambda\gamma_2} \left(e^{-(1+\tau\lambda\gamma_1)\frac{t_2-t_0}{\tau}} - e^{-(2+\tau\lambda\gamma_2)\frac{t_2-t_0}{\tau}}\right)\right)$$

$$- \frac{1}{(1+\tau\lambda\gamma_1)^2} \left(e^{-(1+\tau\lambda\gamma_1)\frac{t_1-t_2}{\tau}} - e^{-(1+\tau\lambda\gamma_1)\frac{t_1-t_0}{\tau}}\right) \left(1 - e^{-(1+\tau\lambda\gamma_1)\frac{t_2-t_0}{\tau}}\right)$$

The remaining two integrals have the following expressions,

$$\frac{1}{\tau}\int_{t_0}^{t_1}\left\langle\left\langle e^{-\frac{1}{\tau}\int_{z_1}^{t_1}(1+Q(u,\xi))du-\frac{1}{\tau}\int_{t_0}^{t_2}(1+Q(v,\xi))dv}\right\rangle\right\rangle dz_1$$

$$=\frac{1}{\tau}e^{-\frac{1}{\tau}(t_2-t_0+\tau\lambda\gamma_1(t_1-t_2))}\int_{t_0}^{t_2}e^{-\frac{1}{\tau}(t_1-z_1+\tau\lambda\gamma_1(z_1-t_0)+\tau\lambda\gamma_2(t_2-z_1))}\,dz_1$$

$$-\frac{1}{\tau}e^{-(1+\tau\lambda\gamma_1)\frac{t_2-t_0}{\tau}}\int_{t_0}^{t_2}e^{-(1+\tau\lambda\gamma_1)\frac{t_1-z_1}{\tau}}\,dz_1$$

$$=\frac{e^{-\frac{1}{\tau}(t_2-t_0+\tau\lambda\gamma_1(t_1-t_2))}}{1-\tau\lambda\gamma_1+\tau\lambda\gamma_2}\left(e^{-\frac{1}{\tau}(t_1-t_2+\tau\lambda\gamma_1(t_2-t_0))}-e^{-\frac{1}{\tau}(t_1-t_0+\tau\lambda\gamma_2(t_2-t_0))}\right)$$

$$-\frac{e^{-(1+\tau\lambda\gamma_1)\frac{t_2-t_0}{\tau}}}{1+\tau\lambda\gamma_1}\left(e^{-(1+\tau\lambda\gamma_1)\frac{t_1-t_2}{\tau}}-e^{-(1+\tau\lambda\gamma_1)\frac{t_1-t_0}{\tau}}\right)$$

$$\frac{1}{\tau}\int_{t_0}^{t_2}\left\langle\left\langle e^{-\frac{1}{\tau}\int_{t_0}^{t_1}(1+Q(u,\xi))du-\frac{1}{\tau}\int_{z_2}^{t_2}(1+Q(v,\xi))dv}\right\rangle\right\rangle dz_2$$

$$=\frac{1}{\tau}e^{-\frac{1}{\tau}(t_1-t_0+\tau\lambda\gamma_1(t_1-t_2))}\int_{t_0}^{t_2}e^{-\frac{1}{\tau}(t_2-z_2+\tau\lambda\gamma_1(z_2-t_0)+\tau\lambda\gamma_2(t_2-z_2))}dz_2$$

$$-\frac{1}{\tau}e^{-(1+\tau\lambda\gamma_1)\frac{t_1-t_0}{\tau}}\int_{t_0}^{t_2}e^{-(1+\tau\lambda\gamma_1)\frac{t_2-z_2}{\tau}}\,dz_2$$

$$=\frac{e^{-\frac{1}{\tau}(t_1-t_0+\tau\lambda\gamma_1(t_1-t_2))}}{1-\tau\lambda\gamma_1+\tau\lambda\gamma_2}\left(e^{-\frac{1}{\tau}(\tau\lambda\gamma_1(t_2-t_0))}-e^{-(1+\tau\lambda\gamma_2)\frac{t_2-t_0}{\tau}}\right)-\frac{e^{-(1+\tau\lambda\gamma_1)\frac{t_1-t_0}{\tau}}}{1+\tau\lambda\gamma_1}\left(1-e^{-(1+\tau\lambda\gamma_1)\frac{t_2-t_0}{\tau}}\right)$$

$$\left\langle\left\langle e^{-\frac{1}{\tau}\int_{t_0}^{t_1}(1+Q(u,\xi))du-\frac{1}{\tau}\int_{t_0}^{t_2}(1+Q(v,\xi))dv}\right\rangle\right\rangle=e^{-\frac{1}{\tau}(t_1-t_0+t_2-t_0+\tau\lambda\gamma_1(t_1-t_2)+\tau\lambda\gamma_2(t_2-t_0))}$$

In the stationary limit this yields,

$$\langle\langle Y_1\,Y_2\rangle\rangle_{\text{stat}}=\frac{1}{\tau^2}\int_{t_0}^{t_1}\int_{t_0}^{t_2}\left\langle\left\langle e^{-\frac{1}{\tau}\int_{z_1}^{t_1}(1+Q(u,\xi))du-\frac{1}{\tau}\int_{z_2}^{t_2}(1+Q(v,\xi))dv}\right\rangle\right\rangle_{\text{stat}}dz_2\,dz_1$$

$$=\frac{2\,e^{-(1+\tau\lambda\gamma_1)\frac{t_1-t_2}{\tau}}}{(1+\tau\lambda\gamma_1)(2+\tau\lambda\gamma_2)}-\frac{e^{-(1+\tau\lambda\gamma_1)\frac{t_1-t_2}{\tau}}}{(1+\tau\lambda\gamma_1)^2}=\frac{\tau\lambda\,(2\gamma_1-\gamma_2)}{(1+\tau\lambda\gamma_1)^2(2+\tau\lambda\gamma_2)}e^{-(1+\tau\lambda\gamma_1)\frac{t_1-t_2}{\tau}}$$

The filtered process $Y(t)$ can also be expressed in terms of the counting process $N(t)$.

$$Y(t)=1-e^{-\frac{t-t_0}{\tau}-\frac{h\tau_s}{\tau}N(t)}-\frac{1}{\tau}\int_{\mathcal{U}}e^{-\frac{t-z}{\tau}-\frac{h\tau_s}{\tau}(N(t)-N(z))}dz$$

which yields the same result for $\langle Y(t)\rangle$, since:

$$\left\langle e^{-\frac{h\tau_s}{\tau}n}\right\rangle=\sum_{n=0}^{\infty}\frac{\left(m(t)\,e^{-\frac{h\tau_s}{\tau}}\right)^n}{n!}e^{-m(t)}=e^{m(t)\,e^{-\frac{h\tau_s}{\tau}}}e^{-m(t)}=e^{-m(t)\left(1-e^{-\frac{h\tau_s}{\tau}}\right)}$$

A.7   Shot Noise Cumulants

Several statistics of shot noise are presented for exponential, alpha and bi-exponential kernels under constant $\lambda(u) = \lambda$. The nonstationary cumulants are evaluated at $T_0 = 0$ and the stationary cumulants are evaluated in the limit $T_0 \to -\infty$.

$$\langle\langle F_1 \ldots F_K \rangle\rangle = \int\limits_{T_0}^{\min(t_1,\ldots,t_K)} f(t_1, x) \cdots f(t_K, x)\, \lambda(x)\, dx$$

Box Kernel

Let $f(t, x) = h\, H(x + \tau_s - t)\, H(t - x)$.

$$\langle\langle F_1 \cdots F_K \rangle\rangle = \begin{cases} h^K \int_{\max(0,\max(t_1,\ldots,t_K)-\tau_s)}^{\min(t_1,\ldots,t_K)} \lambda(x)\, dx & \text{if } \max(t_1,\ldots,t_K) - \min(t_1,\ldots,t_K) \leq \tau_s \\[2ex] 0 & \text{otherwise} \end{cases}$$

Exponential Kernel

Let $f(t, u) = h\, e^{-\frac{t-x}{\tau_s}}\, H(t - x)$ and $\lambda(x) = \lambda$.

$$\langle\langle F_1 \cdots F_K \rangle\rangle = \frac{\lambda h^K \tau_s}{K}\, e^{\sum_{k=1}^{K} -\frac{t_k}{\tau_s}} \left(e^{\frac{K \min(t_1,\ldots,t_K)}{\tau_s}} - 1 \right)$$

In the stationary limit,

$$\langle\langle F_1 \cdots F_K \rangle\rangle_{\text{stat}} = \frac{\lambda h^K \tau_s}{K}\, e^{\sum_{k=1}^{K} -\frac{t_k - \min(t_1,\ldots,t_K)}{\tau_s}}$$

In particular,

$$\langle F_t \rangle = \lambda h \tau_s \left(1 - e^{-\frac{t}{\tau_s}} \right)$$

$$\langle\langle F_t^2 \rangle\rangle = \frac{\lambda h^2 \tau_s}{2} \left(1 - e^{-\frac{2t}{\tau_s}} \right)$$

$$\langle\langle F_1 F_2 \rangle\rangle = \frac{\lambda h^2 \tau_s}{2} \left(e^{-\frac{t_1 + t_2 - 2\min(t_1,t_2)}{\tau_s}} - e^{-\frac{t_1 + t_2}{\tau_s}} \right)$$

In the stationary limit,

$$\langle F_t \rangle_{\text{stat}} = \lambda h \tau_s$$

$$\langle\langle F_t^2 \rangle\rangle_{\text{stat}} = \frac{\lambda h^2 \tau_s}{2}$$

$$\langle\langle F_1 F_2 \rangle\rangle_{\text{stat}} = \frac{\lambda h^2 \tau_s}{2}\, e^{-\frac{t_1 + t_2 - 2\min(t_1,t_2)}{\tau_s}}$$

Alpha Kernel

Let $f(t, u) = h \frac{t-x}{\tau_s} e^{-\frac{t-x}{\tau_s}} H(t - x)$ and $\lambda(u) = \lambda$.

$$\langle F_t \rangle = \lambda h \left(\tau_s - (t + \tau_s) e^{-\frac{t}{\tau_s}} \right)$$

$$\langle\langle F_t^2 \rangle\rangle = \frac{\lambda h^2}{4 \tau_s} \left(\tau_s^2 - \left(2t^2 + \tau_s(2t + \tau_s) \right) e^{-\frac{2t}{\tau_s}} \right)$$

$$\langle\langle F_1 F_2 \rangle\rangle = \frac{\lambda h^2}{4 \tau_s} e^{-\frac{t_1 + t_2}{\tau_s}} \left(\left(e^{\frac{2 \min(t_1, t_2)}{\tau_s}} - 1 \right) (2t_1 t_2 + \tau_s(t_1 + t_2 + \tau_s)) \right.$$

$$\left. - 2 \min(t_1, t_2) e^{\frac{2 \min(t_1, t_2)}{\tau_s}} (t_1 + t_2 + \tau_s - \min(t_1, t_2)) \right)$$

In the stationary limit,

$$\langle F_t \rangle_{\text{stat}} = \lambda h \tau_s$$

$$\langle\langle F_t^2 \rangle\rangle_{\text{stat}} = \frac{\lambda h^2 \tau_s}{4}$$

$$\langle\langle F_1 F_2 \rangle\rangle_{\text{stat}} = \frac{\lambda h^2}{4 \tau_s} e^{-\frac{t_1 + t_2 - 2 \min(t_1, t_2)}{\tau_s}} (2t_1 t_2 + \tau_s(t_1 + t_2 + \tau_s) - 2 \min(t_1, t_2)(t_1 + t_2 + \tau_s - \min(t_1, t_2)))$$

Bi-Exponential Kernel

Let $f(t, x) = h \frac{\tau_s}{\tau_s - \tau_r} \left(e^{-\frac{t-x}{\tau_s}} - e^{-\frac{t-x}{\tau_r}} \right) H(t - x)$ with $\tau_s \neq \tau_r$ and $\lambda(u) = \lambda$.

$$\langle F_t \rangle = \frac{\lambda h \tau_s}{\tau_s - \tau_r} \left(\tau_s \left(1 - e^{-\frac{t}{\tau_s}} \right) - \tau_r \left(1 - e^{-\frac{t}{\tau_r}} \right) \right)$$

$$\langle\langle F_t^2 \rangle\rangle = \frac{\lambda}{2(\tau_s + \tau_r)} \left(\frac{h \tau_s}{\tau_s - \tau_r} \right)^2 \left(\tau_s (\tau_s + \tau_r) \left(1 - e^{-\frac{2t}{\tau_s}} \right) + \tau_r (\tau_s + \tau_r) \left(1 - e^{-\frac{2t}{\tau_r}} \right) \right.$$

$$\left. -4 \tau_s \tau_r \left(1 - e^{-\frac{t}{\tau_s} - \frac{t}{\tau_r}} \right) \right)$$

$$\langle\langle F_1 F_2 \rangle\rangle = \frac{\lambda}{2(\tau_s + \tau_r)} \left(\frac{h \tau_s}{\tau_s - \tau_r} \right)^2 \left(\tau_s (\tau_s + \tau_r) \left(e^{\frac{2 \min(t_1, t_2)}{\tau_s}} - 1 \right) e^{-\frac{t_1 + t_2}{\tau_s}} \right.$$

$$+ \tau_r (\tau_s + \tau_r) \left(e^{\frac{2 \min(t_1, t_2)}{\tau_r}} - 1 \right) e^{-\frac{t_1 + t_2}{\tau_r}}$$

$$\left. -2 \tau_s \tau_r \left(e^{\left(\frac{1}{\tau_s} + \frac{1}{\tau_r} \right) \min(t_1, t_2)} - 1 \right) \left(e^{-\frac{t_1}{\tau_s} - \frac{t_2}{\tau_r}} + e^{-\frac{t_1}{\tau_r} - \frac{t_2}{\tau_s}} \right) \right)$$

In the stationary limit,

$$\langle F_t \rangle_{\text{stat}} = \lambda h \tau_s$$

$$\langle\langle F_t^2 \rangle\rangle_{\text{stat}} = \frac{\lambda (h \tau_s)^2}{2(\tau_s + \tau_r)}$$

$$\langle\langle F_1 F_2 \rangle\rangle_{\text{stat}} = \frac{\lambda}{2(\tau_s + \tau_r)} \left(\frac{h \tau_s}{\tau_s - \tau_r} \right)^2 \left(\tau_s (\tau_s + \tau_r) e^{-\frac{t_1 + t_2 - 2 \min(t_1, t_2)}{\tau_s}} + \tau_r (\tau_s + \tau_r) e^{-\frac{t_1 + t_2 - 2 \min(t_1, t_2)}{\tau_r}} \right.$$

$$\left. -2 \tau_s \tau_r e^{\left(\frac{1}{\tau_s} + \frac{1}{\tau_r} \right) \min(t_1, t_2)} \left(e^{-\frac{t_1}{\tau_s} - \frac{t_2}{\tau_r}} + e^{-\frac{t_1}{\tau_r} - \frac{t_2}{\tau_s}} \right) \right)$$

A.8 Expectation of Random Product

Writing $\mathcal{S} = [T_0, T[$ and $m(t) \equiv \int_{T_0}^{t} \lambda(x)\,dx$ with $t \geq T_0$ and $f(u, x) = g(u - x)\,H(u - x)$,

$$\ln \left\langle e^{-\int_z^t Q(u,\xi)\,du} \right\rangle = \int_{\mathcal{S}} \left(e^{-\int_z^t g(u-x)\,H(u-x)\,du} - 1 \right) \lambda(x)\,dx$$

$$= -m(t) + \int_{T_0}^{z} e^{-\int_z^t g(u-x)\,du} \lambda(x)\,dx + \int_z^t e^{-\int_y^t g(v-y)\,dv} \lambda(y)\,dy$$

Random Dirac Delta Sums

Let $g(t, x)_{\text{delta}} = h\,\tau_s\,\delta(t - x)$,

$$\ln \left\langle e^{-\frac{1}{\tau}\int_z^t Q(u,\xi)\,du} \right\rangle = \int_{\mathcal{S}} \left(e^{-\frac{h\tau_s}{\tau}(H(t-x)-H(z-x))} - 1 \right) \lambda(x)\,dx$$

$$= -(m(t) - m(z)) \left(1 - e^{-\frac{h\tau_s}{\tau}} \right)$$

$$\ln \left\langle e^{-\frac{1}{\tau}\int_{z_1}^{t_1} Q(u,\xi)\,du - \frac{1}{\tau}\int_{z_2}^{t_2} Q(u,\xi)\,du} \right\rangle = \int_{\mathcal{S}} \left(e^{-\frac{h\tau_s}{\tau}(H(t_1-x)-H(z_1-x)) - \frac{h\tau_s}{\tau}(H(t_2-x)-H(z_2-x))} - 1 \right) \lambda(x)\,dx$$

$$= -\left(1 - e^{-\frac{h\tau_s}{\tau}} \right) (m(x_3) - m(x_4) + m(x_1) - m(x_2))$$

$$- \left(1 - e^{-\frac{2h\tau_s}{\tau}} \right) (m(x_2) - m(x_3))\,(H(t_2 - z_1)\,H(t_1 - t_2) + H(t_1 - z_2)\,H(t_2 - t_1))$$

with $\{x_1, x_2, x_3, x_4\}$ being a reordering of $\{z_1, t_1, z_2, t_2\}$ such that $x_1 \geq x_2 \geq x_3 \geq x_4$.

Box Kernel

Let $g(t, x)_{\text{delta}} = h\,H(t - x)\,H(x + \tau - t)$,

For $z \leq t \leq \tau$:

$$\ln \left\langle e^{-\int_z^t Q(u,\xi)\,du} \right\rangle_{\text{box}} = z\,e^{\alpha h(t-z)} + \frac{1}{\alpha h} \left(e^{\alpha h(t-z)} - 1 \right)$$

For $\{z, t - z\} \leq \tau \leq t$:

$$\ln \left\langle e^{-\int_z^t Q(u,\xi)\,du} \right\rangle_{\text{box}} = -\lambda t + \lambda(\tau - (t - z))\,e^{\alpha h(t-z)}\,du - \frac{\lambda}{\alpha h} \left(e^{\alpha h(\tau-z)} - e^{\alpha h(t-z)} \right) + \frac{\lambda}{\alpha h} \left(e^{\alpha h(t-z)} - 1 \right)$$

For $z \leq \tau \leq t - z \leq t$:

$$\ln \left\langle e^{-\int_z^t Q(u,\xi)\,du} \right\rangle_{\text{box}} = -\lambda t + \frac{\lambda}{\alpha h} \left(1 - e^{-\alpha h z} \right) e^{\alpha h\tau} + \frac{\lambda}{\alpha h} \left(e^{\alpha h\tau} - 1 \right) + \lambda(t - z - \tau)\,e^{\alpha h\tau}$$

For $t - z \leq \tau \leq z \leq t$:

$$\ln \left\langle e^{-\int_z^t Q(u,\xi)\,du} \right\rangle_{\text{box}} = -\lambda t + \lambda(\tau - (t - z))\,e^{\alpha h(t-z)} + \frac{2\lambda}{\alpha h} \left(e^{\alpha h(t-z)} - 1 \right) + \lambda(z - \tau)$$

For $\tau \leq \{z, t - z\}$:

$$\ln \left\langle e^{-\int_z^t Q(u,\xi)\,du} \right\rangle_{\text{box}} = -\lambda t + \frac{2\lambda}{\alpha h} \left(e^{\alpha h\tau} - 1 \right) + \lambda(z - \tau) + \lambda(t - z - \tau)\,e^{\alpha h\tau}$$

Exponential Kernel

Let $g(t, x) = h\, e^{-\frac{t-x}{\tau_s}}\, H(t - x)$.

$$\ln \left\langle e^{-\frac{1}{\tau} \int_z^t Q(u,\xi)\, du} \right\rangle_{\exp} = -\lambda t - \lambda \tau_s\, \Gamma \left(0, \frac{h\tau_s}{\tau} \left(1 - e^{-\frac{t-z}{\tau_s}} \right), \frac{h\tau_s}{\tau} \left(1 - e^{-\frac{t-z}{\tau_s}} \right) e^{-\frac{z}{\tau_s}} \right)$$

$$- \lambda \tau_s\, e^{-\frac{h\tau_s}{\tau}}\, \Gamma \left(0, -\frac{h\tau_s}{\tau}, -\frac{h\tau_s}{\tau}\, e^{-\frac{t-z}{\tau_s}} \right)$$

where $\Gamma(z, a, b) = \int_a^b e^{-x}\, x^{z-1}\, dx$ is the generalized incomplete gamma function.

Part II

Research Articles

Chapter 3

Nonstationary filtered shot-noise processes and applications to neuronal membranes

Summary

In this article we derive the exact nonstationary cumulants for a passive neuronal membrane model with a single synapse type with conductance synapses. The synaptic input is modeled by a shot noise process with variable rate. This very basic case is important since it introduces most techniques that are applied to more complex membrane models in the research articles in Chapters 4 and 5. A single shot noise input enables to write the solution of the membrane equation in terms of the key statistic of the model: the exponential of integrated shot noise. This simplifies the derivation of the *central moments expansion* (CME) and avoids the longer expressions that result from applying the Slivnyak-Mecke theorem directly.

We start by presenting a simple model of filtered shot noise process with multiplicative noise and variable input rate that is a scaled and translated version of the membrane equation. The solution of the system is derived for an arbitrary realization of shot noise, followed by an integration by parts step that re-expresses the solution in terms of an integral of the exponential of integrated shot noise. A small review of PPP statistics in the real line follows and the notion of causal PPP transformation is introduced. The solution of the filtered system corresponds to two PPP transformations: integral transform and random product. We investigate the moments and cumulants of these PPP transformations and use them to establish the cumulants of the filtered process. The different steps of this derivation are comprised of well-known results and its merit is to establish the cumulants of the filtered process from first principles, and extending to nonstationary input rate. Comparison with numerical simulations is made to illustrate the exact nature of these results.

The case of single synapse type already leads to long and complex expressions for the cumulants of the filtered process. The original formulation would result in even longer expressions, with the variance written in three lines instead of one, for example. However, the exact solution is still not trivial to analyze due to the superposed levels of integration, and in particular, does not show explicitly which shot noise cumulants have major contributions to the cumulants of the filtered process. The central moments expansion provides such insight. The CME corresponds to a delta method for approximating the moments of a random variable with terms up to the second order kept. The zeroth order corresponds to the deterministic solution of the filtered system, where the shot noise input is replaced by its mean value. The first order CME for a cumulant of order K is expressed in cumulants of integrated shot noise of same order.

54

The second order includes cumulants of integrated shot noise of order up to $2K$. Numerical simulations illustrate the excellent accuracy for the mean of the filtered process since it is second order of the delta method. The second order cumulants of the filtered process are well approximated by the first order CME, but some parameter regimes may require the second order CME. The stationary limit of CME enables to recover previously established results for the exponential and alpha kernels in regards to the mean and variance. A novel expression for the autocovariance is also provided.

These results are applied to a simple model of neuronal membrane with continuously variable rate of presynaptic spikes. The membrane equation is a scaled and translated version of the filtered process and its cumulants are obtained from the properties of cumulants under such transformations. The nonstationary cumulants are used to approximate the time-evolving distribution of V_m, which illustrates their importance in the statistical dynamics of the system. A gaussian approximation is constructed with nonstationary mean and variance of V_m. Higher order approximations integrate higher order cumulants of membrane potential using a truncated Edegeworth series based on the gaussian distribution. The skweness and kurtosis are well captured by the third and fourth order as illustrated by numerical simulations. A second application of this formalism uses the nonstationary mean of shot noise to estimate the presynaptic rate from a small number of intracellular recordings of V_m recordings. The simulated traces were corrupted with additive noise to simulate instrumental measurement noise.

The flow of derivations and results presented in the first part of this article are similar to those included in Chapters 4 and 5.

This article has been accepted for publication in the journal Physical Review E on the 26th March 2015.

Résumé

L'évolution de systèmes aux entrées stochastiques de type *"shot noise"* (appelé aussi *bruit de grenaille*) a souvent été modelisée avec succès par des processus de *shot noise filtré* sur une large variété de domaines d'application, allant de l'électronique à la biologie. En particuler, ces processus peuvent modéliser le potentiel de membrane V_m des neurones sujet à des entrées stochastiques. Ces processus filtrés arrivent à représenter les caractéristiques non-stationnaires des fluctuations du V_m en réponse à des entrées pré-synaptiques à taux variable. Dans cet article, nous appliquons le formalisme général des transformations de *processus ponctuels de Poisson* dans le but d'analyser ces systèmes dans le cadre général de systèmes à taux d'entrée variable. Nous avons obtenu des expressions analytiques exactes, ainsi que des approximations très efficaces, pour les cumulants joints des processus de *shot noise filtré* avec bruit multiplicatif. Ensuite, ces résultats généraux ont été appliqués à un modèle de membrane neuronale à conductance synaptique alimenté par *shot noise* à taux variable. Nous proposons des approximations très efficaces pour l'évolution temporelle de la distribution du V_m, ainsi qu'une méthode simple pour estimer le taux pré-synaptique à partir d'un nombre très réduit de traces du V_m. Ces résultats ouvrent la perspective d'obtenir un accès analytique à différentes statistiques importantes des modèles neuronaux à conductance tels que le *temps de premier passage*.

Nonstationary filtered shot-noise processes and applications to neuronal membranes

Marco Brigham, Alain Destexhe

26/03/2015

Abstract

Filtered shot noise processes have proven to be very effective in modeling the evolution of systems exposed to shot noise sources and have been applied to a wide variety of fields ranging from electronics through biology. In particular, they can model the membrane potential V_m of neurons driven by stochastic input, where these filtered processes are able to capture the nonstationary characteristics of V_m fluctuations in response to presynaptic input with variable rate. In this paper we apply the general framework of Poisson point processes transformations to analyze these systems in the general case of nonstationary input rates. We obtain exact analytic expressions, as well as different approximations, for the joint cumulants of filtered shot noise processes with multiplicative noise. These general results are then applied to a model of neuronal membranes subject to conductance shot noise with a continuously variable rate of presynaptic spikes. We propose very effective approximations for the time evolution of the V_m distribution and a simple method to estimate the presynaptic rate from a small number of V_m traces. This work opens the perspective of obtaining analytic access to important statistical properties of conductance-based neuronal models such as the first passage time.

1 Introduction

We investigate the statistical properties of systems that can be described by the filtering of shot noise input through a linear first-order ordinary differential equation (ODE) with variable coefficients. Such systems give rise to filtered shot noise processes with multiplicative noise. The membrane potential V_m fluctuations of neurons can be modeled as filtered shot noise currents or conductances [Verveen and De-Felice, 1974, Tuckwell, 1988]. These fluctuations have been previously analyzed in the stationary limit of shot noise conductances with constant rate [Kuhn *et al.*, 2004, Richardson and Gerstner, 2005, Rudolph and Destexhe, 2005, Burkitt, 2006a], and an exact analytical solution has been obtained for the mean and joint moments of exponential shot noise [Wolff and Lindner, 2008, 2010]. However, many neuronal systems evolve in nonstationary regimes driven by shot noise with variable input rate. A typical example is provided by visual system neurons that receive presynaptic input with time-varying rate that reflects an evolving visual landscape. Modeling studies often consider the exponential shot noise case, whereas biological systems may display larger diversity including slow rising impulse response functions similar to alpha and bi-exponential functions, for example. Previous studies have addressed nonstationary exponential shot noise conductances and nonstationary currents [Cai *et al.*, 2006, Amemori and Ishii, 2001, Burkitt, 2006b].

Poisson point processes (PPP) provide a natural model of random input arrival times that are distributed according to a Poisson law that may vary in time. Application-oriented treatments of PPP theory and PPP transformations can be found in Refs. [Moller and Waagepetersen, 2003, Streit, 2010]. The key idea of this article is to express the filtered process as a transformation of random input arrival times and to apply the properties of PPP transformations to derive its nonstationary statistics. Using this formalism we derive exact analytical expressions for the mean and joint cumulants of the filtered process in the general case of variable input rate. We develop an approximation based on a power expansion of the expectation about the deterministic solution. We apply these results to a simple neuronal membrane model of sub-threshold membrane potential V_m fluctuations that evolves under shot noise conductance with continuously variable rate of presynaptic spikes.

Shot noise processes are simple yet powerful models of stochastic input that correspond to the superposition of impulse responses arriving at random times according to a Poisson law. Systems evolving under

shot noise input have been observed across many domains, such as electronics [Campbell, 1909, Schottky, 1918], optics [Picinbono *et al.*, 1970, Rousseau, 1971], and many other fields [Snyder and Miller, 1991, Parzen, 1999]. Shot noise was discovered in the early works of Campbell and Schottky [Campbell, 1909, Schottky, 1918]. Key theoretical results were obtained by Rice [Rice, 1945] and a modern review of their probabilistic structure is presented in Ref. [Rice, 1977]. Filtered shot noise processes with multiplicative noise are an extension of *filtered Poisson process* [Snyder and Miller, 1991, Parzen, 1999, Streit, 2010] that are generated by linear transformations of PPPs.

In this article, we start by presenting a simple model of filtered shot noise process with multiplicative noise and variable input rate (Sec. 2). We next consider the general case of PPP transformations and their properties (Sec. 3). Exact analytic expressions for the joint cumulants of the filtered process are derived (Sec. 4) in addition to an approximation of the exact analytical solution (Sec. 5). Finally, we apply these results to a simple neuronal membrane model of sub-threshold V_m fluctuations with continuously variable rate of presynaptic spikes and explore several practical applications (Sec. 6).

2 Model of Filtered Shot Noise Process

In this section we present a simple model of filtered shot noise process with multiplicative noise. This stochastic process results from the filtering of shot noise input through a linear first-order ODE with variable coefficients. We show that under very simple input rate conditions the filtered process is non-stationary. We derive the time course of the filtered process in terms of the shot noise arrival times. The numerical simulation parameters are presented at the end of this section.

Consider the time evolution $Y(t)$ of a system governed by a linear first-order ODE with variable coefficients that is driven by shot noise input $Q(t)$:

$$\tau \frac{d}{dt} Y(t) = -Y(t) + (1 - Y(t)) Q(t) \tag{1}$$

$$Q(t) = \sum_{x_j \in \xi} g(t - x_j) H(t - x_j) \tag{2}$$

where τ is a time constant, ξ is the set of shot noise arrival times, $g(t - x_j) H(t - x_j)$ is the impulse response function at time t for arrival time $x_j \in \xi$ and $H(u)$ is the Heaviside function. The impulse response function is also known as *shot noise kernel*.

The input arrival times ξ in Eq. (2) are distributed according to a Poisson law as is characteristic of shot noise. The time evolution of this system is both stochastic and deterministic: stochastic since it is driven by random input arrival times ξ, but also deterministic since to each ξ corresponds a unique outcome. The system response $Y(t, \xi)$ is said to be a filtered version of the shot noise process $Q(t, \xi)$ since Eq. (1) changes its spectral characteristics.

Nonstationary dynamics are introduced in the model by restricting input arrival times to occur between t_a and $t_b \geq t_a$ with constant Poisson rate λ. A single realization of shot noise input $Q(t, \xi)$ and the resulting system response $Y(t, \xi)$ are shown in Fig. 1. The mean and standard deviation ($\mu \pm \sigma$) of both processes are clearly nonstationary since they vary in time.
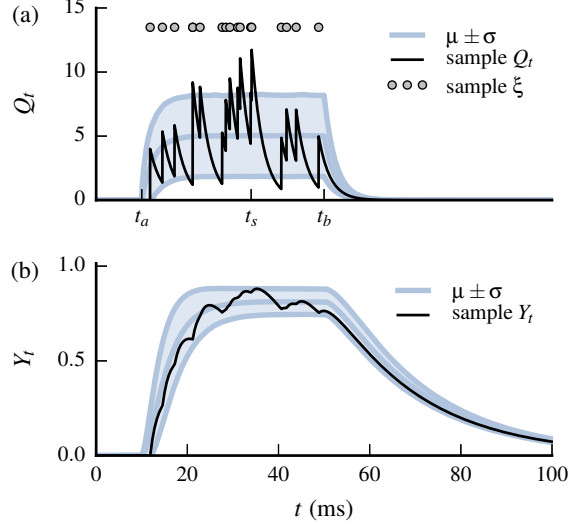
Figure 1 – *Single realization and basic statistics of filtered shot noise process Y_t under shot noise input Q_t. (a) Random input arrival times $x_j \in \xi$ generate nonstationary shot noise $Q_t \equiv Q(t, \xi)$. The input arrival times are distributed with a variable Poisson rate $\lambda(t)$ that restricts the arrivals to occur between t_a and t_b. (b) Nonstationary system response $Y_t \equiv Y(t, \xi)$ driven by shot noise Q_t. A single realization of random arrival times ξ is represented by gray dots; realizations of Q_t and Y_t are shown in black lines. The mean and standard deviation ($\mu \pm \sigma$) of Q_t and Y_t are shown by gray lines and are clearly nonstationary.*

The system response $Y(t, \xi)$ for a particular shot noise input $Q(t, \xi)$ is obtained by solving Eq. (1). For a given set of input arrival times ξ and initial value $Y_0 = 0$,

$$
Y(t, \xi) = \frac{1}{\tau} \int_{-\infty}^{t} e^{-\frac{t-z}{\tau}} \, Q(z, \xi) \, e^{-\frac{1}{\tau} \int_z^t Q(u, \xi) \, du} \, dz
$$

$$
= \frac{1}{\tau} \int_{-\infty}^{t} e^{-\frac{t-z}{\tau}} \sum_{x_j \in \xi} g(z - x_j) \, H(z - x_j) \prod_{x_i \in \xi} e^{-\frac{1}{\tau} \int_z^t g(u - x_i) \, H(u - x_i) \, du} \, dz \tag{3}
$$

The input arrival times ξ completely determine the time evolution of $Y(t, \xi)$. Equation (3) also shows that the response at time t for each input arrival x_j also depends on later input arrivals $x_i \leq t$. For a single shot noise source the solution can be further simplified using integration by parts:

$$
Y(t, \xi) = 1 - \frac{1}{\tau} \int_{-\infty}^{t} e^{-\frac{t-z}{\tau}} \prod_{x_i \in \xi} e^{-\frac{1}{\tau} \int_z^t g(u - x_i) \, H(u - x_i) \, du} \, dz \tag{4}
$$

The remainder of this article addresses the question of how to obtain the cumulants of the quantity on the left side of Eq. (4) from those on the right side, in the particular case of Poisson distributed input arrival times ξ with variable rate $\lambda(t)$. For reasons of concise presentation, instead of Eq. (3), we consider the equivalent Eq. (4).

The numerical simulations were generated with the rate function $\lambda(t)$ represented in Fig. 2(a) and exponential kernel shot noise with $g(t - x) = h \exp\left(-(t - x)/\tau_s\right)$. Other parameters are $t_{max} = 0.1$ s, $\tau = 0.02$ s, $\lambda = 500$ Hz, $h = 4$ and $\tau_s = 0.0025$ s.

3   Causal Point Process Transformations

We review the basic properties of PPP transformations and analyze the stochastic process generated by causal PPP transformations. The expectation of PPP transformations yields the joint cumulants of the

associated processes. We illustrate this approach with the shot noise process and compare the predicted mean and second order cumulants with numerical simulations.

We consider a PPP $\Xi(\mathcal{S}, \lambda)$ that generates *points* in the interval $\mathcal{S} \subseteq \mathbb{R}$ of the real line with rate function $\lambda(x) \geq 0$ such that $m(\mathcal{S}) \equiv \int_{\mathcal{S}} \lambda(x)\,dx$ is finite for any bounded interval $\mathcal{S}$. A realization ξ of Ξ contains a set of $n \geq 0$ points $\{x_1, \ldots, x_n\} \in \mathcal{S}$ that we associate with input arrival times. A PPP is said to be homogeneous for constant $\lambda(t) = \lambda$ and inhomogeneous otherwise. Example rate functions and sample realizations of the associated inhomogeneous PPP are shown in Fig. 2. These rate functions were used to generate input arrival times for the filtered shot noise process of Sec. 2 and the presynaptic spikes for the neuronal membrane of Sec. 6.
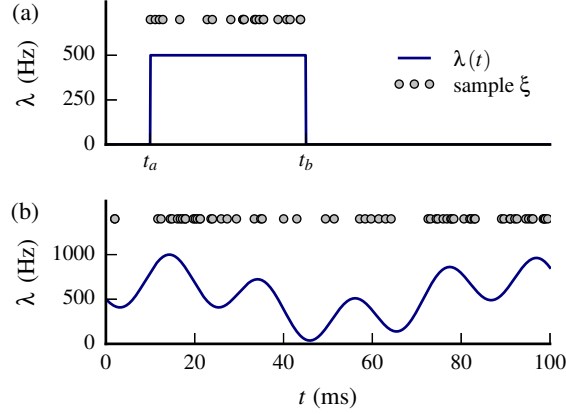

Figure 2 – *Rate function $\lambda(t)$ examples for inhomogeneous PPP. A single realization of input arrival times ξ is represented by gray dots above the rate functions (blue lines) marking the location of input arrival times $x_j \in \xi$. (a) Rate function used to generate input arrival times for the filtered shot noise process of Sec. 2. (b) Rate function used to generate presynaptic spike times for the neuronal membrane of Sec. 6.*

We consider a transformation $F(t, \xi)$ that for each real parameter $t \in \mathcal{S}$ and realization ξ evaluates to a positive real number $F_t = F(t, \xi)$. The transformation is assumed invariant under permutation of $x_j \in \xi$, such that when written as a regular function we have $F(t, x_1, \ldots, x_n) = F(t, \{x_1, \ldots, x_n\})$.

The expectation of $F(t, \xi)$ is obtained from the ensemble average over the number n of points and their locations $\{x_1, \ldots, x_n\}$:

$$\langle F(t, \xi) \rangle = \sum_{n=0}^{\infty} \frac{1}{n!} e^{-m(\mathcal{S})} \int_{\mathcal{S}} \cdots \int_{\mathcal{S}} F(t, x_1, \ldots, x_n) \prod_{j=1}^{n} \lambda(x_j)\,dx_j \tag{5}$$

We now focus on the class of PPP transformations that are causal in the time parameter t. Such transformations ensure that arrivals $x_j \in \xi$ later than t cannot affect the value of $F(t, \xi)$. A single realization ξ generates the entire time course of $F(t, \xi)$ and we therefore associate a *slave stochastic process* $F_t \equiv F(t, \xi)$ to the causal PPP transformation $F(t, \xi)$. By construction, the expectation of F_t is the expectation of $F(t, \xi)$ given by Eq. (5). This is illustrated in Fig. 3, where the value of shot noise process F_t at different times is evaluated from the same realization ξ.
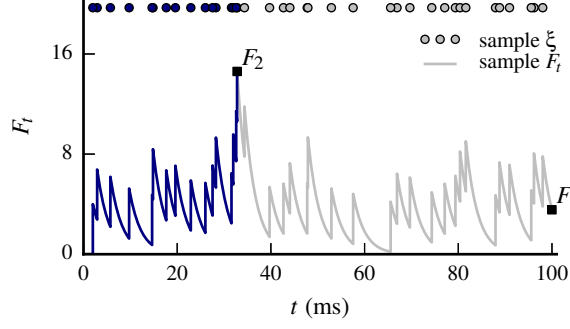
4

Figure 3 – *A shot noise process F_t is a causal PPP transformation $F(t, \xi)$ of input arrival times $x_j \in \xi$. This particular PPP transformation is defined in Eq. (2) and its causality ensures that F_t is not affected by input arrivals later than t. For example, the value of $F_2 = F(t_2, \xi)$ is determined by input arrivals $x_j \in \xi$ up to t_2 (blue line) and is not affected by input arrivals later than t_2 (light gray line). The dots above F_t mark the location of input arrival times $x_j \in \xi$.*

We write $F_1, \ldots, F_K$ for the values of stochastic process F_t at times $t_1, \ldots, t_K$, $\langle F_1 \cdots F_K \rangle$ for its joint moments and $\langle\langle F_1 \cdots F_K \rangle\rangle$ for its joint cumulants. The expectation of PPP transformations enables to obtain analytical expressions for the joint moments and joint cumulants of F_t: its joint moments are obtained by evaluating the expectation of suitable products $F(t_1, \xi) \cdots F(t_K, \xi)$ and its joint cumulants can be constructed explicitly from the joint moments. For example, the moment $\langle F_1 F_2^2 \rangle$ is evaluated by the expectation $\langle F(t_1, \xi) F(t_2, \xi)^2 \rangle$.

The causality of $F(t, \xi)$ enables to consider the PPP in the entire real line ($\mathcal{S} = \mathbb{R}$) with finite activity intervals constructed by setting $\lambda(t) = 0$ outside the activity windows. This approach yields exact analytical expressions for the joint cumulants of nonstationary processes generated from causal PPP transformations as illustrated next with the nonstationary shot noise process from Sec. 2. A shot noise process is a particular type of *random sum*, which is a PPP transformation that factors as $F(t, \xi) = \sum_{x_j \in \xi} f(t, x_j)$. The joint cumulants of random sums are given by the *Campbell Theorem* [Campbell, 1909, Rice, 1945] and are also derived for reference in Appendix A:

$$\langle\langle F_1 \ldots F_K \rangle\rangle = \int_{\mathcal{S}} f(t_1, x) \cdots f(t_K, x) \, \lambda(x) \, dx \tag{6}$$

where $f(t, x)$ is the impulse response function at time t for an input arrival time x. Shot noise is a causal random sum with $f(t, x) = g(t - x) H(t - x)$.

The expectation of more general forms of random sums, such as those in Eq. (3), are provided by the *Slivnyak-Mecke Theorem* [Slivnyak, 1962, Mecke, 1967]. A comparison between numerical simulations and *Campbell Theorem* predictions is shown in Fig. 4 with excellent agreement for the mean and second order cumulants. The autocorrelation at times t_1 and t_2 is given by $\rho(F_1 F_2) = \langle\langle F_1 F_2 \rangle\rangle / (\sigma(F_1) \sigma(F_2))$ where $\langle\langle F_1 F_2 \rangle\rangle$ is the autocovariance at times t_1 and t_2 and $\sigma(F_t)$ is the standard deviation at time t.
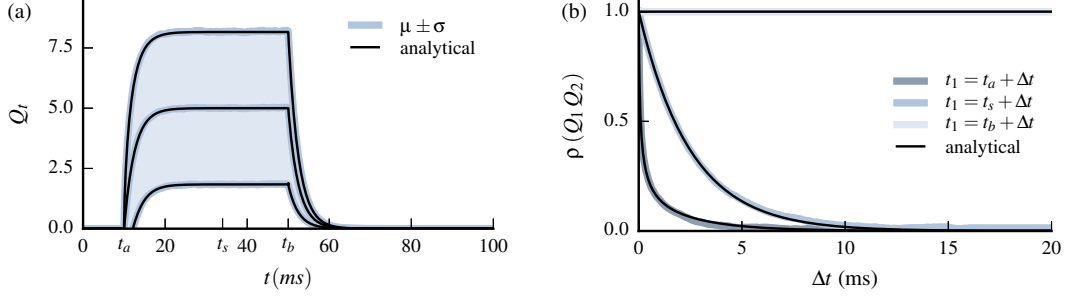
5

Figure 4 – *Comparison with numerical simulations for (a) the mean and standard deviation and (b) the autocorrelation of the shot noise process Q_t from Sec. 2 as predicted by the Campbell Theorem (Eq. (6)). There is excellent agreement between the simulations (gray lines) and the analytic predictions (black lines) with the respective lines overlapping. The autocorrelation ρ is evaluated at t_a, t_s, and t_b corresponding respectively to the onset of PPP activity, quasi-stationary Q_t, and extinction of PPP activity.*

4 Exact Analytical Solution

We use the properties of PPP transformations to derive exact analytical expressions for the cumulants of filtered shot noise processes with multiplicative noise and variable input rate. We investigate transformations that are relevant to these filtered processes: integral transform and random products. We evaluate their cumulants and compare with numerical simulations the predicted mean and second order cumulants of the filtered process.

According to Eq. (4), the filtered process Y_t is the integral of a causal PPP transformation that factors as a product of exponentials of input arrival times $x_j \in \xi$. We now investigate these transformations and define an *integral transform* of $F(t, \xi)$ with regards to a positive and bounded function w:

$$SF(t,\xi) = \int_{-\infty}^{t} F(u,\xi)\, w(u,t)\, du \tag{7}$$

The mean and joint moments of the integral transform are calculated by interchanging the infinite sum and integrals of the expectation Eq. (5) with the integral of the transform provided any one side of the equalities is finite (*Fubini-Tonelli Theorem*).

$$\langle SF_t \rangle = \left\langle \int_{-\infty}^{t} F(u,\xi)\, w(u,t)\, du \right\rangle = \int_{-\infty}^{t} \langle F(u,\xi) \rangle\, w(u,t)\, du \tag{8}$$

$$\langle SF_1 \cdots SF_K \rangle = \int_{-\infty}^{t_1} \cdots \int_{-\infty}^{t_K} \langle F(u_1,\xi) \cdots F(u_K,\xi) \rangle \prod_{l=1}^{K} w(u_l, t_l)\, du_l \tag{9}$$

The linearity of integration extends Eq. (9) to the joint cumulants:

$$\langle\langle SF_1 \cdots SF_K \rangle\rangle = \int_{-\infty}^{t_1} \cdots \int_{-\infty}^{t_K} \langle\langle F(u_1,\xi) \cdots F(u_K,\xi) \rangle\rangle \prod_{l=1}^{K} w(u_l, t_l)\, du_l \tag{10}$$

We now analyze *random products* that are PPP transformations factoring as $F(t,\xi) = \prod_{x_j \in \xi} f(t, x_j)$. The joint moments of random products are well known, and as shown in Appendix A:

$$\langle F_1 \ldots F_K \rangle = \exp\left(\int_{\mathcal{S}} \left(\prod_{k=1}^{K} f(t_k, x) - 1 \right) \lambda(x)\, dx \right) \tag{11}$$

6

We have gathered all the elements to derive the mean and joint cumulants of the filtered process Y_t. Writing $Q(t, \xi) = Q(t)$ and using the properties of joint cumulants,

$$\langle Y_t \rangle = 1 - \frac{1}{\tau} \int_{-\infty}^{t} \left\langle e^{-\frac{1}{\tau} \int_z^t Q(u)\,du} \right\rangle e^{-\frac{t-z}{\tau}}\,dz \tag{12}$$

$$\langle\langle Y_1 \cdots Y_K \rangle\rangle = \left(-\frac{1}{\tau}\right)^K \int_{-\infty}^{t_1} \cdots \int_{-\infty}^{t_K} \left\langle\left\langle \prod_{k=1}^{K} e^{-\frac{1}{\tau} \int_{z_k}^{t_k} Q(u)\,du} \right\rangle\right\rangle \prod_{l=1}^{K} e^{-\frac{t_l - z_l}{\tau}}\,dz_l \tag{13}$$

The expectation of the random product of exponentials is obtained from Eq. (11) and yields:

$$\left\langle \prod_{k=1}^{K} e^{-\frac{1}{\tau} \int_{z_k}^{t_k} Q(u)\,du} \right\rangle = \exp\left(\int_{\mathcal{S}} \left(\prod_{k=1}^{K} e^{-\frac{1}{\tau} \int_{z_k}^{t_k} g(u-x)\,H(u-x)\,du} - 1 \right) \lambda(x)\,dx \right) \tag{14}$$

Replacing Eq. (14) into Eqs. (12) and (13) yields the exact solution for the joint cumulants of filtered shot noise process with multiplicative noise and variable input rate. The random product expectation of Eq. (14) is the key element in the evaluation of the mean and joint cumulants, which was already identified in previous work [Wolff and Lindner, 2008, 2010], where closed expressions were obtained for expo- nential kernel shot noise with constant rate. As our derivation shows, this extends to any shot noise kernel $g(t-x)\,H(t-x)$ and variable input rate $\lambda(t)$ and is the main original contribution of this work.

The comparison between numerical simulations and the predictions from Eqs. (12) and (13) are shown in Fig. 5. There is excellent agreement even in such a nonstationary scenario with the system undergoing transient evolution. The numerical evaluation of Eqs. (12) and (13) can be performed very efficiently with the trapezoidal rule due to the double exponential in the integrand.
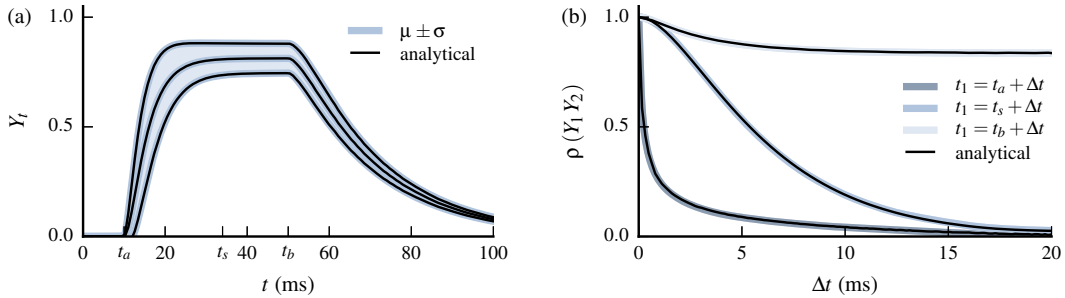

Figure 5 – *Comparison with numerical simulations for (a) the mean and standard deviation and (b) the autocorrelation of the filtered process Y_t predicted by the exact analytic solution given by Eqs. (12) and (13). There is excellent agreement between the simulations (gray lines) and the analytic predictions (black lines) with the respective lines overlapping. The autocorrelation ρ is evaluated at t_a, t_s, and t_b corresponding respectively to the onset of PPP activity, quasi-stationary Y_t, and extinction of PPP activity.*

5   Central Moments Expansion

We propose an approximation of the exact analytical solution that is based on a power expansion about the deterministic solution. The central moments expansion (CME) yields a series in the central moments of integrated shot noise. We compare this approximation for the mean and second order cumulants with numerical simulations, including the case of constant Poison rate.

The deterministic solution of Eq. (1) with mean shot noise input $\langle Q(u) \rangle$ is given by:

$$\langle Y_t \rangle_0 = 1 - \frac{1}{\tau} \int_{-\infty}^{t} e^{-\frac{t-z}{\tau}} e^{-\frac{1}{\tau} \int_z^t \langle Q(u) \rangle\,du}\,dz$$

This suggests an expansion about the deterministic solution $\langle Y_t \rangle_0$ by performing power expansions of the random product expectations in Eqs. (12) and (13). The integrated mean shot noise is first factored out of the random product and a power expansion of the resulting exponential is performed. This corresponds to the delta method technique [Cramér, 1946, Oehlert, 1992] for approximating expectations of random variable transformations and yields a series in the central moments of integrated shot noise. As shown in Appendix B, the second order expansion for a single random product yields:

$$\left\langle e^{-\frac{1}{\tau} \int_z^t Q(u)\, du} \right\rangle \simeq e^{-\frac{1}{\tau} \int_z^t \langle Q(u) \rangle\, du} \left(1 + \frac{1}{2} \left\langle \left(-\frac{1}{\tau} \int_z^t (Q(u) - \langle Q(u) \rangle)\, du \right)^2 \right\rangle \right)$$

This provides the following approximation for the mean of the filtered process:

$$\langle Y_t \rangle_2 = 1 - \frac{1}{\tau} \int_{-\infty}^t e^{-\frac{1}{\tau} \int_z^t (1 + \langle Q(u) \rangle)\, du} \left(1 + \frac{1}{2\tau^2} \int_z^t \int_z^t \langle\langle Q(u_1)\, Q(u_2) \rangle\rangle\, du_1\, du_2 \right) dz \tag{15}$$

where the subscript 2 represents the second order of the expansion.

Extending to joint cumulants is straightforward by expanding each exponential individually and collecting terms of same order in $1/\tau$. The first order expansion for the autocovariance is given by:

$$\langle\langle Y_1\, Y_2 \rangle\rangle_1 = \frac{1}{\tau^4} \int_{-\infty}^{t_1} \int_{-\infty}^{t_2} e^{-\frac{1}{\tau} \int_{z_1}^{t_1} (1 + \langle Q(u) \rangle)\, du - \frac{1}{\tau} \int_{z_2}^{t_2} (1 + \langle Q(v) \rangle)\, dv} \int_{z_1}^{t_1} \int_{z_2}^{t_2} \langle\langle Q(u_1)\, Q(u_2) \rangle\rangle\, du_1\, du_2\, dz_1\, dz_2 \tag{16}$$

The first order expansion for the variance is obtained from Eq. (16) by replacing $t_1 = t_2 = t$. The comparison between numerical simulations and the predictions from Eqs. (15) and (16) are shown in Fig. 6. There is good agreement for the mean but lower accuracy for second order cumulants. This can be improved with the second order expansion for the autocovariance that is provided in Appendix B.
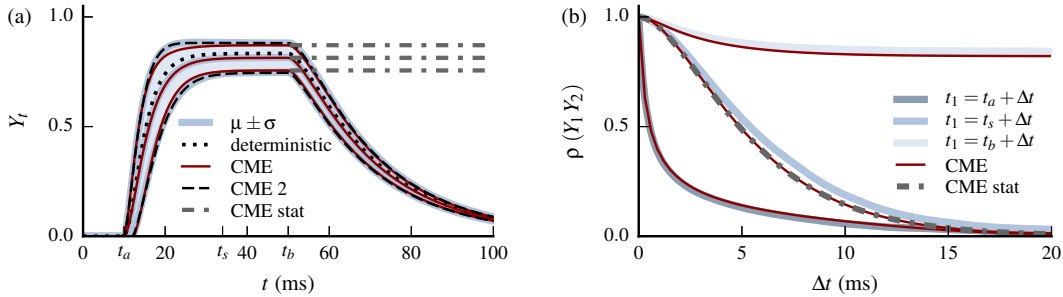

Figure 6 – *Comparison with numerical simulations for (a) the mean and standard deviation and (b) the autocorrelation of the central moments expansion given by Eqs. (15) and (16). There is good agreement between the simulations (full gray lines) and the approximation (full red lines) for the mean but lower accuracy for second order cumulants. This is corrected by the second order expansion for the autocovariance (dashed black lines) that is provided in Appendix B. The stationary limit (dashed dotted gray lines) is also shown. The deterministic solution (dotted black line) displays considerable approximation error.*

We found that the second order expansion for the mean and autocovariance consistently provided good results in the parameter regimes of neuron cells (as seen in Fig. 6(a) and Fig. 9 below). Under these conditions, third and fourth order expansions either did not provide significant improvements over the second order or even resulted in worse approximations, in which case much higher order expansions would be required to improve on the second order. Under certain parameter regimes the first order expansion for the autocovariance (Eq. (16)) may already provide good results (see Fig. 8 below).

The stationary limit of the filtered process reflects the statistics of long running trials under shot noise input with constant rate. The cumulants for this regime can be obtained by placing the onset of input arrival times at $-\infty$ and replacing the mean and second order cumulants of shot noise in Eqs (15) and (16) with their stationary limits. After integration by parts,

$$\langle Y_t \rangle_2 = \frac{\langle Q \rangle}{1 + \langle Q \rangle} - \frac{\langle\langle Q^2 \rangle\rangle}{(1 + \langle Q \rangle)^2} \frac{1}{\tau} \int_{-\infty}^{t} e^{-\frac{t-z}{\tau}(1 + \langle Q \rangle)} r(t - z) \, dz \tag{17}$$

$$\langle\langle Y_1 Y_2 \rangle\rangle_1 = \frac{\langle\langle Q^2 \rangle\rangle}{(1 + \langle Q \rangle)^2} \frac{1}{\tau^2} \int_{-\infty}^{t_1} \int_{-\infty}^{t_2} e^{-\frac{t_1 - z_1 + t_2 - z_2}{\tau}(1 + \langle Q \rangle)} r(|z_1 - z_2|) \, dz_1 \, dz_2 \tag{18}$$

where $\langle Q \rangle$, $\langle\langle Q^2 \rangle\rangle$ and $\langle\langle Q_1 Q_2 \rangle\rangle = \langle\langle Q^2 \rangle\rangle r(|t_1 - t_2|)$ are, respectively, the mean, variance, and auto-covariance of stationary shot noise.

The stationary limits for the mean and second order cumulants of the exponential and alpha kernels are presented in Appendix B.1.

6   Application to Neuronal Membranes

We apply the previous results to a simple model of membrane potential $V_m(t)$ fluctuations and explore several practical applications. We first calculate the nonstationary cumulants and compare them with numerical simulations. The central moment expansion (CME) is compared with previously published analytical estimates for the stationary limit of $V_m(t)$. The nonstationary cumulants are integrated in truncated Edgeworth series to approximate the time-evolving distribution of $V_m(t)$, which is compared with numerical simulations. We propose a simple method to estimate $\lambda(t)$ from a small number of noisy realizations of $V_m(t)$ and compare the inferred rate to the original presynaptic rate function. The numerical simulation parameters are presented below.

We consider a simple model of the membrane potential $V_m(t)$ for a passive neuron without spiking mechanism that is driven by shot noise conductance $G(t)$. This model has a single synapse type and is directly applicable to experiments where one type of synapse is isolated [Okun and Lampl, 2008]. The time evolution of $V_m(t)$ under conductance shot noise input $G(t)$ is given by the following membrane equation:

$$\tau_m \frac{d}{dt} V_m(t) = E_l - V_m(t) + (E_s - V_m(t)) \frac{1}{g_l} G(t) \tag{19}$$

$$\frac{1}{g_l} G(t) = \sum_{x_j \in \xi} g(t - x_j) H(t - x_j) \tag{20}$$

where τ_m is the membrane time constant, E_l is the resting potential, E_s is the synaptic reversal potential, g_l is the leak conductance and ξ is a set of presynaptic spike times.

The membrane equation is a scaled and translated version of Eq. (1) with the following change of variables:

$$V_m(t) = (E_s - E_l) Y(t) + E_l \qquad\qquad Q(t) = \frac{1}{g_l} G(t)$$

A single realization of conductance shot noise $G_t \equiv G(t, \xi)$ and the resulting membrane potential response $V_t \equiv V_m(t, \xi)$ are shown in Fig. 7, where the mean and standard deviation of both processes are also represented. The numerical simulations were generated with the rate function $\lambda(t)$ represented in Fig. 2(b) and alpha kernel shot noise with $g(t - x) = h(t - x/\tau_s) \exp(-(t - x)/\tau_s)$. Other parameters are $\tau_m = 0.02$ s, $E_l = -0.06$ V, $E_s = 0$ V and $g_l = 10\text{E-}9$ S in addition to those detailed in Section 2. The quantal conductance is $4\text{E-}9$ S corresponding to $h = 0.4$.
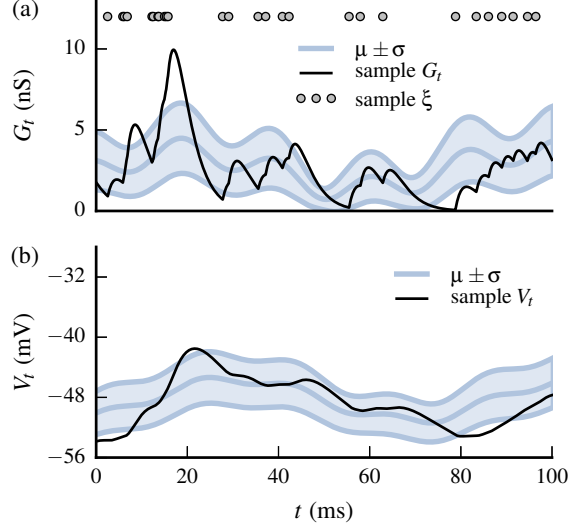
Figure 7 – *Single realization and basic statistics of membrane potential V_t fluctuations under conductance shot noise input G_t. (a) Random presynaptic spike times $x_j \in \xi$ generate nonstationary shot noise conductance $G_t \equiv G(t,\xi)$. The presynaptic spike times are distributed with a continuously varying rate $\lambda(t)$. (b) Nonstationary membrane potential $V_t \equiv V(t,\xi)$ driven by shot noise conductance G_t. A single realization of spike times ξ is represented by gray dots; realizations of G_t and V_t are shown in black lines. The mean and standard deviation ($\mu \pm \sigma$) of G_t and V_t are shown with gray lines.*

6.1 Nonstationary Cumulants

A first application of this formalism is to derive the mean and joint cumulants of V_t from those of Y_t. Using the properties of the mean and cumulants of random variables for each value of t yields the required relationships:

$$\langle V_t \rangle = (E_s - E_l)\langle Y_t \rangle + E_l \qquad\qquad \langle\langle V_1 \cdots V_K \rangle\rangle = (E_s - E_l)^K \langle\langle Y_1 \cdots Y_K \rangle\rangle \tag{21}$$

The comparison between numerical simulations and the predictions from Eq. (21) is shown in Fig. 8. There is excellent agreement with the predictions from both the exact analytical solution given by Eqs. (12) and (13) and the CME given by Eqs (15) and (16). The deterministic solution is obtained from Eq. (21) by replacing $\langle Y_t \rangle$ with $\langle Y_t \rangle_0$ and displays good agreement with mean V_t.
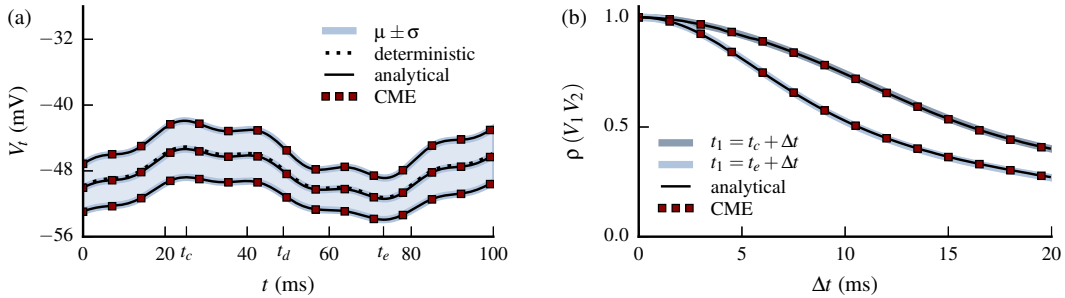
Figure 8 – *Comparison with numerical simulations for (a) the mean and standard deviation and (b) the autocorrelation of membrane potential V_t predicted by the exact analytical solution (full black lines) and the central moments expansion (red squares). There is excellent agreement between the simulations (full gray lines) and the analytic prediction for both methods with the respective lines overlapping. The deterministic solution (dotted black line) also displays good agreement with mean V_t. The autocorrelation ρ is evaluated at local maxima (t_c) and minima (t_e) of mean V_t.*

In this parameter regime, the approximation error of the CME is very low (on the order of 0.01 mV).

However, additional terms of the expansion may be required to reach similar precision in other parameter regimes. In order to illustrate this, we increase the quantal conductance by a factor of 20 (to 80 nS) with the effect of raising mean V_t very close to the reversal potential E_s. As shown in Fig. 9, the CME is still in very good agreement for the mean but the approximation error is larger for the standard deviation (on the order of several millivolts). The second order expansion for the standard deviation results in lower approximation error (in the order of 1 mV) but requires evaluating third and fourth order cumulants of integrated shot noise. The approximation error for the deterministic solution also increases to several mV.
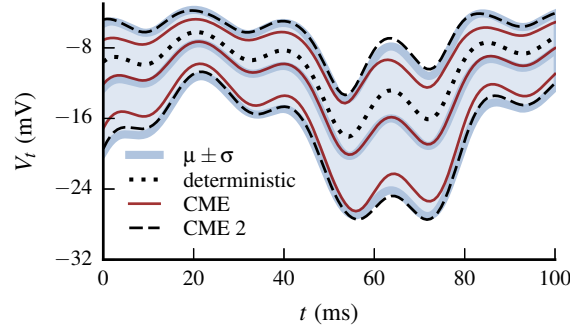

Figure 9 – *Same parameter regime as Fig. 8 but with quantal conductance increased by a factor of 20 ($h = 80$ nS). The mean and standard deviation of the numerical simulations (full gray lines) display excellent agreement with the exact analytical solution but are omitted for clarity. The approximation error for the CME (full red lines) remains low for the mean but increases significantly for both the standard deviation and the deterministic solution (dotted black line). The second order expansion for the standard deviation (dashed black lines) results in lower approximation error.*

The Appendix B.2 provides analytical expressions for the CME in the stationary limit of V_t for the mean and second order cumulants of exponential and alpha kernels. These expressions are obtained by applying Eq. (21) to Eqs. (17) and (18) and are consistent with previous analytical estimates for the mean and standard deviation that were derived with different approaches: Fokker-Planck methods for exponential kernel shot noise [Richardson and Gerstner, 2005, Rudolph and Destexhe, 2005] given by Eqs. (24), and a shot noise approach for alpha kernel shot noise [Kuhn *et al.*, 2004] given by Eqs. (26). The extension to the autocovariance is given by Eqs. (25), and (27) respectively.

6.2 Probability Distribution Approximation

A second application of this formalism is to use the nonstationary cumulants to approximate the time evolving distribution of membrane potential fluctuations. The mean and standard deviation of V_t yield a Gaussian approximation that successfully captures the time evolution of $p(V_t)$ as illustrated in Fig. 10. As expected, the skew of the distribution is not well captured by the Gaussian approximation, which has been reported in both experimental [Destexhe and Paré, 1999] and theoretical studies [Richardson and Gerstner, 2005, Rudolph and Destexhe, 2005]. The quantal conductance was increased by a factor of 4 (to 16 nS) in these simulations.
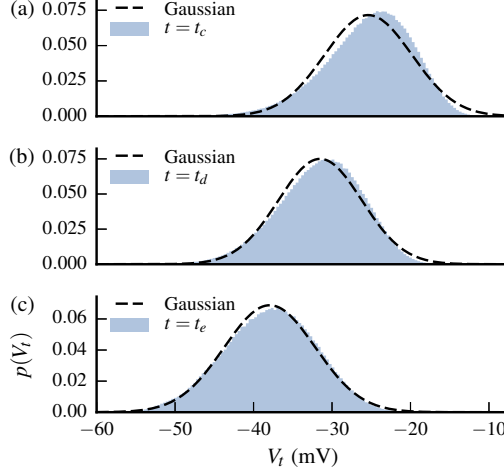
Figure 10 – *Nonstationary density of membrane potential $p(V_t)$ evaluated at three different times times: t_c, t_d, and t_e corresponding to (a), (b), and (c), respectively, (see abscissa of Fig. 8(a)). Comparison between the empirical histogram (gray) and the Gaussian approximation (dashed line) based on nonstationary mean and variance of V_t. The time evolution of $p(V_t)$ is captured successfully by this approximation, which as expected also misses the skew of $p(V_t)$.*

Deviations from the Gaussian distribution are expected whenever cumulants of order three or higher are present in $p(V_t)$. We use a truncated Edgeworth series [Edgeworth, 1907, Cramér, 1946, Wallace, 1958] to account for these deviations since it provides an asymptotic expansion of $p(V_t)$ in terms of its cumulants. In particular, we use the Edgeworth series expanded from the Gaussian distribution distribution as discussed in [Badel, 2011]. This has the advantage of coinciding with the Gaussian approximation whenever cumulants of order three or higher are negligible. This is an important aspect since approximately Gaussian shapes of $p(V_t)$ are sometimes present in experimental intracellular recordings. In terms of the normalized process $X_t = (V_t - \langle V_t \rangle)/\sigma_t$ with $\sigma_t \equiv \sqrt{\langle\langle V_t^2 \rangle\rangle}$, the truncated fourth order Edgeworth series is given by:

$$
p_{Ew4}\left(X_t = x\right) = \frac{1}{\sigma_t}\left(1 + \frac{1}{3!}\frac{\langle\langle V_t^3 \rangle\rangle}{\sigma_t^3}\left(x^3 - 3x\right)\right.
$$
$$
\left. + \frac{1}{4!}\frac{\langle\langle V_t^4 \rangle\rangle}{\sigma_t^4}\left(x^4 - 6x^2 + 3\right) + \frac{10}{6!}\frac{\langle\langle V_t^3 \rangle\rangle^2}{\sigma_t^6}\left(x^6 - 15x^4 + 45x^2 - 15\right)\right)\mathcal{N}(x)
$$
(22)

where $\mathcal{N}(x) = \exp(-x^2/2)/\sqrt{2\pi}$ is the standard normal density and $p(V_t = v) \simeq p_{Ew}\left(x = \frac{v - \langle V_t \rangle}{\sigma_t}\right)$. The third order Edgeworth series is given by the the first two terms.

As illustrated in the left side of Fig. 11, the skewness of $p(V_t)$ is indeed captured by the third order of the Edgeworth series. Figure 11(c) also shows a slight overestimation near the peak of $p(V_t)$, which is successfully captured by the fourth order, as shown in the right side of this figure.
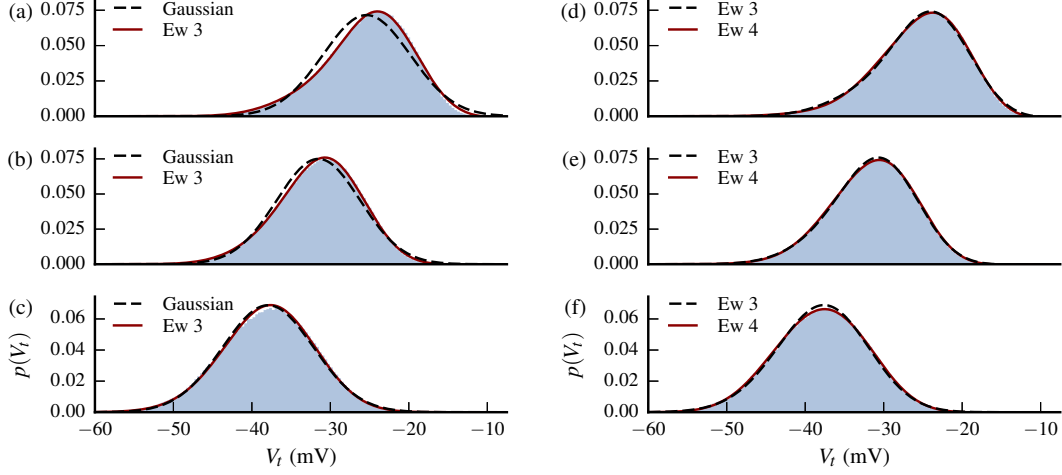
Figure 11 – *(a)-(c): Comparison at times t_c, t_d, and t_e between the empirical histogram (gray), Gaussian approximation (dashed black line), and the third order Edgeworth series (full red line). (d)-(f): Comparison at times t_c, t_d, and t_e between the empirical histogram (gray), third order Edgeworth series (dashed black line), and fourth order Edgeworth series (full red line). The slight discrepancy at the peak of the empirical histogram in (c) is successfully captured by the fourth order Edgeworth series in (f).*

Under more extreme parameter regimes, additional terms of the Edgeworth series may be needed to approximate $p(V_t)$. In such cases, the asymptotic character of the series becomes relevant since the truncation error is of the same order as the first neglected term of the series. An important caveat is that the truncated series may yield negative values for certain values of x. This is intrinsic to Edgeworth series that are constructed in the set of orthogonal polynomials associated with the base distribution (*Hermite polynomials* in the case of the standard normal distribution). The truncated series integrates to unity but may result in an invalid density function since negatives values are possible. Algorithms for computing an Edgeworth series to an arbitrary order are provided in Refs. [Petrov, 1962, Blinnikov and Moessner, 1998].

6.3 presynaptic Rate Estimation

Another application of this formalism is to estimate the nonstationary presynaptic rate $\lambda(t)$ from a small number ($N = 10$) of membrane potential V_t traces that are independently generated from the same PPP. Each trace has small amounts of additive noise to simulate measurement error that are independent from the PPP. The traces of V_t are sampled at rate $1/\Delta t$. A single realization of the noisy membrane potential with mean and variance estimated from a small number of traces is shown in Fig. 12. The noisy membrane equation is given by:

$$\tau_m \frac{d}{dt} V_m(t) = E_l - V_m(t) + (E_s - V_m(t)) \frac{1}{g_l} G(t) + \epsilon(t) \tag{23}$$

where $\epsilon(t)$ is a zero mean Gaussian white noise in units of voltage with $\sigma(\epsilon) = 0.2$ mV.
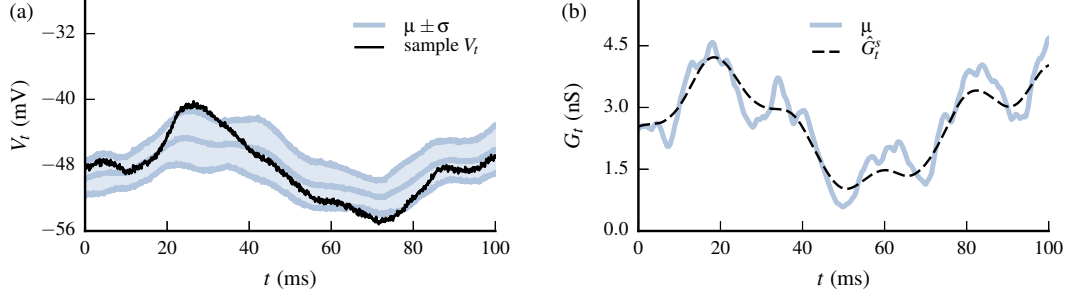
Figure 12 – *(a) Single realization (black line) and basic statistics (gray lines) generated from a small number (N = 10) of membrane potential V_t traces with additive noise to simulate measurement error. (b) Extracted mean conductance (full gray line) and smoothed version G_t^s (dashed black line) obtained with non-parametric smoothing.*

The key expression that enables to estimate $\lambda(t)$ from traces of V_t is the Campbell Theorem for the mean of nonstationary shot noise given by Eq. (6). If the shot noise kernel is known then the rate function can in principle be obtained by deconvolution of the mean conductance. However, this operation is very sensitive to noise since small changes in the estimated mean conductance will result in large changes of the estimated rate function. This aspect is dealt with by smoothing the estimated mean conductance prior to performing the deconvolution step. From each trace of V_t we extract the input conductance by inverting Eq. (23) and average them to obtain the estimated mean conductance:

$$\left\langle \hat{G}_t \right\rangle = \frac{1}{N} \sum_{n=1}^{N} \frac{g_l}{\Delta t} \frac{\tau_m \left(V_{t+\Delta t}^n - V_t^n \right) - \Delta t \left(E_l - V_t^n \right)}{E_s - V_t^n}$$

where V_t^n is the n-th trace of V_t and Δt is the sampling interval.

The estimated mean conductance will be a noisy version of the actual mean conductance due to the effects of the additive noise $\epsilon(t)$ in each trace of V_t. Non-parametric smoothing is performed using a local linear smoother with tricube kernel and kernel bandwidth selected by cross-validation [Wasserman, 2006], yielding the smoothed version $\left\langle \hat{G}_t^s \right\rangle$ shown in Fig. 12(b). Finally, we use the discrete convolution theorem to estimate the presynaptic rate $\hat{\lambda}(t)$ from the smoothed mean conductance:

$$\hat{\lambda}(t) = \frac{1}{\Delta t} \mathrm{DFT}^{-1} \left[\frac{\mathrm{DFT}\left\{ \left\langle \hat{G}_t^s \right\rangle \right\}}{\mathrm{DFT}\{g\}} \right]$$

The result is shown in Fig. 13, where the estimated $\hat{\lambda}(t)$ rate compares favorably to the original presynaptic rate $\lambda(t)$. Estimating $\lambda(t)$ from noisy shot noise data has been previously addressed [Sequeira and Gubner, 1995] in addition to methods that enable to estimate the shot noise kernel [Sequeira and Gubner, 1997].
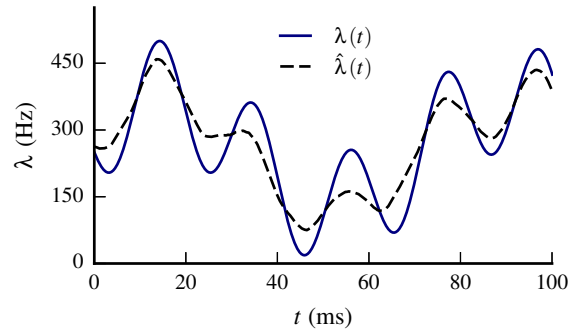

Figure 13 – *Estimated presynaptic rate $\hat{\lambda}(t)$ (black dashed line) compared with original rate function $\lambda(t)$ (full blue line). The magnitude and variations are reasonably well captured considering the small number (N = 10) of membrane potential traces used.*

14

7 Discussion

In this paper, we investigated important statistical properties of filtered shot noise processes with multiplicative noise, in the general case of variable input rate. These properties provide a compact description of time-evolving dynamics of the system. Such processes arise from the filtering of nonstationary shot noise input through a linear first-order ODE with variable coefficients. We have obtained general results for this class of stochastic processes and results specific to applications in neuronal models.

We first identified the causal PPP transformation that corresponds to filtered shot noise with multiplicative noise. We investigated the statistical properties of this transformation to derive the exact analytical solution for the joint cumulants of the filtered process with variable input rate. Excellent agreement with numerical simulations was found for the mean and second order cumulants. We proposed an approximation based on a CME about the solution of the deterministic system. We have shown with numerical simulations that under parameter regimes relevant to neuronal membranes the second order of this approximation provides good results for the mean and second order cumulants. Under certain parameter regimes, the first order expansion for the second order cumulants may already provide effective approximations.

These general results were then applied to a simple model of subthreshold membrane potential V_m fluctuations subject to shot noise conductance with continuously variable rate of presynaptic spikes. Excellent agreement with numerical simulations was found for the mean and second order cumulants for both the exact analytical solution and the second order CME. This approximation is consistent with previously published analytical estimates for stationary V_m. An expression for the stationary limit of autocovariance is provided for exponential and alpha kernel shot noise input. An approximation for the time-evolving distribution of V_m is proposed that is based on a truncated Edgeworth series using the nonstationary cumulants obtained analytically. This approximation successfully captures the time evolution of V_m under a large range of conditions. The nonstationary mean of shot noise is used to estimate the presynaptic rate from a small number of intracellular V_m recordings with additive noise simulating measurement error.

In future work we will extend this formalism to multiple independent shot noise inputs by applying the Slivnyak-Mecke Theorem. Such development would yield direct applications for neuronal membrane models with different synapse types (such as excitatory and inhibitory synapses). Preliminary work indicates that analytic treatment of filtered shot noise with correlated input is accessible with this formalism. The present work also opens perspectives for the analytical development first passage time statistics based on nonstationary approxima- tions of the filtered process distribution.

Acknowledgments

Appendix

A   Random Sums and Random Products

Random products are transformations of PPP that factor as $F(t, \xi) = \prod_{x_j \in \xi} f(t, x_j)$. The expectation of random products is obtained as follows:

$$\langle F_t \rangle = \sum_{n=0}^{\infty} \frac{1}{n!} e^{-m(\mathcal{S})} \left(\int_{\mathcal{S}} f(t, x) \lambda(x) \, dx \right)^n = \exp \left(\int_{\mathcal{S}} (f(t, x) - 1) \lambda(x) \, dx \right)$$

$$\langle F_1 \dots F_K \rangle = \left\langle \prod_{x_j \in \xi} \prod_{k=1}^{K} f(t_k, x_j) \right\rangle = \exp \left(\int_{\mathcal{S}} (f(t_1, x) \cdots f(t_K, x) - 1) \lambda(x) \, dx \right)$$

In the case of the random product with $f(t, x_j) = e^{-\frac{1}{\tau} \int_z^t g(u-x_j)H(u-x_j)du}$ and $\mathcal{S} = \mathbb{R}$,

$$\left\langle e^{-\frac{1}{\tau} \int_z^t Q(u,\xi)\,du} \right\rangle = \exp\left(\int\limits_{-\infty}^{z} \left(e^{-\frac{1}{\tau} \int_z^t g(u-x)\,du} - 1 \right) \lambda(x)\,dx + \int\limits_{z}^{t} \left(e^{-\frac{1}{\tau} \int_y^t g(v-y)\,dv} - 1 \right) \lambda(y)\,dy \right)$$

Random sums are transformations of PPP that factor as $F(t,\xi) = \sum_{x_j \in \xi} f(t, x_j)$. The joint cumulants of random sums are given by the *Campbell Theorem* [Campbell, 1909, Rice, 1945]. The *characteristic function* $\phi(s_1, \ldots, s_K)$ is the expectation of a random product, and its derivatives yield the joint cumulants:

$$\phi(s_1, \ldots, s_K) \equiv \left\langle e^{is_1 F(t_1,\xi) + \cdots + is_K F(t_K,\xi)} \right\rangle = \left\langle \prod_{x_j \in \xi} \prod_{k=1}^{K} e^{is_k f(t_k, x_j)} \right\rangle = \exp\left(\int_{\mathcal{S}} \left(e^{\sum_{k=1}^{K} is_k f(t_k, x)} - 1 \right) \lambda(x)\,dx \right)$$

$$\langle\langle F(t_1, \xi) \ldots F(t_K, \xi) \rangle\rangle = \left(\frac{1}{i}\frac{d}{ds_1} \right) \cdots \left(\frac{1}{i}\frac{d}{ds_K} \right) \ln \phi(s_1, \ldots, s_K) \bigg|_{s_1, \ldots, s_K = 0} = \int_{\mathcal{S}} f(t_1, x) \cdots f(t_K, x)\, \lambda(x)\,dx$$

B   Central Moments Expansion

A Taylor expansion of the random product about mean shot noise input results in a series of central moments of the integrated shot noise. Expanding the exponential inside the expectation, keeping terms of order $(1/\tau_m)^2$ and re-expressing in terms of cumulants, yields:

$$\left\langle e^{-\frac{1}{\tau} \int_z^t Q(u,\xi)\,du} \right\rangle = e^{-\frac{1}{\tau} \int_z^t \langle Q(u) \rangle\, du} \left(1 + \sum_{m=2}^{+\infty} \frac{1}{m!} \left\langle \left(-\frac{1}{\tau} \int_z^t (Q(u,\xi) - \langle Q(u) \rangle)\, du \right)^m \right\rangle \right)$$

$$\simeq e^{-\frac{1}{\tau} S\bar{Q}} \left(1 + \frac{1}{2\,\tau^2} \langle\langle SQ^2 \rangle\rangle \right)$$

where $SQ \equiv \int_z^t Q(v, \xi)\, dv$ and $S\bar{Q} \equiv \int_z^t \langle Q(u) \rangle\, du$.

Higher order cumulants are obtained in a similar manner by expanding each exponential individually and collecting terms in the same order of $1/\tau_m$. The second order expansion for second order cumulants involves the expansion of two random products and keeping terms up to order $(1/\tau_m)^4$, yielding:

$$\left\langle\left\langle e^{-\frac{1}{\tau} \int_{z_1}^{t_1} Q(u_1,\xi)\,du_1} e^{-\frac{1}{\tau} \int_{z_2}^{t_2} Q(u_2,\xi)\,du_2} \right\rangle\right\rangle$$

$$\simeq e^{-\frac{1}{\tau} S\bar{Q}_1 - \frac{1}{\tau} S\bar{Q}_2} \left(\frac{1}{\tau^2} \langle\langle SQ_1\, SQ_2 \rangle\rangle - \frac{1}{2\tau^3} \left(\langle\langle SQ_1^2\, SQ_2 \rangle\rangle + \langle\langle SQ_1\, SQ_2^2 \rangle\rangle \right) \right.$$

$$+ \frac{1}{2\tau^4} \left(\frac{1}{3} \langle\langle SQ_1^3\, SQ_2 \rangle\rangle + \frac{1}{3} \langle\langle SQ_1\, SQ_2^3 \rangle\rangle + \frac{1}{2} \langle\langle SQ_1^2\, SQ_2^2 \rangle\rangle \right.$$

$$\left. \left. + \langle\langle SQ_1\, SQ_2 \rangle\rangle \left(\langle\langle SQ_1^2 \rangle\rangle + \langle\langle SQ_2^2 \rangle\rangle + \langle\langle SQ_1\, SQ_2 \rangle\rangle \right) \right) \right)$$

where $SQ_1 \equiv \int_{z_1}^{t_1} Q(v, \xi)\, dv$ and $S\bar{Q}_1 \equiv \int_{z_1}^{t_1} \langle Q(u) \rangle\, du$, etc.

B.1   Stationary limit for Y_t

The stationary limit of shot noise autocovariance can be written $\langle\langle Q_1\, Q_2 \rangle\rangle = \langle\langle Q^2 \rangle\rangle\, r(|t_1 - t_2|)$, since:

$$\langle\langle Q_1\, Q_2 \rangle\rangle = \lambda \int\limits_{-\infty}^{\min(t_1, t_2)} g(t_1 - x)\, g(t_2 - x)\, dx = \lambda \int\limits_{0}^{+\infty} g(u)\, g(|t_1 - t_2| + u)\, du = \langle\langle Q^2 \rangle\rangle\, r(|t_1 - t_2|)$$

with $r\left(|t_1 - t_2|\right) \equiv \int_0^{+\infty} g(u)\, g(|t_1 - t_2| + u)\, du / \int_0^{+\infty} g(v)^2\, dv$.

For the exponential kernel shot noise $r\left(|t_1 - t_2|\right) = e^{-\frac{|t_1 - t_2|}{\tau_s}}$ and the stationary mean and second order cumulants are given by:

$$\langle Q \rangle = \lambda h \tau_s \qquad\qquad \langle\langle Q_1\, Q_2 \rangle\rangle = \frac{\lambda h^2 \tau_s}{2}\, e^{-\frac{|t_1 - t_2|}{\tau_s}} = \langle\langle Q^2 \rangle\rangle\, e^{-\frac{|t_1 - t_2|}{\tau_s}}$$

Writing $Q_0 \equiv 1 + \langle Q \rangle$ and applying Eq. (17) yields the mean:

$$\langle Y_t \rangle_2 = \frac{\langle Q \rangle}{Q_0} - \frac{\langle\langle Q^2 \rangle\rangle}{Q_0^2}\frac{1}{\tau}\int_{-\infty}^{t} e^{-\frac{t-z}{\tau}}\, Q_0 \int_z^{t} e^{-\frac{u-z}{\tau_s}}\, dz\, du = \langle Y_t \rangle_0 - \frac{\langle\langle Q^2 \rangle\rangle}{Q_0^2\left(Q_0 + \frac{\tau}{\tau_s}\right)}$$

Applying Eq. (18) yields the autocovariance:

$$\langle\langle Y_1\, Y_2 \rangle\rangle_1 = \frac{\langle\langle Q^2 \rangle\rangle}{Q_0^2}\frac{1}{\tau^2}\int_{-\infty}^{t_1}\int_{-\infty}^{t_2} e^{-\frac{t_1 - z_1 + t_2 - z_2}{\tau}}\, Q_0\, e^{-\frac{|z_1 - z_2|}{\tau_s}}\, dz_1\, dz_2$$

$$= \begin{cases} \dfrac{\langle\langle Q^2 \rangle\rangle}{Q_0^2\left(Q_0 + \frac{\tau}{\tau_s}\right)\left(Q_0 - \frac{\tau}{\tau_s}\right)}\left(e^{-\frac{|t_1 - t_2|}{\tau_s}} - \frac{1}{Q_0}\frac{\tau}{\tau_s}\, e^{-\frac{|t_1 - t_2|}{\tau}}\, Q_0\right) & \text{if } Q_0 \neq \frac{\tau}{\tau_s} \\[2em] \dfrac{\langle\langle Q^2 \rangle\rangle}{2\,\tau\, Q_0^3}\left(\tau_s + |t_1 - t_2|\right) e^{-\frac{|t_1 - t_2|}{\tau_s}} & \text{otherwise} \end{cases}$$

Setting $t_1 = t_2 = t$ in the previous result yields the variance:

$$\langle\langle Y_t^2 \rangle\rangle_1 = \frac{\langle\langle Q^2 \rangle\rangle}{Q_0^3\left(Q_0 + \frac{\tau}{\tau_s}\right)}$$

For the alpha kernel shot noise $r(|t_1 - t_2|) = e^{-\frac{|t_1 - t_2|}{\tau_s}}\left(1 + \frac{|t_1 - t_2|}{\tau_s}\right)$ and the stationary mean and second order cumulants are given by:

$$\langle Q \rangle = \lambda h \tau_s \qquad \langle\langle Q_1\, Q_2 \rangle\rangle = \frac{\lambda h^2 \tau_s}{4}\, e^{-\frac{|t_1 - t_2|}{\tau_s}}\left(1 + \frac{|t_1 - t_2|}{\tau_s}\right) = \langle\langle Q^2 \rangle\rangle\, e^{-\frac{|t_1 - t_2|}{\tau_s}}\left(1 + \frac{|t_1 - t_2|}{\tau_s}\right)$$

Proceeding as before yields:

$$\langle Y_t \rangle_2 = \frac{\langle Q \rangle}{Q_0} - \frac{\left(Q_0 + 2\frac{\tau}{\tau_s}\right)\langle\langle Q^2 \rangle\rangle}{Q_0^2\left(Q_0 + \frac{\tau}{\tau_s}\right)^2} \qquad\qquad \langle\langle Y_t^2 \rangle\rangle_1 = \frac{\left(Q_0 + 2\frac{\tau}{\tau_s}\right)\langle\langle Q^2 \rangle\rangle}{Q_0^3\left(Q_0 + \frac{\tau}{\tau_s}\right)^2}$$

$$\langle\langle Y_1\, Y_2 \rangle\rangle_1 = \begin{cases} \dfrac{\langle\langle Q^2 \rangle\rangle}{Q_0^2\left(Q_0 + \frac{\tau}{\tau_s}\right)^2\left(Q_0 - \frac{\tau}{\tau_s}\right)^2} \\[1em] \times\left(\left(\left(1 + \frac{|t_1 - t_2|}{\tau_s}\right)\left(Q_0 + \frac{\tau}{\tau_s}\right)\left(Q_0 - \frac{\tau}{\tau_s}\right) - 2\left(\frac{\tau}{\tau_s}\right)^2\right) e^{-\frac{|t_1 - t_2|}{\tau_s}}\right. \\[1em] \qquad\qquad\qquad\qquad\qquad \left. + \frac{2}{Q_0}\left(\frac{\tau}{\tau_s}\right)^3 e^{-\frac{|t_1 - t_2|}{\tau}}\, Q_0\right) \quad \text{if } Q_0 \neq \frac{\tau}{\tau_s} \\[2em] \dfrac{\langle\langle Q^2 \rangle\rangle}{4\,\tau\, Q_0^3}\left(3(\tau_s + |t_1 - t_2|) + \frac{1}{\tau_s}|t_1 - t_2|^2\right) e^{-\frac{|t_1 - t_2|}{\tau_s}} \quad \text{otherwise} \end{cases}$$

B.2   Stationary limit for V_t

We apply the transformation given by Eq. (21) to the results from the previous section to obtain the cumulants for the membrane potential V_t. The expression for the stationary mean of the deterministic system is the same for both shot noise kernels:

$$\langle V_t \rangle_0 = \frac{\langle G \rangle}{G_0}\left(E_s - E_l\right) + E_l = \frac{g_l\, E_l + \langle G \rangle\, E_s}{G_0} \qquad\qquad G_0 = g_l + \langle G \rangle$$

17

The mean and variance of exponential and alpha kernel shot noise are consistent with those given in Refs. [Richardson and Gerstner, 2005, Rudolph and Destexhe, 2005] and Ref. [Kuhn *et al.*, 2004], respectively. The extension to the autocovariance is also provided below. For exponential kernel shot noise and using $E_e - E_l = \frac{G_0}{g_l}(E_e - \langle V_t \rangle_0)$,

$$\langle V_t \rangle_2 = \langle V_t \rangle_0 - \frac{\langle\langle G^2 \rangle\rangle}{g_l\left(\frac{G_0}{g_l} + \frac{\tau}{\tau_s}\right)G_0}\left(E_s - \langle V_t \rangle_0\right) \qquad \langle\langle V_t^2 \rangle\rangle_1 = \frac{\langle\langle G^2 \rangle\rangle}{g_l\left(\frac{G_0}{g_l} + \frac{\tau}{\tau_s}\right)G_0}\left(E_s - \langle V_t \rangle_0\right)^2 \qquad (24)$$

$$\langle\langle V_1 V_2 \rangle\rangle_1 = \begin{cases} \frac{\langle\langle G^2 \rangle\rangle}{g_l^2\left(\frac{G_0}{g_l} + \frac{\tau}{\tau_s}\right)\left(\frac{G_0}{g_l} - \frac{\tau}{\tau_s}\right)}\left(e^{-\frac{t_1-t_2}{\tau_s}} - \frac{\tau}{\tau_s}\frac{g_l}{G_0}e^{-\frac{t_1-t_2}{\tau}\frac{G_0}{g_l}}\right)\left(E_s - \langle V_t \rangle_0\right)^2 & \text{if } \frac{G_0}{g_l} \neq \frac{\tau}{\tau_s} \\[3mm] \frac{\langle\langle G^2 \rangle\rangle}{2\,\tau\,g_l\,G_0}\left(\tau_s + |t_1 - t_2|\right)e^{-\frac{|t_1-t_2|}{\tau_s}}\left(E_s - \langle V_t \rangle_0\right)^2 & \text{otherwise} \end{cases}$$
$$(25)$$

For alpha kernel shot noise,

$$\langle V_t \rangle_2 = \langle V_t \rangle_0 - \frac{\left(\frac{G_0}{g_l} + 2\frac{\tau}{\tau_s}\right)\langle\langle G^2 \rangle\rangle}{g_l\left(\frac{G_0}{g_l} + \frac{\tau}{\tau_s}\right)^2 G_0}\left(E_s - \langle V_t \rangle_0\right) \qquad \langle\langle V_t^2 \rangle\rangle_1 = \frac{\left(\frac{G_0}{g_l} + 2\frac{\tau}{\tau_s}\right)\langle\langle G^2 \rangle\rangle}{g_l\left(\frac{G_0}{g_l} + \frac{\tau}{\tau_s}\right)^2 G_0}\left(E_s - \langle V_t \rangle_0\right)^2$$
$$(26)$$

$$\langle\langle V_1 V_2 \rangle\rangle_1 = \begin{cases} \frac{\langle\langle G^2 \rangle\rangle}{g_l^2\left(\frac{G_0}{g_l} + \frac{\tau}{\tau_s}\right)^2\left(\frac{G_0}{g_l} - \frac{\tau}{\tau_s}\right)^2}\left(E_s - \langle V_t \rangle_0\right)^2 \\[2mm] \quad \times\left(\left(\left(1 + \frac{t_1-t_2}{\tau_s}\right)\left(\frac{G_0}{g_l} + \frac{\tau}{\tau_s}\right)\left(\frac{G_0}{g_l} - \frac{\tau}{\tau_s}\right) - 2\left(\frac{\tau}{\tau_s}\right)^2\right)e^{-\frac{t_1-t_2}{\tau_s}}\right. \\[4mm] \qquad\qquad\qquad\qquad\qquad \left. +2\left(\frac{\tau}{\tau_s}\right)^3\frac{g_l}{G_0}e^{-\frac{t_1-t_2}{\tau}\frac{G_0}{g_l}}\right) \quad \text{if } \frac{G_0}{g_l} \neq \frac{\tau}{\tau_s} \\[4mm] \frac{\langle\langle G^2 \rangle\rangle}{4\,\tau\,g_l\,G_0}\left(3(\tau_s + |t_1 - t_2|) + \frac{1}{\tau_s}|t_1 - t_2|^2\right)e^{-\frac{|t_1-t_2|}{\tau_s}}\left(E_s - \langle V_t \rangle_0\right)^2 \quad \text{otherwise} \end{cases}$$
$$(27)$$

References

A. Verveen and L. DeFelice, Progress in biophysics and molecular biology **28**, 189 (1974).

H. C. Tuckwell, *Introduction to theoretical neurobiology: volume 2, nonlinear and stochastic theories* (Cambridge University Press, 1988).

A. Kuhn, A. Aertsen, and S. Rotter, The Journal of neuroscience **24**, 2345 (2004).

M. Richardson and W. Gerstner, Neural Computation **17**, 923 (2005).

M. Rudolph and A. Destexhe, Neural Computation **17**, 2301 (2005).

A. N. Burkitt, Biological cybernetics **95**, 1 (2006a).

L. Wolff and B. Lindner, Physical Review E **77**, 041913 (2008).

L. Wolff and B. Lindner, Neural Computation **22**, 94 (2010).

D. Cai, L. Tao, A. Rangan, and D. McLaughlin, Communications in Mathematical Sciences **4**, 97 (2006).

K.-i. Amemori and S. Ishii, Neural computation **13**, 2763 (2001).

A. N. Burkitt, Biological cybernetics **95**, 97 (2006b).

J. Moller and R. P. Waagepetersen, *Statistical inference and simulation for spatial point processes* (CRC Press, 2003).

R. L. Streit, *Poisson Point Processes: Imaging, Tracking, and Sensing* (Springer, 2010).

N. Campbell, in *Proc. Camb. Phil. Soc*, Vol. 15 (1909) pp. 310–328.

W. Schottky, Annalen der Physik **362**, 541 (1918).

B. Picinbono, C. Bendjaballah, and J. Pouget, Journal of Mathematical Physics **11**, 2166 (1970).

M. Rousseau, JOSA **61**, 1307 (1971).

D. L. Snyder and M. I. Miller, *Random Point Processes in Time and Space* (Springer, 1991).

E. Parzen, *Stochastic processes*, Vol. 24 (SIAM, 1999).

S. Rice, Bell System Technical Journal **24**, 46 (1945).

J. Rice, Advances in Applied Probability , 553 (1977).

I. Slivnyak, Theory of Probability & Its Applications **7**, 336 (1962).

J. Mecke, Wahrscheinlichkeitsth **9**, 36 (1967).

H. Cramér, *Mathematical methods of statistics*, Vol. 1 (Princeton university press, 1946).

G. W. Oehlert, The American Statistician **46**, 27 (1992).

M. Okun and I. Lampl, Nature neuroscience **11**, 535 (2008).

A. Destexhe and D. Paré, Journal of neurophysiology **81**, 1531 (1999).

F. Edgeworth, Journal of the Royal Statistical Society , 102 (1907).

D. L. Wallace, The Annals of Mathematical Statistics , 635 (1958).

L. Badel, Physical Review E **84**, 041919 (2011).

V. Petrov, "On some polynomials occurring in probability theory (russian)," (1962).

S. Blinnikov and R. Moessner, Astronomy and Astrophysics Supplement Series **130**, 193 (1998).

L. Wasserman, *All of nonparametric statistics* (Springer Science & Business Media, 2006).

R. E. Sequeira and J. A. Gubner, Signal Processing, IEEE Transactions on **43**, 1527 (1995).

R. E. Sequeira and J. A. Gubner, Signal Processing, IEEE Transactions on **45**, 421 (1997).

Chapter 4

The impact of synaptic conductance inhomogeneities on membrane potential statistics

Summary

This article extends to N independent conductance inputs the simple case presented in Chapter 3 for a single shot noise conductance input. The effect of synaptic inhomogeneities in the statistics of membrane potential is also investigated.

A basic model of N synapse types is first introduced with one shot noise process per synapse type. This corresponds for $N = 2$ to the the popular model of single excitatory and inhibitory synapse types. Multiple synapse types ($N > 2$) can account for different reversal potentials within the same synapse type. This basic model assumes homogeneous biological parameters for the synapses of each synapse type. The exact cumulants are derived using the Slivnyak-Mecke theorem and comparison with numerical simulations illustrates the accuracy for mean and second order cumulants. A truncated Edgeworth series with cumulants up to third order is used to approximate the time-evolving distribution of membrane potential fluctuations. The key statistic in this model is a product of shot noise and the exponential of integrated shot noise. The central moments expansion (CME) introduced in the article from Chapter 3 is extended to multiple independent shot noise inputs and requires some adaptation in order to avoid terms containing both moments and central moments of shot noise.

This basic model is extended to take into consideration biological characteristics of individual synapses. This is implemented by introducing synapses within each synapse type and each synapse is driven by independent shot noise process with particular biological parameters. The limiting case of a large number of synapses is analyzed in more detail, where variation in biological parameters is reflected in each postsynaptic response. The exact cumulants and CME expansion are derived for this model. Interesting predictions on synaptic inhomogeneities effects in comparison to the homogeneous model can be derived by simple analysis of the CME expansion. This extended model relates synaptic inhomogeneity to membrane potential statistics and corresponds to the statistical model of V_t already mentioned in Sec. 1.3. This model may provide basis for improvement of statistical inference models due to the exact nature of these results and access to higher order statistics of V_t.

Résumé

Les inhomogénéités synaptiques dues à la variabilité biologique affectent les propriétés statistiques des entrées synaptiques, ainsi que les fluctuations du potentiel de membrane. Leur impact est étudié dans un modéle de membrane passive qui évolue suivant des entrées à conductance non stationnaires du type *shot noise*. Le cas de synapses multiples est considéré dans la limite d'un grand nombre de synapses où la variation des paramètres biologiques se produit à chaque réponse post-synaptique. Les cumulants exacts sont obtenus et leur approximation en termes des cumulants de *shot noise* est dérivé dans le cadre d'une expansion des moments centraux. Cela permet d'explorer les effets des cumulants d'ordre supérieur du *shot noise* dans les statistiques des fluctuations du potentiel de membrane à la fois quantitativement et qualitativement.

The impact of synaptic conductance inhomogeneities on membrane potential statistics

Marco Brigham, Alain Destexhe

26/03/2015

Abstract

Synaptic noise is usually modeled as arising from a large number of identical synapses, but in real neurons, there is considerable diversity in the characteristics of synaptic responses. We investigate the impact of these inhomogeneities by applying a generalization of the classic shot noise approach to a passive membrane model evolving under nonstationary shot noise conductance with multiple synapse types. Synaptic inhomogeneities are introduced in the limit of very large number of synapses where diversity in synaptic properties is reflected in each postsynaptic response. Exact expressions for the cumulants of membrane potential (Vm) fluctuations are derived, in addition to various approximations based on a central moments expansion (CME). This enables to explore the effects of higher order shot noise cumulants in the statistics of Vm fluctuations both quantitatively and qualitatively.

1   Introduction

The biological characteristics of synapses are often assumed identical for a given synapse type [Stein, 1965, Tuckwell, 1988, Burkitt, 2006a,b] in order to improve the tractability of neural population activity models [Brunel and Hakim, 1999, Brunel, 2000, Gerstner, 2000, Abbott and van Vreeswijk, 1993, Gerstner and van Hemmen, 1993] with very few exceptions in the literature [Richardson and Swarbrick, 2010]. However, biological neurons have considerable diversity in the characteristics of synaptic responses [Markram et al., 1997, Golowasch et al., 1999]. In order to understand and quantify the impact of synaptic inhomogeneities in the dynamical properties of neurons, we investigate the effects of synaptic parameter variation in the statistics of membrane potential Vm. For this purpose we use a simple neuron model with passive membrane that evolves under shot noise conductance with nonstationary rates. Variation of synaptic parameters, such as synaptic strength and synaptic time constant, changes the statistical properties of input conductance, which in turn affects the statistics of Vm.

We first consider a membrane model with N synapse types, each driven by an independent shot noise process. In this *homogeneous model*, the synaptic responses from the same synapse type are identical. This is extended to multiple independent synapses of the same synapse type with individual synaptic parameters. Finally, the limit of very large number of synapses is considered where the variation of synaptic parameters is reflected in each synaptic response. The exact nonstationary cumulants of these membrane models are derived with the formalism of Poisson point process (PPP) transformations introduced in previous work [Brigham and Destexhe, 2015]. Various approximations are obtained with a central moments expansion (CME) about the deterministic solution of the system. Using these tools, we explore how the hierarchy of shot noise cumulants, which directly reflects the inhomogeneities in synaptic parameters, impacts the statistics of Vm fluctuations.

The homogeneous model is presented in Section 2, where exact cumulants and CME for the mean and second order cumulants are derived. Synaptic inhomogeneities are introduced in Section 3 and the limiting case of large number of synapses is examined in greater detail. The impact of exponential and uniform distributions in synaptic strength are analyzed with the CME in Section 4. We discuss these results and their applications in Section 5.

2   Model Description

We consider a simple passive membrane model with N types of conductance synapses characterized by their reversal potentials E_n ($1 \leq n \leq N$). The synaptic input is modeled by independent shot noise
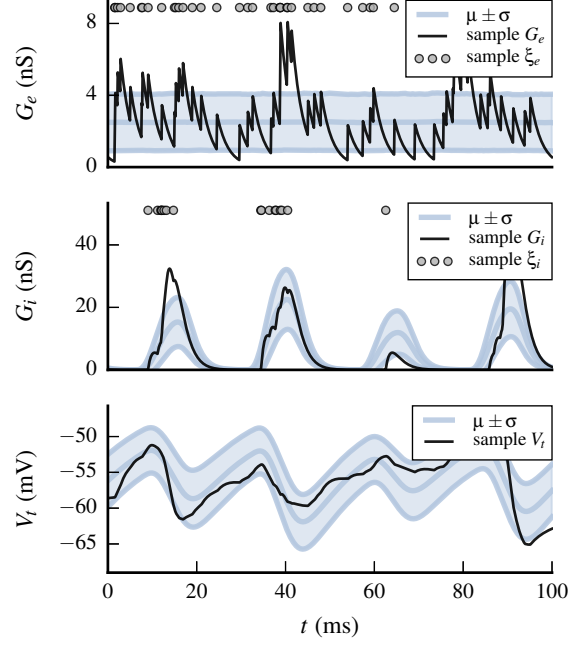
Figure 1 – *Single realizations, mean and standard deviation for simple passive membrane model with single excitatory and single inhibitory synapse types. Excitatory conductances G_e (top) and inhibitory conductances G_i (middle) drive the membrane potential V_t (bottom). Single realizations of G_e, G_i and V_t are shown in black, realizations of ξ_e and ξ_i are represented by gray dots. Mean and standard deviations ($\mu \pm \sigma$) are shown in gray.*

processes $G_n(t)$ with presynaptic events $x_j \in \xi_n$ generated by a multivariate PPP $\boldsymbol{\Xi}$ with independent components $\{\Xi_1, \ldots, \Xi_N\}$. The shot noise conductance $G_n(t)$ drive the evolution of the membrane potential $V(t)$ according to the *membrane equation*:

$$\tau_m \frac{d}{dt} V(t) = E_l - V(t) + \sum_{n=1}^{N} (E_n - V(t)) \frac{1}{g_l} G_n(t) \tag{1}$$

$$\frac{1}{g_l} G_n(t, \xi_n) = \sum_{x_j \in \xi_n} g_n(t - x_j) H(t - x_j) \tag{2}$$

where τ_m is the membrane time constant, E_l is the leak potential, g_l is the leak conductance, E_n is the synaptic reversal potential for synapse type n, $g_n(t - x_j) H(t - x_j)$ is the impulse response function, or shot noise kernel, for synapse type n and $H(u)$ is the Heaviside function. The presynaptic spike times are realizations from independent PPP $\Xi_n (\mathcal{S}, \lambda_n(t))$ that are characterized by rate functions $\lambda_n(t) > 0$, such that $m_n(\mathcal{S}) \equiv \int_{\mathcal{S}} \lambda_n(x) \, dx$ is finite for any bounded interval $\mathcal{S} \subseteq \mathbb{R}$ of the real line.

The Fig. 1 illustrates a membrane model with single excitatory and inhibitory synapse types ($N = 2$) that is driven by stationary excitatory and nonstationary inhibitory shot noise conductances. The corresponding PPP rates $\lambda_e(t)$ and $\lambda_i(t)$ are represented in Fig. 2. The numerical simulations are generated with exponential kernel $g(t - x)_{exp} = h \exp\left(-(t - x)/\tau_s\right)$ for excitatory conductance and alpha kernel $g(t - x)_{alpha} = h\left((t - x)/\tau_s\right) \exp\left(-(t - x)/\tau_s\right)$ for inhibitory conductance. The excitatory and inhibitory rate are $\lambda_e = 500$ Hz and $\lambda_i = 1000$ Hz, respectively. Other parameters are $\tau_m = 0.02$ s, $E_l = -0.06$ V, $E_e = 0$ V, $E_i = -0.08$ V, $g_l = 10\text{E-}9$ S, $h_e = 2\text{E-}9$ S, $h_i = 15\text{E-}9$ S, $\tau_e = 0.0025$ s, $\tau_i = 0.0015$ s.

2.1 Exact Solution

The exact nonstationary cumulants for the homogeneous model are derived next. The membrane equation is first transformed into a unitless system by writing E_1 and E_N for the highest and lowest reversal
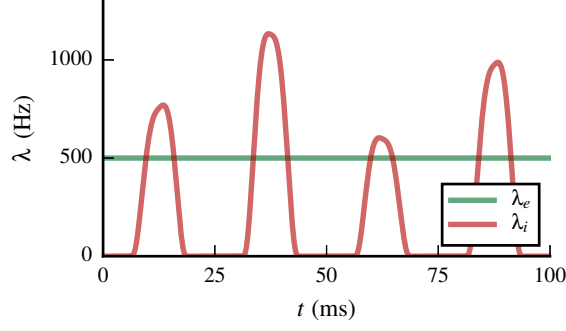
Figure 2 – *Presynaptic rate functions for shot noise processes generating input conductance for single excitatory and inhibitory synapse types ($N = 2$). The excitatory rate $\lambda_e(t)$ is stationary (green line) and inhibitory rate $\lambda_i(t)$ is nonstationary (red line).*

potentials, $\tau = \tau_m$ and performing the following transformations:

$$Y(t) = \frac{V(t) - E_l}{E_1 - E_N} \qquad w_n = \frac{E_n - E_l}{E_1 - E_N} \qquad Q_n(t) = \frac{1}{g_l} G_n(t) \qquad Q_0(t) = 1 + \sum_{n=1}^{N} Q_n(t) \quad (3)$$

yields the following unit-less system:

$$\tau \frac{d}{dt} Y(t) = -Y(t) + \sum_{n=1}^{N} (w_n - Y(t)) Q_n(t) \tag{4}$$

$$Q_n(t, \xi_n) = \sum_{x_j \in \xi_n} g_n(t - x_j) H(t - x_j) \tag{5}$$

The system response $Y(t, \boldsymbol{\xi})$ for shot noise inputs $\{Q_1(t, \xi_1), \ldots, Q_N(t, \xi_N)\}$ is obtained by solving Eq. (4) for the realization $\boldsymbol{\xi} = \{\xi_1, \ldots, \xi_N\}$ of $\boldsymbol{\Xi}$. Assuming without loss of generality $Y_0 = 0$,

$$Y(t, \boldsymbol{\xi}) = \frac{1}{\tau} \int_{-\infty}^{t} e^{-\frac{t-z}{\tau}} \sum_{n=1}^{N} w_n \, Q_n(z, \xi_n) \, e^{-\frac{1}{\tau} \int_z^t Q_0(u, \boldsymbol{\xi}) \, du} \, dz$$

The cumulants of Y_t are obtained by first forming the relevant products of $Y(t, \boldsymbol{\xi})$ and evaluating their expectation under $\boldsymbol{\Xi}$, as detailed in Appendix A. This is multiple synapse extension of the method introduced in previous work [Brigham and Destexhe, 2015] and generalizes the case of stationary input rates addressed in [Wolff and Lindner, 2008, 2010]. For example, the autocovariance $\langle\langle Y_1 Y_2 \rangle\rangle$ between times t_1 and t_2 is obtained by evaluating $\langle Y(t_1, \boldsymbol{\xi}) Y(t_2, \boldsymbol{\xi}) \rangle - \langle Y(t_1, \boldsymbol{\xi}) \rangle \langle Y(t_2, \boldsymbol{\xi}) \rangle$ under $\boldsymbol{\Xi}$. The mean and joint cumulants of Y_t are given by:

$$\langle Y_t \rangle = \frac{1}{\tau} \int_{-\infty}^{t} \sum_{n=1}^{N} \left\langle w_n \, Q_n(z) \, e^{-\frac{1}{\tau} \int_z^t Q_0(u) \, du} \right\rangle dz \tag{6}$$

$$\langle\langle Y_1 \cdots Y_K \rangle\rangle = \frac{1}{\tau^K} \int_{-\infty}^{t_1} \cdots \int_{-\infty}^{t_K} \sum_{n_1=1}^{N} \cdots \sum_{n_K=1}^{N} \left\langle\!\!\left\langle \prod_{k=1}^{K} w_{n_k} \, Q_{n_k}(z_k) \, e^{-\frac{1}{\tau} \int_{z_k}^{t_k} Q_0(u) \, du} \right\rangle\!\!\right\rangle dz_1 \cdots dz_K \tag{7}$$

The independence of the components $\boldsymbol{\Xi}_n$ and the *Slivnyak-Mecke Theorem* [Slivnyak, 1962, Mecke, 1967] yield the expectations in the integrands. Explicit expressions for the mean and autocovariance are provided in Appendix A with the key expectations given by:

$$\left\langle Q_n(z) \, e^{-\frac{1}{\tau} \int_z^t Q_0(u) \, du} \right\rangle = \left\langle e^{-\frac{1}{\tau} \int_z^t Q_0(u) \, du} \right\rangle \int_{-\infty}^{z} g_n(z - x) \, e^{-\frac{1}{\tau} \int_z^t g_n(u-x) H(u-x) du} \, \lambda_n(x) \, dx \tag{8}$$

3

$$\left\langle \prod_{k=1}^{K} e^{-\frac{1}{\tau} \int_{z_k}^{t_k} Q_n(u)\, du} \right\rangle = \exp\left(\int_{\mathcal{S}} \left(\prod_{k=1}^{K} e^{-\frac{1}{\tau} \int_{z_k}^{t_k} g_n(u-x) H(u-x) du} - 1 \right) \lambda_n(x)\, dx \right) \tag{9}$$

The cumulants of V_t are recovered from Eqs. (6) and (7) with the following transformation:

$$\langle V_t \rangle = (E_1 - E_N)\langle Y_t \rangle + E_l \qquad\qquad \langle\langle V_1 \cdots V_K \rangle\rangle = (E_1 - E_N)^K \langle\langle Y_1 \cdots Y_K \rangle\rangle \tag{10}$$

A comparison between numerical simulations and predictions from Eqs. (6) and (7) are shown in Fig. 3 for the mean and second order cumulants, where the autocorrelation is given by $\rho(V_1 V_2) = \langle\langle V_1 V_2 \rangle\rangle / (\sigma(V_1)\sigma(V_2))$.
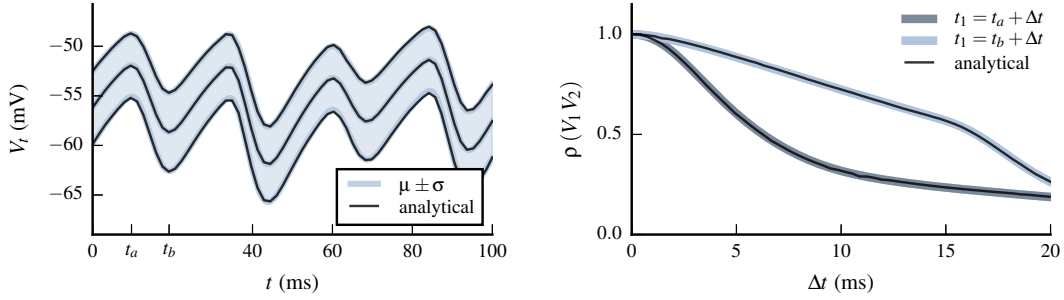

Figure 3 – *Comparison with numerical simulations for the mean and second order cumulants of membrane potential $V(t)$ predicted by the exact solution given by Eqs. (6) and (7). There is excellent agreement between the simulations (gray) and the analytic prediction (black). The autocorrelation ρ is evaluated at t_a and t_b corresponding to local maxima and minima of V_t, respectively.*

The exact cumulants given by Eqs (6) and (7) can be used to build very accurate approximations of the time-evolving distribution of membrane potential with a truncated Edgeworth series [Edgeworth, 1907, Wallace, 1958]. This series is an asymptotic expansion of $p(V_t)$ in terms of its cumulants [Cramér, 1946] and is provided for reference in Appendix C. The first term is a gaussian approximation with the second and third terms adding the contribution from the skewness and kurtosis of the distribution, respectively. As illustrated in Fig. 4, the skewness of $p(V_t)$ at the local minima t_b is well captured by the third order of the truncated Edgeworth series.
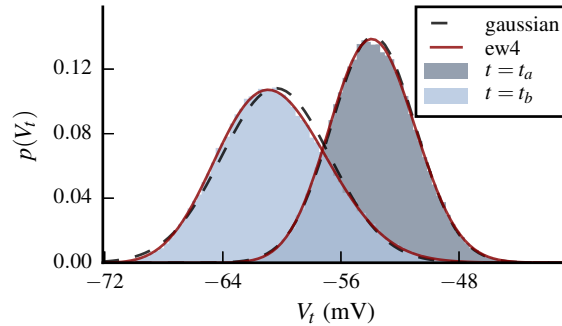
Figure 4 – *Comparison with numerical simulations for the probability density function (pdf) of membrane potential $p(V_t)$ given by truncated Edgeworth series using exact second and third cumulant of V_t. The pdf is evaluated at t_a and t_b that corresponds to local maxima and minima of V_t respectively (see Fig. 3). There is good agreement between the simulations (gray) and the gaussian approximation (black dash) at t_a. The effect of third order cumulant (kurtosis) at t_b is well captured by the third order of the series.*

2.2 Central Moments Expansion

The central moments expansion (CME) was also introduced in previous work [Brigham and Destexhe, 2015] and enables to evaluate the contribution of shot noise cumulants to the statistics of Y_t. This method corresponds to first and second order delta method expansions [Cramér, 1946, Oehlert, 1992] about the deterministic solution of the system. This is obtained by driving the system with input conductance with amplitude equal to the mean of shot noise $\langle Q_n(t) \rangle$ and is given by:

$$\langle Y_t \rangle_0 = \frac{1}{\tau} \int\limits_{-\infty}^{t} e^{-\frac{1}{\tau} \int_z^t \langle Q_0(u) \rangle du} \sum_{n=1}^{N} w_n \langle Q_n(z) \rangle \, dz \tag{11}$$

Directly expanding the exponential of integrated shot noise results in terms with mixed products of moments and central moments of shot noise. An expansion in terms of central moments is derived in Appendix B. The second order of the expansion for the mean is given by:

$$\langle Y_t \rangle_2 = \langle Y_t \rangle_0 + \frac{1}{\tau} \int\limits_{-\infty}^{t} e^{-\frac{1}{\tau} \int_z^t \langle Q_0(u) \rangle du}$$

$$\sum_{n=1}^{N} \left(-\frac{1}{\tau} \int\limits_z^t w_n \langle\langle Q_n(z) \, Q_n(u) \rangle\rangle \, du \right.$$

$$\left. + w_n \langle Q_n(z) \rangle \frac{1}{2\tau^2} \int\limits_z^t \int\limits_z^t \sum_{m=1}^{N} \langle\langle Q_m(u_1) \, Q_m(u_2) \rangle\rangle \, du_1 \, du_2 \right) dz \tag{12}$$

where the subscript 2 represents the second order of the expansion for the mean.

Extending to joint cumulants is obtained in similar manner and yields for the first order expansion for the autocovariance:

$$\langle\langle Y_1 \, Y_2 \rangle\rangle_1 = \frac{1}{\tau^2} \int\limits_{-\infty}^{t_1} \int\limits_{-\infty}^{t_2} e^{-\frac{1}{\tau} \int_{z_1}^{t_1} \langle Q_0(u_1) \rangle du_1 - \frac{1}{\tau} \int_{z_2}^{t_2} \langle Q_0(u_2) \rangle du_2}$$

$$\sum_{n=1}^{N} \left(w_n^2 \langle\langle Q_n(z_1) \, Q_n(z_2) \rangle\rangle \right.$$

$$+ \sum_{m=1}^{N} \sum_{m'=1}^{N} w_n \, w_m \langle Q_n(z_1) \rangle \langle Q_m(z_2) \rangle \frac{1}{\tau^2} \int\limits_{z_1}^{t_1} \int\limits_{z_2}^{t_2} \langle\langle Q_{m'}(u_1) \, Q_{m'}(u_2) \rangle\rangle \, du_1 \, du_2$$

$$- \sum_{l=1}^{N} w_n \, w_l \left(\langle Q_n(z_1) \rangle \frac{1}{\tau} \int\limits_{z_1}^{t_1} \langle\langle Q_l(u_1) \, Q_l(z_2) \rangle\rangle \, du_1 \right.$$

$$\left. \left. + \langle Q_n(z_2) \rangle \frac{1}{\tau} \int\limits_{z_2}^{t_2} \langle\langle Q_l(u_2) \, Q_l(z_1) \rangle\rangle \, du_2 \right) \right) dz_1 \, dz_2 \tag{13}$$

where the subscript 1 represents the first order of the expansion for the autocovariance.

The comparison between numerical simulations and the predictions for the mean and second order cumulants are shown in Fig. 5. The deterministic solution and first order of the autocorrelation display good agreement in this parameter regime, with the second order of the mean yielding higher accuracy.
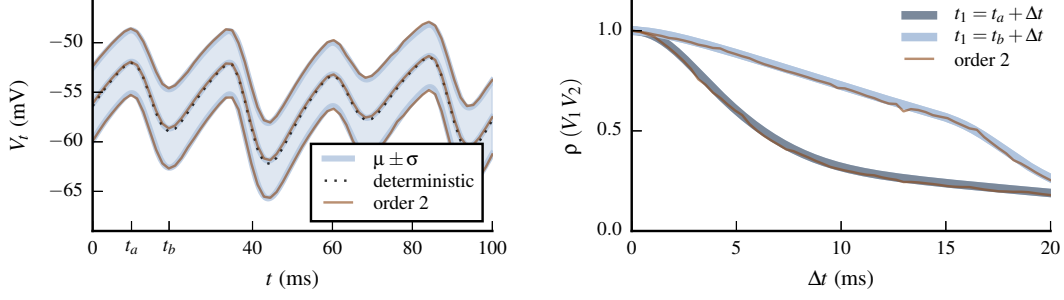
Figure 5 – *Comparison with numerical simulations for the mean and second order cumulants of V_t predicted by the central moments expansion (CME). The agreement between the simulations (gray lines) and the approximation is good for the deterministic solution (black dots) and first order expansion for the autocorrelation and variance (brown lines). The second order of the expansion for the mean shows higher accuracy, as expected. The second order of the expansion for the autocovariance may be required for more extreme parameter regimes.*

The stationary limit yields the statistics of Y_t under shot noise input with constant rate after dissipation of initial transients. The cumulants for this regime are obtained by setting the onset of PPP activity at $-\infty$ and replacing the cumulants of shot noise by their stationary limits. Explicit expressions for the mean and second order cumulants of exponential and alpha kernels are presented in the Appendix B.1.

$$\langle Y_t \rangle_0 = \frac{1}{\langle Q_0 \rangle} \sum_{n=1}^{N} w_n \langle Q_n \rangle \tag{14}$$

$$\langle Y_t \rangle_2 = \langle Y_t \rangle_0 - \sum_{n=1}^{N} \frac{1}{\langle Q_0 \rangle} (w_n - \langle Y_t \rangle_0) \langle\langle Q_n^2 \rangle\rangle \frac{1}{\tau} \int_{-\infty}^{t} e^{-\frac{t-z}{\tau} \langle Q_0 \rangle} r_n(t-z) \, dz \tag{15}$$

$$\langle\langle Y_1 Y_2 \rangle\rangle_1 = \sum_{n=1}^{N} (w_n - \langle Y_t \rangle_0)^2 \langle\langle Q_n^2 \rangle\rangle \frac{1}{\tau^2} \int_{-\infty}^{t_1} \int_{-\infty}^{t_2} e^{-\frac{t_1 - z_1 + t_2 - z_2}{\tau} \langle Q_0 \rangle} r_n(|z_1 - z_2|) \, dz_1 \, dz_2 \tag{16}$$

where $\langle Q_n \rangle$, $\langle\langle Q_n^2 \rangle\rangle$ and $\langle\langle Q_n(t_1) Q_n(t_2) \rangle\rangle_{stat} = \langle\langle Q_n^2 \rangle\rangle r(|t_1 - t_2|)$ are respectively the mean, variance and autocovariance of stationary shot noise input $Q_n(t)$.

3 Synaptic Inhomogeneities

Variations in the synaptic responses of the same synapse type are expected to occur due to biological differences in the synapses. These synaptic inhomogeneities are modeled by introducing individual synapses with particular synaptic parameters $\boldsymbol{\Theta}_n = \{\theta_1, \ldots, \theta_{N_n}\}$ that are distributed according to $p(\boldsymbol{\Theta}_n)$. Each synapse is driven by an independent shot noise processes with rate $\lambda_n(t)/N_n$. This leads to the the following model of input shot noise:

$$Q_n(t, \boldsymbol{\xi}_n, \boldsymbol{\Theta}_n) = \sum_{m=1}^{N_n} Q_m(t, \xi_m, \boldsymbol{\theta}_m) = \sum_{m=1}^{N_n} \sum_{x_j \in \xi_m} g_m(t - x_j, \boldsymbol{\theta}_m) H(t - x_j) \tag{17}$$

where $\boldsymbol{\theta}_m \sim p(\boldsymbol{\Theta}_n)$ are the synaptic parameters of synapse m of synapse type n.

For example, the exponential shot noise kernel is characterized by two parameters $\boldsymbol{\theta} = \{h, \tau_s\}$ representing the synaptic strength and synaptic time constant. The synaptic input from synapse m is generated with parameters $\boldsymbol{\theta}_m = \{h_m, (\tau_s)_m\}$ that are drawn at the beginning of the simulations from $p(\boldsymbol{\Theta}_n)$. This is illustrated in the left plot of Fig. 6 where color-coded presynaptic spike times reflect the synapse of origin.
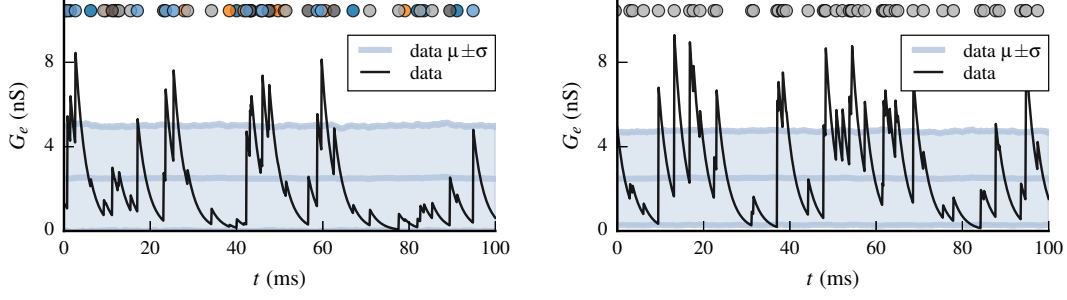
Figure 6 – *Example of synaptic input with small number of synapses ($N_e = 5$) with individual synaptic parameters from the same synapse type (left plot) where the presynaptic spikes are color-coded to represent the synapse of origin. In the limit of very large number of synapses the synaptic parameters change with each postsynaptic response (right plot). Comparing the realizations of both cases illustrates that the limit case may yield good approximations for a small number of synapses, depending on particular biological parameter distributions and simulation parameters.*

The limiting case of large number of synapses corresponds to varying the synaptic parameters $\boldsymbol{\theta}$ of shot noise kernel for each presynaptic spike. This is a compact representation in computational and analytical terms and leads to the following model of input shot noise:

$$Q_n(t, \xi_n^{\boldsymbol{\theta}}) = \sum_{x_j \in \xi_n^{\boldsymbol{\theta}}} g_n(t - x_j, \boldsymbol{\theta}_j) \, H(t - x_j) \tag{18}$$

where $\boldsymbol{\theta}$ are the synaptic parameters of the post synaptic response elicited by presynaptic spike time x_j.

This input model is illustrated in the right plot of Fig. 6 for excitatory conductance with synaptic strength distribution following an exponential law $p(h)$ with same mean as the homogenous model. The limiting case is rapidly approached, with a few dozen synapses being sufficient to yield similar synaptic input statistics. This is illustrated in Fig. 7 where a comparison for mean and variance is made for 5 and 50 synapses of each synapse type.
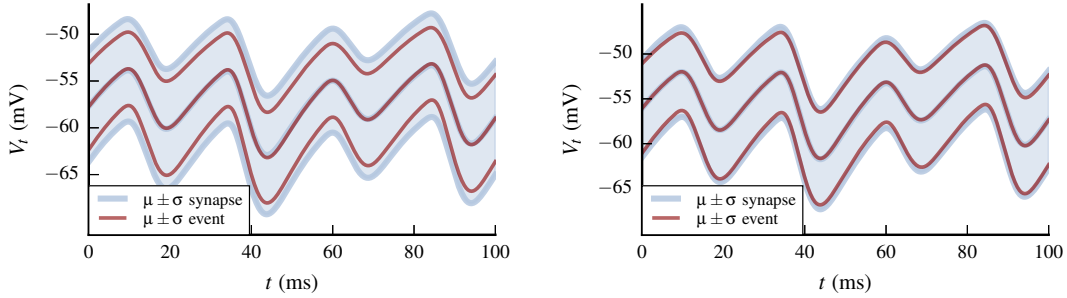

Figure 7 – *Comparison of membrane potential statistics for synaptic input generated from models with small number of synapses (left plot: $N_e = 5$, $N_i = 5$, right plot: $N_e = 50$, $N_i = 50$) and the limiting case of very large number of synapses (brown). The limiting case is approached quite rapidly from just a few dozen synapses under this parameter regime.*

This conductance input model corresponds to a general class of PPP transformations known as *Filtered Poisson Processes* [Snyder and Miller, 1991, Parzen, 1999, Streit, 2010, Rice, 1977]. The presynaptic spike times are generated by a *Compound PPP* $\boldsymbol{\Xi}^{\boldsymbol{\theta}}$ that for each point $x_j \in \xi$ generates a mark $\boldsymbol{\theta}_j$ independent of x_j that represents the synaptic parameters, i.e. $\boldsymbol{\theta}_j = \{h_j, (\tau_s)_j\}$ in the previous example of exponential kernel. A realization $\xi^{\boldsymbol{\theta}}$ specifies both the presynaptic spikes and the marks: $\xi^{\boldsymbol{\theta}} = \{(x_1, \theta_1), \ldots, (x_n, \theta_n)\}$. The *Slivnyak-Mecke Theorem* also applies to transformations of compound PPP since the properties of the PPP are not changed, as shown in Appendix D. The exact cumulants of this model are given by Eqs. (6) and (7). As before, the independence of $\boldsymbol{\Xi}^{\boldsymbol{\theta}}$ and the Slivnyak-Mecke Theorem yield the expectations in

the integrands, with the key expectations given by:

$$\left\langle Q_n(z)\, e^{-\frac{1}{\tau}\int_z^t Q_0(u)\, du} \right\rangle = \left\langle e^{-\frac{1}{\tau}\int_z^t Q_0(u)\, du} \right\rangle$$

$$\int_\Theta \int_{-\infty}^z g_n(z,x,\boldsymbol{\theta}_n)\, e^{-\frac{1}{\tau}\int_z^t g_n(u,x,\boldsymbol{\theta}_n)du}\, \lambda_n(x)\, dx\, p(\boldsymbol{\theta}_n)\, d\boldsymbol{\theta}_n \tag{19}$$

$$\left\langle \prod_{k=1}^K e^{-\frac{1}{\tau}\int_{z_k}^{t_k} Q_n(u)\, du} \right\rangle = \exp\left(\int_\Theta \int_{-\infty}^t \left(\prod_{k=1}^K e^{-\frac{1}{\tau}\int_{z_k}^{t_k} g_n(u,x,\boldsymbol{\theta}_n)\, du} - 1 \right) \lambda(x)\, dx\, p(\boldsymbol{\theta})\, d\boldsymbol{\theta} \right) \tag{20}$$

A comparison between numerical simulations and predictions from Eqs. (6) and (7) with Eqs. (19) and (20) is shown in Fig. 8 for the mean and standard deviation. The deterministic solution $\langle Y_t \rangle_0$ of this model corresponds to input with mean shot noise under $\boldsymbol{\Xi}^{\boldsymbol{\theta}}$:

$$\langle Q_n(t) \rangle = \int_\Theta \int_{-\infty}^t g_n(z,x,\boldsymbol{\theta}_n)\, \lambda_n(x)\, dx\, p(\boldsymbol{\theta}_n)\, d\boldsymbol{\theta}_n$$

The central moments expansion is developed around the deterministic solution and results in the same expressions as Eqs. (11), (12) and (13) but with shot noise expectations evaluated under $\boldsymbol{\Xi}^{\boldsymbol{\theta}}$.
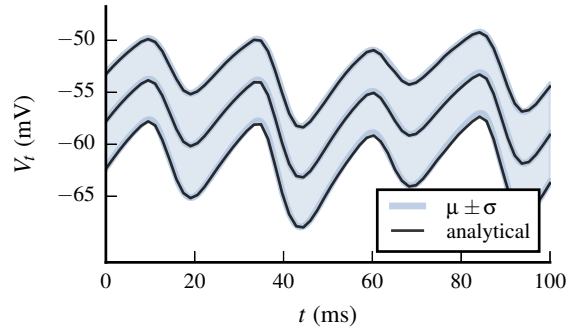

Figure 8 – *Comparison with numerical simulations for the exact mean and standard deviation evaluated with Eqs. (19) (20) for the model with large number of synapses. There is excellent agreement between the simulations (gray) and the analytic prediction (black).*

4 Impact of Synaptic Inhomogeneities

In this section we investigate the impact of synaptic inhomogeneity distributions in the statistics of Vm fluctuations. The examples from the previous section illustrate that synaptic input can be modeled with different synaptic responses for each presynaptic spike due to the important number of synapses present in biological neurons (from hundreds to many thousands). We assume the mean of the synaptic parameter distribution to be the same as the homogeneous model, noted $\bar{\boldsymbol{\theta}}$, i.e. $\langle h_n \rangle = \bar{h}_n$ for synaptic strenght of synapse type n. The effect of exponential and uniform distributions for the synaptic strength parameter h are compared to the homogeneous model.

As shown in Fig. 9, the mean value of V_t is similar in all cases and the standard deviation increases in the exponential case.
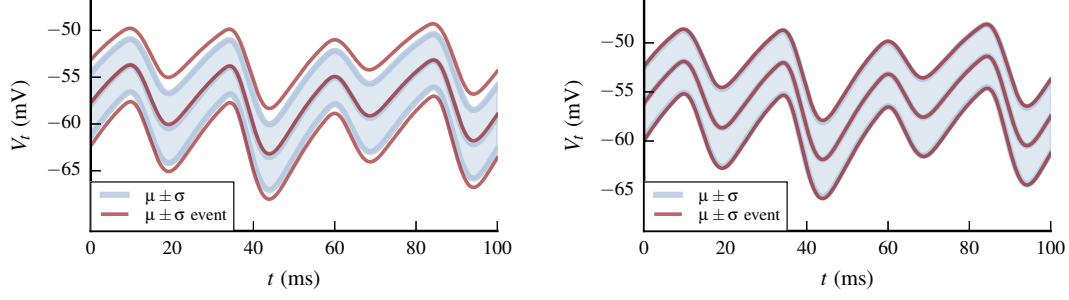
Figure 9 – *Effect of exponential and uniform distributions of synaptic strenghts on mean and standard deviation of membrane potential fluctuations. The mean is very similar in both cases and standard deviation increases for the exponential case. Mean and standard deviation ($\mu \pm \sigma$) shown in gray and brown for the homogeneous and inhomogeneous models, respectively.*

The CME enables to estimate this result under the assumption that the shot noise kernel is separable in the synaptic strength parameter h, such that $g(t) = \bar{h} f(t, \tau_s)$. This results in the following factorization of shot noise cumulants:

$$\langle Q_n(t) \rangle = h \, f_1(t, \tau_s, \lambda(t))$$

$$\langle\langle Q_n(t)^2 \rangle\rangle = h^2 \, f_2(t, \tau_s, \lambda(t))$$

$$\langle\langle Q_n(t_1) \, Q_n(t_2) \rangle\rangle = h^2 \, f_3(t_1 - t_2, \tau_s, \lambda(t))$$

The mean of shot noise input $\langle Q_n(t) \rangle_\theta$ remains unchanged since $\langle h_n \rangle = \bar{h}_n$. The deterministic solution also remains unchanged since it only depends on the mean input (Eq. (11)). The shot noise autocovariance changes by a common multiplicative factor $\langle h_n^2 \rangle / \bar{h}_n^2$ since the synaptic parameters are assumed to be drawn from the same distribution (but with different parameters). In consequence, the second order expansion for the mean (Eq. (12)) and first order expansion for the autocovariance (Eq. (13)) are changed by the multiplicative factor $\langle h_n^2 \rangle / \bar{h}_n^2$. For the exponential distribution $\langle h_n^2 \rangle = 2 \bar{h}_n^2$ and for uniform distribution $\langle h_n^2 \rangle = \bar{h}_n^2 (1 + 1/12)$. This explains the small change in the mean since the correction from the deterministic solution is already small in this parameter regime (see Fig. 5) and remains small when multiplied by a small factor. The small change in the standard deviation of the uniform distribution is due to the factor $\sqrt{1 + 1/12} \approx 1.04$. The variance and autocovariance are expected to increase by a factor of two in the case of exponential distribution, as illustrated in Fig. 10. The Gaussian approximation in the same figure is estimated from the homogeneous model with the variance multiplied by a factor $\langle h_n^2 \rangle / \bar{h}_n^2$.
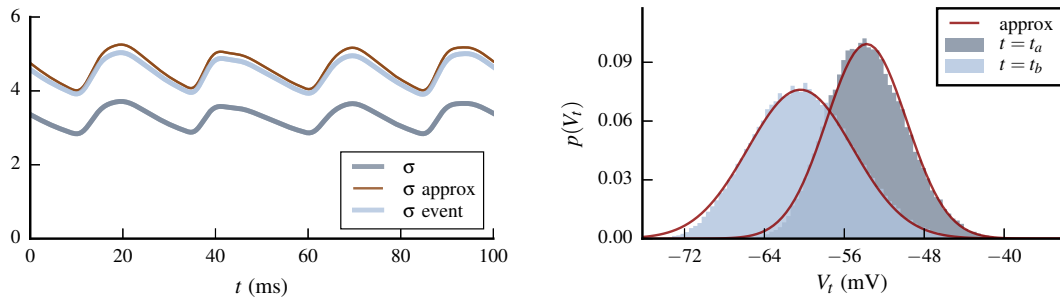

Figure 10 – *Estimating statistics of the inhomogeneous model from those of the homogeneous model. To the first order of the CME, the variance increases by a factor of 2 when synaptic strength parameter $h \sim p(h)$ is distributed exponentially with same mean as the homogeneous case. This approximation is used to estimate the standard deviation (left) and gaussian approximation of probability distribution (right). The distribution is evaluated at t_a and t_b corresponding respectively to the local maxima and minima of $\langle V_t \rangle$ shown in the left plot of Fig. 3.*

The autocorrelation is expected to remain unchanged since the changes in second order cumulants of shot noise is given by a constant factor. This prediction is compared to numerical simulations in Fig. 11 where the autocovariance is estimated separately.
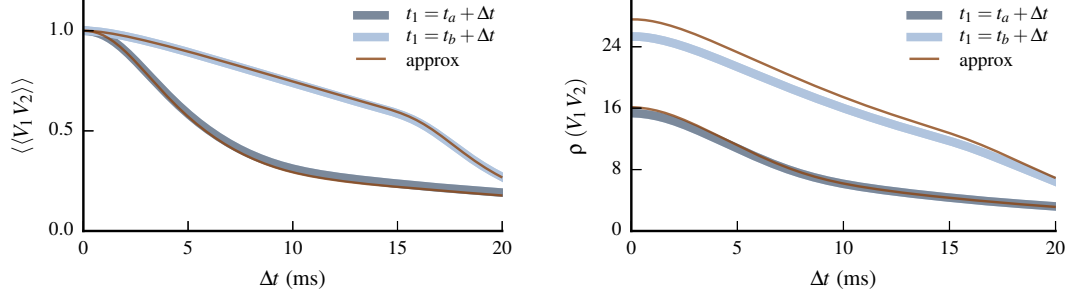
Figure 11 – *The CME predicts no change in the autocorrelation (to the first order of correlation) when introducing synaptic inhomogeneities under the same conditions in fig. 10 and predicts a doubling of autocovariance magnitude. The approximations were estimated by multiplying by a factor of two the second order statistics of the homogeneous model. The evaluations are made is evaluated at t_a and t_b (see Figs. 3 and 10).*

5 Discussion

The effects of synaptic inhomogeneities in the statistical properties of membrane potential (Vm) fluctuations is investigated. A simple passive membrane model is used with conductance synapses driven by nonstationary shot noise. An homogeneous model of synaptic input with N synapse types with identical synaptic properties for each synapse type is first examined. This model is then extended to include independent synapses with individual synaptic characteristics for each synapse type. In the limit of very large number of synapses the synaptic inhomogeneity is reflected in the variation of synaptic responses for each presynaptic spike.

The exact cumulants of the these models is obtained with the formalism of Poisson point process transformations. The central moments expansion (CME) is derived in order to understand how the hierarchy of shot noise cumulants impacts the statistics of Vm fluctuations. Under mild assumptions on factoring properties of the shot noise kernel, the cumulants of Vm are estimated from those of the homogeneous model.

The CME establishes the relationship between synaptic input statistics with synaptic inhomogeneities and the statistics of Vm. This may contribute to refine existing models of statistical inference that address the inverse problem of estimating the statistics of synaptic input from measures of membrane potential statistics. Improvements may be obtained by including measures of autocovariance in addition to the more common point statistics of mean and variance. An important pre-requisite is the experimental estimation of biological parameter distributions for neurons.

Acknowledgments

Appendix

A   Multivariate PPP Transformation

The expectation of a bounded transformation $F(t, \boldsymbol{\xi})$ of realizations $\boldsymbol{\xi} \equiv \{\xi_1, \ldots, \xi_N\}$ of the multivariate PPP Ξ [Cox and Isham, 1980] with independent components $\{\Xi_1(\mathcal{S}, \lambda_1(t)), \ldots, \Xi_N(\mathcal{S}, \lambda_N(t)\}$ is obtained by summing over every possible number of arrivals for each component PPP and integrating over the

location of each arrival.

$$\langle F(t, \boldsymbol{\xi}) \rangle = \sum_{n_1=0}^{\infty} \cdots \sum_{n_N=0}^{\infty} \frac{1}{n_1!} e^{-m_1(\mathcal{S})} \cdots \frac{1}{n_N!} e^{-m_N(\mathcal{S})}$$

$$\int_{\mathcal{S}} \cdots \int_{\mathcal{S}} \cdots \cdots \int_{\mathcal{S}} \cdots \int_{\mathcal{S}} F\left(t, x_1^1, \ldots, x_{n_1}^1, \ldots, x_1^N, \ldots, x_{n_N}^N\right) \prod_{n=1}^{N} \prod_{j_n=1}^{n_n} \lambda_n(x_{j_n}^n) \, dx_{j_n}^n$$

where x_j^n is the time of the j-th event from realization ξ_n.

The independence of the PPPs and the *Slivnyak-Mecke Theorem* [Slivnyak, 1962, Mecke, 1967] yields the expectations inside the integrals of Eqs. (6) and (7). For the mean and autocovariance:

$$\left\langle Q_n(z) \, e^{-\frac{1}{\tau} \int_z^t Q_0(u) \, du} \right\rangle = \left\langle e^{-\frac{1}{\tau} \int_z^t Q_0(u) \, du} \right\rangle \int_{-\infty}^{z} g_n(z, x) \, e^{-\frac{1}{\tau} \int_z^t g_n(u,x) \, du} \, \lambda_n(x) \, dx$$

$$\sum_{n=1}^{N} \sum_{m=1}^{N} \left\langle w_n \, Q_n(z_1) \, w_m \, Q_m(z_2) \prod_{k=1}^{2} e^{-\frac{1}{\tau} \int_{z_k}^{t_k} Q_0(u) \, du} \right\rangle$$

$$= \left\langle \prod_{k=1}^{2} e^{-\frac{1}{\tau} \int_{z_k}^{t_k} Q_0(u) \, du} \right\rangle \left(\sum_{n=1}^{N} w_n^2 \int_{-\infty}^{\min(z_1,z_2)} g_n(z_1 - x) \, g_n(z_2 - x) \prod_{k=1}^{2} e^{-\frac{1}{\tau} \int_{z_k}^{t_k} g_n(u-x) \, H(u-x) \, du} \, \lambda_n(x) \, dx \right.$$

$$+ \sum_{m=1}^{N} w_m \int_{-\infty}^{z_1} g_m(z_1 - y) \prod_{k=1}^{2} e^{-\frac{1}{\tau} \int_{z_k}^{t_k} g_m(v-y) \, H(v-y) \, dv} \, \lambda_m(y) \, dy$$

$$\left. \sum_{l=1}^{N} w_l \int_{-\infty}^{z_2} g_l(z_2 - z) \prod_{k=1}^{2} e^{-\frac{1}{\tau} \int_{z_k}^{t_k} g_l(w-z) \, H(w-z) \, dw} \, \lambda_l(z) \, dz \right)$$

since for $n = m$,

$$w_n^2 \left\langle Q_n(z_1) \, e^{-\frac{1}{\tau} \int_{z_1}^{t_1} Q_0(u_1) du_1} \, Q_n(z_2) \, e^{-\frac{1}{\tau} \int_{z_2}^{t_2} Q_0(u_2) du_2} \right\rangle$$

$$= w_n^2 \left\langle Q_n(z_1) \, Q_n(z_2) \, e^{-\frac{1}{\tau} \int_{z_1}^{t_1} Q_n(u_1) du_1 - \frac{1}{\tau} \int_{z_2}^{t_2} Q_n(u_2) du_2} \right\rangle \left\langle e^{-\frac{1}{\tau} \int_{z_1}^{t_1} Q_{0 \backslash n}(v_1) dv_1 - \frac{1}{\tau} \int_{z_2}^{t_2} Q_{0 \backslash n}(v_2) dv_2} \right\rangle$$

$$= w_n^2 \, e^{-\frac{t_1 - z_1 + t_2 - z_2}{\tau}} \prod_{l=1}^{N} \left\langle e^{-\frac{1}{\tau} \int_{z_1}^{t_1} Q_l(u_1) du_1 - \frac{1}{\tau} \int_{z_2}^{t_2} Q_l(u_2) \, du_2} \right\rangle$$

$$\left(\int_{-\infty}^{\min(t_1,t_2)} g_n(z_1 - x) \, g_n(z_2 - x) \, e^{-\frac{1}{\tau} \int_{z_1}^{t_1} g_n(u_1-x) du_1 - \frac{1}{\tau} \int_{z_2}^{t_2} g_n(u_2-x) du_2} \lambda_n(x) \, dx \right.$$

$$+ \int_{-\infty}^{t_1} g_n(z_1 - y) \, e^{-\frac{1}{\tau} \int_{z_1}^{t_1} g_n(u_1-y) du_1 - \frac{1}{\tau} \int_{z_2}^{t_2} g_n(u_2-y) du_2} \lambda_n(y) \, dy$$

$$\left. \int_{-\infty}^{t_2} g_n(z_2 - w) \, e^{-\frac{1}{\tau} \int_{z_1}^{t_1} g_n(u_1-w) du_1 - \frac{1}{\tau} \int_{z_2}^{t_2} g_n(u_2-w) du_2} \lambda_n(w) \, dw \right)$$

For $n \neq m$,

$$w_n\, w_m \left\langle Q_n(z_1)\, e^{-\frac{1}{\tau}\int_{z_1}^{t_1} Q_0(u_1)du_1}\, Q_m(z_2)\, e^{-\frac{1}{\tau}\int_{z_2}^{t_2} Q_0(u_2)du_2} \right\rangle$$

$$= w_n\, w_m \left\langle Q_n(z_1)\, e^{-\frac{1}{\tau}\int_{z_1}^{t_1} Q_n(u_1)du_1 - \frac{1}{\tau}\int_{z_2}^{t_2} Q_n(u_2)du_2} \right\rangle \left\langle Q_m(z_2)\, e^{-\frac{1}{\tau}\int_{z_1}^{t_1} Q_{0\backslash n}(v_1)dv_1 - \frac{1}{\tau}\int_{z_2}^{t_2} Q_{0\backslash n}(v_2)dv_2} \right\rangle$$

$$= w_n\, w_m \prod_{l=1}^{N} \left\langle e^{-\frac{1}{\tau}\int_{z_1}^{t_1} Q_l(u_1)du_1 - \frac{1}{\tau}\int_{z_2}^{t_2} Q_l(u_2)\, du_2} \right\rangle$$

$$\int_{-\infty}^{t_1} g_n(z_1 - x)\, e^{-\frac{1}{\tau}\int_{z_1}^{t_1} g_n(u_1-x)du_1 - \frac{1}{\tau}\int_{z_2}^{t_2} g_n(u_2-x)du_2}\, \lambda_n(x)\, dx$$

$$\int_{-\infty}^{t_2} g_I(z_2 - y)\, e^{-\frac{1}{\tau}\int_{z_1}^{t_1} g_I(v_1-y)\, dv_1 - \frac{1}{\tau}\int_{z_2}^{t_2} g_I(v_2-y)\, dv_2}\, \lambda_I(y)\, dy$$

And in the general case,

$$\left\langle \prod_{k=1}^{K} e^{-\frac{1}{\tau}\int_{z_k}^{t_k} Q_0(u)\, du} \right\rangle = \prod_{n=1}^{N} \left\langle \prod_{k=1}^{K} e^{-\frac{1}{\tau}\int_{z_k}^{t_k} Q_n(u)\, du} \right\rangle \prod_{k'=1}^{K} e^{-\frac{t_{k'} - z_{k'}}{\tau}}$$

$$\left\langle \prod_{k=1}^{K} e^{-\frac{1}{\tau}\int_{z_k}^{t_k} Q_n(u)\, du} \right\rangle = \exp\left(\int_{\mathcal{S}} \left(\prod_{k=1}^{K} e^{-\frac{1}{\tau}\int_{z_k}^{t_k} g_n(u-x)\, H(u-x)\, du} - 1 \right) \lambda_n(x)\, dx \right)$$

B   Central Moments Expansion

The independence properties of Ξ lead to the following factorization for the mean of Y_t. Writing $Q_{0\backslash n}$ as Q_0 without Q_n,

$$\langle Y_t \rangle = \frac{1}{\tau} \int_{-\infty}^{t} \sum_{n=1}^{N} w_n \left\langle Q_n(z)\, e^{-\frac{1}{\tau}\int_z^t Q_0(u)du} \right\rangle dz = \frac{1}{\tau} \int_{-\infty}^{t} \sum_{n=1}^{N} w_n \left\langle Q_n(z)\, e^{-\frac{1}{\tau}\int_z^t Q_n(u)du} \right\rangle \left\langle e^{-\frac{1}{\tau}\int_z^t Q_{0\backslash n}(v)dv} \right\rangle dz$$

The expectation of exponential integrated shot noise on the right is derived in [Brigham and Destexhe, 2015] and we just need to derive the expectation the product of shot noise with the exponential integrated shot noise. Directly expanding the exponential term would yield mixed products of moments and central moments:

$$\left\langle Q(z)_n\, e^{-\frac{1}{\tau}\int_z^t Q_n(u)\, du} \right\rangle = e^{-\frac{1}{\tau}\int_z^t \langle Q_n(u)\rangle du} \left(\langle Q_n(z) \rangle + \sum_{m=1}^{+\infty} \frac{1}{m!} \left\langle Q_n(z) \left(-\frac{1}{\tau} \int_z^t (Q_n(u) - \langle Q_n(u)\rangle)\, du \right)^m \right\rangle \right)$$

To recover an expansion in terms of central moments, we first form the shot noise central moment inside the expectation before expanding the exponential term,

$$\left\langle Q_n(z)\, e^{-\frac{1}{\tau}\int_z^t Q_n(u)du} \right\rangle$$

$$= e^{-\frac{1}{\tau}\int_z^t \langle Q_n(u)\rangle du} \left(\left\langle (Q_n(z) - \langle Q_n(z)\rangle)\, e^{-\frac{1}{\tau}\int_z^t (Q_n(u) - \langle Q_n(u)\rangle)du} \right\rangle + \langle Q_n(z) \rangle \left\langle e^{-\frac{1}{\tau}\int_z^t (Q_n(v) - \langle Q_n(v)\rangle)dv} \right\rangle \right)$$

$$= e^{-\frac{1}{\tau}\int_z^t \langle Q\rangle(u)du} \left(\langle Q_n(z) \rangle + \sum_{m=1}^{+\infty} \frac{1}{m!} \left(\left\langle (Q_n(z) - \langle Q_n(z)\rangle) \left(-\frac{1}{\tau} \int_z^t (Q_n(u) - \langle Q_n(u)\rangle)\, du \right)^m \right\rangle \right. \right.$$

$$\left. \left. + \frac{1}{m+1}\, \langle Q_n(z) \rangle \left\langle \left(-\frac{1}{\tau} \int_z^t (Q_n(v) - \langle Q_n(v)\rangle)\, dv \right)^{m+1} \right\rangle \right) \right)$$

Keeping terms up to the second order in the central moments ($m = 1$) and expressing in terms of shot noise autocovariance yields the final result:

$$\left\langle Q_n(z) \, e^{-\frac{1}{\tau} \int_z^t Q_n(u)du} \right\rangle$$

$$\simeq e^{-\frac{1}{\tau} \int_z^t \langle Q_n(u) \rangle du} \left(\langle Q_n(z) \rangle - \frac{1}{\tau} \int_z^t \langle\langle Q_n(z) \, Q_n(u) \rangle\rangle \, du + \langle Q_n(z) \rangle \frac{1}{2\tau^2} \int_z^t \int_z^t \langle\langle Q_n(u_1) \, Q_n(u_2) \rangle\rangle \, du_1 \, du_2 \right)$$

In terms of Y_t,

$$\langle Y_t \rangle_0 = \frac{1}{\tau} \int_{-\infty}^t e^{-\frac{1}{\tau} \int_z^t \langle Q_0(u) \rangle du} \sum_{n=1}^N w_n \, \bar{Q}_n(z) dz$$

$$\langle Y_t \rangle_2 = \langle Y_t \rangle_0 + \frac{1}{\tau} \int_{-\infty}^t e^{-\frac{1}{\tau} \int_z^t \langle Q_0(u) \rangle du}$$

$$\sum_{n=1}^N \left(-\frac{1}{\tau} \int_z^t w_n \, \langle\langle Q_n(z) \, Q_n(u) \rangle\rangle \, du + w_n \, \langle Q_n(z) \rangle \frac{1}{2\tau^2} \int_z^t \int_z^t \sum_{m=1}^N \langle\langle Q_m(u_1) \, Q_m(u_2) \rangle\rangle \, du_1 \, du_2 \right) dz$$

The autocovariance requires the evaluation of terms of the form:

$$\langle\langle Y_1 \, Y_2 \rangle\rangle_1 = \frac{1}{\tau^2} \int_{-\infty}^{t_1} \int_{-\infty}^{t_2} \sum_{n=1}^N \sum_{m=1}^N w_n \, w_m \left\langle\left\langle Q_n(z_1) \, e^{-\frac{1}{\tau} \int_{z_1}^{t_1} Q_0(u_1)du_1} \, Q_m(z_2) \, e^{-\frac{1}{\tau} \int_{z_2}^{t_2} Q_0(v) \, dv} \right\rangle\right\rangle dz_1 \, dz_2$$

Expanding each exponential and forming products with central moments, for the case $m = n$,

$$w_n^2 \left\langle\left\langle Q_n(z_1) \, e^{-\frac{1}{\tau} \int_{z_1}^{t_1} Q_0(u_1)du_1} \, Q_n(z_2) \, e^{-\frac{1}{\tau} \int_{z_2}^{t_2} Q_0(u_2)du_2} \right\rangle\right\rangle$$

$$= w_n^2 \left\langle\left\langle (Q_n(z_1) - \langle Q_n(z_1) \rangle) \, e^{-\frac{1}{\tau} \int_{z_1}^{t_1} Q_0(u_1)du_1} \, (Q_n(z_2) - \langle Q_n(z_2) \rangle) \, e^{-\frac{1}{\tau} \int_{z_2}^{t_2} Q_0(u_2)du_2} \right\rangle\right\rangle$$

$$+ w_n^2 \, \langle Q_n(z_1) \rangle \left\langle\left\langle e^{-\frac{1}{\tau} \int_{z_1}^{t_1} Q_0(u_1)du_1} \, (Q_n(z_2) - \langle Q_n(z_2) \rangle) \, e^{-\frac{1}{\tau} \int_{z_2}^{t_2} Q_0(u_2)du_2} \right\rangle\right\rangle$$

$$+ w_n^2 \, \langle Q_n(z_2) \rangle \left\langle\left\langle (Q_n(z_1) - \langle Q_n(z_1) \rangle) \, e^{-\frac{1}{\tau} \int_{z_1}^{t_1} Q_0(u_1)du_1} \, e^{-\frac{1}{\tau} \int_{z_2}^{t_2} Q_0(u_2)du_2} \right\rangle\right\rangle$$

$$+ w_n^2 \, \langle Q_n(z_1) \rangle \langle Q_n(z_2) \rangle \left\langle\left\langle e^{-\frac{1}{\tau} \int_{z_1}^{t_1} Q_0(u_1)du_1} \, e^{-\frac{1}{\tau} \int_{z_2}^{t_2} Q_0(u_2)du_2} \right\rangle\right\rangle$$

Up to the 2nd order in the cumulants,

$$\simeq w_n^2 \, e^{-\frac{1}{\tau} \int_{z_1}^{t_1} \langle Q_0(u_1) \rangle du_1 - \frac{1}{\tau} \int_{z_2}^{t_2} \langle Q_0(u_2) \rangle du_2}$$

$$\left(\langle\langle (Q_n(z_1) - \langle Q_n(z_1) \rangle) \, (Q_n(z_2) - \langle Q_n(z_2) \rangle) \rangle\rangle + \langle Q_n(z_1) \rangle \langle Q_n(z_2) \rangle \left\langle\left\langle \frac{1}{\tau} \int_{z_1}^{t_1} Q_0(u_1) \, du_1 \, \frac{1}{\tau} \int_{z_2}^{t_2} Q_0(u_2) \, du_2 \right\rangle\right\rangle \right.$$

$$- \langle Q_n(z_1) \rangle \left\langle\left\langle \frac{1}{\tau} \int_{z_1}^{t_1} Q_0(u_1) \, du_1 \, (Q_n(z_2) - \langle Q_n(z_2) \rangle) \right\rangle\right\rangle$$

$$\left. - \langle Q_n(z_2) \rangle \left\langle\left\langle (Q_n(z_1) - \langle Q_n(z_1) \rangle) \frac{1}{\tau} \int_{z_2}^{t_2} Q_0(u_2) \, du_2 \right\rangle\right\rangle \right)$$

13

Removing terms with independent values yields the final expression:

$$\simeq w_n^2\, e^{-\frac{1}{\tau}\int_{z_1}^{t_1}\langle Q_0(u_1)\rangle du_1 - \frac{1}{\tau}\int_{z_2}^{t_2}\langle Q_0(u_2)\rangle du_2}$$

$$\left(\langle\langle Q_n(z_1)\, Q_n(z_2)\rangle\rangle - \langle Q_n(z_1)\rangle\, \frac{1}{\tau}\int_{z_1}^{t_1} \langle\langle Q_n(u)\, Q_n(z_2)\rangle\rangle\, du - \langle Q_n(z_2)\rangle\, \frac{1}{\tau}\int_{z_2}^{t_2}\langle\langle Q_n(z_1)\, Q_n(v)\rangle\rangle\, dv \right.$$

$$\left. + \langle Q_n(z_1)\rangle\, \langle Q_n(z_2)\rangle\, \frac{1}{\tau^2}\int_{z_1}^{t_1}\int_{z_2}^{t_2}\sum_{m=1}^N \langle\langle Q_m(u_1)\, Q_m(u_2)\rangle\rangle\, du_1\, du_2 \right)$$

For the mixed terms $m \neq n$ and following similar steps,

$$w_n\, w_m\, \left\langle\left\langle Q_n(z_1)\, e^{-\frac{1}{\tau}\int_{z_1}^{t_1} Q_0(u)du_1}\, Q_m(z_2)\, e^{-\frac{1}{\tau}\int_{z_2}^{t_2} Q_0(u_2)du_2}\right\rangle\right\rangle$$

$$\simeq w_n\, w_m\, e^{-\frac{1}{\tau}\int_{z_1}^{t_1}\langle Q_0(u_1)\rangle du_1 - \frac{1}{\tau}\int_{z_2}^{t_2}\langle Q_0(u_2)\rangle du_2}$$

$$\left(-\langle Q_n(z_1)\rangle\, \frac{1}{\tau}\int_{z_1}^{t_1}\langle\langle Q_m(u)\, Q_m(z_2)\rangle\rangle\, du - \langle Q_m(z_2)\rangle\, \frac{1}{\tau}\int_{z_2}^{t_2}\langle\langle Q_n(z_1)\, Q_n(v)\rangle\rangle\, dv \right.$$

$$\left. + \langle Q_n(z_1)\rangle\, \langle Q_m(z_2)\rangle\, \frac{1}{\tau^2}\int_{z_1}^{t_1}\int_{z_2}^{t_2}\left(\langle\langle Q_n(u_1)\, Q_n(u_2)\rangle\rangle + \langle\langle Q_m(u_1)\, Q_m(u_2)\rangle\rangle \right) du_1\, du_2 \right)$$

In terms of the filtered process,

$$\langle\langle Y_1\, Y_2\rangle\rangle_1 = \frac{1}{\tau^2}\int_{-\infty}^{t_1}\int_{-\infty}^{t_2}\sum_{n=1}^N \left(w_n^2\, \left\langle\left\langle Q_n(z_1)\, e^{-\frac{1}{\tau}\int_{z_1}^{t_1} Q_0(u_1)du_1}\, Q_n(z_2)\, e^{-\frac{1}{\tau}\int_{z_2}^{t_2} Q_0(u_2)\, du_2}\right\rangle\right\rangle \right.$$

$$\left. + \sum_{m\neq n} w_n\, w_m\, \left\langle\left\langle Q_n(z_1)\, e^{-\frac{1}{\tau}\int_{z_1}^{t_1} Q_0(u_1)du_1}\, Q_m(z_2)\, e^{-\frac{1}{\tau}\int_{z_2}^{t_2} Q_0(u_2)\, du_2}\right\rangle\right\rangle \right) dz_1\, dz_2$$

$$= \frac{1}{\tau^2}\int_{-\infty}^{t_1}\int_{-\infty}^{t_2} e^{-\frac{1}{\tau}\int_{z_1}^{t_1}\langle Q_0(u_1)\rangle du_1 - \frac{1}{\tau}\int_{z_2}^{t_2}\langle Q_0(u_2)\rangle du_2}$$

$$\sum_{n=1}^N \left(w_n^2\, \langle\langle Q_n(z_1)\, Q_n(z_2)\rangle\rangle + \sum_{m=1}^N\sum_{m'=1}^N w_n\, w_m \bar{Q}_n(z_1)\, \bar{Q}_m(z_2)\, \frac{1}{\tau^2}\int_{z_1}^{t_1}\int_{z_2}^{t_2}\langle\langle Q_{m'}(u_1)\, Q_{m'}(u_2)\rangle\rangle\, du_1\, du_2 \right.$$

$$\left. - \sum_{l=1}^N w_n\, w_l\left(\bar{Q}_n(z_1)\, \frac{1}{\tau}\int_{z_1}^{t_1}\langle\langle Q_l(u_1)\, Q_l(z_2)\rangle\rangle\, du_1 + \bar{Q}_n(z_2)\, \frac{1}{\tau}\int_{z_2}^{t_2}\langle\langle Q_l(u_2)\, Q_l(z_1)\rangle\rangle\, du_2 \right) \right) dz_1\, dz_2$$

B.1 Stationary Limit

The stationary limit is obtained by setting the onset of PPP activity at an earlier point than membrane potential integration, such that the cumulants of shot noise can be replaced by their stationary limits.

$$\langle Y_t\rangle_0 = \sum_{n=1}^N w_n\, \langle Q_n\rangle\, \frac{1}{\tau}\int_{-\infty}^t e^{-\frac{t-z}{\tau}\langle Q_0\rangle}\, dz = \frac{1}{\langle Q_0\rangle}\sum_{n=1}^N w_n\, \langle Q_n\rangle$$

The stationary limit of shot noise autocovariance can be written $\langle\langle Q_1\, Q_2\rangle\rangle_{stat} = \langle\langle Q^2\rangle\rangle\, r\,(|t_1 - t_2|)$, since:

$$\langle\langle Q_1\, Q_2\rangle\rangle_{stat} = \lambda\int_{-\infty}^{\min(t_1,t_2)} f(t_1 - x)\, f(t_2 - x)\, dx = \lambda\int_0^{+\infty} f(u)\, f(|t_1 - t_2| + u)\, du = \langle\langle Q^2\rangle\rangle\, r\,(|t_1 - t_2|)$$

14

with $r\left(|t_1 - t_2|\right) \equiv \int_0^{+\infty} f(u)\, f(|t_1 - t_2| + u)\, du / \int_0^{+\infty} f(v)^2\, dv$

For the second order of the mean, integrating by parts the inner integrals yields:

$$\langle Y_t \rangle_2 = \langle Y_t \rangle_0 + \sum_{n=1}^{N} \left\langle\!\left\langle Q_n^2 \right\rangle\!\right\rangle \frac{1}{\tau} \int_{-\infty}^{t} e^{-\frac{t-z}{\tau} \langle Q_0 \rangle}$$

$$\left(-w_n \frac{1}{\tau} \int_0^{t-z} r_n(u)\, du + \sum_{m=1}^{N} w_m \langle Q_m \rangle \frac{1}{2\tau^2} \int_z^t \int_z^t r_n(|u_1 - u_2|)\, du_1\, du_2 \right) dz$$

$$= \langle Y_t \rangle_0 + \sum_{n=1}^{N} \left\langle\!\left\langle Q_n^2 \right\rangle\!\right\rangle \frac{1}{\langle Q_0 \rangle} \frac{1}{\tau} \int_{-\infty}^{t} e^{-\frac{t-z}{\tau} \langle Q_0 \rangle} \left(-w_n\, r_n(t-z) + \sum_{m=1}^{N} w_m \langle Q_m \rangle \frac{1}{\tau} \int_0^{t-z} r_n(v)\, dv \right) dz$$

$$= \langle Y_t \rangle_0 - \sum_{n=1}^{N} \frac{1}{\langle Q_0 \rangle} \left(w_n - \langle Y_t \rangle_0 \right) \left\langle\!\left\langle Q_n^2 \right\rangle\!\right\rangle \frac{1}{\tau} \int_{-\infty}^{t} e^{-\frac{t-z}{\tau} \langle Q_0 \rangle}\, r_n(t-z)\, dz$$

Proceeding in the same manner for the autocovariance,

$$\left\langle\!\left\langle Y_1 Y_2 \right\rangle\!\right\rangle_1 = \frac{1}{\tau^2} \int_{-\infty}^{t_1} \int_{-\infty}^{t_2} e^{-\frac{t_1 - z_1 + t_2 - z_2}{\tau} \langle Q_0 \rangle}$$

$$\sum_{n=1}^{N} \left(w_n^2 \left\langle\!\left\langle Q_n^2 \right\rangle\!\right\rangle r_n(|z_1 - z_2|) + \sum_{m=1}^{N} \sum_{m'=1}^{N} w_n w_m \langle Q_n \rangle \langle Q_m \rangle \left\langle\!\left\langle Q_{m'}^2 \right\rangle\!\right\rangle \frac{1}{\tau^2} \int_{z_1}^{t_1} \int_{z_2}^{t_2} r_{m'}(|u_1 - u_2|)\, du_1\, du_2 \right.$$

$$\left. - \sum_{l=1}^{N} w_n w_l \langle Q_n \rangle \left\langle\!\left\langle Q_l^2 \right\rangle\!\right\rangle \left(\frac{1}{\tau} \int_{z_1}^{t_1} r_l(|u_1 - z_2|)\, du_1 + \frac{1}{\tau} \int_{z_2}^{t_2} r_l(|z_1 - u_2|)\, du_2 \right) \right) dz_1\, dz_2$$

$$= \frac{1}{\tau^2} \int_{-\infty}^{t_1} \int_{-\infty}^{t_2} e^{-\frac{t_1 - z_1 + t_2 - z_2}{\tau} \langle Q_0 \rangle}$$

$$\sum_{n=1}^{N} \left(w_n^2 \left\langle\!\left\langle Q_n^2 \right\rangle\!\right\rangle r_n(|z_1 - z_2|) + \frac{w_n \langle Q_n \rangle}{\langle Q_0 \rangle} \sum_{m=1}^{N} \left(\langle Y_t \rangle_0 - 2w_m \right) \left\langle\!\left\langle Q_m^2 \right\rangle\!\right\rangle r_m(|z_1 - z_2|)\, dz_1\, dz_2 \right)$$

$$= \sum_{n=1}^{N} \left(w_n - \langle Y_t \rangle_0 \right)^2 \left\langle\!\left\langle Q_n^2 \right\rangle\!\right\rangle \frac{1}{\tau^2} \int_{-\infty}^{t_1} \int_{-\infty}^{t_2} e^{-\frac{t_1 - z_1 + t_2 - z_2}{\tau} \langle Q_0 \rangle}\, r_n(|u_1 - u_2|)\, dz_1\, dz_2$$

For exponential kernel shot noise,

$$\langle Y_t \rangle_2 = \langle Y_t \rangle_0 - \sum_{n=1}^{N} \frac{\left\langle\!\left\langle Q_n^2 \right\rangle\!\right\rangle}{\langle Q_0 \rangle} \left(w_n - \langle Y_t \rangle_0 \right) \frac{1}{\tau} \int_{-\infty}^{t} e^{-\frac{t-z}{\tau} \langle Q_0 \rangle} e^{-\frac{t-z}{\tau_n}}\, dz = \langle Y_t \rangle_0 - \sum_{n=1}^{N} \frac{\left\langle\!\left\langle Q_n^2 \right\rangle\!\right\rangle}{\langle Q_0 \rangle \left(\langle Q_0 \rangle + \frac{\tau}{\tau_n} \right)} \left(w_n - \langle Y_t \rangle_0 \right)$$

where τ_n is the synaptic time constant of shot noise conductance $G_n(t)$.

For the autocovariance,

$$\left\langle\!\left\langle Y_1 Y_2 \right\rangle\!\right\rangle_1 = \sum_{n=1}^{N} \left(w_n - \langle Y_t \rangle_0 \right)^2 \left\langle\!\left\langle Q_n^2 \right\rangle\!\right\rangle \frac{1}{\tau^2} \int_{-\infty}^{t_1} \int_{-\infty}^{t_2} e^{-\frac{t_1 - z_1 + t_2 - z_2}{\tau} \langle Q_0 \rangle} e^{-\frac{|z_1 - z_2|}{\tau_n}}\, dz_1\, dz_2$$

15

Assuming $t_1 \geq t_2$,

$$\langle\langle Y_1 Y_2\rangle\rangle_1$$

$$= \sum_{n=1}^{N} (w_n - \langle Y_t\rangle_0)^2 \langle\langle Q_n^2\rangle\rangle$$

$$\frac{1}{\tau^2} \int_{-\infty}^{t_2} e^{-\frac{t_2-z_2}{\tau}\langle Q_0\rangle} \left(\int_{-\infty}^{z_1} e^{-\frac{t_1-z_1}{\tau}\langle Q_0\rangle} e^{-\frac{z_1-z_2}{\tau_n}} \, dz_1 + \int_{z_1}^{t_2} e^{-\frac{t_1-z_1}{\tau}\langle Q_0\rangle} e^{-\frac{z_2-z_1}{\tau_n}} \, dz_1 + \int_{t_2}^{t_1} e^{-\frac{t_1-z_1}{\tau}\langle Q_0\rangle} e^{-\frac{z_1-z_2}{\tau_n}} \, dz_1 \right) dz_2$$

Evaluating the integrals yields the final expression:

$$\langle\langle Y_1 Y_2\rangle\rangle_1 = \sum_{n=1}^{N} \frac{\langle\langle Q_n^2\rangle\rangle}{\left(\langle Q_0\rangle + \frac{\tau}{\tau_n}\right)\left(\langle Q_0\rangle - \frac{\tau}{\tau_n}\right)} \left(e^{-\frac{|t_1-t_2|}{\tau_n}} - \frac{\tau}{\tau_n} \frac{1}{\langle Q_0\rangle} e^{-\frac{|t_1-t_2|}{\tau}\langle Q_0\rangle} \right) (w_n - \langle Y_t\rangle_0)^2$$

$$\langle\langle Y^2\rangle\rangle_1 = \sum_{n=1}^{N} \frac{\langle\langle Q_n^2\rangle\rangle}{\langle Q_0\rangle \left(Q_0 + \frac{\tau}{\tau_n}\right)} (w_n - \langle Y_t\rangle_0)^2$$

Expressing in terms of V_t yields:

$$\langle V_t\rangle_0 = \frac{1}{\langle G_0\rangle} \left(g_l E_l + \sum_{n=1}^{N} \langle G_n\rangle E_n \right)$$

$$\langle V_t\rangle_2 = \langle V_t\rangle_0 - \sum_{n=1}^{N} \frac{\langle\langle G_n^2\rangle\rangle}{g_l \langle G_0\rangle \left(\frac{\langle G_0\rangle}{g_l} + \frac{\tau}{\tau_n}\right)} (E_n - \langle V_t\rangle_0) \quad \langle\langle V_t^2\rangle\rangle = \sum_{n=1}^{N} \frac{\langle\langle G_n^2\rangle\rangle}{g_l \langle G_0\rangle \left(\frac{\langle G_0\rangle}{g_l} + \frac{\tau}{\tau_n}\right)} (E_n - \langle V_t\rangle_0)^2$$

$$\langle\langle V_1 V_2\rangle\rangle_1 = \sum_{n=1}^{N} \frac{\langle\langle G_n^2\rangle\rangle}{g_l^2 \left(\frac{\langle G_0\rangle}{g_l} + \frac{\tau}{\tau_n}\right)\left(\frac{\langle G_0\rangle}{g_l} - \frac{\tau}{\tau_n}\right)} \left(e^{-\frac{t_1-t_2}{\tau_n}} - \frac{\tau}{\tau_n} \frac{g_l}{\langle G_0\rangle} e^{-\frac{t_1-t_2}{\tau}\frac{\langle G_0\rangle}{g_l}} \right) (E_n - \langle V_t\rangle_0)^2$$

For alpha kernel shot noise,

$$\langle Y_t\rangle_2 = \langle Y_t\rangle_0 - \sum_{n=1}^{N} \frac{\left(\langle Q_0\rangle + 2\frac{\tau}{\tau_n}\right)\langle\langle Q_n^2\rangle\rangle}{\langle Q_0\rangle \left(\langle Q_0\rangle + \frac{\tau}{\tau_n}\right)^2} (w_n - \langle Y_t\rangle_0) \quad \langle\langle Y_t^2\rangle\rangle = \sum_{n=1}^{N} \frac{\left(\langle Q_0\rangle + 2\frac{\tau}{\tau_n}\right)\langle\langle Q_n^2\rangle\rangle}{\langle Q_0\rangle \left(\langle Q_0\rangle + \frac{\tau}{\tau_n}\right)^2} (w_n - \langle Y_t\rangle_0)^2$$

$$\langle\langle Y_1 Y_2\rangle\rangle_1 = \sum_{n=1}^{N} \frac{\langle\langle Q_n^2\rangle\rangle}{\left(\langle Q_0\rangle + \frac{\tau}{\tau_n}\right)^2 \left(\langle Q_0\rangle - \frac{\tau}{\tau_n}\right)^2} (w_n - \langle Y_t\rangle_0)^2$$

$$\left(\left(\left(1 + \frac{|t_1-t_2|}{\tau_n}\right)\left(\langle Q_0\rangle + \frac{\tau}{\tau_n}\right)\left(\langle Q_0\rangle - \frac{\tau}{\tau_n}\right) - 2\left(\frac{\tau}{\tau_n}\right)^2 \right) e^{-\frac{|t_1-t_2|}{\tau_n}} \right.$$

$$\left. + 2\left(\frac{\tau}{\tau_n}\right)^3 \frac{1}{\langle Q_0\rangle} e^{-\frac{|t_1-t_2|}{\tau}\langle Q_0\rangle} \right)$$

In terms of V_t,

$$\langle V_t\rangle_2 = \langle V_t\rangle_0 - \sum_{n=1}^{N} \frac{\left(\frac{\langle G_0\rangle}{g_l} + 2\frac{\tau}{\tau_n}\right)\langle\langle G_n^2\rangle\rangle}{g_l \left(\frac{\langle G_0\rangle}{g_l} + \frac{\tau}{\tau_n}\right)^2 \langle G_0\rangle} (E_n - \langle V_t\rangle_0) \quad \langle\langle V_t^2\rangle\rangle_1 = \sum_{n=1}^{N} \frac{\left(\frac{\langle G_0\rangle}{g_l} + 2\frac{\tau}{\tau_n}\right)\langle\langle G_n^2\rangle\rangle}{g_l \left(\frac{\langle G_0\rangle}{g_l} + \frac{\tau}{\tau_n}\right)^2 \langle G_0\rangle} (E_n - \langle V_t\rangle_0)^2$$

16

$$\langle\langle V_1 V_2\rangle\rangle_1 = \sum_{n=1}^{N} \frac{\langle\langle G_n^2\rangle\rangle}{g_l^2 \left(\frac{\langle G_0\rangle}{g_l} + \frac{\tau}{\tau_n}\right)^2 \left(\frac{\langle G_0\rangle}{g_l} - \frac{\tau}{\tau_n}\right)^2} \left(E_n - \langle V_t\rangle_0\right)^2$$

$$\left(\left(\left(1 + \frac{|t_1 - t_2|}{\tau_n}\right)\left(\frac{\langle G_0\rangle}{g_l} + \frac{\tau}{\tau_n}\right)\left(\frac{\langle G_0\rangle}{g_l} - \frac{\tau}{\tau_n}\right) - 2\left(\frac{\tau}{\tau_n}\right)^2\right) e^{-\frac{|t_1 - t_2|}{\tau_n}}\right.$$

$$\left. + 2\left(\frac{\tau}{\tau_n}\right)^3 \frac{g_l}{\langle G_0\rangle} e^{-\frac{|t_1 - t_2|}{\tau} \frac{\langle G_0\rangle}{g_l}}\right)$$

C   Edgeworth Expansion

In terms of the normalized process $X_t = (V_t - \langle V_t\rangle)/\sigma_t$ with $\sigma_t \equiv \sqrt{\langle\langle V_t^2\rangle\rangle}$, the truncated fourth order Edgeworth series is given by:

$$p_{ew}(X_t = x) \simeq \frac{1}{\sigma_t}\left(1 + \frac{1}{3!}\frac{\langle\langle V_t^3\rangle\rangle}{\sigma_t^3}\left(x^3 - 3x\right)\right.$$

$$\left. + \frac{1}{4!}\frac{\langle\langle V_t^4\rangle\rangle}{\sigma_t^4}\left(x^4 - 6x^2 + 3\right) + \frac{10}{6!}\frac{\langle\langle V_t^3\rangle\rangle^2}{\sigma_t^6}\left(x^6 - 15x^4 + 45x^2 - 15\right)\right)\mathcal{N}(x) \quad (21)$$

where $\mathcal{N}(x) = \exp(-x^2/2)/\sqrt{2\pi}$ is the standard normal density and $p(V_t = v) = p_{ew}\left(x = \frac{v - \langle V_t\rangle}{\sigma_t}\right)$. The third order and fourth order of the series is given by the first and second lines, respectively.

D   Compound PPP Transformations

The expectation of $F(t,\xi)$ under the compound process Ξ is given by:

$$\langle F(t,\xi)\rangle = \sum_{n=0}^{\infty} \frac{1}{n!} e^{-m(\mathcal{S})} \int_{\mathcal{S}}\cdots\int_{\mathcal{S}}\int_{\Theta}\cdots\int_{\Theta} F\left(t, (x_1, \boldsymbol{\theta}_1), \ldots, (x_n, \boldsymbol{\theta}_n)\right) \prod_{j=1}^{n} p(\boldsymbol{\theta}_j)\, d\boldsymbol{\theta}_j\, \lambda(x_j)\, dx_j$$

If $F(t,\xi) \equiv G_t$ is a shot noise process we obtain the familiar factorization:

$$\left\langle e^{isG_t(\xi)}\right\rangle = e^{-m(\mathcal{S})} \sum_{n=0}^{\infty}\frac{1}{n!}\left(\int_{\mathcal{S}}\int_{\Theta} e^{isg(t,x,\boldsymbol{\theta})}\, p(\boldsymbol{\theta})\,\lambda(x)\, d\boldsymbol{\theta}\, dx\right)^n = \exp\left(\int_{\mathcal{S}}\int_{\Theta}\left(e^{isg(t,x,\boldsymbol{\theta})} - 1\right) p(\boldsymbol{\theta})\,\lambda(x)\, d\boldsymbol{\theta}\, dx\right)$$

The k-th cumulants of G_t and $G_1, \ldots, G_K$ are given by:

$$\langle\langle G_t^k\rangle\rangle = \left(\frac{1}{i}\frac{d}{ds}\right)^k \log\left\langle e^{isG_t(\xi)}\right\rangle\bigg|_{s=0} = \int_{\mathcal{S}}\int_{\Theta} g(t,x,\boldsymbol{\theta})^k\, p(\boldsymbol{\theta})\,\lambda(x)\, d\boldsymbol{\theta}\, dx$$

$$\langle\langle G_1 \cdots G_K\rangle\rangle = \left(\frac{1}{i}\frac{d}{ds_1}\right)\cdots\left(\frac{1}{i}\frac{d}{ds_K}\right) \log\left\langle e^{isG_1(\xi)+\cdots isG_K(\xi)}\right\rangle\bigg|_{s_1=\cdots=s_K=0}$$

$$= \int_{\mathcal{S}}\int_{\Theta} g(t_1, x, \boldsymbol{\theta})\cdots g(t_K, x, \boldsymbol{\theta})\, p(\boldsymbol{\theta})\,\lambda(x)\, d\boldsymbol{\theta}\, dx$$

The *Slivnyak-Mecke Theorem* extends to transformations of compound PPP, which can be verified as

follows:

$$\left\langle \sum_{x_j \in \xi} f\left(t, x_j, \xi_{\setminus x_j}, \boldsymbol{\theta}\right) \right\rangle$$

$$= \sum_{n=0}^{\infty} \frac{1}{n!} e^{-m(\mathcal{S})} \int_{\mathcal{S}} \cdots \int_{\mathcal{S}} \int_{\Theta} \cdots \int_{\Theta} \sum_{x_j \in \xi} f\left(t, (x_j, \boldsymbol{\theta}_j), \{(x_1, \boldsymbol{\theta}_1) \ldots, (x_n, \boldsymbol{\theta}_n)\} \setminus (x_j, \boldsymbol{\theta}_j)\right) \prod_{j=1}^{n} p(\boldsymbol{\theta}_j) \, d\boldsymbol{\theta}_j \, \lambda(x_j) \, dx_j$$

$$= \sum_{n=0}^{\infty} \frac{1}{(n-1)!} e^{-m(\mathcal{S})} \int_{\mathcal{S}} \cdots \int_{\mathcal{S}} \int_{\Theta} \cdots \int_{\Theta} f\left(t, (x_n, \boldsymbol{\theta}_n), \{(x_1, \boldsymbol{\theta}_1) \ldots, (x_{n-1}, \boldsymbol{\theta}_{n-1})\}\right) \prod_{j=1}^{n} p(\boldsymbol{\theta}_j) \, d\boldsymbol{\theta}_j \, \lambda(x_j) \, dx_j$$

$$= \int_{\mathcal{S}} \int_{\Theta} \sum_{n=0}^{\infty} \frac{1}{(n-1)!} e^{-m(\mathcal{S})} \int_{\mathcal{S}} \cdots \int_{\mathcal{S}} \int_{\Theta} \cdots \int_{\Theta} f\left(t, (x, \boldsymbol{\theta}), \{(x_1, \boldsymbol{\theta}_1) \ldots, (x_{n-1}, \boldsymbol{\theta}_{n-1})\}\right)$$
$$\prod_{j=1}^{n-1} p(\boldsymbol{\theta}_j) \, d\boldsymbol{\theta}_j \, \lambda(x_j) \, dx_j \, p(\boldsymbol{\theta}) \, d\boldsymbol{\theta} \, \lambda(x) \, dx$$

$$= \int_{\mathcal{S}} \int_{\Theta} \langle f\left(t, x, \boldsymbol{\theta}, \xi\right) \rangle \, p(\boldsymbol{\theta}) \, d\boldsymbol{\theta} \, \lambda(x) \, dx$$

In particular, the expectation of a sum of products is given by:

$$\left\langle \sum_{x_j \in \xi} f(t, x_j, \boldsymbol{\theta}_j) \prod_{x_k \in \xi} w(t, x_k, \boldsymbol{\theta}_k) \right\rangle = \left\langle \prod_{x_k \in \xi} w(t, x_k, \boldsymbol{\theta}_k) \right\rangle \int_{\mathcal{S}} \int_{\Theta} f(t, x, \boldsymbol{\theta}) \, w(t, x, \boldsymbol{\theta}) \, p(\boldsymbol{\theta}) \, d\boldsymbol{\theta} \, \lambda(x) \, dx$$

References

LF Abbott and Carl van Vreeswijk. Asynchronous states in networks of pulse-coupled oscillators. *Physical Review E*, 48(2):1483, 1993.

Marco Brigham and Alain Destexhe. Nonstationary filtered shot-noise processes and applications to neuronal membranes. *Physical Review E*, 91(6):062102, 2015.

N. Brunel. Dynamics of sparsely connected networks of excitatory and inhibitory spiking neurons. *Journal of computational neuroscience*, 8(3):183–208, 2000.

Nicolas Brunel and Vincent Hakim. Fast global oscillations in networks of integrate-and-fire neurons with low firing rates. *Neural computation*, 11(7):1621–1671, 1999.

Anthony N Burkitt. A review of the integrate-and-fire neuron model: I. homogeneous synaptic input. *Biological cybernetics*, 95(1):1–19, 2006a.

Anthony N Burkitt. A review of the integrate-and-fire neuron model: Ii. inhomogeneous synaptic input and network properties. *Biological cybernetics*, 95(2):97–112, 2006b.

David Roxbee Cox and Valerie Isham. *Point processes*, volume 12. CRC Press, 1980.

Harald Cramér. *Mathematical methods of statistics*, volume 1. Princeton university press, 1946.

FY Edgeworth. On the representation of statistical frequency by a series. *Journal of the Royal Statistical Society*, pages 102–106, 1907.

Wulfram Gerstner. Population dynamics of spiking neurons: fast transients, asynchronous states, and locking. *Neural computation*, 12(1):43–89, 2000.

Wulfram Gerstner and J Leo van Hemmen. Coherence and incoherence in a globally coupled ensemble of pulse-emitting units. *Physical review letters*, 71(3):312, 1993.

Jorge Golowasch, LF Abbott, and Eve Marder. Activity-dependent regulation of potassium currents in an identified neuron of the stomatogastric ganglion of the crab cancer borealis. *Journal of Neuroscience*, 19:RC33–1, 1999.

Henry Markram, Joachim Lübke, Michael Frotscher, Arnd Roth, and Bert Sakmann. Physiology and anatomy of synaptic connections between thick tufted pyramidal neurones in the developing rat neocortex. *The Journal of physiology*, 500(2):409–440, 1997.

J Mecke. Stationäre zufällige masse auf localcompakten abelischen gruppen. *Wahrscheinlichkeitsth*, 9: 36–58, 1967.

Gary W Oehlert. A note on the delta method. *The American Statistician*, 46(1):27–29, 1992.

Emanuel Parzen. *Stochastic processes*, volume 24. SIAM, 1999.

J. Rice. On generalized shot noise. *Advances in Applied Probability*, pages 553–565, 1977.

M.J.E. Richardson and R. Swarbrick. Firing-rate response of a neuron receiving excitatory and inhibitory synaptic shot noise. *Physical review letters*, 105(17):178102, 2010.

IM Slivnyak. Some properties of stationary flows of homogeneous random events. *Theory of Probability & Its Applications*, 7(3):336–341, 1962.

Donald L Snyder and Michael I Miller. *Random Point Processes in Time and Space.* Springer, 1991.

Richard B Stein. A theoretical analysis of neuronal variability. *Biophysical Journal*, 5(2):173–194, 1965.

Roy L Streit. *Poisson Point Processes: Imaging, Tracking, and Sensing.* Springer, 2010.

Henry C Tuckwell. *Introduction to theoretical neurobiology: volume 2, nonlinear and stochastic theories.* Cambridge University Press, 1988.

David L Wallace. Asymptotic approximations to distributions. *The Annals of Mathematical Statistics*, pages 635–654, 1958.

Lars Wolff and Benjamin Lindner. Method to calculate the moments of the membrane voltage in a model neuron driven by multiplicative filtered shot noise. *Physical Review E*, 77(4):041913, 2008.

Lars Wolff and Benjamin Lindner. Mean, variance, and autocorrelation of subthreshold potential fluctuations driven by filtered conductance shot noise. *Neural Computation*, 22(1):94–120, 2010.

Chapter 5

How causal correlations between synaptic inputs affect membrane potential fluctuations

Summary

This article builds on the extension to multiple synapse types presented in Chapter 4 and investigates the effects of correlations in synaptic input. Experimental and computational studies report various degrees of correlation that are reflected in the statistics of membrane potential fluctuations and may convey information to the neuron. This article proposes a simple model of synaptic correlation and evaluates its impact in membrane potential statistics.

A basic model of passive membrane with two synapse types (excitatory and inhibitory) is first introduced with synaptic correlations being generated by inserting common presynaptic spikes in the inputs. This model displays strong correlation effects since common spikes are coincident between synapse types. Adding random displacements to common spikes removes spike coincidence and enables arbitrary cross-correlation function between presynaptic spikes. This enables to generate causal correlations between synapse types by adding strictly positive random displacements to one synapse type. The exact cumulants of both models are derived in addition to the central moments expansion (CME). These analytical results are compared with numerical simulations.

This approach to analyze correlated synaptic input is possible by explicitly considering the effect of individual presynaptic spikes in the evolution of membrane potential.

This research article is work in progress with its main analytical results already derived.

Résumé

Les corrélations des entrées pré-synaptiques sont sensées avoir un rôle important dans la dynamique de populations neuronales et ces corrélations se reflètent aussi dans le potentiel de membrane de neurones individuels. Nous étudions l'effet des entrées synaptiques corrélées dans les statistiques des fluctuations du potentiel de membrane pour une modèle passif de membrane neuronale avec des synapses excitatrices et inhibitrices à conductance alimentées par des processus *shot noise*. Les cumulants exacts et leurs approximations sont obtenus en termes des cumulants du *shot noise* dans le cadre d'une expansion des moments centraux. Un modèle simple de corrélations causales des entrées synaptiques est analysé.

How causal correlations between synaptic inputs affect membrane potential fluctuations

Marco Brigham, Alain Destexhe

26/03/2015

Abstract

Correlations in presynaptic input are thought to have an important role in the dynamics of neuronal populations and are reflected in the membrane potential of individual neurons. We investigate the effect of correlated synaptic input in the statistics of membrane potential fluctuations for a passive neuronal membrane with excitatory and inhibitory synapses driven y shot noise conductance. Exact cumulants are obtained and their approximation in terms of shot noise cumulants is derived with a central moments expansion. A simple model of causal correlation between synaptic input is investigated.

1 Introduction

Experimental studies have reported varying degrees of correlation in membrane potential of neurons and related neural correlates [Ts'o et al., 1986, Gray et al., 1989, Gawne and Richmond, 1993, Zohary et al., 1994, Prut et al., 1995, Lee et al., 1998, Renart et al., 2010]. Several theoretical and computational studies have investigated the impact of correlations in input spike trains [Brette, 2009, Macke et al., 2009], synaptic input currents and conductances [Rudolph and Destexhe, 2006], neuronal membranes [Rosenbaum et al., 2010] and neuronal firing [Salinas and Sejnowski, 2000, Moreno et al., 2002, Kuhn et al., 2003, Renart et al., 2010, Rossant et al., 2011, Hertz, 2010].

In this article we investigate the effects of presynaptic correlation in membrane potential statistics for a passive membrane model driven by excitatory and inhibitory shot noise conductance with nonstationary input rates. Correlations are generated by adding common spikes to presynaptic inputs. Several models of presynaptic correlations are investigated. Arbitrary crosscovariance functions between excitatory and inhibitory spike trains are enabled by adding random displacements to common spikes [Brette, 2009]. Strictly positive or negative displacements results in causal correlations. The exact cumulants are obtained for each case and the central moments expansion is used to analyze the structure and consequence of synaptic correlation in membrane potential statistics.

2 Model of Correlated Shot Noise Input

We consider a simple passive membrane model with excitatory and inhibitory conductance synapses. Each synapse type is driven by independent shot noise processes generated by presynaptic events ξ_e and ξ_i. We introduce correlation between excitatory and inhibitory synapses by adding a third set of independent presynaptic events ξ_c to each synapse type. This results in the following shot noise input model:

$$G_e(t) = \sum_{x_j \in \xi_e} g_e(t - x_j)\, H(t - x_j) + \sum_{x_l \in \xi_c} g_e(t - x_l)\, H(t - x_l) \tag{1}$$

$$G_i(t) = \sum_{x_i \in \xi_i} g_i(t - x_i)\, H(t - x_i) + \sum_{x_l \in \xi_c} g_i(t - x_l)\, H(t - x_l) \tag{2}$$

where g_s is the impulse response function (shot noise kernel) for synapse type $s \in \{e, i\}$ and $H(u)$ is the Heaviside function. The presynaptic events $\boldsymbol{\xi} = \{\xi_e, \xi_i, \xi_c\}$ are realizations of three independent components of multivariate Poisson point processes (PPP) $\boldsymbol{\Xi}$ on the real line with rate functions $\lambda_n(t) > 0$, $n = \{e, i, c\}$ such that $m_n(\mathcal{S}) \equiv \int_{\mathcal{S}} \lambda_n(x)\, dx$ is finite for any bounded interval $\mathcal{S} \subseteq \mathbb{R}$ of the real line.

The shot noise input drives the evolution of the membrane potential $V(t)$ according to the following *membrane equation*:

$$\tau_m \frac{d}{dt} V(t) = E_l - V(t) + (E_e - V(t)) \frac{1}{g_l} G_e(t) + (E_i - V(t)) \frac{1}{g_l} G_i(t) \tag{3}$$

where τ_m is the membrane time constant, E_l is the leak potential, g_l is the leak conductance, E_s is the synaptic reversal potential of synapse type *se*.

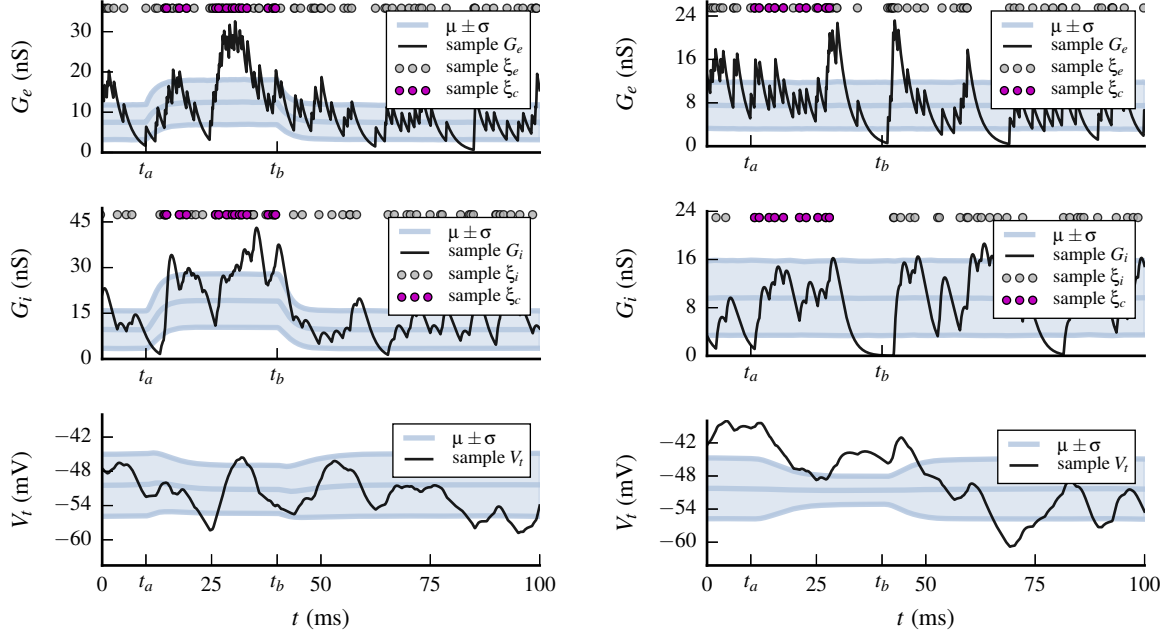Two examples of synaptic correlation generated by this model are illustrate in Fig. 1.

Figure 1 – *Two examples of neuron model with excitatory and inhibitory conductance synapses under correlated synaptic input between t_a and $t_b \geq t_a$. Excitatory conductance G_e (top) and inhibitory conductance G_i (middle) drive the membrane potential evolution V_t (bottom). Single realizations of G_e, G_i and V_t are shown in black, realizations of ξ_e and ξ_i are marked by gray dots and $x_l \in \xi_c$ is marked by magenta dots. Mean and standard deviation $(\mu \pm \sigma)$ are shown in gray. Correlated input is implemented by adding common presynaptic spikes to G_e and G_i. In the example from the left plot common input is cumulative with the original rates. In the right plot the total synaptic rates are unchanged. The simulation parameters are detailed at the end of this Section.*

In both examples the membrane potential is first driven to a stationary regime at time $t_a > 0$ with shot noise conductances with constant rates λ_e and λ_i. The original realizations of presynaptic spike times ξ_e and ξ_i from these processes are represented by gray dots. Between times t_a and $t_b > t_a$ common presynaptic events ξ_c are added to synaptic input. In the first scenario, the common input rate is cumulative to the original rates and in the second scenario the synaptic rates remain constant. The rate functions used to implement them are shown in Fig. 2.
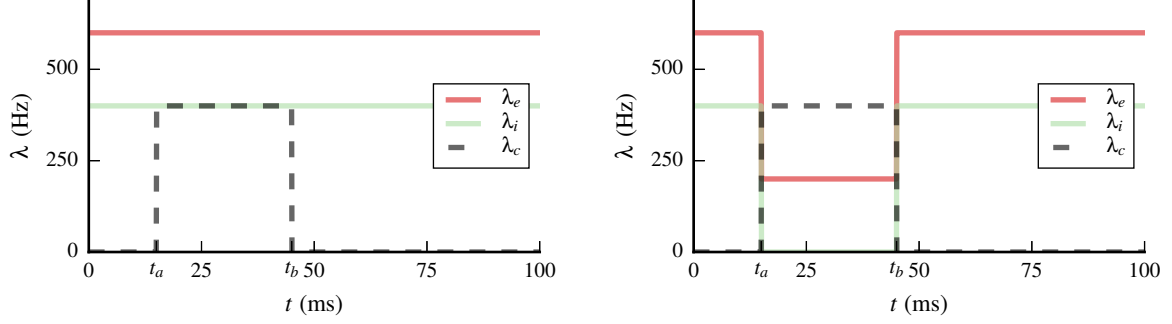
2

Figure 2 – *Rate functions for the examples of synaptic correlation shown in Fig. 1. The excitatory and inhibitory rates are represented with red and green lines, respectively. The common input rate is represented with dashed gray line.*

The introduction of common presynaptic spikes between t_a and t_b affects the membrane potential and input conductance in different ways. According to the Campbell theorem, the mean and variance of the synaptic input are linear in the rate and their values between t_a and t_b are given by:

$$\langle G_n(t) \rangle = \lambda_n \int_{-\infty}^{t_a} g_n(t-x)\,dx + \left(\tilde{\lambda}_n + \lambda_c \right) \int_{t_a}^{t} g_n(t-x)\,dx$$

$$\langle\langle G_n(t)^2 \rangle\rangle = \lambda_n \int_{-\infty}^{t_a} g_n(t-x)^2\,dx + \left(\tilde{\lambda}_n + \lambda_c \right) \int_{t_a}^{t} g_n(t-x)^2\,dx$$

where $n \in \{e, i\}$ and $\tilde{\lambda}_n$ is the rate of independent synaptic input between t_a and t_b.

In this first scenario the mean membrane potential $\langle V(t) \rangle$ experiences a transient increase followed by a decrease, with its variance $\langle\langle V(t)^2 \rangle\rangle$ also decreasing after the initial transient. This decrease in variance occurs while the variance of the conductance inputs increases (linearly). In the second example $\langle V(t) \rangle$ experiences a slight decrease, and $\langle\langle V(t)^2 \rangle\rangle$ displays a considerable reduction. These two examples illustrate that correlations in the synaptic input can affect the statistics of membrane potential fluctuations in non-trivial ways. We are interested in understanding qualitatively and quantitatively such effects, and more generally, in understanding how the statistics of common presynaptic input events affect the statistics of mean membrane potential $\langle V(t) \rangle$.

The numerical simulations were generated with exponential kernel $g(t-x)_{exp} = h \exp\left(-(t-x)/\tau_s \right)$ for excitatory conductance and alpha kernel $g(t-x)_{alpha} = h\left((t-x)/\tau_s \right) \exp\left(-(t-x)/\tau_s \right)$ for inhibitory conductance. The excitatory and inhibitory rate are $\lambda_e = 600$ Hz and $\lambda_i = 400$ Hz, respectively. The conductance rate functions are represented in Fig. 2 for both examples. Other parameters are $\tau_m = 0.02$ s, $E_l = -0.06$ V, $E_e = 0$ V, $E_i = -0.08$ V, $g_l = 10\text{E-}9$ S, $h_e = 5\text{E-}9$ S, $h_i = 16\text{E-}9$ S, $\tau_e = 0.0025$ s, $\tau_i = 0.0015$ s.

2.1 Exact Solution

In this section we derive the exact cumulants for this neuron model with correlated synaptic input due to injection of common spikes between synapse types. The membrane equation Eq. (3) is first transformed to its unit-less version and responses to common presynaptic events ξ_c are grouped into a third shot noise process since ξ_c is independent from ξ_e and ξ_i. The analytical structure of this correlated input model is in fact equivalent to a membrane model with three independent conductance synapse types.

The membrane equation (Eq. 3) is transformed to its unit-less version by applying the following transformations:

$$Y(t) = \frac{V(t) - E_l}{E_e - E_i} \qquad w_1 = \frac{E_e - E_l}{E_e - E_i} \qquad w_2 = \frac{E_i - E_l}{E_e - E_i} \qquad w_3 = 1$$

3

yielding,

$$\tau \frac{d}{dt} Y(t) = -Y(t) Q_0(t) + w_1 Q_1(t) + w_2 Q_2(t) + w_3 Q_3(t) \tag{4}$$

where,

$$Q_0(t) = 1 + Q_1(t) + Q_2(t) + \hat{Q}_3(t)$$

$$Q_1(t) = \frac{1}{g_l} G_e(t, \xi_e) = \sum_{x_j \in \xi_e} g_1(t - x_j) H(t - x_j)$$

$$Q_2(t) = \frac{1}{g_l} G_i(t, \xi_i) = \sum_{x_i \in \xi_i} g_2(t - x_i) H(t - x_i)$$

$$\hat{Q}_3(t) = \frac{1}{g_l} G_e(t, \xi_c) + \frac{1}{g_l} G_i(t, \xi_c) \equiv \sum_{x_l \in \xi_c} \hat{g}_3(t - x_l) H(t - x_l)$$

$$Q_3(t) = \frac{w_1}{g_l} G_e(t, \xi_c) + \frac{w_2}{g_l} G_i(t, \xi_c) \equiv \sum_{x_l \in \xi_c} g_3(t - x_l) H(t - x_l)$$

where $G_s(t, \xi_n)$ represents synaptic input of synapse type s restricted to spike arrivals from realization ξ_n, and $\hat{g}_k(t - x_l) = g_k(t - x_l)$ for $k \in \{1, 2\}$.

Writing explicitly in terms of conductances,

$$\hat{Q}_3(t) = \frac{1}{g_l} \sum_{x_l \in \xi_c} g_e(t - x_l) H(t - x_l) + g_i(t - x_l) H(t - x_l)$$

$$Q_3(t) = \frac{1}{g_l} \sum_{x_l \in \xi_c} w_1 g_e(t - x_l) H(t - x_l) + w_2 g_i(t - x_l) H(t - x_l)$$

The system response $Y(t)$ for arbitrary and independent shot noise conductance $Q_1(t)$, $Q_2(t)$ and $Q_3(t)$ is obtained by solving Eq. (4) for the corresponding realizations of presynaptic events $\boldsymbol{\xi} = \{\xi_e, \xi_i, \xi_c\}$. Assuming without loss of generality an initial value $Y_0 = 0$,

$$Y(t, \boldsymbol{\xi}) = \frac{1}{\tau} \int_{-\infty}^{t} \sum_{n=1}^{3} w_n Q_n(z) e^{-\frac{1}{\tau} \int_z^t Q_0(u) \, du} \, dz$$

The cumulants of $Y_t \equiv Y(t, \boldsymbol{\xi})$ correspond to filtering of three independent shot noise inputs with multiplicative noise. As shown in [Brigham and Destexhe, 2015], the mean and higher order cumulants of the filtered process are given by:

$$\langle Y_t \rangle = \frac{1}{\tau} \int_{-\infty}^{t} \sum_{n=1}^{3} \left\langle w_n Q_n(z) e^{-\frac{1}{\tau} \int_z^t Q_0(u) \, du} \right\rangle dz \tag{5}$$

$$\langle \langle Y_1 \cdots Y_K \rangle \rangle = \frac{1}{\tau^K} \int_{-\infty}^{t_1} \cdots \int_{-\infty}^{t_K} \sum_{n_1=1}^{3} \cdots \sum_{n_K=1}^{3} \left\langle \left\langle \prod_{k=1}^{K} w_{n_k} Q_{n_k}(z_k) e^{-\frac{1}{\tau} \int_{z_k}^{t_k} Q_0(u) \, du} \right\rangle \right\rangle dz_1 \cdots dz_K \tag{6}$$

Using independence of $\boldsymbol{\Xi}$ and applying the Slivnyak-Mecke Theorem yields the expectations inside the integrals. Explicit expressions for the mean and autocovariance are provided in Appendix A with key expectations given by:

$$\left\langle Q_n(z) e^{-\frac{1}{\tau} \int_z^t Q_0(u) \, du} \right\rangle = \left\langle e^{-\frac{1}{\tau} \int_z^t Q_0(u) \, du} \right\rangle \int_{-\infty}^{z} g_n(z - x) e^{-\frac{1}{\tau} \int_z^t \hat{g}_n(u-x) H(u-x) \, du} \lambda_n(x) \, dx$$

$$\left\langle \prod_{k=1}^{K} e^{-\frac{1}{\tau} \int_{z_k}^{t_k} Q_n(u) \, du} \right\rangle = \exp \left(\int_{\mathcal{S}} \left(\prod_{k=1}^{K} e^{-\frac{1}{\tau} \int_{z_k}^{t_k} \hat{g}_n(u-x) H(u-x) \, du} - 1 \right) \lambda_n(x) \, dx \right)$$

4

Comparison with numerical simulations for the mean and standard deviation is shown in Fig. 3 and illustrates the excellent accuracy provided by the exact solutions.
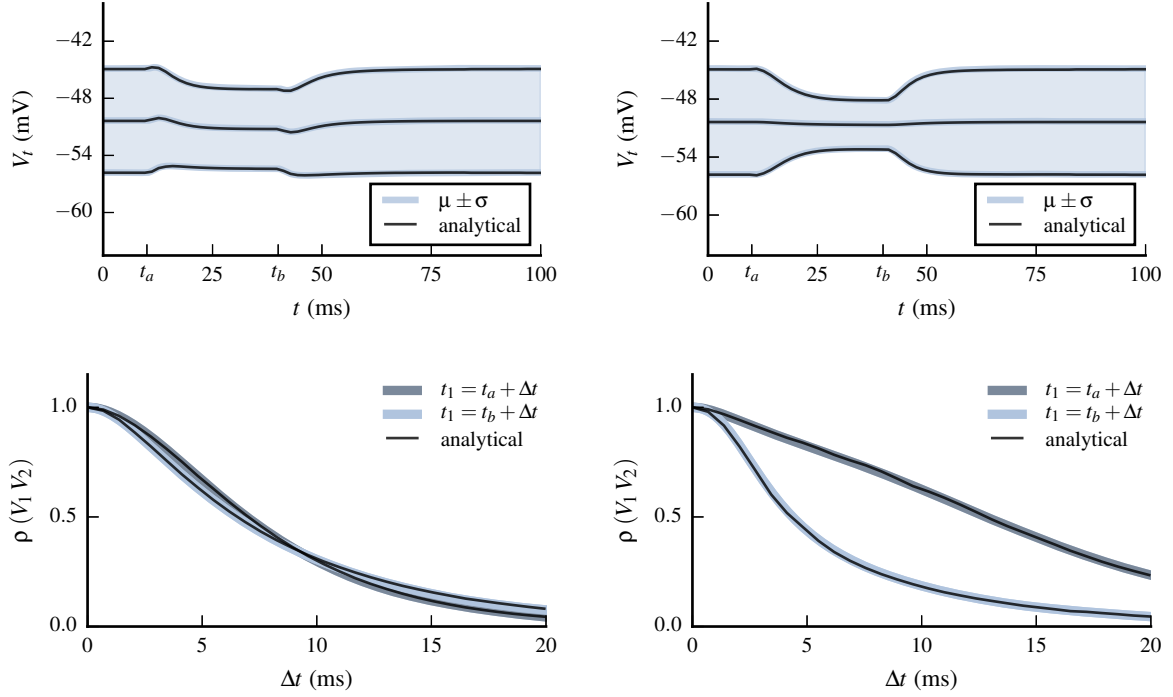

Figure 3 – *Comparison of exact solutions with numerical simulations for mean and second order cumulants of membrane potential $V(t)$. There is excellent agreement between the simulations (gray) and the analytic prediction (black).*

The exact cumulants of membrane potential fluctuations (Eqs (5) and (6)) can be used to build very accurate approximations of the time-evolving distribution of membrane potential with truncated Edgeworth series [Edgeworth, 1907, Cramér, 1946, Wallace, 1958]. This series is an asymptotic expansion of $p(V_t)$ in terms of its cumulants and the second order coincides with the gaussian approximation. The third and fourth order take into consideration the skewness and kurtosis of the distribution, respectively. The truncated series up to the fourth order is included in Appendix B. As illustrated in Fig. 4, the skewness of $p(V_t)$ at the local minima t_b is well captured by the third order of the truncated Edgeworth series.
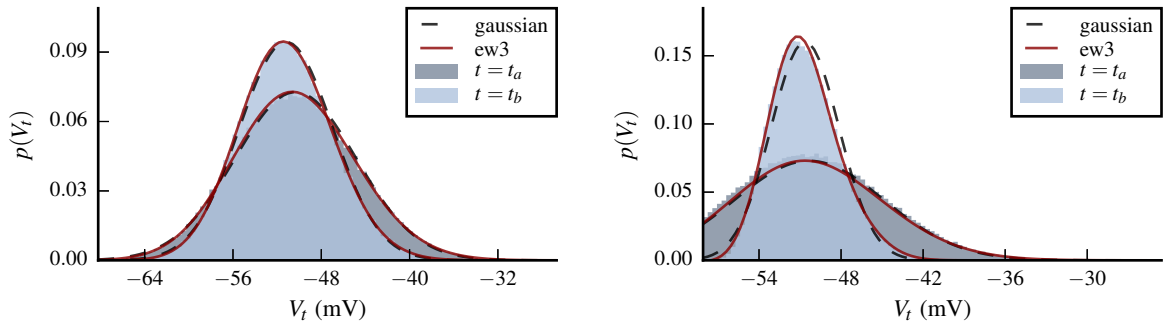

Figure 4 – *Comparison with numerical simulations for the probability density function (pdf) of membrane potential $p(V_t)$ given by truncated Edgeworth series using exact second and third cumulant of V_t. The pdf is evaluated at t_a and t_b that corresponds to local maxima and minima of V_t respectively (see Fig. 5). There is good agreement between the simulations (gray) and the gaussian approximation (black dash) at t_a. The effect of third order cumulant (kurtosis) at t_b is well captured by the third order of the series.*

2.2 Central Moments Expansion

The central moments expansion (CME) provides an approximation of the exact cumulants in terms of integrated shot noise. This enables to investigate the role of shot noise cumulants in membrane potential statistics and directly exposes the shot noise process generated by common input. This is the particular case for $N = 3$ that is developed in general in [Brigham and Destexhe, 2015]. The deterministic solution of Eq. (4) with mean shot noise input $\langle Q_n(t) \rangle$ is given by:

$$\langle Y_t \rangle_0 = \frac{1}{\tau} \int_{-\infty}^{t} e^{-\frac{1}{\tau} \int_z^t \langle Q_0(u) \rangle du} \sum_{n=1}^{3} w_n \, \langle Q_n(z) \rangle \, dz \tag{7}$$

The correction to the mean $\langle Y_t \rangle$ due to the stochastic nature of shot noise input is given by the second order of the CME for the mean:

$$\langle Y_t \rangle_2 = \langle Y_t \rangle_0 + \frac{1}{\tau} \int_{-\infty}^{t} e^{-\frac{1}{\tau} \int_z^t \langle Q_0(u) \rangle du}$$

$$\sum_{n=1}^{3} \left(-\frac{1}{\tau} \int_z^t w_n \, \langle\langle Q_n(z) \, Q_n(u) \rangle\rangle \, du \right.$$

$$\left. + \sum_{m=1}^{3} w_n \, \langle Q_n(z) \rangle \, \frac{1}{2\tau^2} \int_z^t \int_z^t \langle\langle Q_m(u_1) \, Q_m(u_2) \rangle\rangle \, du_1 \, du_2 \right) dz \tag{8}$$

where the subscript 2 represents the second order of the expansion of the mean.

The above expression makes explicit the important role of shot noise autocovariance in the stochastic correction of the mean $\langle Y_t \rangle$ in regards to the deterministic solution $\langle Y_t \rangle_0$. The first order of CME for the autocovariance is given by:

$$\langle\langle Y_1 Y_2 \rangle\rangle_1 = \frac{1}{\tau^2} \int_{-\infty}^{t_1} \int_{-\infty}^{t_2} e^{-\frac{1}{\tau} \int_{z_1}^{t_1} \langle Q_0(u_1) \rangle du_1 - \frac{1}{\tau} \int_{z_2}^{t_2} \langle Q_0(u_2) \rangle du_2}$$

$$\sum_{n=1}^{3} \left(w_n^2 \, \langle\langle Q_n(z_1) \, Q_n(z_2) \rangle\rangle \right.$$

$$+ \sum_{m=1}^{3} \sum_{m'=1}^{3} w_n \, w_m \, \langle Q_n(z_1) \rangle \, \langle Q_m(z_2) \rangle \, \frac{1}{\tau^2} \int_{z_1}^{t_1} \int_{z_2}^{t_2} \langle\langle Q_{m'}(u_1) \, Q_{m'}(u_2) \rangle\rangle \, du_1 \, du_2$$

$$- \sum_{l=1}^{3} w_n w_l \left(\langle Q_n(z_1) \rangle \, \frac{1}{\tau} \int_{z_1}^{t_1} \langle\langle Q_l(u_1) \, Q_l(z_2) \rangle\rangle \, du_1 \right.$$

$$\left. \left. + \langle Q_n(z_2) \rangle \, \frac{1}{\tau} \int_{z_2}^{t_2} \langle\langle Q_l(u_2) \, Q_l(z_1) \rangle\rangle \, du_2 \right) \right) dz_1 \, dz_2 \tag{9}$$

where the subscript 1 represents the first order of the expansion for the autocovariance.

The first order of CME for the autocovariance generally provides good approximations in the range of biological parameters. Some conditions may require the the second order of the expansion that includes contributions up to fourth order cumulants.
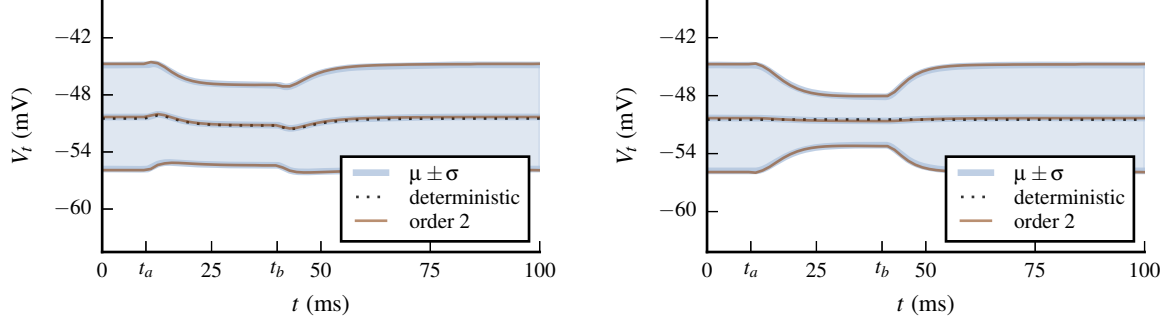
6

Figure 5 – *Comparison with numerical simulations of approximate solution given by central moments expansion (CME) for mean and standard deviation of membrane potential $V(t)$. There is excellent agreement between the simulations (gray) and the approximate solution (brown).*

The stationary limit of V_t yields the statistics shot noise input with constant rate after dissipation of initial transients and is obtained by setting the onset of PPP activity at an earlier time than the start of membrane potential integration. Under such conditions the cumulants of shot noise can be replaced by their stationary limits.

$$\langle Y_t \rangle_0 = \frac{1}{\langle Q_0 \rangle} \sum_{n=1}^{3} w_n \langle Q_n \rangle \tag{10}$$

$$\langle Y_t \rangle_2 = \langle Y_t \rangle_0 - \sum_{n=1}^{3} \frac{1}{\langle Q_0 \rangle} \left(w_n - \langle Y_t \rangle_0 \right) \left\langle\left\langle Q_n^2 \right\rangle\right\rangle \frac{1}{\tau} \int_{-\infty}^{t} e^{-\frac{t-z}{\tau} \langle Q_0 \rangle} r_n(t-z)\, dz \tag{11}$$

$$\left\langle\left\langle Y_1\, Y_2 \right\rangle\right\rangle_1 = \sum_{n=1}^{3} \left(w_n - \langle Y_t \rangle_0 \right)^2 \left\langle\left\langle Q_n^2 \right\rangle\right\rangle \frac{1}{\tau^2} \int_{-\infty}^{t_1} \int_{-\infty}^{t_2} e^{-\frac{t_1 - z_1 + t_2 - z_2}{\tau} \langle Q_0 \rangle} r_n(|z_1 - z_2|)\, dz_1\, dz_2 \tag{12}$$

where $\langle Q_n \rangle$, $\left\langle\left\langle Q_n^2 \right\rangle\right\rangle$ and $\left\langle\left\langle Q_n(t_1)\, Q_n(t_2) \right\rangle\right\rangle_{stat} = \left\langle\left\langle Q_n^2 \right\rangle\right\rangle r\left(|t_1 - t_2|\right)$ are respectively the mean, variance and autocovariance of stationary shot noise conductance $Q_n(t)$.

3   Random displacements

Adding random displacements to common presynaptic spikes enables to implement arbitrary crosscovariance functions between the spike trains and results in the following synaptic input model:

$$G_e(t) = \sum_{x_j \in \xi_e} g_e(t - x_j)\, H(t - x_j) + \sum_{x_l \in \xi_c} g_e(t - (x_l + \eta_l))\, H(t - (x_l + \eta_l))$$

$$G_i(t) = \sum_{x_i \in \xi_i} g_i(t - x_i)\, H(t - x_i) + \sum_{x_l \in \xi_c} g_i(t - (x_l + \theta_l))\, H(t - (x_l + \theta_l))$$

where $\eta_l \sim p_e(\eta)$ and $\theta_l \sim p_i(\theta)$ are independent random displacements.

The common spikes are generated by a *Compound PPP* Ξ_c^η that assigns independent marks $\eta_l \sim p_e(\eta)$ and $\theta_l \sim p_i(\theta)$ to each arrival time $t_l \in \xi_c$. A realization ξ_c of the compound PPP specifies both the common arrival times and the random displacements, i.e. $\xi_c = \{(x_1, \eta_1, \theta_1), \ldots, (x_L, \eta_L, \theta_L)\}$.

The correlated input model analyzed in the previous sections results in delta-correlated crosscovariance between excitatory and inhibitory spike trains. Arbitrary crosscovariance functions are generated

by adding random displacements to the common spikes [Brette, 2009]. The results from the previous sections can be used with the following changes:

$$\hat{Q}_3(t) = \frac{1}{g_l} \sum_{x_l \in \xi_c} g_e(t - x_l - \eta_l) H(t - x_l - \eta_l) + g_i(t - x_l - \theta_l) H(t - x_l - \theta_l)$$

$$Q_3(t) = \frac{1}{g_l} \sum_{x_l \in \xi_c} w_1 g_e(t - x_l - \eta_l) H(t - x_l - \eta_l) + w_2 g_i(t - x_l - \theta_l) H(t - x_l - \theta_l)$$

The structure of the solution given by Eqs. (5) and (6) remains unchanged for this model. The independence of Ξ and the Slivnyak-Mecke theorem yields the expectations inside the integrals with expectations involving ξ_c evaluated under Ξ_c^η. The key expectations are given by:

$$\left\langle Q_3(z) e^{-\frac{1}{\tau} \int_z^t Q_0(u)\,du} \right\rangle = \left\langle e^{-\frac{1}{\tau} \int_z^t Q_0(u)\,du} \right\rangle \int \int \int_{-\infty}^{z} e^{-\frac{1}{\tau} \int_z^t (g_1(u-x-\eta)H(u-x-\eta) + g_2(u-x-\theta)H(u-x-\theta))\,du}$$

$$\left(w_1 g_1(z - x - \eta) H(z - x - \eta) \right.$$
$$\left. + w_2 g_2(z - x - \theta) H(z - x - \theta) \right)$$
$$\lambda_c(x)\, p_e(\eta)\, p_i(\theta)\, dx\, d\eta\, d\theta \qquad (13)$$

$$\left\langle \prod_{k=1}^{K} e^{-\frac{1}{\tau} \int_{z_k}^{t_k} Q_3(u)\,du} \right\rangle = \exp\left(\int \int \int_{\mathcal{S}} \left(\prod_{k=1}^{K} e^{-\frac{1}{\tau} \int_{z_k}^{t_k} (g_1(u-x-\eta)H(u-x-\eta) + g_2(u-x-\theta)H(u-x-\theta))\,du} - 1 \right) \right.$$
$$\left. \lambda_c(x)\, p_e(\eta)\, p_i(\theta)\, dx\, d\eta\, d\theta \right) \qquad (14)$$

The deterministic solution $\langle Y_t \rangle_0$ of this model is evaluated as in the previous section with the following change:

$$\langle Q_3(t) \rangle = \int \int \int_{-\infty}^{t} (w_1 g_1(z - x - \eta) + w_2 g_2(z - x - \theta))\, \lambda_c(x)\, p_e(\eta)\, p_i(\theta)\, dx\, d\eta\, d\theta$$

The central moments expansion is developed around the deterministic solution and results in the same expressions as Eqs. (7), (8) and (9) but with expectations involving ξ_c evaluated under Ξ_c^η.

Introducing random displacements in one synapse type and allowing strictly positive or negative displacements in the other synapse type generates causal correlations in the synaptic input. We apply these results to a membrane model with periodic common input shown in Fig. 6 and random displacements with exponential distribution ($\mu = 5$ ms) on common spikes from inhibitory input.
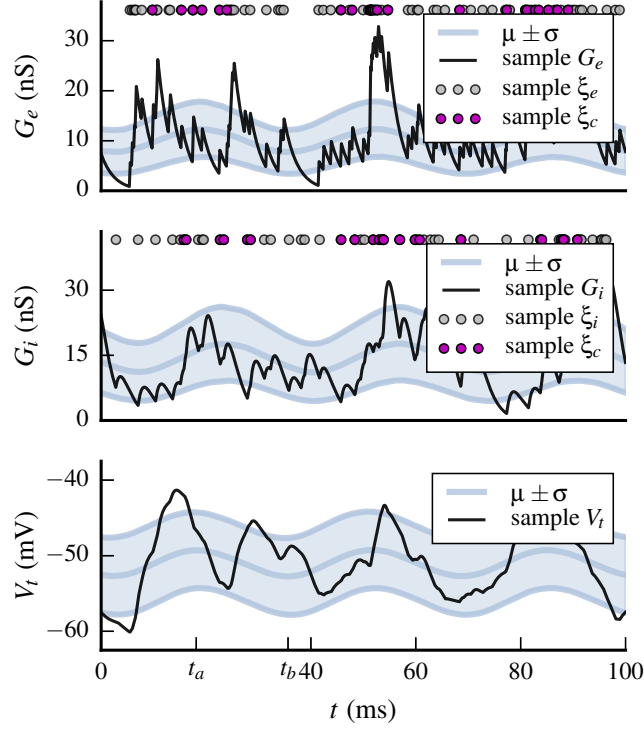
Figure 6 – *Neuron model with excitatory and inhibitory conductance synapses under periodic correlated synaptic input. The synaptic input rates for excitatory and inhibitory synapses is constant and the common input oscillates periodically. Random displacements with exponential distribution ($\mu = 5$ ms) are added to common spikes from inhibitory input.*

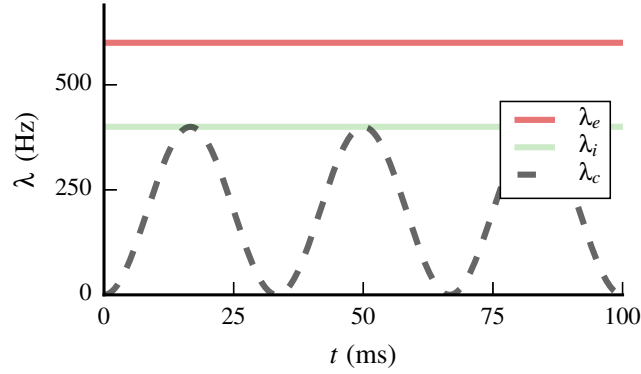The rate functions used to implement this model are shown in Fig. 7.

Figure 7 – *Rate functions for periodic common input (dashed gray) and constant excitatory and inhibitory rates (red and green, respectively).*

Comparison with numerical simulations for the mean and standard deviation is shown in Fig. 8 for mean and variance and result in excellent accuracy. An approximation for the membrane potential distribution using truncated Edgeworth series is also shown.
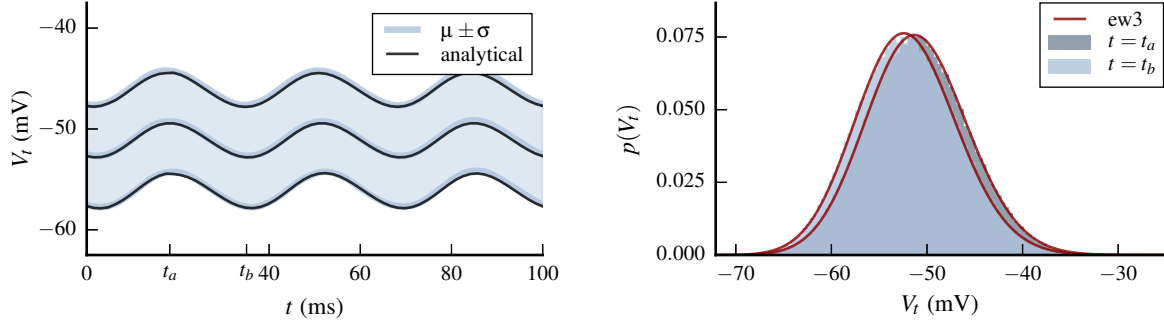
Figure 8 – *(Left) Comparison of exact solutions with numerical simulations for mean and second order cumulants of membrane potential $V(t)$. There is excellent agreement between the simulations (gray) and the analytic prediction (black). (Right) Approximation of probability density function (pdf) using truncated Edgeworth series of third order. The pdf is evaluated at t_a and t_b that corresponds to local maxima and minima of V_t shown in the left plot.*

4 Conclusion

The effect of synaptic input correlations in the statistics of membrane potential is investigated, in the case of passive neuronal membrane driven by nonstationary shot noise conductance. Input correlations are introduced by adding common presynaptic spikes to the inputs. Such input model displays a degree of coincident presynaptic spikes that may not be biologically relevant. Arbitrary crosscorrelation functions are implemented by adding random displacements to common input spikes. Causality can be enforced by only adding random displacements to one synapse type and choosing a distribution with strictly positive or negative values. The exact cumulants of these models is obtained under the formalism of Poisson Point Process transformations. The central moments expansion (CME) is derived and expresses the cumulants of membrane potential fluctuations in terms of the correlated shot noise inputs. Approximations to the time-evolving distribution are obtained with truncated Edgeworth series based on the nonstationary cumulants.

The CME relates the hierarchy of correlated shot noise cumulants to the statistics of membrane potential fluctuations and may contribute to refine existing models of statistical inference by including the effects of correlation in synaptic input. Future research questions will address the effect of input correlation in the firing rate of the cell.

Acknowledgments

Appendix

A   Exact Cumulants

Using independence of Ξ and applying the *Slivnyak-Mecke Theorem* [Slivnyak, 1962, Mecke, 1967] yields the expectations inside the integrals. For the mean and autocovariance,

$$\left\langle Q_n(z)\, e^{-\frac{1}{\tau}\int_z^t Q_0(u)\,du} \right\rangle = \left\langle e^{-\frac{1}{\tau}\int_z^t Q_0(u)\,du} \right\rangle \int_{-\infty}^{z} g_n(z,x)\, e^{-\frac{1}{\tau}\int_z^t \hat{g}_n(u,x)\,du}\, \lambda_n(x)\, dx$$

$$\sum_{n=1}^{3}\sum_{m=1}^{3}\left\langle w_n\, Q_n(z_1)\, w_m\, Q_m(z_2)\prod_{k=1}^{2}e^{-\frac{1}{\tau}\int_{z_k}^{t_k}Q_0(u)\,du}\right\rangle$$

$$=\left\langle\prod_{k=1}^{2}e^{-\frac{1}{\tau}\int_{z_k}^{t_k}Q_0(u)\,du}\right\rangle\left(\sum_{n=1}^{3}w_n^2\int_{-\infty}^{\min(z_1,z_2)}g_n(z_1-x)\,g_n(z_2-x)\prod_{k=1}^{2}e^{-\frac{1}{\tau}\int_{z_k}^{t_k}\hat{g}_n(u-x)\,H(u-x)\,du}\,\lambda_n(x)\,dx\right.$$

$$+\sum_{m=1}^{3}w_m\int_{-\infty}^{z_1}g_m(z_1-y)\prod_{k=1}^{2}e^{-\frac{1}{\tau}\int_{z_k}^{t_k}\hat{g}_m(v-y)\,H(v-y)\,dv}\,\lambda_m(y)\,dy$$

$$\left.\sum_{l=1}^{3}w_l\int_{-\infty}^{z_2}g_l(z_2-z)\prod_{k=1}^{2}e^{-\frac{1}{\tau}\int_{z_k}^{t_k}\hat{g}_l(w-z)\,H(w-z)\,dw}\,\lambda_l(z)\,dz\right)$$

In the general case,

$$\left\langle\prod_{k=1}^{K}e^{-\frac{1}{\tau}\int_{z_k}^{t_k}Q_0(u)\,du}\right\rangle=\prod_{n=1}^{3}\left\langle\prod_{k=1}^{K}e^{-\frac{1}{\tau}\int_{z_k}^{t_k}Q_n(u)\,du}\right\rangle e^{-\frac{t_1-z_1+t_2-z_2}{\tau}}$$

$$\left\langle\prod_{k=1}^{K}e^{-\frac{1}{\tau}\int_{z_k}^{t_k}Q_n(u)\,du}\right\rangle=\exp\left(\int_{\mathcal{S}}\left(\prod_{k=1}^{K}e^{-\frac{1}{\tau}\int_{z_k}^{t_k}\hat{g}_n(u-x)\,H(u-x)\,du}-1\right)\lambda_n(x)\,dx\right)$$

B   Truncated Edgeworth Expansion

In terms of the normalized process $X_t=(V_t-\langle V_t\rangle)/\sigma_t$ with $\sigma_t\equiv\sqrt{\langle\langle V_t^2\rangle\rangle}$, the truncated fourth order Edgeworth series is given by:

$$p_{ew}\left(X_t=x\right)\simeq\frac{1}{\sigma_t}\left(1+\frac{1}{3!}\frac{\langle\langle V_t^3\rangle\rangle}{\sigma_t^3}\left(x^3-3x\right)\right.$$

$$\left.+\frac{1}{4!}\frac{\langle\langle V_t^4\rangle\rangle}{\sigma_t^4}\left(x^4-6x^2+3\right)+\frac{10}{6!}\frac{\langle\langle V_t^3\rangle\rangle^2}{\sigma_t^6}\left(x^6-15x^4+45x^2-15\right)\right)\mathcal{N}(x)\quad(15)$$

where $\mathcal{N}(x)=\exp(-x^2/2)/\sqrt{2\pi}$ is the standard normal density and $p(V_t=v)=p_{ew}\left(x=\frac{v-\langle V_t\rangle}{\sigma_t}\right)$. The third order and fourth order of the series is given by the first and second lines, respectively.

References

Romain Brette. Generation of correlated spike trains. *Neural computation*, 21(1):188–215, 2009.

Marco Brigham and Alain Destexhe. Nonstationary filtered shot-noise processes and applications to neuronal membranes. *Physical Review E*, 91(6):062102, 2015.

Harald Cramér. *Mathematical methods of statistics*, volume 1. Princeton university press, 1946.

FY Edgeworth. On the representation of statistical frequency by a series. *Journal of the Royal Statistical Society*, pages 102–106, 1907.

Timothy J Gawne and Barry J Richmond. How independent are the messages carried by adjacent inferior temporal cortical neurons? *The Journal of neuroscience*, 13(7):2758–2771, 1993.

Charles M Gray, Peter König, Andreas K Engel, Wolf Singer, et al. Oscillatory responses in cat visual cortex exhibit inter-columnar synchronization which reflects global stimulus properties. *Nature*, 338 (6213):334–337, 1989.

John Hertz. Cross-correlations in high-conductance states of a model cortical network. *Neural Computation*, 22(2):427–447, 2010.

Alexandre Kuhn, Ad Aertsen, and Stefan Rotter. Higher-order statistics of input ensembles and the response of simple model neurons. *Neural Computation*, 15(1):67–101, 2003.

Daeyeol Lee, Nicholas L Port, Wolfgang Kruse, and Apostolos P Georgopoulos. Variability and correlated noise in the discharge of neurons in motor and parietal areas of the primate cortex. *The Journal of neuroscience*, 18(3):1161–1170, 1998.

Jakob H Macke, Philipp Berens, Alexander S Ecker, Andreas S Tolias, and Matthias Bethge. Generating spike trains with specified correlation coefficients. *Neural Computation*, 21(2):397–423, 2009.

J Mecke. Stationäre zufällige masse auf localcompakten abelischen gruppen. *Wahrscheinlichkeitsth*, 9: 36–58, 1967.

Rubén Moreno, Jaime de La Rocha, Alfonso Renart, and Néstor Parga. Response of spiking neurons to correlated inputs. *Physical Review Letters*, 89(28):288101, 2002.

Y Prut, H Slovin, and A Aertsen. Dynamics of neuronal interactions in monkey cortex in relation to behavioural events. *Nature*, 373:9, 1995.

Alfonso Renart, Jaime de la Rocha, Peter Bartho, Liad Hollender, Néstor Parga, Alex Reyes, and Kenneth D Harris. The asynchronous state in cortical circuits. *science*, 327(5965):587–590, 2010.

Robert J Rosenbaum, James Trousdale, and Krešimir Josić. Pooling and correlated neural activity. *Frontiers in computational neuroscience*, 4, 2010.

Cyrille Rossant, Sara Leijon, Anna K Magnusson, and Romain Brette. Sensitivity of noisy neurons to coincident inputs. *The Journal of Neuroscience*, 31(47):17193–17206, 2011.

M. Rudolph and A. Destexhe. A multichannel shot noise approach to describe synaptic background activity in neurons. *The European Physical Journal B*, 52(1):125–132, 2006.

Emilio Salinas and Terrence J Sejnowski. Impact of correlated synaptic input on output firing rate and variability in simple neuronal models. *The Journal of Neuroscience*, 20(16):6193–6209, 2000.

IM Slivnyak. Some properties of stationary flows of homogeneous random events. *Theory of Probability & Its Applications*, 7(3):336–341, 1962.

Daniel Y Ts'o, Charles D Gilbert, and Torsten N Wiesel. Relationships between horizontal interactions and functional architecture in cat striate cortex as revealed by cross-correlation analysis. *The Journal of Neuroscience*, 6(4):1160–1170, 1986.

David L Wallace. Asymptotic approximations to distributions. *The Annals of Mathematical Statistics*, pages 635–654, 1958.

Ehud Zohary, Michael N Shadlen, and William T Newsome. Correlated neuronal discharge rate and its implications for psychophysical performance. *Nature*, 1994.

Chapter 6

Estimating stochastic process memory in neuronal membranes

Summary

This article explores a complementary aspect of membrane potential dynamics, namely memory effects due to recent activity. Actual physical processes may have a characteristic memory time during which recent history is important for the evolution of the system. In the case of neuronal membranes with conductance synapses, the solution of the membrane equation displays long range memory: the contribution of a past presynaptic spike depends on all subsequent spikes. However, the most recent presynaptic input has higher impact on membrane potential evolution resulting in an effective memory range of finite duration. The membrane equation for current synapses does not have this type of memory effects since the contribution of presynaptic spikes is independent of other spikes. However, the form of postsynaptic response may also introduce a characteristic memory time.

In order to explore this question, we analyze the relaxation properties of these filtered processes following the extinction of presynaptic activity. The second time derivative of the autocorrelation can capture the effect of recent history when evaluated in a sliding window after the extinction time. Beyond a critical time interval τ_{crit} only residual memory effects remain by this measure.

However, there is a free parameter related to the residual value of decorrelation that can be neglected. We propose to constrain it by testing the loss of markov property with a two sample Kolmogorov-Smirnov (K-S) test. This test rejects to a p-level of significance the baseline hypothesis that the samples originate from the same distribution, which is chosen according to the Markov hypothesis.

Quantifying the extent of memory effects and establishing their range provides a time scale for the dynamics of neuronal population activity models beyond which memory effects can be neglected. The characteristic memory time of membrane potential fluctuations in biological neurons can be estimated from intracellular recordings containing up and down epochs by aligning the end of up states.

Résumé

La présence d'effets de mémoire augmente la complexité de l'analyse des processus stochastiques, et ce type d'effet est souvent négligé au profit de processus sans effet de mémoire dans

les applications pratiques. Neanmoins, ces effets peuvent être étudiés analytiquement pour des processus de *shot noise* simples ou filtrés, en analysant leurs propriétés de relaxation suite à l'extinction du *processus ponctuel de Poisson* associé. Les effets de temps de mémoire caractéristique se manifestent par la décorrélation résiduelle dans la phase de relaxation. Une échelle du temps pour cet effet de mémoire peut être estimée en se fixant un seuil de décorrélation résiduelle maximale. Ceci permet d'évaluer une échelle de temps effective endeans laquelle le processus présenterait des corrélations à longue portée tout en ayant des effets de mémoire négligeables. Cependant, ce seuil critique est un paramètre libre du modèle qui peut être restreint par des simulations numériques avec le test de *Kolmogorov-Smirnov* à deux échantillons.

Estimating stochastic process memory in neuronal membranes

Marco Brigham, Alain Destexhe

26/03/2015

Abstract

Memory effects often impair the tractability of stochastic processes and lead to consider their memory-less approximations in actual applications. These effects can be investigated analytically for shot noise and filtered shot noise processes by analyzing their relaxation properties after extinguishing the associated Poisson point process. Any existing characteristic memory time results in residual decorrelation in the relaxation phase. A time scale for process memory can be estimated by setting a critical threshold of maximal residual decorrelation. This enables to determine the effective time scale for which the process still has long range correlations but negligible memory effects. This critical threshold is a free parameter of the method that can be constrained by numerical simulations with two sample Kolmogorov-Smirnov (K-S) test.

1 Introduction

The prospect of only evaluating the present in order to successfully estimate the future is an important property across many activities. This is also the case in the study of stochastic processes to the extent of carrying a dedicated name: *the Markov Property*. The tractability of stochastic processes is greatly improved by this property since only a very small set of conditional densities is required to completely define them [Gillespie, 1992, Van Kampen, 1992]. Actual physical processes may have a characteristic memory time during which recent history is important [Gardiner, 2009] and defines the shortest time scale for which system dynamics can be modeled as Markovian. Computational neuroscience models often assume the Markov property in state variables such as neuronal membrane potential or synaptic input. Such hypothesis is an approximation for membrane models with conductance synapses since the membrane equation has long term memory effects [Tuckwell, 1988, Gerstner et al., 2014]. Quantifying the extent of these effects and establishing their characteristic memory time provides a time scale for models of neuronal population activity beyond which memory effects can be considered minimal.

We explore this question by considering a passive membrane model with conductance synapses driven by shot noise input and analyze the relaxation properties of membrane potential following the extinction of synaptic input. The membrane potential and the synaptic input of this model are deterministic transformations of presynaptic spike times. Stopping the arrival of new spikes produces a transition between the stochastic evolution of these filtered processes and their deterministic regimes and enables to gain access to the characteristic memory time. The autocorrelation is measured after input extinction in order to assess the level of residual decorrelation that typically decreases during relaxation. This provides a quantitative measure of process memory effects that can be applied to both membrane potential fluctuations and synaptic input. These results extend to membrane models with current synapses since the latter kind can also be considered shot noise processes.

This method has a free parameter related to the level of residual decorrelation that is considered negligible. We use an empirical test of effective memory timescale with the two sample version of the Kolmogorov-Smirnov (K-S) test [Kolmogorov, 1933, Smirnov, 1939, Kolmogoroff, 1941]. The K-S test has the ability to reject to a p-level of significance whether samples originate from the same (unknown) distribution. We test samples from relevant empirical conditional distributions that are equivalent under the Markov hypothesis. If the K-S test rejects the hypothesis that samples are drawn from the same distribution then the Markov hypothesis does not hold. This procedure has the power to reject the Markov hypothesis but not to confirm it, which is sufficient for our purposes. The problem of evaluating the Markov property from time series data is complex and has been the subject of recent interest [De Matos and Fernandes, 2007, Aït-Sahalia et al., 2010, Chen and Hong, 2012]. This empirical procedure estimates

the level of memory effects that violates the Markov property over a large number of realizations and therefore constraints the free parameter related to residual decorrelation.

2   Filtered Process Memory

We consider shot noise and filtered shot noise processes that are generated from a *Poisson point process* (PPP) with nonstationary rate. These processes can display different time scales of memory effects as can be appreciated by their relaxation following the extinction of PPP events. This is illustrated in Fig. 1, where superposed realizations are shown for exponential and alpha kernel shot noise and their filtered versions by a conductance-base membrane. The PPP extinction time t_{ext} is marked by a vertical line. The exponential kernel shot noise decays in an orderly manner after t_{ext} . Realizations from the other processes may display amplitude increases after t_{ext} but after a short period all realizations also decay rather orderly. The cases of amplitude increase beyond t_{ext} reflects memory effects for these examples since they originate in the particular history of the realizations prior to t_{ext}.
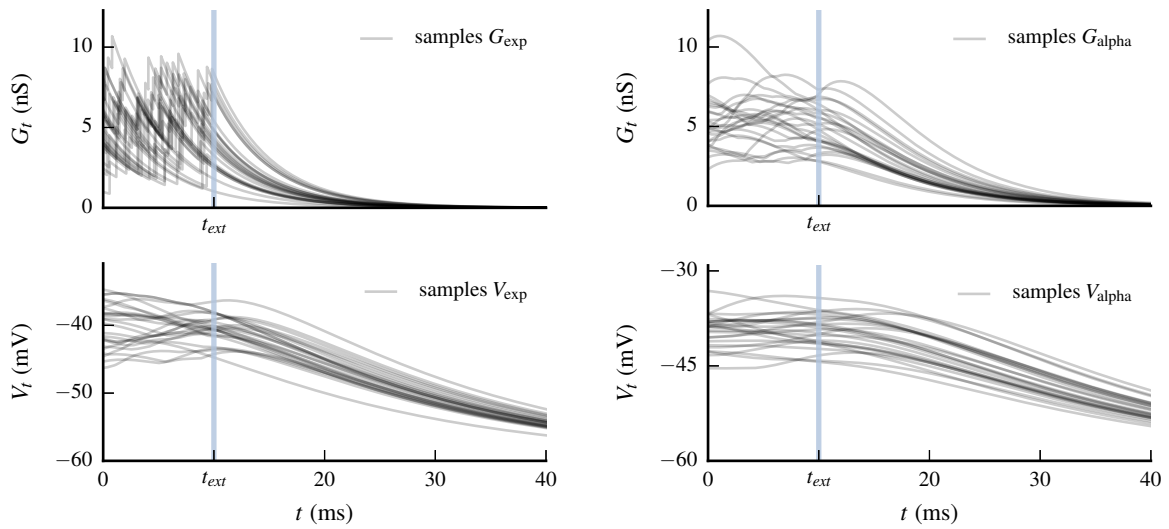

Figure 1 – *Realizations from exponential (left) and alpha kernel (right) shot noise and their filtered versions by a conductance-base neuronal membrane following the extinction of the underlying Poisson Point Process (PPP) at time t_{ext}. The realizations of exponential shot noise decay in an orderly manner after t_{ext} whereas realizations of the other processes may still display amplitude increases after t_{ext}. These amplitude increases after the extinction of PPP reflect deviations from the mean decay trajectory of the processes and are a form of recent history effect.*

A measure of decay uniformity is given by the autocorrelation ρ, since the possibility that some realizations increase in amplitude while the mean decays after t_{ext} contributes to a decrease in ρ. The autocorrelation $\rho(X_1\,X_2)$ is given by $\rho(X_1\,X_2) = \langle\langle X_1\,X_2\rangle\rangle\,/(\sigma(X_1)\,\sigma(X_2))$ where $\langle\langle X_1\,X_2\rangle\rangle$ is the autocovariance at times t_1 and t_2 and $\sigma(X_t)$ is the standard deviation at time t. In what follows, the autocorrelation will be measured at times posterior to t_s and t_{ext} with $t_s < t_{ext}$. This is illustrated in Fig. 2 with realizations from the alpha kernel shot noise.
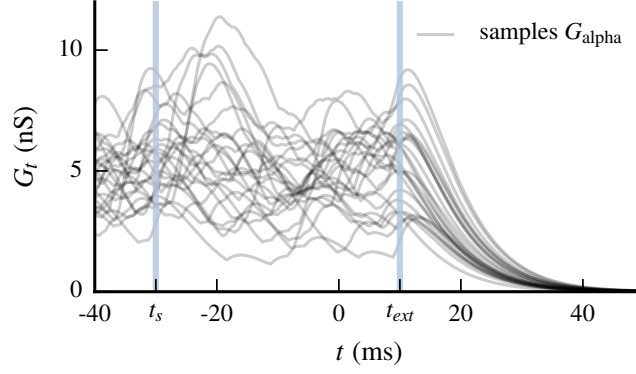
Figure 2 – *Shot noise and filtered shot noise processes are generated from transformations of Poisson point process (PPP) realizations. The PPP is active at time t_s and inactive from time t_{ext} onwards (extinction time). The times t_s and t_{ext} are marked with vertical blue lines. The extinction time marks a transition between the stochastic evolution of these filtered processes and their deterministic regime.*

Measuring the autocorrelation at t_s while the PPP is still active is not very informative of decay behavior following the extinction of the PPP. All processes from Fig. 1 have long tailed autocorrelations as shown in the left plot of Fig. 3. A very different picture is obtained when measuring the autocorrelation after t_{ext}, as shown in the right plot of the same figure. At times later than t_{ext}, the exponential kernel shot noise G_{exp} is fully autocorrelated and its filtered process V_{exp} displays higher autocorrelation ρ than both of the alpha kernel-based processes.
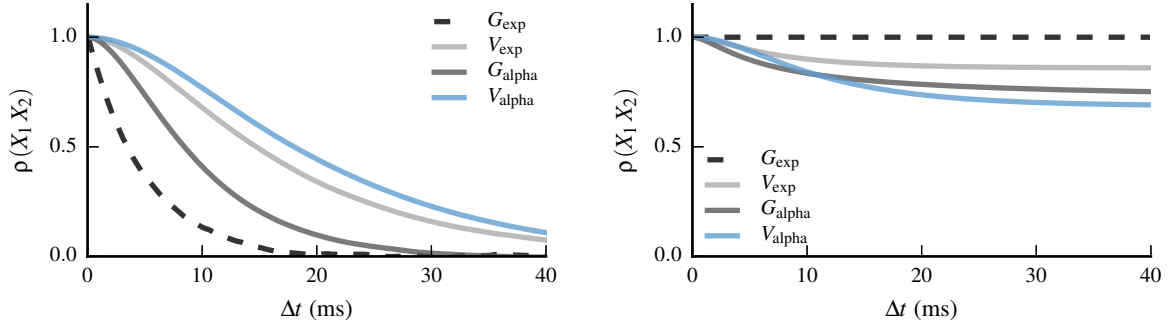

Figure 3 – *The autocorrelation ρ displays quite different characteristics when measured from time t_s (left) and time t_{ext} onwards (right). The exponential kernel shot noise G_{exp} is fully autocorrelated from t_{ext} onwards, and its filtered process V_{exp} displays higher autocorrelation than the alpha kernel-based processes. The ranking in autocorrelation as measured at $\Delta t = 20$ ms can be compared with decay orderliness at time $t_{ext} + 20$ ms in Fig. 1.*

The numerical simulations were generated with shot noise input with exponential kernel $g(t - x)_{\exp} = h \exp\left(-(t - x)/\tau_s\right)$ and alpha kernel $g(t-x)_{alpha} = h\left((t-x)/\tau_s\right) \exp\left(-(t - x)/\tau_s\right)$ for excitatory conductance. The stationary PPP rate $\lambda = 500$ Hz is the same in both cases. Other parameters are $\tau_m = 0.02$ s, $E_l = -0.06$ V, $E_e = 0$ V, $g_l = 10\text{E-9}$ S, $h_e = 2\text{E-9}$ S, $\tau_s = 0.0025$ s.

3   Estimating Memory Time Scale

Measuring autocorrelation ρ after the extinction of the PPP reflects the evolution of decay uniformity for each process but also between them. For example, the reversal in autocorrelation for alpha kernel-based processes that occurs between times $\Delta t = 5$ ms and $\Delta t = 20$ ms corresponds to the reversal in decay uniformity between these processes. The alpha kernel shot noise has lower decay uniformity at time $\Delta t = 5$ ms due to its higher initial variance, whereas the situation is reversed at time $\Delta t = 20$ ms due to the possible amplitude increases for the filtered process.

3

The autocorrelation $\rho(X_1 X_2)$ of the process X_t at times $t_1 \geq t_2$ is measured from t_2 to $t_1 = t_2 + \Delta t$. Moving the starting time t_2 to the right of t_{ext} results in increasingly autocorrelated processes, as illustrated in the left plot of Fig. 4 for filtered alpha kernel shot noise. Beyond a critical value $t_2 = t_{ext} + \tau_{crit}$ particular to each process, all processes become very autocorrelated reflecting states where most realizations follow the mean decay trajectory to their rest value. This time interval τ_{crit} is our estimate for the characteristic memory time of these processes with $\tau_{crit} = 0$ for exponential shot noise and $\tau_{crit} > 0$ for the other examples.
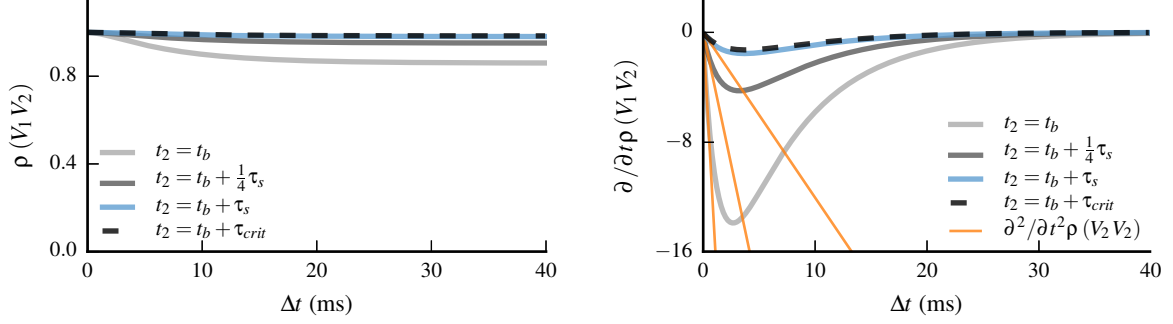

Figure 4 – *The autocorrelation (left) and its first derivative (right) measured from extinction time t_{ext} onwards for the filtered process of alpha kernel shot noise. The filtered process becomes increasingly autocorrelated and its first derivative approaches zero as the starting time of measure t_2 moves to the right of t_{ext}. The characteristic memory time of the process is estimated by τ_{crit}, which is the smallest value of t_2 that yields a process nearly autocorrelated with first derivative close to zero (dashed line). The second derivative of ρ evaluated at the origin decreases as the first derivative approaches zero.*

The value of τ_{crit} can be estimated from the first derivative of ρ evaluated at t_2 as it decreases and approaches zero when moving to the right of t_{ext}. This is illustrated in the right plot of Fig. 4. Setting a small threshold value c for this first derivative leads to $\rho \simeq 1$ close to unity. In more quantitative terms,

$$\tau_{crit} = \arg\min_{\tau} \left. \frac{\partial^2}{\partial t_2^2} \rho(X_1 X_2) \right|_{t_1 = t_2 = t_{ext} + \tau} > c \tag{1}$$

with,

$$\left. \frac{\partial^2}{\partial t_2^2} \rho(X_1 X_2) \right|_{t_1 = t_2 = t} = \frac{\langle\langle X_t \frac{d}{dt} X_t \rangle\rangle^2}{\langle\langle X_t^2 \rangle\rangle} - \frac{\left\langle\left\langle \left(\frac{d}{dt} X_t\right)^2 \right\rangle\right\rangle^2}{\langle\langle X_t^2 \rangle\rangle^2} \tag{2}$$

The simple derivation of the second partial derivative of ρ is shown in Appendix A and explicit expressions for PPP transformations can be evaluated using using expressions provided in Appendix B.

Setting $c = 1$ results in $\tau_{crit} = 9.9$ ms or filtered alpha kernel shot noise and yields the dashed trace of ρ and its first derivative shown in Fig. 4. However, this process already has ρ quite close to unity with $\Delta t \simeq \tau_s$ and illustrates the ambiguity in defining the level of residual decorrelation. For alpha kernel shot noise and the filtered process of exponential kernel shot noise setting $c = 1$ yields $\tau_{crit} = 5.4$ ms and $\tau_{crit} = 5.9$ ms, respectively. The second derivative of ρ for each process is shown in the left plot of Fig. 5 and the corresponding traces of ρ are shown in the right plot of the figure.
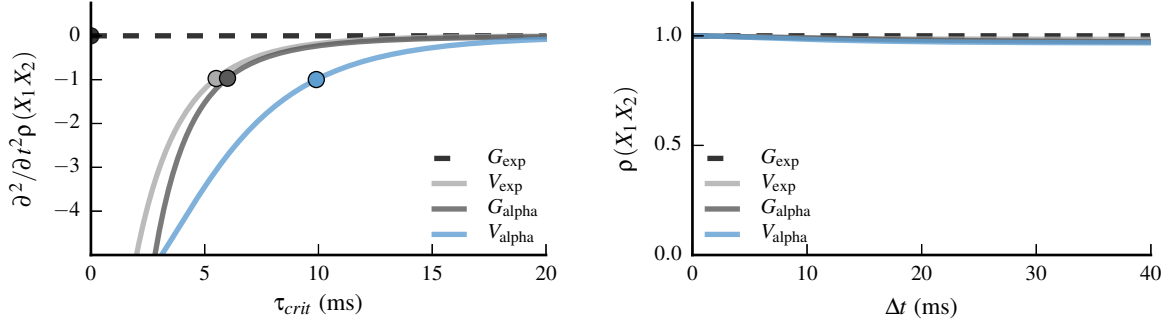
4

Figure 5 – *Setting a threshold value c for the second derivative of ρ evaluated at the origin (left) corresponds to very low levels of residual decorrelation in ρ (right). Each process crosses the threshold c at different values of $t_2 = t_{ext} + \tau$ defining the value of τ_{crit}. As can be appreciated from the traces of ρ in the right plot there is some ambiguity on the level of decorrelation that can be considered negligible.*

4 Testing the Markov Hypothesis

The free parameter c determines the value of τ_{crit} that in turn specifies the level of residual decorrelation deemed negligible. We would like to constrain this parameter to values that are relevant to applications. One possibility is to find the minimal interval τ_{mv} for which the stochastic process can be empirically tested as non-Markovian and ensure that $\tau_{crit} \geq \tau_{mv}$. For any $N \geq 3$ and $x_1 \geq x_2 \geq \cdots \geq x_N$ a first order Markov process is characterized by:

$$p(x_1|x_2, \ldots x_N) = p(x_1|x_2)$$

Choosing particular values of the process at times t_2 and t_3 and showing that $p(x_1|x_2, x_3) \neq p(x_1|x_2)$ violates the condition for $N = 3$ and proves the process is not first order Markovian. In this case, X_1 is the value of the process at time $t_1 \geq t_{ext}$ and we set $t_2 = t_{ext}$ and $t_3 \leq t_{ext}$. This is illustrated in Fig. 6 where realizations of the process are selected when crossing a small neighborhood around the median of the process at times t_2 and both t_2 and t_3. A two sample Kolmogorov-Smirnov (K-S) test can reject to a p-level of significance whether two sets of samples originate from the same (unknown) distribution, i.e. we set $H_0 : p(x_1|x_2, \ldots x_N) = p(x_1|x_2)$. The distance between the conditional distributions $p(x_1|x_2)$ and $p(x_1|x_2, x_3)$ according to K-S statistic is simply the maximum distance between the empirical cumulative distribution functions (CDFs) of both distributions:

$$D = \max |P(x_1|x_2) - P(x_1|x_2, x_3)|$$

where $P(x_1|x_2)$ and $P(x_1|x_2, x_3)$ are the empirical CDFs for separate sets of realizations.
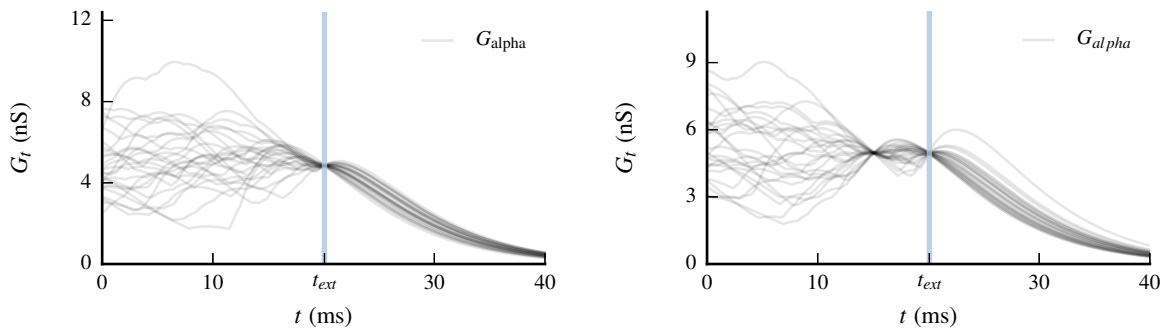

Figure 6 – *Examples of alpha kernel shot noise realizations from the conditional distributions $(X_1 | X_2 = x_2)$ and $(X_1 | X_2 = x_2, X_3 = x_3)$ with $t_1 \geq t_{ext}$, $t_2 = t_{ext}$ and $t_3 \leq t_{ext}$. The realizations are selected in a small neighborhood around the time-evolving median.*

We generate realizations of X_t and extract two sets of samples $\{y_a\}$ and $\{y_b\}$ with the values of the process at $t_1 = t_{ext} + \Delta$. The samples $\{y_a\}$ and $\{y_b\}$ cross a small neighborhood around the median of the process at time $t_2 = t_{ext}$, and those of $\{y_b\}$ also cross the same region at time $t_3 = t_{ext} - \Delta t$. These are samples from the empirical distributions $y_a \sim p(x_1|x_2 = p_{50})$ and $y_b \sim p(x_1|x_2 = p_{50}, x_3 = p_{50})$ where p_{50} denotes the value of the median at those times. The hypothesis H_0 states that y_a and y_b are drawn from the same distribution and the K-S test rejects H_0 with a p-level of significance whenever that is not the case $(p(x_1|x_2) \neq p(x_1|x_2, x_3))$. The result of this procedure is illustrated in Fig. 7 for a single run of stationary alpha kernel shot noise. In the left plot of the figure the K-S test is seen to reject H_0 for $\Delta t \simeq \tau_s/2 = 2$ ms after only a few hundred samples but cannot converge to a low p-value for $\Delta t = 2\tau_s = 10$ ms. The value of the D statistic is shown in the right plot of the figure and is shown to converge very quickly for $\Delta t = 2$ ms.
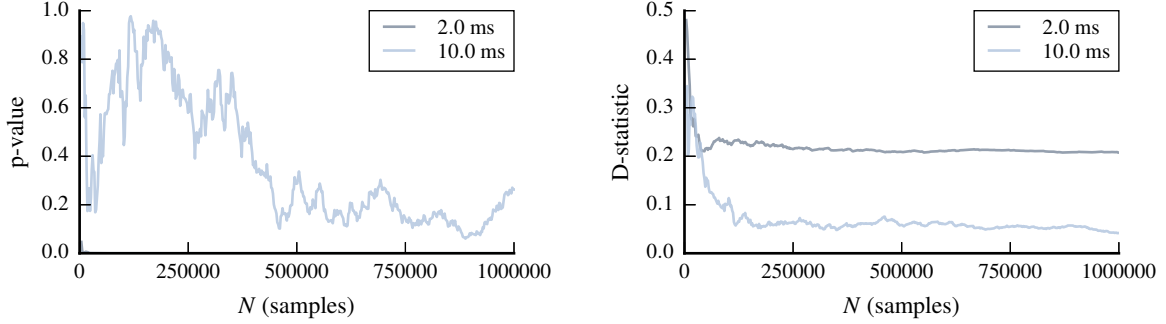

Figure 7 – *Example of P-value and D-statistic for the two sample K-S test evaluated at an increasing number of samples from stationary alpha kernel shot noise. The two sample sets are drawn from empirical conditional distributions $y_a \sim p(x_1|x_2 = p_{50})$ and $y_b \sim p(x_1|x_2 = p_{50}, x_3 = p_{50})$ where p_{50} the median of the process. The samples were evaluated at $t_1 = t_{ext} + \Delta t$ and cross a small neighborhood around the median of the process at time $t_2 = t_{ext}$, and those of $\{y_b\}$ also cross the same region at time $t_3 = t_{ext} - \Delta t$.*

We ran the test for 2 million realizations separated in two sets and applied the K-S test fifty times to evaluate the mean $p - value$ for Δt ranging from 2 ms to 10 ms. We first validate that the test does not reject H_0 for exponential kernel shot noise G_{exp} since it is known to have the Markov property. This is indeed the case as shown in Fig. 8 for this amount of realizations with the case $\Delta t = 2$ ms showing a slight downward trend. The K-S test rejects H_0 for the filtered version of the process V_{exp} for $\Delta t = \{2, 4\}$ ms and displays a downward trend for $\Delta t = 2$ ms.
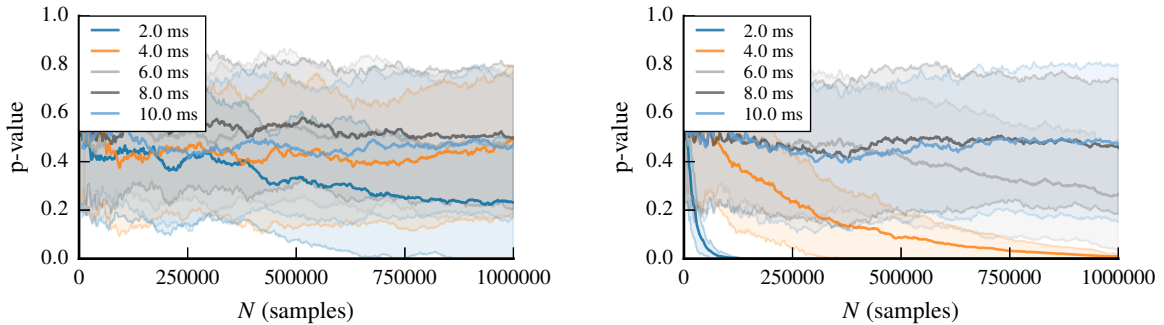

Figure 8 – *P-value and D-statistic averaged over 50 trials for one million realizations for each sample set of the exponential kernel shot noise G_{exp} (left) and its filtered version V_{exp} (right). The K-S test could not reject H_0 for G_{exp}. The test rejects H_0 for V_{exp} at $\Delta t = \{2, 4\}$ ms but cannot converge to a low p-value for higher values of Δt.*

The same procedure was ran for the alpha kernel-based processes and the result is shown in Fig. 9. The K-S test rejects H_0 for G_{alpha} at $\Delta t = \{2, 4\}$ ms and for all but $\Delta t = 10$ ms for the filtered version of the process V_{exp}.
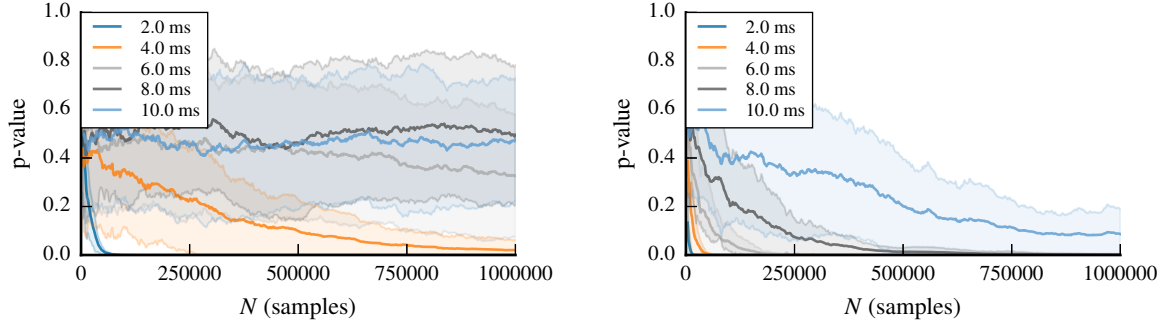
6

Figure 9 – *Result of the K-S test for alpha kernel shot noise G_{exp} (left) and its filtered version V_{exp} (right) under the same conditions as Fig. 8. The K-S test rejects H_0 for G_{exp} at $\Delta t = \{2, 4\}$ ms and V_{exp} for all but $\Delta t = 10$ ms.*

These results show that the K-S statistic is sensitive to deviations from the Markov property under these simulation parameters and for one million of realizations for each sample set. Simulations under different parameters and nonstationary conditions show similar results. For some values of Δt the average p-value displayed a downwards trend indicating that H_0 may be rejected for larger sample sets. In the case of exponential kernel shot noise this may be related to numerical characteristics of the simulations where a trade-off between accuracy and memory size had to be made in terms of sampling frequency and floating point accuracy. For the other cases it seems to indicate that residual process memory effects violating the Markov property are present but are not strong enough to trigger the rejection of H_0. This is precisely the type of constraint required to motivate the choice of free parameter c, which in this case is compatible with the choice $c = 1$.

5 Conclusion

We investigated the memory effects of shot noise and filtered shot noise processes by extinguishing the associated PPP and analyzing their relaxation properties in terms of the autocorrelation. The level of decorrelation in the relaxation phase expresses the extent of memory effects and can therefore be used to estimate the characteristic memory time of these processes. This enables to determine an effective time scale in neural population activity models for which the process has long range correlations and negligible memory effects. However, this method contains a free parameter that sets the level of decorrelation in the relaxation phase that can be neglected.

This measure of characteristic memory is compared with an empirical two sample Kolmogorov-Smirnov (K-S) test on conditional samples of the processes. This non-parametric statistical test rejects to a p-level of significance whether the Markov hypothesis holds for the samples and provides an indication of the level of residual memory effects that can be neglected for practical purposes. This provides a constraint for the free parameter regulating the level of decorrelation in the relaxation phase.

These results can also be applied to estimate the characteristic memory time of membrane potential fluctuations in intracellular recordings containing up and down epochs by measuring the autocorrelation at the extinction of up states.

Future research directions include analysing whether this approach can be applied to other types of synaptic input models, such as white and colored noise and the Ornstein-Uhlenbeck process.

Acknowledgments

Appendix

A   Second Time Derivative of Autocorrelation

In what follows we assume $\rho\left(X_1\,X_2\right)$ to be twice derivable for both arguments. Writing $t_1 = t_2 + \tau$,

$$
\frac{\partial}{\partial\tau}\,\rho(X_1\,X_2) = \frac{\partial}{\partial\tau}\,\frac{\langle\langle X(t_2+\tau)\,X(t_2)\rangle\rangle}{\sqrt{\langle\langle X(t_2+\tau)^2\rangle\rangle}\sqrt{\langle\langle X(t_2)^2\rangle\rangle}}
$$

$$
= \frac{\langle\langle \frac{d}{d\tau}\,X(t_1)\,X(t_2)\rangle\rangle}{\sqrt{\langle\langle X(t_1)^2\rangle\rangle}\sqrt{\langle\langle X(t_2)^2\rangle\rangle}} - \frac{\langle\langle X(t_1)\,\frac{d}{d\tau}\,X(t_1)\rangle\rangle}{\langle\langle X(t_1)^2\rangle\rangle}\,\rho(X_1\,X_2)
$$

Applying the second partial derivative,

$$
\frac{\partial^2}{\partial\tau^2}\,\rho(X_1\,X_2) = \frac{\left\langle\left\langle \frac{d^2}{d\tau^2}\,X(t_1)\,X(t_2)\right\rangle\right\rangle}{\sqrt{\langle\langle X(t_1)^2\rangle\rangle}\sqrt{\langle\langle X(t_2)^2\rangle\rangle}} - \frac{\langle\langle \frac{d}{d\tau}\,X(t_1)\,X(t_2)\rangle\rangle}{\sqrt{\langle\langle X(t_1)^2\rangle\rangle}\sqrt{\langle\langle X(t_2)^2\rangle\rangle}}\,\frac{\langle\langle X(t_1)\,\frac{d}{d\tau}\,X(t_1)\rangle\rangle}{\langle\langle X(t_1)^2\rangle\rangle}
$$

$$
- \left(\frac{\left\langle\left\langle\left(\frac{d}{d\tau}\,X(t_1)\right)^2\right\rangle\right\rangle + \left\langle\left\langle X(t_1)\,\frac{d^2}{d\tau^2}\,X(t_1)\right\rangle\right\rangle}{\langle\langle X(t_1)^2\rangle\rangle} - 2\left(\frac{\langle\langle X(t_1)\,\frac{d}{d\tau}\,X(t_1)\rangle\rangle}{\langle\langle X(t_1)^2\rangle\rangle}\right)^2\right)\rho(X_1\,X_2)
$$

$$
- \frac{\langle\langle X(t_1)\,\frac{d}{d\tau}\,X(t_1)\rangle\rangle}{\langle\langle X(t_1)^2\rangle\rangle}\,\frac{\partial}{\partial\tau}\,\rho(X_1\,X_2)
$$

Setting $\tau = 0$ yields the expression in Eq. (2).

B   First Partial Derivative $d/dt\,\langle F(t,\xi)\rangle$ for PPP transformations

Let $F(t,\xi)$ be a transformation of PPP Ξ The expectation of $F(t,\xi)$ is obtained from the ensemble average over the number n of points and their locations $\{x_1,\ldots,x_n\}$ [Moller and Waagepetersen, 2003, Streit, 2010]:

$$
\langle F(t,\xi)\rangle = \sum_{n=0}^{\infty}\frac{1}{n!}\,e^{-m(\mathcal{S})}\int_{\mathcal{S}}\cdots\int_{\mathcal{S}} F(t,x_1,\ldots,x_n)\prod_{j=1}^{n}\lambda(x_j)\,dx_j
$$

$$
\frac{d}{dt}\,\langle F(t,\xi)\rangle = \frac{d}{dt}\sum_{n=0}^{\infty}\frac{1}{n!}\,e^{-m(\mathcal{S})}\int_{\mathcal{S}}\cdots\int_{\mathcal{S}} F(t,x_1,\ldots,x_n)\prod_{j=1}^{n}\lambda(x_j)\,dx_j = \left\langle\frac{d}{dt}\,F(t,\xi)\right\rangle
$$

For $F(t,\xi)$ a causal transformation of ξ,

$$
\frac{d}{dt}\,\langle F(t,\xi)\rangle = \frac{d}{dt}\sum_{n=0}^{\infty}\frac{1}{n!}\,e^{-m(\mathcal{S})}\int_{\mathcal{S}}\cdots\int_{\mathcal{S}} F(t,x_1,\ldots,x_n)\prod_{j=1}^{n}\lambda(x_j)\,dx_j
$$

$$
= \frac{d}{dt}\sum_{n=0}^{\infty}\frac{1}{n!}\,e^{-m(t)}\int_{-\infty}^{t}\cdots\int_{-\infty}^{t} F(t,x_1,\ldots,x_n)\prod_{j=1}^{n}\lambda(x_j)\,dx_j
$$

$$
= -\lambda(t)\,\langle F(t,\xi)\rangle + \sum_{n=1}^{\infty}\frac{1}{(n-1)!}\,e^{-m(t)}\int_{-\infty}^{t}\cdots\int_{-\infty}^{t} F(t,t,x_1,\ldots,x_{n-1})\prod_{j=1}^{n-1}\lambda(x_j)\,dx_j + \left\langle\tilde{\partial}_t F(t,\xi)\right\rangle
$$

$$
= -\lambda(t)\,\langle F(t,\xi)\rangle + \lambda(t)\,\langle F(t,t,\xi)\rangle + \left\langle\tilde{\partial}_t F(t,\xi)\right\rangle
$$

$$
= \lambda(t)\left(\langle F(t,t,\xi)\rangle - \langle F(t,\xi)\rangle\right) + \left\langle\tilde{\partial}_t F(t,\xi)\right\rangle
$$

where $\left\langle\tilde{\partial}_t F(t,\xi)\right\rangle$ is the expectation of the partial time derivative of $F(t,\xi)$ without explicitly considering causality. In the case of shot noise processes this corresponds to the time derivative of the shot noise

kernel $g(t)$.

Applying to alpha and exponential-based shot noise:

$$\frac{d}{dt}\langle G_{\exp}(t,\xi)\rangle = -\frac{1}{\tau}\langle G_{\exp}(t,\xi)\rangle + h\,\lambda(t)$$

$$\frac{d}{dt}\langle G_{\mathrm{alpha}}(t,\xi)\rangle = \frac{1}{\tau}\langle G_{\exp}(t,\xi)\rangle - \frac{1}{\tau}\langle G_{\mathrm{alpha}}(t,\xi)\rangle$$

These results can be verified directly by evaluating the expectation over the entire real line in order to pass the derivative inside the expectation:

$$\left\langle \frac{d}{dt}\sum_{t_j\in\xi} g(t-t_j)\,H(t-t_j)\right\rangle = \left\langle \sum_{t_j\in\xi}\left(\frac{d}{dt}g(t-t_j)\right)H(t-t_j)\right\rangle + \left\langle \sum_{t_j\in\xi} g(t-t_j)\,\delta(t-t_j)\right\rangle$$

$$= \left\langle \sum_{t_j\in\xi}\left(\frac{d}{dt}g(t-t_j)\right)H(t-t_j)\right\rangle + g(0)\,\lambda(t)$$

However, factoring out the terms ensuring causality in $F(t,\xi)$ may not be very straightforward in some cases, like for example filtered multiplicative noise where terms explicitly involving t appear due to the integration of the input. For the case of single shot noise input $Q(u,\xi)$ and passing the derivative inside the expectation as done previously,

$$Y(t,\xi) = \frac{1}{\tau}\int_0^{+\infty} Q(t-x,\xi)\,e^{-\frac{1}{\tau}\int_{t-x}^t Q(u,\xi)\,du}\,e^{-\frac{x}{\tau}}\,dx = 1 - \frac{1}{\tau}\int_0^{+\infty} e^{-\frac{1}{\tau}\int_{t-x}^t Q(u,\xi)\,du}\,e^{-\frac{x}{\tau}}\,dx$$

$$\frac{d}{dt}\langle Y(t,\xi)\rangle = \left\langle \frac{d}{dt}Y(t,\xi)\right\rangle$$

$$= -\frac{1}{\tau}\int_0^{+\infty}\left\langle \partial_t\, e^{-\frac{1}{\tau}\int_{t-x}^t Q(u)\,du}\right\rangle e^{-\frac{x}{\tau}}\,dx = \frac{1}{\tau^2}\int_0^{+\infty}\left\langle (Q(t)-Q(t-x))\,e^{-\frac{1}{\tau}\int_{t-x}^t Q(u)\,du}\right\rangle e^{-\frac{x}{\tau}}\,dx$$

$$= -\frac{1}{\tau}\langle Y(t,\xi)\rangle + \frac{1}{\tau}\langle Q(t)(1-Y(t,\xi))\rangle$$

References

Yacine Aït-Sahalia, Jianqing Fan, Jiancheng Jiang, et al. Nonparametric tests of the markov hypothesis in continuous-time models. *The Annals of Statistics*, 38(5):3129–3163, 2010.

Bin Chen and Yongmiao Hong. Testing for the markov property in time series. *Econometric Theory*, 28 (01):130–178, 2012.

João Amaro De Matos and Marcelo Fernandes. Testing the markov property with high frequency data. *Journal of Econometrics*, 141(1):44–64, 2007.

C.W. Gardiner. *Stochastic methods.* Springer, 2009.

Wulfram Gerstner, Werner M Kistler, Richard Naud, and Liam Paninski. *Neuronal dynamics: from single neurons to networks and models of cognition.* Cambridge University Press, 2014.

Daniel T Gillespie. *Markov processes: an introduction for physical scientists.* Academic Pr, 1992.

A Kolmogoroff. Confidence limits for an unknown distribution function. *The Annals of Mathematical Statistics*, 12(4):461–463, 1941.

Andrej N Kolmogorov. Sulla determinazione empirica di una legge di distribuzione (on the empirical determination of a distribution law). *Giornale dell'Istituto Italiano degli Attuari*, 4:83–91, 1933.

Jesper Moller and Rasmus Plenge Waagepetersen. *Statistical inference and simulation for spatial point processes*. CRC Press, 2003.

Nikolai V Smirnov. On the estimation of the discrepancy between empirical curves of distribution for two independent samples. *Bull. Math. Univ. Moscou*, 2(2), 1939.

Roy L Streit. *Poisson Point Processes: Imaging, Tracking, and Sensing*. Springer, 2010.

Henry C Tuckwell. *Introduction to theoretical neurobiology: volume 2, nonlinear and stochastic theories*. Cambridge University Press, 1988.

Nicolaas Godfried Van Kampen. *Stochastic processes in physics and chemistry*, volume 1. Elsevier, 1992.

Part III

Discussion

Chapter 7

General Discussion

The work developed in this thesis focuses on statistical properties of nonstationary neuronal membrane fluctuations. These results apply to passive membrane equations without spiking mechanism for both current and conductance synapses when driven by shot noise processes with time-varying rates. These highly variable synaptic input regimes are important since they are thought to reflect synaptic activity during behaving conditions. Exact cumulants are obtained for both synapse types from "first-principles", where the effect of each presynaptic spike on membrane potential is taken into account. This answers the stated research question: *For given statistics of presynaptic spikes, what are the statistics of membrane potential fluctuations?* The exact cumulants can be integrated in truncated Edgeworth series to provide very accurate approximations of time-evolving distribution of membrane potential. These key results are developed in the article *Nonstationary filtered shot noise processes and applications to neuronal membranes* presented in Chapter 3 for the simple case of a single conductance synapse.

Several extensions of this basic results are obtained. The first extension concerns multiple independent synapse types. This is particularly useful for conductance synapses where different excitatory and inhibitory reversal potentials can be associated to relevant ion channels. The effect of synaptic inhomogeneities due to biological differences between synapses is investigated and implemented at the levels of synapse and synapse type. At synapse level, each synapse is modeled by an independent shot noise processes with biological parameters generated from suitable distributions. At the synapse type level, one single shot noise process generates the synaptic input for the synapses of that type, and postsynaptic responses are generated with unique characteristics generated from suitable distributions. This enables to model neurons with a small number of synapses or with multi-modal and sharply distributed biological parameters, in addition to neurons with a large number of synapses. This is exposed in the article *The impact of synaptic conductance inhomogeneities on membrane potential statistics* presented in Chapter 4.

Another extension concerns the effects of synaptic input correlations on membrane potential fluctuations. A simple model of synaptic correlation is analyzed where common presynaptic spikes are added to synaptic input. These spikes can be sharply timed or with random delays or *jitter*. The effects of causal correlations can be accounted by choosing a range of strictly positive values jitter distribution. This simple model enables to investigate the impact of synaptic correlations in the statistics of neuronal membrane fluctuations and is developed in the article *How causal correlations between synaptic inputs affect membrane potential fluctuations* presented in Chapter 5. This approach to analyze correlated synaptic input was made possible by the underlying strategy of explicitly considering the effect of individual presynaptic spikes in the evolution of membrane potential.

The exact cumulants for conductance synapses result in long and complex expressions that may not easily provide insight into the dynamics of membrane statistics. In particular, it does not explicitly show which cumulants of synaptic input have major contributions to membrane potential fluctuations. The central moments expansion (CME) is developed to addresses this question. The CME expresses the statistical dynamics of membrane potential fluctuations in terms of the cumulants of synaptic input. The second order of this expansion yields very accurate approximations in the biological range of parameters and provides a simple path to obtain the stationary limits that are relevant in some applications. The exact cumulants obtained in the articles of Chapters 3, 4 and 5 are approximated with CME versions in each article and facilitate analytical access to the statistical structure of the relevant membrane models.

Conductance synapses induce long range memory effects in membrane potential fluctuations. This memory effect has an effective range due to "forgetting mechanisms" of the membrane that place more importance in the most recent recent presynaptic input. This memory effect is quantifiable by the autocorrelation when measured after extinction of presynaptic input. This enables to measure the time scale of memory effects under nonstationary input. The time scale thus obtained is consistent an empirical test for the loss of Markov property based on the two sample version of Kolmogorov-Smirnov (K-S) test. These results can be applied to estimate the characteristic memory time of membrane potential fluctuations from intracellular recordings containing "up-and-down" states. In this case the autocorrelation is measured by alignment of "down" states under the necessary assumptions of statistical regularity. The memory effects of membrane potential are analyzed in the article *Estimating stochastic process memory in neuronal membranes* in Chapter 6.

The research articles presented in Chapters 3, 4, 5 and 6 focuses in conductance-based synapses due to their higher biological relevance and lower abundance of established results. Treatment of current synapses mostly recovers previous results in the literature and is presented in Chapter 2.

The results developed in this thesis may benefit statistical inference models for biological and dynamical characterization of neurons and their afferent neural networks. These models critically depend on data generation assumptions that can be made more precise and general by including higher order statistics, nonstationary regimes and synaptic inhomogeneities. Using measures of autocorrelation in addition to the more common point statistics given by mean and variance may also yield more robust results. A prerequisite to successfully include synaptic inhomogeneity effects is the development of experimental measures of biological parameter distributions.

Existing models of transfer function, which links membrane potential evolution to neuronal discharge, may also benefit from the exact results and approximations developed in this thesis. The transfer function is a core element of computational models of neuronal activity that compresses internal dynamics of neurons into an input to output firing relationship. The statistics of membrane potential are key to the derivation of transfer functions. These results may contribute with the exact and approximate formulations of higher order statistics and accurate approximations of membrane potential distribution.

Future research possibilities include extending the formalism to synaptic saturation mechanisms and shot-term plasticity. While this represents a departure from the shot noise input model that enabled to obtain exact statistical results, approximations may be developed with the central movements expansion. Another important direction of research is to determine the range of biological and dynamical conditions that requires higher order statistics to fully cap-

ture neuronal dynamics, and perhaps more importantly for applications, the conditions where these can be neglected and more tractable noise models used instead. Determining the convergence properties of the central moments expansion is also an important subject for future research.

Bibliography

Larry F Abbott. Lapicques introduction of the integrate-and-fire model neuron (1907). *Brain research bulletin*, 50(5):303–304, 1999.

Ken-ichi Amemori and Shin Ishii. Gaussian process approach to spiking neurons for inhomogeneous poisson inputs. *Neural computation*, 13(12):2763–2797, 2001.

D.J. Amit and N. Brunel. Model of global spontaneous activity and local structured activity during delay periods in the cerebral cortex. *Cerebral Cortex*, 7(3):237, 1997.

Laurent Badel. Firing statistics and correlations in spiking neurons: a level-crossing approach. *Physical Review E*, 84(4):041919, 2011.

Stuart Bevan, Richard Kullberg, and John Rice. An analysis of cell membrane noise. *The Annals of Statistics*, 7(2):237–257, 1979.

Romain Brette. Generation of correlated spike trains. *Neural computation*, 21(1):188–215, 2009.

N. Brunel. Dynamics of sparsely connected networks of excitatory and inhibitory spiking neurons. *Journal of computational neuroscience*, 8(3):183–208, 2000.

Anthony N Burkitt. Balanced neurons: analysis of leaky integrate-and-fire neurons with reversal potentials. *Biological cybernetics*, 85(4):247–255, 2001.

Anthony N Burkitt. A review of the integrate-and-fire neuron model: I. homogeneous synaptic input. *Biological cybernetics*, 95(1):1–19, 2006a.

Anthony N Burkitt. A review of the integrate-and-fire neuron model: Ii. inhomogeneous synaptic input and network properties. *Biological cybernetics*, 95(2):97–112, 2006b.

D. Cai, L. Tao, A.V. Rangan, and D.W. McLaughlin. Kinetic theory for neuronal network dynamics. *Communications in Mathematical Sciences*, 4(1):97–127, 2006.

N. Campbell. The study of discontinuous phenomena. In *Proc. Camb. Phil. Soc*, volume 15, pages 310–328, 1909.

Mark M Churchland, M Yu Byron, John P Cunningham, Leo P Sugrue, Marlene R Cohen, Greg S Corrado, William T Newsome, Andrew M Clark, Paymon Hosseini, Benjamin B Scott, et al. Stimulus onset quenches neural variability: a widespread cortical phenomenon. *Nature neuroscience*, 13(3):369–378, 2010.

David Roxbee Cox and Valerie Isham. *Point processes*, volume 12. CRC Press, 1980.

Harald Cramér. *Mathematical methods of statistics*, volume 1. Princeton university press, 1946.

DR Curtis and JC Eccles. Synaptic action during and after repetitive stimulation. *The Journal of physiology*, 150(2):374–398, 1960.

Peter Dayan and Laurence F Abbott. *Theoretical neuroscience*. Cambridge, MA: MIT Press, 2001.

P Fatt and B Katz. Spontaneous subthreshold activity at motor nerve endings. *The Journal of physiology*, 117(1):109–128, 1952.

Wulfram Gerstner, Werner M Kistler, Richard Naud, and Liam Paninski. *Neuronal dynamics: from single neurons to networks and models of cognition*. Cambridge University Press, 2014.

EN Gilbert and HO Pollak. Amplitude distribution of shot noise. *Bell Syst. Tech. J*, 39(2):333–350, 1960.

Alan L Hodgkin and Andrew F Huxley. A quantitative description of membrane current and its application to conduction and excitation in nerve. *The Journal of physiology*, 117(4):500–544, 1952.

Ao L Hodgkin, AF Huxley, and B Katz. Measurement of current-voltage relations in the membrane of the giant axon of loligo. *The Journal of physiology*, 116(4):424–448, 1952.

Johan Ludwig William Valdemar Jensen. Sur les fonctions convexes et les inégalités entre les valeurs moyennes. *Acta Mathematica*, 30(1):175–193, 1906.

A. Kuhn, A. Aertsen, and S. Rotter. Neuronal integration of synaptic input in the fluctuation-driven regime. *The Journal of neuroscience*, 24(10):2345, 2004.

A Kuno and K Ikegaya. A statistical investigation of acoustic power radiated by a flow of random point sources. *J. Acoustic Soc. Japan*, 29:662–671, 1973.

Louis Lapicque. Recherches quantitatives sur lexcitation électrique des nerfs traitée comme une polarisation. *J. Physiol. Pathol. Gen*, 9(1):620–635, 1907.

R.B. Lund, R.W. Butler, and R.L. Paige. Prediction of shot noise. *Journal of applied probability*, pages 374–388, 1999.

J. Masoliver. First-passage times for non-markovian processes: Shot noise. *Physical Review A, 1987, vol. 35, núm. 9.*, pages 3918–3928, 1987.

J Mecke. Stationäre zufällige masse auf localcompakten abelischen gruppen. *Wahrscheinlichkeitsth*, 9:36–58, 1967.

Jesper Moller and Rasmus Plenge Waagepetersen. *Statistical inference and simulation for spatial point processes*. CRC Press, 2003.

Gary W Oehlert. A note on the delta method. *The American Statistician*, 46(1):27–29, 1992.

Emanuel Parzen. *Stochastic processes*, volume 24. SIAM, 1999.

B Picinbono, C Bendjaballah, and J Pouget. Photoelectron shot noise. *Journal of Mathematical Physics*, 11(7):2166–2176, 1970.

J. Rice. On generalized shot noise. *Advances in Applied Probability*, pages 553–565, 1977.

S.O. Rice. Mathematical analysis of random noise. *Bell System Technical Journal*, 23(3):282–332, 1944.

S.O. Rice. Mathematical analysis of random noise - conclusion. *Bell System Technical Journal*, 24:46–156, 1945.

Magnus JE Richardson. Effects of synaptic conductance on the voltage distribution and firing rate of spiking neurons. *Physical Review E*, 69(5):051918, 2004.

M.J.E. Richardson and W. Gerstner. Synaptic shot noise and conductance fluctuations affect the membrane voltage with equal significance. *Neural Computation*, 17(4):923–947, 2005.

RW Rodieck, NY-S Kiang, and GL Gerstein. Some quantitative methods for the study of spontaneous activity of single neurons. *Biophysical Journal*, 2(4):351, 1962.

Martine Rousseau. Statistical properties of optical fields scattered by random media. application to rotating ground glass. *JOSA*, 61(10):1307–1316, 1971.

M. Rudolph, M. Pospischil, I. Timofeev, and A. Destexhe. Inhibition determines membrane potential dynamics and controls action potential generation in awake and sleeping cat cortex. *The Journal of neuroscience*, 27(20):5280–5290, 2007.

Michael Rudolph and Alain Destexhe. An extended analytic expression for the membrane potential distribution of conductance-based synaptic noise. *Neural Computation*, 17(11):2301–2315, 2005.

Michael Rudolph, Joe Guillaume Pelletier, Denis Paré, and Alain Destexhe. Characterization of synaptic conductances and integrative properties during electrically induced eeg-activated states in neocortical neurons in vivo. *Journal of neurophysiology*, 94(4):2805–2821, 2005.

Walter Schottky. Uber spontane stromschwankungen in verschiedenen elektrizitatsleitern. *Annalen der Physik*, 362(23):541–567, 1918.

E Siebenga, AWA Meyer, and AA Verveen. Membrane shot-noise in electrically depolarized nodes of ranvier. *Pflügers Archiv*, 341(2):87–96, 1973.

IM Slivnyak. Some properties of stationary flows of homogeneous random events. *Theory of Probability & Its Applications*, 7(3):336–341, 1962.

Donald L Snyder and Michael I Miller. *Random Point Processes in Time and Space*. Springer, 1991.

Richard B Stein. A theoretical analysis of neuronal variability. *Biophysical Journal*, 5(2):173–194, 1965.

Richard B Stein. Some models of neuronal variability. *Biophysical journal*, 7(1):37, 1967.

Charles F Stevens. Inferences about membrane properties from electrical noise measurements. *Biophysical journal*, 12(8):1028–1047, 1972.

Roy L Streit. *Poisson Point Processes: Imaging, Tracking, and Sensing*. Springer, 2010.

Henry C Tuckwell. *Introduction to theoretical neurobiology: volume 2, nonlinear and stochastic theories*. Cambridge University Press, 1988a.

Henry C Tuckwell. *Introduction to theoretical neurobiology: volume 1, Linear Cable Theory and Dendritic Structure*. Cambridge University Press, 1988b.

Jagadish Venkataraman, Martin Haenggi, and Oliver Collins. Shot noise models for outage and throughput analyses in wireless ad hoc networks. In *Military Communications Conference, 2006. MILCOM 2006. IEEE*, pages 1–7. IEEE, 2006.

AA Verveen and LJ DeFelice. Membrane noise. *Progress in biophysics and molecular biology*, 28:189–265, 1974.

Lars Wolff and Benjamin Lindner. Method to calculate the moments of the membrane voltage in a model neuron driven by multiplicative filtered shot noise. *Physical Review E*, 77(4):041913, 2008.

Lars Wolff and Benjamin Lindner. Mean, variance, and autocorrelation of subthreshold potential fluctuations driven by filtered conductance shot noise. *Neural Computation*, 22(1):94–120, 2010.